

University of Warwick institutional repository: <http://go.warwick.ac.uk/wrap>

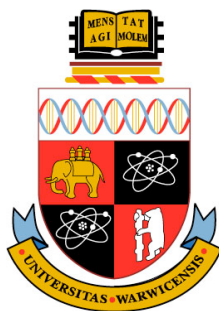
A Thesis Submitted for the Degree of PhD at the University of Warwick

<http://go.warwick.ac.uk/wrap/64116>

This thesis is made available online and is protected by original copyright.

Please scroll down to view the document itself.

Please refer to the repository record for this item for information to help you to cite it. Our policy information is available from the repository home page.



**Biocatalytic valorisation of lignin via genetic or
chemical intervention of bacterial aromatic
degradation pathways**

Paul Sainsbury

A thesis submitted in partial fulfilment of the requirement for the degree of Doctor of
Philosophy in Chemistry

THE UNIVERSITY OF
WARWICK

Department of Chemistry

December 2013

Supervisor: Professor T.D.H Bugg

Contents

Contents	i
Acknowledgements	v
Declaration	vii
Abstract	viii
Abbreviations	x
List of Figures	xii
List of Tables	xxiv
1: Introduction	1
1.1 A bio-based economy	2
1.2 Lignocellulose.....	6
1.2.1 Lignin biosynthesis	9
1.3 Commercial sources of lignin	14
1.3.1 Kraft lignin	14
1.3.2 Sulphite pulping	16
1.3.3 Organosolv lignin.....	17
1.4 Enzymatic breakdown of lignin.....	18
1.4.1 Lignin Peroxidase (LiP)	20
1.4.2 Manganese Peroxidase (MnP).....	24
1.4.3 Versatile Peroxidase (VP).....	26
1.4.4 Laccase	27
1.4.5 Evidence of bacterial lignin degradation.....	30
1.4.6 Dye-decolorizing peroxidases.....	32
1.4.7 Existence of aromatic degradation pathways in bacteria	34

1.5 Extracting value from lignin	40
1.5.1 Chemocatalytic approaches to obtaining high value chemicals.....	42
1.5.2 Vanillic acid pathway as a target for pathway engineering	44
1.6 Aims and Objectives	49
2: Results and Discussion I: The use of <i>Rhodococcus jostii</i> RHA1 gene deletion strains for targeted metabolite production from the breakdown of lignocellulose	51
2.1 Investigation into lignin degradation by <i>R. jostii</i> RHA1	51
2.2 Identification of vanillin catabolic genes in <i>Rhodococcus jostii</i> RHA1	54
2.3 Testing of Δvdh and $\Delta vanA$ gene deletion strains in incubations with wheat straw lignocellulose.	60
2.3.1 Growth observations with the Δvdh and $\Delta vanA$ gene deletion strains in incubations with wheat straw lignocellulose in liquid growth media P1.	61
2.3.2 Metabolite analysis on samples taken from the Δvdh and $\Delta vanA$ incubations with wheat straw lignocellulose in liquid growth media P1.	62
2.3.3 Testing of Δvdh and $\Delta vanA$ gene deletion strains in incubations with hemicellulose.	73
2.3.4 Testing of Δvdh and $\Delta vanA$ gene deletion strains in incubations with ferulic acid.	75
2.4 Attempts to confirm partial bacterial lignin degradation pathways.....	76
2.4.1 Testing of Δvdh and $\Delta vanA$ gene deletion strains in incubations with alkali treated wheat straw lignocellulose	79
2.5 Kraft lignin.....	81
3: Results and Discussion II: Chemical inhibition of selected enzymes proposed to be involved in lignin breakdown	86
3.1 Vanillin aldehyde dehydrogenase (VDH) as a target for chemical inhibition.....	87
3.1.1 Inhibition of aldehyde dehydrogenase by disulfiram.....	87
3.1.2 Growth studies in the presence of disulfiram.....	89

3.1.3 Inhibition of betaine aldehyde dehydrogenase (BADH).....	93
3.2 Known inhibitors of mono-oxygenase enzymes.....	96
3.2.1 Design of potential mechanism-based inhibitors of vanillate monooxygenase (VMO).....	98
3.2.2 Testing in vivo of potential mechanism-based inhibitors of VMO.....	100
3.3 Hydroxamic acid based inhibitors for non-heme iron oxygenases.....	102
3.3.1 Chemical inhibition of <i>E. coli</i> 2,3-dihydroxyphenyl propionate 1,2-dioxygenase (MhpB).....	104
3.3.2 Chemical inhibition of protocatechuate 3,4-dioxygenase (3,4-PCD).....	111
4: Conclusions.....	125
5: Experimental.....	128
5.1: General experimental.....	128
5.1.1 Chemicals and reagents.....	128
5.1.2 Instruments and equipment.....	128
5.1.3 Enzymes and commercially prepared kits.....	130
5.1.4 Solutions and buffers.....	130
5.1.5 Media.....	131
5.1.6 Bacterial Strains.....	133
5.2: Methods.....	134
5.2.1 Culture growth conditions and storage of cells.....	134
5.2.2 Incubations with sources of lignin.....	135
5.2.3 Metabolite extractions.....	137
5.2.4 Thin layer chromatography.....	138
5.2.5 HPLC-UV analysis.....	138
5.2.6 LC-MS analysis.....	138
5.2.7 GC-MS analysis.....	139
5.2.8 Protein purification.....	139

5.2.9 Enzyme assays	141
5.2.10 In-vitro Chemical Inhibition Assays	143
5.2.11 In-vivo Chemical Inhibition Assays.....	144
5.3: Synthesis	145
5.3.1 Synthesis of 3-(prop-2-ynyloxy)benzoic acid (21) ^[219]	145
5.3.1 Synthesis of 3-(prop-2-ynyloxy)-4-hydroxy benzoic acid (22) ^[219]	146
5.3.7 Synthesis of 3,4-Dimethoxycinnamohydroxamic acid (23) ^[212]	148
5.3.8 Synthesis of 3-(3,4-Dimethoxyphenyl)propiohydroxamic acid (24)	149
5.3.9 Synthesis of 4-methoxycinnamohydroxamic acid (D13) ^[212]	150
5.3.10 Synthesis of 3-(4-methoxyphenyl)propiohydroxamic acid (25)	151
6: References.....	152
7: Appendix.....	172
7.1 GC-MS Fragmentation patterns of identified metabolites and authentic standards	172

Acknowledgements

Sometimes its best to be like the snail.

In your life I believe you should go slowly in all matters.

Don't worry if you take a different route, you will eventually get to your destination.

You have been designed to carry a heavy load on your back.

Be honest, be yourself and be the best that you can be in that moment.

Make mistakes.

It's okay to be vulnerable, you are protected.

That's your shell

You can't change yourself, but you can be honest about who and what you are capable of being.

Follow your dreams, take chances and reach for the impossible.

Let the people that love you, love you for the person you are already and not the person you think they want you to be.

Sometimes you may find yourself alone even though others surround you.

But never forget.

We'll know where you are.

That's the shiny trail you leave

You're a snail, a magnificent snail

Paul Sainsbury

Without question I would like to thank Professor Tim Bugg for giving me the opportunity to change my path in life.

To Dr Lidz Hardiman, for being one of the loveliest people in the world.

To Pete and Rahman for their friendship and patient tutelage. Thanks to Goran, Jo, Maria and Fridgefreezer for stopping to make me smile.

To all the past and present Challis, Tosylates, Correttes and Dixlets for making my time at Warwick a memorable one.

Thank you Anne, a friend when mine seemed so distant.

To the BOC for keeping me sane.

To Scott, Vanessa, Steve, Alan, Chris, Jim and Jamie for making the path easier
.....and finally thanks to my mum, who gives so much and expects so little.

Declaration

This thesis represents original research and has not been previously submitted to this or any other institution for any degree, diploma or other qualification. All experimental work has been carried out by the author in the Department of Chemistry at the University of Warwick, between 2010 and 2014.

No material contained herein has been submitted for any other degree, or at any other institution.

.....

Paul Sainsbury

.....

(Date)

Abstract

Global dependence on fossil fuels is not only finite, but also environmentally unsound. A move from petroleum-based chemicals to an alternative based on renewable sources such as agricultural lignocellulosic waste materials could provide significant environmental and economic gains. Lignin, a component of such feedstocks represents an abundant source of aromatic compounds if an effective method for controlled conversion to fine chemicals can be discovered.

Despite the many potential benefits of chemicals derived from lignin, it still remains an unlocked source of more valuable substances.

Lignin is a complex polymer that gives rigidity and protection to plant cell walls. By its very nature it is inherently very hard to break down. Pre-treatments so far have revolved around removing lignin to access the more exploitable sugars from cellulose and hemicellulose.

If a biocatalytic approach to valorisation could combine the natural microbial breakdown of lignin with advances in genetics, then potentially this may offer a method to derive useful aromatic by-products.

In the present thesis, a combined approach was taken for the valorisation of natural state and industrial sources of lignin. Genetic mutants of lignin-degrading bacteria were prepared by targeting enzymes for deletion based on hypothetical lignin degradation pathways. These mutants were used in incubations with different sources of lignin. A chemical approach using mechanism-based and commercially available enzyme inhibitors is also proposed.

These techniques were investigated and various procedures explored and employed, to varying degrees of success, most notably the production of up to 96 mg/L after 144 h of vanillin using a Δvdh mutant of *Rhodococcus jostii* RHA1 in incubations with 2.5% wheat straw lignocellulose (w/v).

A chemical approach identified a potent *in vitro* hydroxamic acid as an inhibitor of protocatechuate 3,4-dioxygenase, with tentative results also suggesting *in vivo* inhibition.

These results in combination, or as stand-alone technique, may provide a valuable method for the valorisation of lignin from agricultural waste feedstocks. They may also bring the possibility of a commercially viable and environmentally sound concept closer to realisation.

Abbreviations

ABTS	2,2'-azino-bis(3-ethylbenthiazoline-6-sulphonic acid)
°C	Degrees Celsius
CoA	Coenzyme A
d	Doublet
da	Dalton
DCM	Dichloromethane
DMF	Dimethylformamide
DNA	Deoxyribonucleic acid
ESI	Electrospray ionisation
EtOH	Ethanol
GC	Gas chromatography
GSH	Glutathione
GPC	Gel permeation chromatography
Hz	Hertz
HPLC	High pressure liquid chromatography
IR	Infra red
kDa	Kilodalton
RT	Room temperature
LB	Luria Broth
LiP	Lignin Peroxidase
LP	Light fraction of light petroleum distilling between 40 and 60 °C
m	Multiplet
Mb/d	Million barrels per day

MeOH	Methanol
MnP	Manganese Peroxidase
mp	Melting point
MS	Mass spectrometry
Mz	Z average molar mass
m/z	Mass to charge ratio
NAD ⁺	Nicotinamide adenine dinucleotide (oxidised)
NADH	Nicotinamide adenine dinucleotide (reduced)
nm	Nanometres
Pd/C	Palladium on carbon
PCA	Protocatechuic acid
PCD	Protocatechuate 3,4-dioxygenase
q	Quartet
s	Singlet
SDS-PAGE	Sodium dodecyl sulphate polyacrylamide gel electrophoresis
t	Triplet
TLC	Thin layer chromatography
Tris	Tris(hydroxymethyl)aminomethane
VP	Versatile Peroxidase
UV	Ultra-violet
λ	Wave length

List of Figures

- Figure 1: The fractional distillation of crude oil returns a number of different hydrocarbons that modern society has become dependent on.1**
- Figure 2: Simplified schematic representation of the first-generation production of bioethanol3**
- Figure 3: The schematic shows that base catalysed transesterification of triglycerides in oils results in fatty acid methyl esters used to fuel compatible biodiesel engines3**
- Figure 4: Biorefineries would use biological and/or thermochemical routes for the production of second-generation products to be used for transportation fuels, burnt for energy or upgraded to more useful products.4**
- Figure 5: The repetitive β -1,4 glycosidic linkages within cellulose enable the polysaccharide to aggregate into strong, insoluble microfibrills. Branching within starch via α -1,4 and α -1,6-glycosidic bonds disallows this stacking.7**
- Figure 6: The hemicellulose polymer typically consists sugar backbone reinforced with sugar and sugar acid substituents and is cross-linked to itself and the other components of the secondary cell wall with ferulate and diferulate bridges.8**
- Figure 7: This simplified section from a secondary cell wall displays how the aromatic polymer lignin might thicken and strengthen the secondary cell wall by attaching to the cellulose microfibrills by hemicellulosic bridges.9**
- Figure 8: The phenylpropanoids p-coumaryl alcohol, coniferyl alcohol and sinapyl alcohol are respectively responsible for the so-called H, G and S type lignin.10**
- Figure 9: A confocal microscopy image of wheat straw after pre-treatment with the stain phloroglucinol-HCl (used to dye lignified cell walls red) indicates the presence of lignin. The hypothetical chemical structure of a section of lignin indicates how the β -aryl ether, phenylcoumaran, diaryl ether, diaryl propane and biphenyl linkages may be linked together in a 2D fashion. Microscope image obtained with Dr Liz Hardiman**

at the Warwick University Life Sciences Imaging Suite funded by a Wellcome Trust grant.	11
Figure 10: The coupling of two coniferyl alcohol monolignols produces β -aryl ether (β -O-4), phenylcoumaran (β -5), pinoresinol (β - β) or diarylpropane (β -1) dimer outcomes	12
Figure 11: Continuing lignification of the G type lignin results in mainly β -aryl ether, phenylcoumarin, biphenyl and diaryl ether linkages.....	13
Figure 12: The α -aryl ether of a para phenolic unit is cleaved during the kraft process via quinone methide intermediate (4) that can then undergo further degradation with the loss of formaldehyde (CH ₂ O) to form enol ether (5). The hydrosulphide ions generated during the kraft process can also form thiirane intermediate (6) to cleave the β -aryl ether.....	15
Figure 13: The cleavage of a β -aryl ether in non-phenolic units can occur from a nucleophilic attack of an alkoxide ion formed on the neighbouring α -C via the formation of an oxirane intermediate.	16
Figure 14: Cations formed from acid cleaved α -aryl ether units are readily sulphonated during the sulphite pulping process.	17
Figure 15: Heme-peroxidases initiate lignin degradation reactions via the use of radical mediators such as hydrogen peroxide, veratryl alcohol (7) and metal chelates of the oxalate anion (8).	19
Figure 16: After initial oxidation of the native enzyme with hydrogen peroxide to form compound I, a generic mechanism of a heme-peroxidase shows compound I existing as an iron porphyrin radical cation intermediate. This intermediate can then oxidise reducing substrates (RS) such as veratryl alcohol by a one electron steps to give Compound II which again oxidises reducing substrates by a subsequent one electron step returning the enzyme to its resting state. In the manganese peroxidase (MnP) reaction, Mn ²⁺ is oxidized by compounds I and II to generate Mn ³⁺ , which by various means diffuses to the surface to oxidize the lignin structure.	20

Figure 17: The buried heme group of lignin peroxidase (LiP) is accessible through two small channels and cannot directly access the lignin polymer. The slightly larger opening (top) is assumed accessible only by small substrates such as veratryl alcohol. An even smaller channel on the distal side of the protein (bottom) appears to only be suitable for the transport and occupancy of one hydrogen peroxide molecule. PDB ID: 1LLP^[63]21

Figure 18: The Asp-His-Fe triad is a common stabilizer of the heme Fe in peroxidases. PDB ID: 1LLP^[63]22

Figure 19: Cleavage between the α -C and β -C in non-phenolic lignin substructures can proceed after the formation of an aryl cation radical23

Figure 20: The oxidation of the substrate is thought initiated via long-range electron transfer to the Trp171 residue on the protein surface. This residue is conserved in all lignin peroxidases and mutation leads to complete loss of activity. PDB ID: 1LLP^[63] 24

Figure 21: The α -C and β -C bond in non-phenolic lignin structures are cleaved via hydrogen and one electron abstraction.....25

Figure 22: The manganese is coordinated by a Glu-Glu-Asp triad and the propionate of a heme moiety. PDB ID: 1MNP^[80]26

Figure 23: The versatile peroxidase (VP) shares a heme binding site coordinating a Mn^{2+} cation in keeping with MnP and a surface based tryptophan residue as seen in LiP. PDB ID: 2BOQ^[83]27

Figure 24: Fungal laccases contain 4 copper atoms, three of which are orientated in a trinuclear cluster, typical of laccases. PDB ID: 2H5U^[91]28

Figure 25: General laccase mediated oxidation of phenolic compounds results in the concomitant release of two molecules of water29

Figure 26: In the nitrated lignin assay tetranitromethane ($C(NO_2)_4$) is used to nitrate the milled wheat straw lignin. Positive microbial degradation of this substrate releases nitrated aromatic products that cause an increase in absorbance at A_{430}31

Figure 27: An enzymatic reaction with hydrogen peroxide forms compound I with a porphyrin located radical. Reduction of compound II proceeds either via the oxidation of Mn^{II} to Mn^{III} (Pathway A) or direct interaction with a reducing substrate such as the β -aryl ether dimer (Pathway B). Either pathway can create an aryl radical that can undergo non-enzymatic cleavage of the C_{α} - C_{β} bond.^[106]33

Figure 28: *meta* and *ortho* cleavage of catechol.....34

Figure 29: Bacterial β -ketoadipate and α -ketoacid pathways for the substituted catechol protocatechuate. Enzymatic steps are indicated by initials. β -ketoadipate pathway steps: 3,4-PCD protocatechuate 3,4-dioxygenase; CMLE β -carboxymuconate lactonizing enzyme; CMD γ -carboxymuconolactone decarboxylase; ELH enolactone hydrolase; TR β -ketoadipate:succinyl-CoA transferase; TH β -ketoadipyl-CoA thiolase. α -ketoacid pathway steps: P4,5O protocatechuate 4,5-dioxygenase; CHMSDH 4-carboxy-2-hydroxymuconate-6-semialdehyde dehydrogenase; PDCL 2-pyrone-4,6-dicarboxylate lactonase; 4OMH 4-oxalomesaconate hydratase; 4HOAL 4-hydroxy-4methyl-2oxoglutarate aldolase.^[114]35

Figure 30: It is hypothesised that the DypB catalysed degradation of the β -aryl ether component of lignin could release vanillin (11). Vanillin may be further oxidised via a dehydrogenase to vanillic acid (10).37

Figure 31: 5-carboxyvanillic acid (12) could potentially arise from lignin related structure 5,5' -dehydrodivanillate (13) by a demethylation catalysed by LigX, a concomitant ring cleavage by LigZ followed by a C-C hydrolase step (LigY) step of the biphenyl component of lignin. Vanillic acid (10) may also be formed by a decarboxylation of 5-carboxyvanillic acid.....38

Figure 32: A phenylcoumaran model compound is first oxidized in the coumaran ring to give the propiosyringone derivative by the action of a peroxidase.^[71] This may then be followed by a reduction to form the diarylpropane structure. An alternative pathway from the propiosyringone derivative could involve cleavage between C_{α} and

C β to vanillic acid (10). The diarylpropane degradation pathway itself may also proceed via a cleavage between C α and C β by a peroxidase or alternatively via a cleavage of the inter phenyl double bonds of lignostilbene (14) by lignostilbene dioxygenases39

Figure 33: Protocatechuic acid (15), guaiacol (16), syringol (17) and catechol (18)42

Figure 34: Catalytic hydrodeoxygenation of guaiacol (16) found in high percentage in the bio-oil from lignin pyrolysis can proceed via a number demethylated and ring methylated products to form benzene and toluene. This provides a possible route from lignin to the BTX (benzene-toluene-xylene) fraction require for jet fuel.^[137]43

Figure 35: Ether substrates were selectively cleaved in the order of Ar-OAr >> Ar-OMe > ArCH₂-OMe without further hydrogenation and loss of aromaticity when treated with H₂ and a soluble nickel carbene catalyst.^[138]44

Figure 36: Postulated bacterial breakdown pathways of lignin substructures based on metabolites (9, 10, 11 and 12) observed by research within the group highlights the prominent involvement of the vanillic acid pathway. In the pathway, it is suggested vanillin (11) is oxidised by a vanillin dehydrogenase (VDH) to vanillic acid (10), which is further demethylated by either a tetrahydrofolate dependent demethylase (THF-DM) or vanillate mono-oxygenase (VMO) to protocatechuic acid (15) for entry into ring cleavage pathways.....45

Figure 37: Glycosylation of vanillin by nucleotide-sugar dependent glycosyltransferases (UGTs) produces the far less toxic metabolite vanillin β -D-glucoside.....47

Figure 38: Total ion chromatogram by GC/MS with EI ionisation from a sample taken after 6 days from an incubation with *R. jostii* RHA1 and 2.5% w/v wheat straw lignocellulose in LB media (a), the total ion chromatogram of an oxalic acid standard (b) and the mass spectrum fragmentation pattern of the peak that was also consistent with that of the standard (c).....53

Figure 39: A hypothetical pathway for the production of oxalic acid by *R. jostii* RHA1. The breakdown of a β -aryl ether type linkage could release a glycoaldehyde fragment that with subsequent oxidations by aldehyde oxidase (ALOD) could form a route to oxalic acid biosynthesis.....54

Figure 40: Enzymes hypothesised to responsible for the bacterial degradation of vanillin via the vanillic acid catabolic pathway include vanillin aldehyde dehydrogenase (VDH), vanillate monooxygenase (VMO) and 3,4-protocatechuate dioxygenase (3,4-PCD).....55

Figure 41: Oxidation of vanillin to form vanillic acid catalysed by the cysteine residue of a vanillin dehydrogenase with a concomitant reduction of NAD^+ 56

Figure 42: Chemical inhibitors of the catalytic cysteine residues of benzaldehyde dehydrogenases include disulfiram (20) and N-ethylmaleimide (19).....56

Figure 43: The monooxygenase system of vanillate mono-oxygenase contains ferredoxin reductase (VanB) (left) and oxygenase (VanA) (right) components. PDB ID: 3GLO^[168] & PDB ID: 1Q1R^[169]57

Figure 44: VMO catalysed conversion of vanillic acid to protocatechuic acid is initiated by oxygenation from the mononuclear ferrous iron within the oxygenase component.....58

Figure 45: One-carbon movement by the THF-dependent methyltransferases from vanillate to tetrahydrofolate59

Figure 46: An example of the cell growth of *R. jostii* RHA1 wild type and the Δvdh and ΔvanA gene deletion strains grown in growth media P1 with 2.5% lignocellulose (w/v) and 0.1% glucose (w/v) appears to show a pattern of cellular growth in two to three phases, and illustrates a diauxic-type growth curve.61

Figure 47: Detection by GC–MS of aromatic metabolites from cultures of Δvdh mutant RHA045 (top), compared with wild-type strain (bottom), grown on minimal media containing 2.5% wheat straw lignocellulose (w/v) and 0.1% glucose (w/v) in M9 minimal media, after 120 h.63

Figure 48: The protocatechuic acid observed in GC-MS spectra could be formed by the oxidation of 3,4-dihydroxybenzaldehyde formed from a slow enzymatic demethylation of vanillin.....64

Figure 49: EIC for m/z 153.8 corresponding to the positively charged ions of vanillin (RT 15.0 min) from cultures of Δvdh mutant RHA045 (top), compared with control @ $t=72h$ (no bacteria), grown on minimal media containing 2.5% wheat straw lignocellulose (w/v) and 0.1% glucose (w/v) in M9 minimal media. (LC-MS was unable to detect the appearance of any metabolites not in control samples before $t=72 h$).....66

Figure 50: EIC for m/z 124.0 corresponding to the positively charged ions of p-hydroxybenzaldehyde (RT 13.2 mins) from cultures of Δvdh mutant RHA045 (top), compared with control @ $t=72h$ (no bacteria), grown on minimal media containing 2.5% wheat straw lignocellulose (w/v) and 0.1% glucose (w/v) in M9 minimal media. (LC-MS was unable to detect the appearance of any metabolites not in control samples before $t=72 h$).....67

Figure 51: EIC for m/z 165.7 corresponding to the positively charged ions of p-coumaric acid (RT 15.6 mins) from cultures of Δvdh mutant RHA045 (top), compared with control @ $t=72h$ (no bacteria), grown on minimal media containing 2.5% wheat straw lignocellulose (w/v) and 0.1% glucose (w/v) in M9 minimal media. (LC-MS was unable to detect the appearance of any metabolites not in control samples before $t=72 h$).....68

Figure 52: EIC for m/z 195.5 corresponding to the positively charged ions of ferulic acid (RT 17.1 mins) from cultures of Δvdh mutant RHA045 (top), compared with control @ $t=72h$ (no bacteria), grown on minimal media containing 2.5% wheat straw lignocellulose (w/v) and 0.1% glucose (w/v) in M9 minimal media. (LC-MS was unable to detect the appearance of any metabolites not in control samples before $t=72 h$).....69

Figure 53: EIC for m/z 169.7 corresponding to the positively charged ions of vanillic acid (RT 11.1 mins) from cultures of Δvdh mutant RHA045 (top), compared with control @ $t=72h$ (no bacteria), grown on minimal media containing 2.5% wheat straw

lignocellulose (w/v) and 0.1% glucose (w/v) in M9 minimal media. (LC-MS was unable to detect the appearance of any metabolites not in control samples before t=72 h).....70

Figure 54: Concentrations of detected metabolites plotted against growth curve from same experiment.72

Figure 55: A simplified example of how ferulic acid may crosslink the arabinoglucoronoxylan hemicellulose to lignin.....74

Figure 56: Strains of *R. jostii* RHA1 grown on 0.1% ferulic acid and 0.1% glucose in M9 minimal media. Samples taken at 96 h. EIC 169.2 m/z for Δ vanA mutant (blue), Δ vdh mutant (pink) wild type (green) control with no bacteria (orange). The peaks were confirmed as vanillic acid from the EIC of an authentic standard with a retention time of 15.9 min.76

Figure 57: A hydrolysis of the ester linkages in lignocellulose could account for the initial release of the phenylpropanoid units seen after 72 hours. Theoretically this would also be accompanied by the simultaneous release of a lignin fragment77

Figure 58: The β -oxidation pathway for the metabolism of ferulic acid to vanillic acid.78

Figure 59: In this example of a lignin fragment it can be seen how an oxidative cleavage of the α - β carbon bond and the benzylic C-O bond could generate vanillin and ferulic acid linkages in lignocellulose.....79

Figure 60: Concentrations of detected metabolites from incubations with wheat straw alkali lignin plotted against growth curve from same experiment.....80

Figure 61: Cell growth of *R. jostii* wild type and the Δ vdh and Δ vanA strains grown in growth media P1 with 0.5% kraft lignin and 0.1% glucose.82

Figure 63: The enzymes selected for chemical inhibition on the vanillic acid pathway include vanillin aldehyde dehydrogenase (VDH), vanillate monooxygenase (VMO) and 3,4-protocatechuate dioxygenase (3,4-PCD).....86

Figure 64: The oxidation of alcohol to acetaldehyde and then to acetic acid is disrupted by inhibition of aldehyde dehydrogenase (ALDH) and leads to a toxic build-up of the intermediate.....88

Figure 65: Intracellular glutathione reductase (GSR) is thought responsible for the liberation of DDTC which is further metabolised via a thiol methyl transferase (TMT) and then several oxidative transformations to produce a toxic metabolite capable of irreversible carbamylation to the catalytic cysteine residue.^[187]88

Figure 66: Growth of selected bacteria observed at OD600 in incubations with M9 minimal media, 0.1% glucose (w/v) and 100 µM disulfiram90

Figure 67: The base peak chromatogram shows a peak with a retention time of 2.6 min obtained the sample taken at 24 h from the *P. fluorescens* incubation (a) in comparison with that of a control incubation without disulfiram (b) for the same time period. The dominant ions at m/z 120.0 and 134.0 are displayed in the spectrum (c). Incubations were performed in M9 minimal media, 2.5% wheat straw lignocellulose (w/v), 0.1% glucose (w/v) and with or without 100 µM disulfiram.91

Figure 68: HR-MS analysis identified a molecular formula of C₅H₁₂NO.....92

Figure 69: Glycine betaine aldehyde (N,N,N-trimethyl-2-oxoethanaminium) and betaine aldehyde hydrate (2,2 Dihydroxy-N,N,N-trimethylethanaminium) were identified as potential compounds isolated from the intracellular metabolite extraction of *P. fluorescens* from a 24 hour incubation with 2.5% wheat straw lignocellulose (w/v) and 100 µM disulfiram in P1 growth media.92

Figure 70: An EIC chromatogram for m/z 102.1 (m+H)⁺ shows a peak with a retention time of 2.6 min obtained from the sample taken at 24 h from the *P. fluorescens* incubation (a) in comparison with that of an analytical standard (b) confirming the compound to be glycine betaine aldehyde.93

Figure 71: The metabolic pathway of glycine from choline is disrupted after the oxidation of choline by a choline oxidase oxidase (COX).^[192]94

Figure 72: <i>m</i> -Anisic acid (3-methoxy benzoic acid) shown to be degraded via the THF-dependent methyltransferase system in certain bacteria and vanillic acid (4-hydroxy-3-methoxybenzoic acid) thought to be degraded by an oxygenase and reductase system.	97
Figure 73: De Montelano and Komives proposed activation of acetylene to ketene via a hydride shift and concomitant reaction with a nucleophilic active site residue.....	97
Figure 74: Synthesis of 3-(prop-2-ynyl)-4-hydroxybenzoic acid (21) from 3,4-dihydroxybenzoic acid	98
Figure 75: Synthesis of 3-(prop-2-ynyl) benzoic acid (22) from 3,4-dihydroxybenzoic acid	99
Figure 76: Growth curve for <i>P. putida</i> and <i>R. jostii</i> RHA1 in liquid M9 minimal media with 0.1% glucose and 500 μ M of putative inhibitor.	101
Figure 77: Two subfamilies of catechol dioxygenase enzymes exist; the extradiol and intradiol dioxygenases that incorporate molecular oxygen to break open the aromatic ring structure.....	102
Figure 78: Core structure of hydroxamic acid reported as a selective chelator of the ferric Fe^{3+} ion.....	103
Figure 79: Cleavage of β -carotene by β -carotene-15,15'-dioxygenase to retinal	103
Figure 80: The enzyme 2,3-dihydroxyphenyl propionate 1,2-dioxygenase (MhpB) from <i>E. coli</i> catalyses the extradiol cleavage of 2,3-dihydroxyphenyl propionate (DHPP) to give 2-hydroxy-6-oxo-nona-2,4-diene-1,9-dicarboxylate.....	104
Figure 81: SDS-PAGE gel showing the relative abundance of MhpB in each fraction, which showed a main band at ~ 33 kDa ± 3	105
Figure 82: Microtitre plate experiments in which inhibitors at various concentrations slowed or stopped the formation of the yellow coloured MhpB catalysed reaction product over 1 min (A) and 60 min (B). D3, D7 and D8 were highlighted as potentiating a negative effect on enzyme activity.	106
Figure 83: Potential inhibitors D3, D7 and D8.....	107

Figure 84: Inhibition of the MhpB by D8.....	107
Figure 85: Hydroxamic acid D3 proved to be the most effective on enzyme activity with an IC₅₀ value of approximately 110 μM ± 5.....	108
Figure 86: Mutants of E. coli lacking MhpB or MhpC and defective in catabolism of 3-phenylpropionate accumulated colourful substrates when grown in colour enhancing indicator media (CEM).....	109
Figure 87: Accumulation of 2,3-dihydroxyphenyl propionate (in LW 366) or 2-hydroxy-6-oxo-nona-2,4-diene-1,9-dicarboxylic acid (in LW353) in indicator media (CEM) led to the formation of dark red or bright yellow colours respectively.	110
Figure 88: Inoculations in the presence of D3 at final concentrations of 110 μM, 220 μM and 330 μM failed to reproduce the vibrant purple colour expected with inhibition of MhpB and accumulation of DHPP. A darker slight colour change was observed with 220 μM D3 but subsequent analysis did not reveal expected products.	111
Figure 89: Protocatechuate 3,4-dioxygenase (3,4-PCD) catalyses the cleavage of protocatechuic acid (PCA) to produce 3-carboxy-<i>cis,cis</i>-muconate.	112
Figure 90: Using the D13 structure as a scaffold, (23), (24) and (25) were synthesised.	115
Figure 91: Synthesis of 3,4 dimethoxy-cinnamohydroxamic acid from 3,4 dimethoxycinnamic acid.....	116
Figure 92: Reduction of substituted cinnamohydroxamic acids.	116
Figure 93: The IC₅₀ of 3,4-methoxyphenyl propiohydroxamic acid (24) was obtained by plotting the data as % inhibition as a function of inhibitor concentration	117
Figure 94: The IC₅₀ of 3,4-dimethoxyphenyl propiohydroxamic acid (25) was obtained by plotting the data as % inhibition as a function of inhibitor concentration.	118
Figure 95: The IC₅₀ of 3,4 dimethoxy cinnamohydroxamic acid (23) was obtained by plotting the data as % inhibition as a function of inhibitor concentration.	118

Figure 96: The IC₅₀ of 4-methoxycinnamohydroxamic acid (D13) was obtained by plotting the data as % inhibition as a function of inhibitor concentration.119

Figure 97: Logarithmic growth curve showing the effects of 3,4-dimethoxycinnamohydroxamic acid (23) and 4-methoxycinnamohydroxamic acid (D13) on *R. jostii* RHA1. Bacteria grown with 0.4% glucose (w/v) were exposed to inhibitors at a concentration of 50 μM for up to 46 h. Controls without inhibitor and without additional PCA carbon source were also monitored. Each data point is an average of three samples counted from the same time point.....120

Figure 98: Proposed mechanism of the hydrolysis of a hydroxamic acid structure by a serine protease to release the bacteria toxin hydroxylamine (NH₂OH).....121

Figure 99: An EIC for *m/z* 153.12 shows a peak with a retention time of 15.6 min obtained in the sample taken at 96 h from the *R. jostii* RHA1 incubation (a). The small peak was first observed in the UV chromatogram @ 280 nm and not present in controls. The dominant ions at *m/z* 153.3 correspond to the expected [M-H]⁻ ion (c). Incubations were performed in P1 media, 10 mM ferulic acid and 0.1% glucose (w/v) with inhibitor (23) introduced after 16 h (final concentration 50 μM).122

Figure 100: The bacterial *ortho* and *meta* catechol cleavage routes offer an opportunity to combine chemical and genetic pathway manipulation to afford useful agrochemical such as 1,3-pyridinecarboxylate.127

List of Tables

Table 1: Current value of identified potential lignin breakdown products. (Prices obtained from Borregaard Ingredients, ICIS Pricing and Rhodia Group. Correct as of 12/09/13).....	41
Table 2: The highest concentrations of detected metabolites found during an experiment are displayed. The metabolites were identified using LC-MS and their concentrations determined by plotting calibration curves (mg/L).....	71
Table 3: The percentage decrease in specific activity for the 11 hydroxamic acid based ‘D-Series’ at 200 μM concentration that tested positive in the plate reader screening assay	114
Table 4: Concentrations of PCA from the intracellular extractions obtained from incubations of <i>R. jostii</i> RHA1 with 10 mM ferulic acid in P1 media (inhibitor (23) concentration 50 μM) by application of the Beer-Lambert law. The molar absorption coefficient value used for protocatechuate was 3800 $M^{-1} cm^{-1}$ @290 nm (pH7.5) in a 1 cm path length quartz cuvette. Absorbance values are the average of triplicate reads	123

1: Introduction

Fractional distillation of crude oil provides a vast number of different hydrocarbons used not only as transportation fuels and energy, but precursors for everyday products, such as plastics and pharmaceuticals (Figure 1). Crude oil is not only a finite resource, but also the gases emitted in its extraction and uses are responsible for a rapidly changing world climate that has far-reaching and devastating social and economic trends.

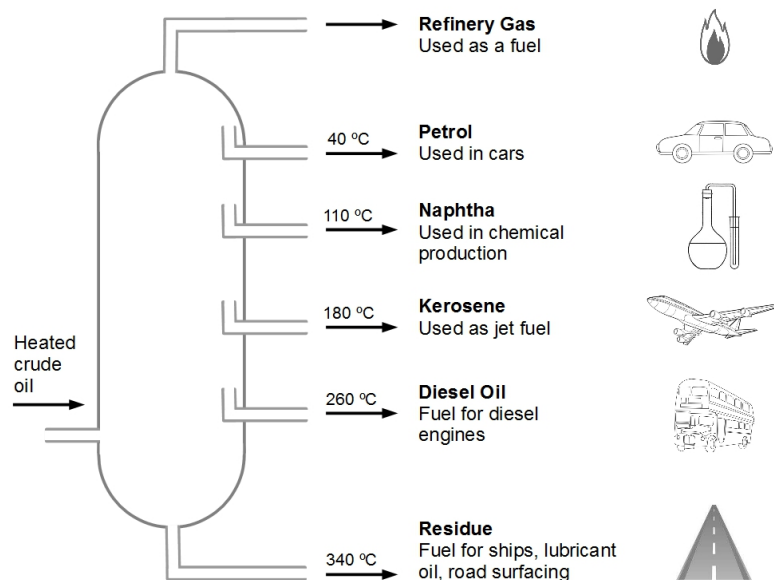


Figure 1: The fractional distillation of crude oil returns a number of different hydrocarbons that modern society has become dependent on.

The latest International Energy Agency (IEA) report predicts that global demand for crude oil will be 92.6 million barrels per day (Mb/d) in 2014 growing to 101 Mb/d in 2035.^[1] With 1668.9 billion in proven reserves, at current use without further increases or decreases to these reserves there is only enough oil to last for approximately 50 years.^[2]

Although reliance on oil as a source of energy can theoretically be mitigated by further investment into existing alternative methods such as shale gas, solar, wind and nuclear, cleaner, greener options to replace crude oil as a reliable source of fuel and petrochemicals are few and far between. Technologies using renewable biological resources (biofuels) as an alternative need to be developed further.

1.1 A bio-based economy

Biofuels represent a significant potential as an alternative to crude oil because they can be generated from renewable and locally available agricultural material. First-generation biofuels such as bioethanol and biodiesel are recovered from a biomass that is usually edible such as corn, sugarcane or barley. The recovered products are then generally blended into motor fuels at levels between 10 to 25% (v/v).^[3]

Bioethanol production happens mainly in larger countries, specifically the United States and Brazil, resulting from the enzymatic fermentation of the C₆ sugars (mainly glucose) of the biomass by strains of yeast. Brazil is currently the leading producer of bioethanol and processing plants in the country achieve concentrations of 8–11% (v/v) after fermentation of liquefied sugarcane with industrial strains of *Saccharomyces cerevisiae*.^[4] As sugarcane only grows in tropical and temperate climates, the other major producer of bioethanol, the USA, ferments milled corn grain and achieves similar yields.^[5] This process requires an extra step in which the corn kernel is mixed with amylase enzymes to release the fermentable sugars from the starch polysaccharide (Figure 2).^[6]

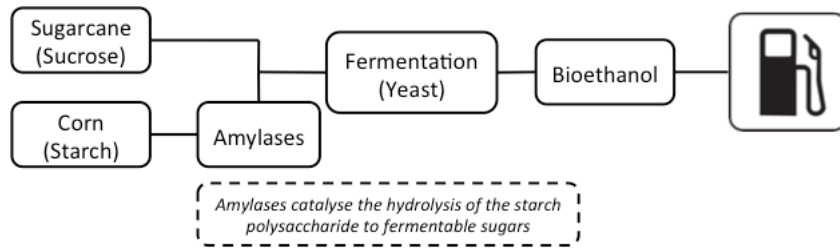


Figure 2: Simplified schematic representation of the first-generation production of bioethanol

Biodiesel is the other main first-generation biofuel and is produced mainly using base catalysed transesterification of the triglycerides of vegetable oil and animal fats in the presence of methanol (Figure 3). Readily grown across the EU, the rapeseed plant *Brassica napus* is already cultivated for human and animal consumption due its high oil content and is therefore the major crop used in biodiesel production.^[7]

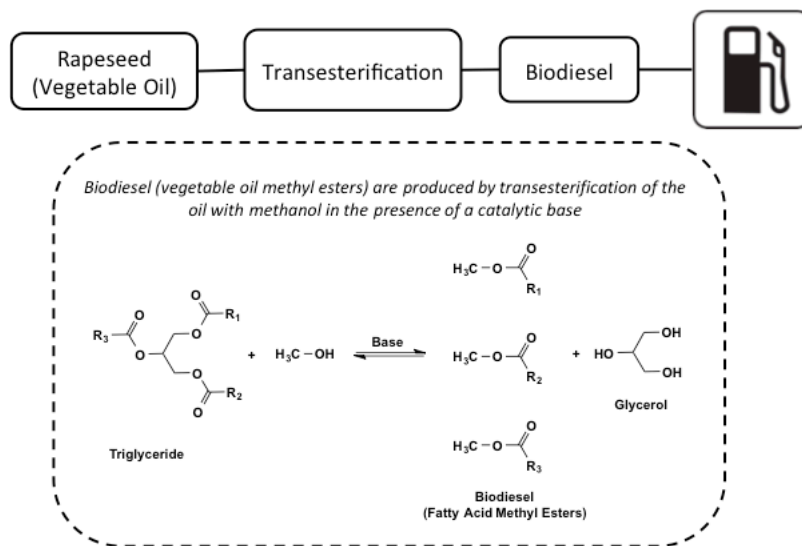


Figure 3: The schematic shows that base catalysed transesterification of triglycerides in oils results in fatty acid methyl esters used to fuel compatible biodiesel engines

The use of *B. napus* in biodiesel production highlights the major obstacle facing first-generation biofuels in that it diverts crops away from the global food market. This leads to a shortage of the crop available for food and an increase in crop prices. First-generation biofuel production is also noteworthy for a number of other socioeconomic and environmental issues including the effects on greenhouse gas

emissions by large scale deforestation, atmospheric pollution and extensive water consumption.^[5]

To overcome these issues arising from the production of first-generation biofuels, a wider array of different non-edible feedstocks, especially agricultural lignocellulosic and domestic waste is used. This biomass is generally more complex to convert and the products produced from these feedstocks are defined as second-generation. A hypothetical “biorefinery” would employ a number of processes to deconstruct this waste into useful products, categorised into either “thermochemical” or “bio” pathways.^[8]

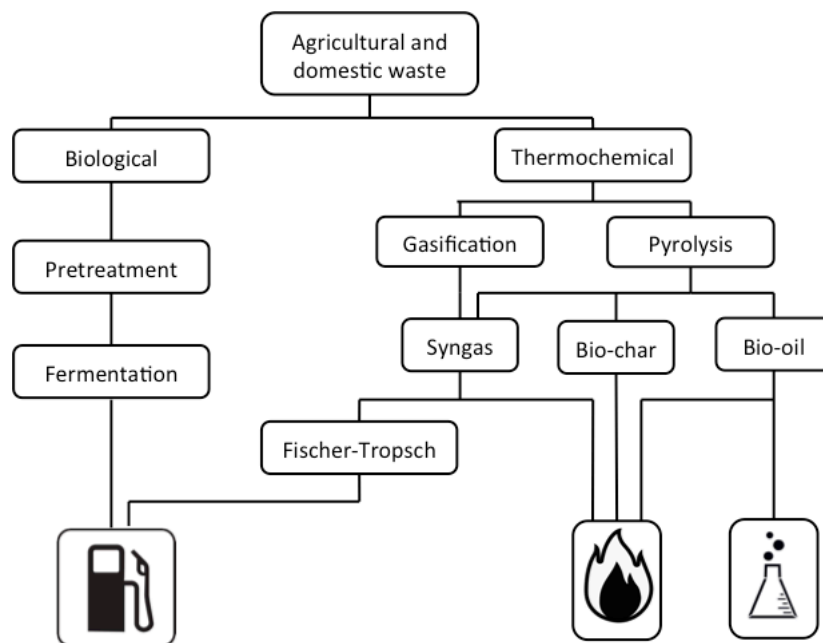


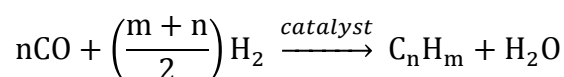
Figure 4: Biorefineries would use biological and/or thermochemical routes for the production of second-generation products to be used for transportation fuels, burnt for energy or upgraded to more useful products.

The biological route involves the enzymatic fermentation of extractable C₅ and C₆ sugars and their subsequent fermentation to bioethanol. The residue left can be fractionated into a high-protein animal feed and fractions to be burned as fuel.^[9] The

thermochemical approach consists mainly, but not limited to, pyrolysis and gasification techniques. Gasification uses a combination of high heat, pressure and a limited amount of oxygen to convert the biomass into combustible gases carbon monoxide (CO), methane (CH₄) hydrogen (H₂), nitrogen (N₂) and carbon dioxide (CO₂). These gases are collectively referred to as synthesis gas or syngas and can be used directly as fuel.^[6] Pyrolytic “cracking” of lignocellulose involves the deconstruction of biomass in the absence of oxygen at various temperatures and speeds, with and without the presence of chemical catalysts to yield a solid charcoal-like residue (bio-char), a mixture of oxygenated hydrocarbons (bio-oil) and a mixture of non-condensable gases (syn gas).^{[10], [11]}

Although pyrolysis produces a large amount of bio-oils □60-95% (w/w),^[12] direct use as a fuel is limited by its properties. Bio-oils have been shown to contain a mixture of phenolics, carboxylic acids, ketones, aldehydes (lignin fragments and residue hemicellulosic sugar units are also present).^{[12], [13]} Bio-oils are immiscible with other hydrocarbons and have a number of factors reducing their suitability such as high viscosity and oxygen content. The bio-oil obtained from pyrolysis can be catalytically upgraded to more useful products, with China at the forefront of this technology,^[14] but it is still prohibitively expensive to be of any real commercial value.^[15]

The syngas obtained from thermochemical processes can be converted to green biodiesel via Fischer-Tropsch catalysis in which the CO and H₂ components react over a transition metal catalyst to form hydrocarbon building blocks following the equation:



The major limitations of the Fischer-Tropsch process are not only financial, due to the control of the highly exothermic reaction but selectivity for CO and H₂ over the other gases present in syngas.^[16] The use of zeolites and aluminium based adsorbents for efficient gas separation has enabled some progress to making this an economically viable process as recently optimised by Perez-Carbajo *et al* (2014).^[17]

A bio-based economy based on the conversion of agricultural waste products into higher value products has proved extremely difficult to realise, mainly due to the difficulties arising from the inherent strong resistance of lignocellulose to enzymatic and chemical breakdown treatments.

1.2 Lignocellulose

Members of the plant kingdom share an enormous amount of characteristics that can be assumed responsible for their longevity and success. Many have developed ways to ensure resistance to harsh environmental conditions, complex water and nutrient transport systems along with varying degrees of protection from microbial attack. Primarily, it is the differing composition of the cell walls of plants that confer these abilities and provides understanding to the difficulties faced by biorefineries in breaking down lignocellulosic plant matter (biomass).

It should be remembered that plant cell walls are multifaceted and diverse with varying configurations that result in complex compositions even within members of the same species. However, to simplify our understanding we can divide them into primary and secondary walls. Primary cell walls surround a developing cell and consist mainly of cellulose and hemicellulose polysaccharides encapsulating the starch stores a plant requires to grow. Secondary cell walls are found within more specialised cells that have stopped growing such as those used for vascular purposes

and although similar structures, they are thickened by a lignin matrix.^[18] Lignocellulosic biomass can be seen as the non-starch based fibrous material.

Although starch and cellulose are both polysaccharides of glucose, distinctions in the glycosidic linkages between the monomeric glucose units gives rise to their different properties. The glucose in starch are linked mainly via α -1,4-glycosidic bonds with branched α -1,6 bonds present in very small amounts. These types of linkages confer a degree of branching making aggregation difficult and as a consequence enables starch to be soluble and easy to digest/ferment. Unlike starch, cellulose is formed via β -1,4 glycosidic bonds forming long, straight chains that stack via hydrogen bonding into strong insoluble microfibrils.

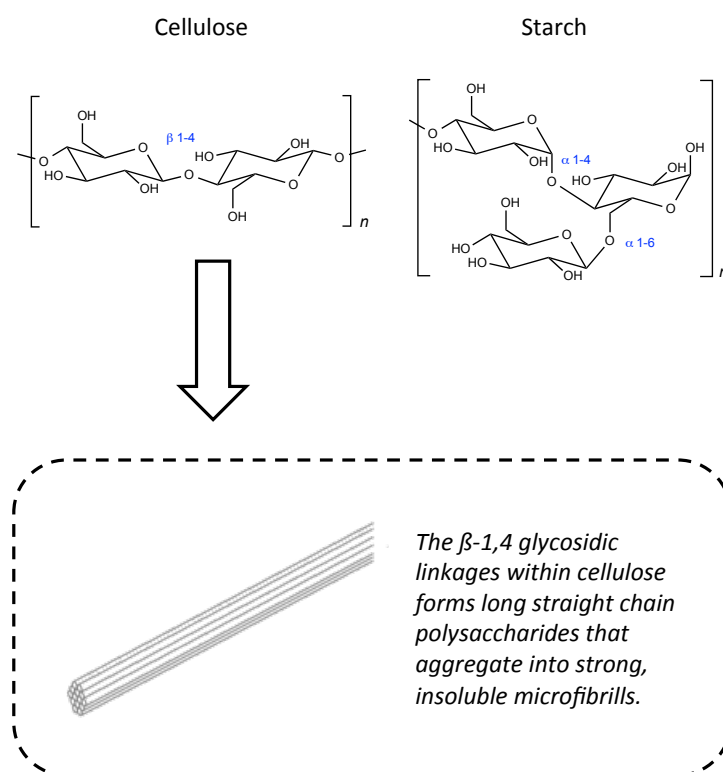


Figure 5: The repetitive β -1,4 glycosidic linkages within cellulose enable the polysaccharide to aggregate into strong, insoluble microfibrils. Branching within starch via α -1,4 and α -1,6-glycosidic bonds disallows this stacking.

Cellulose is the most abundant component of lignocellulose representing over 50% of all woody biomass.^[19]

Another part of lignocellulose is the hemicellulosic component. In contrast to cellulose, the hemicelluloses are polymers that are made up of differing sugar residues including five carbon sugar pentoses (arabinose and xylose) and six carbon sugar hexoses (glucose, galactose, mannose). Typically, the hemicelluloses consist of a xylan (xylose, arabinose and glucuronic acid) backbone substituted with sugar and sugar acid side chains. These glycans are then highly cross-linked to each other and the other components of the cell wall with ferulic acid and diferulate bridges reinforcing the robust secondary cell wall (Figure 6).

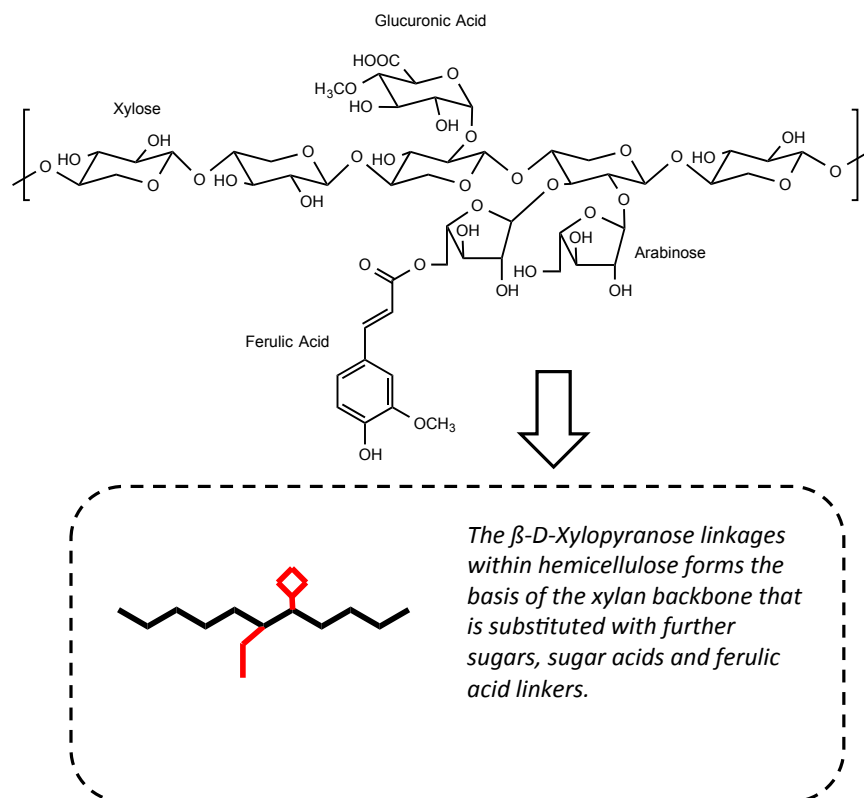


Figure 6: The hemicellulose polymer typically consists sugar backbone reinforced with sugar and sugar acid substituents and is cross-linked to itself and the other components of the secondary cell wall with ferulate and diferulate bridges.

Although cellulose and hemicellulose give a degree of structure and rigidity to the plant, one of the most outstanding features of the secondary plant cell wall however is lignin. Through evolution, the hardier plants have enabled a way to indurate and thicken their cell walls by constructing a complex matrix by using just a few primary phenylpropanoid monomers derived from the plant shikimate pathway.

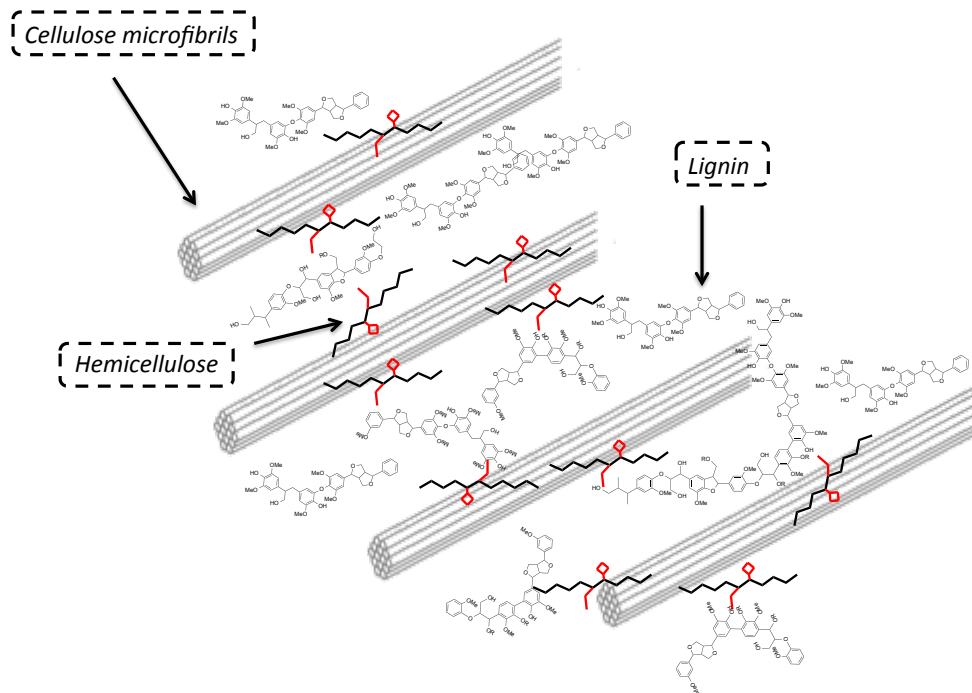


Figure 7: This simplified section from a secondary cell wall displays how the aromatic polymer lignin might thicken and strengthen the secondary cell wall by attaching to the cellulose microfibrills by hemicellulosic bridges.

Making up over 30% of all woody biomass, this phenolic biopolymer lignin is the most abundant aromatic material on Earth.^[20]

1.2.1 Lignin biosynthesis

The content and structure of the lignified cell wall varies between different species of plant, with the exact biosynthetic and degradation pathways still unresolved and under

debate.^[21] It is generally believed that primarily, lignin is formed from the phenylpropanoids *p*-coumaryl alcohol (1), coniferyl alcohol (2) and sinapyl alcohol (3) and that these units, known as monolignols, are linked together by radical-radical coupling reactions (Figure 8).^{[22], [23]}

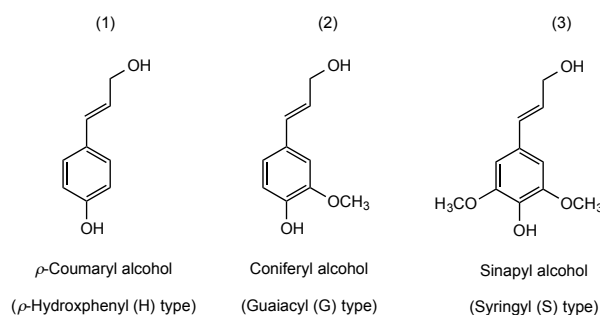


Figure 8: The phenylpropanoids *p*-coumaryl alcohol, coniferyl alcohol and sinapyl alcohol are respectively responsible for the so-called H, G and S type lignin.

The first step in the polymerisation of these monolignols involves an initial enzymatic dehydrogenation reaction by a peroxidase or laccase. These oxidative enzymes catalyse the formation of radicals and lead to a dimerisation of two individual units or the addition of one unit to a growing polymeric lignin chain in a process known as lignification. This process continues to produce a polydisperse complex structure that can then be characterised by the number of guaiacyl (G), syringyl (S) and *p*-hydroxyphenyl (H) units derived from the three main monolignols.

Grasses, including cereal crop varieties, have a mixture of G and H, the hardwood trees and some palms have G and S units, while softwoods have mostly G units.^[24]

The inter-unit linkages between these G, S and H sub-components of lignin form further identifiable subdivisions and include β -aryl ether (β -O-4), phenylcoumaran (β -5), pinoresinol (β - β), biphenyl (5-5) and diphenyl ether (4-O-5) substructures.

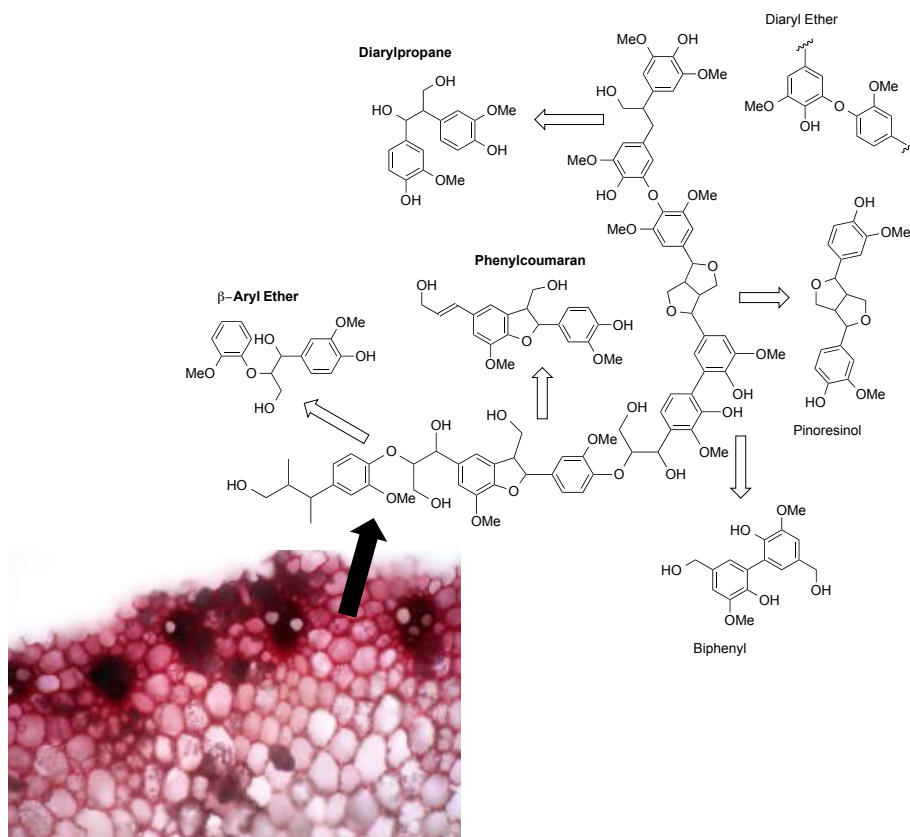


Figure 9: A confocal microscopy image of wheat straw after pre-treatment with the stain phloroglucinol-HCl (used to dye lignified cell walls red) indicates the presence of lignin. The hypothetical chemical structure of a section of lignin indicates how the β -aryl ether, phenylcoumaran, diaryl ether, diaryl propane and biphenyl linkages may be linked together in a 2D fashion. Microscope image obtained with Dr Liz Hardiman at the Warwick University Life Sciences Imaging Suite funded by a Wellcome Trust grant.

Dimerisation of two G units almost always result in a dimer where one unit is coupled at its β position. This produces the β -aryl ether (β -O-4), phenylcoumaran (β -5), pinoresinol (β - β) or diarylpropane (β -1) dimer outcomes (Figure 10).^[25]

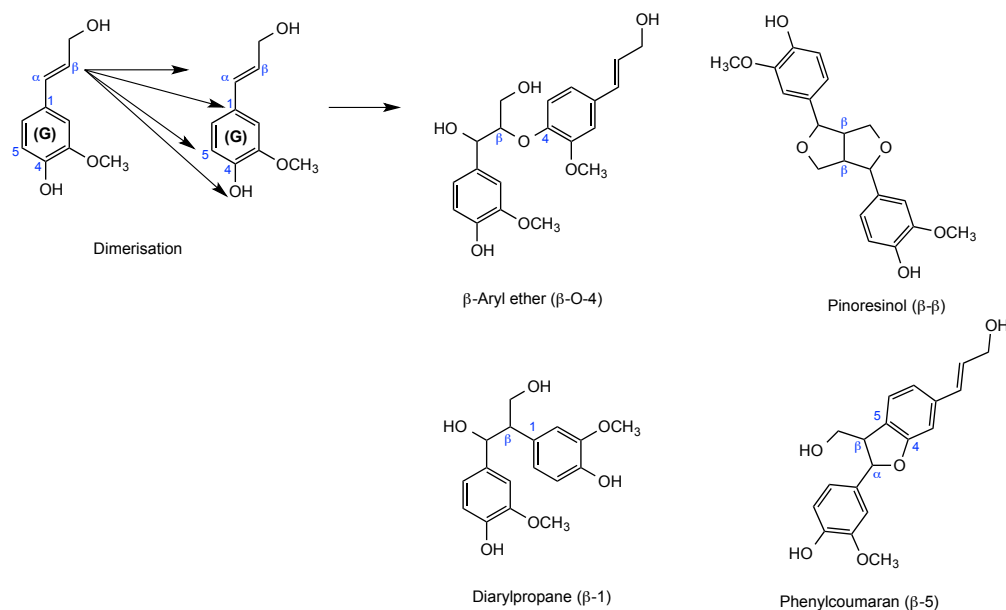


Figure 10: The coupling of two coniferyl alcohol monolignols produces β -aryl ether (β -O-4), phenylcoumaran (β -5), pinoresinol (β - β) or diarylpropane (β -1) dimer outcomes

The addition of a coniferyl alcohol monolignol to a G unit in lignification again joins from its β position to the developing lignin frame resulting in mainly β -aryl ether (β -O-4) and phenylcoumaran (β -5) linkages. The biphenyl (5-5) and diphenyl ether (4-O-5) substructures are generally formed as a consequence of the radical-radical coupling of two G units within the same or from different growing lignin matrices (Figure 11).^{[26]–[29]}

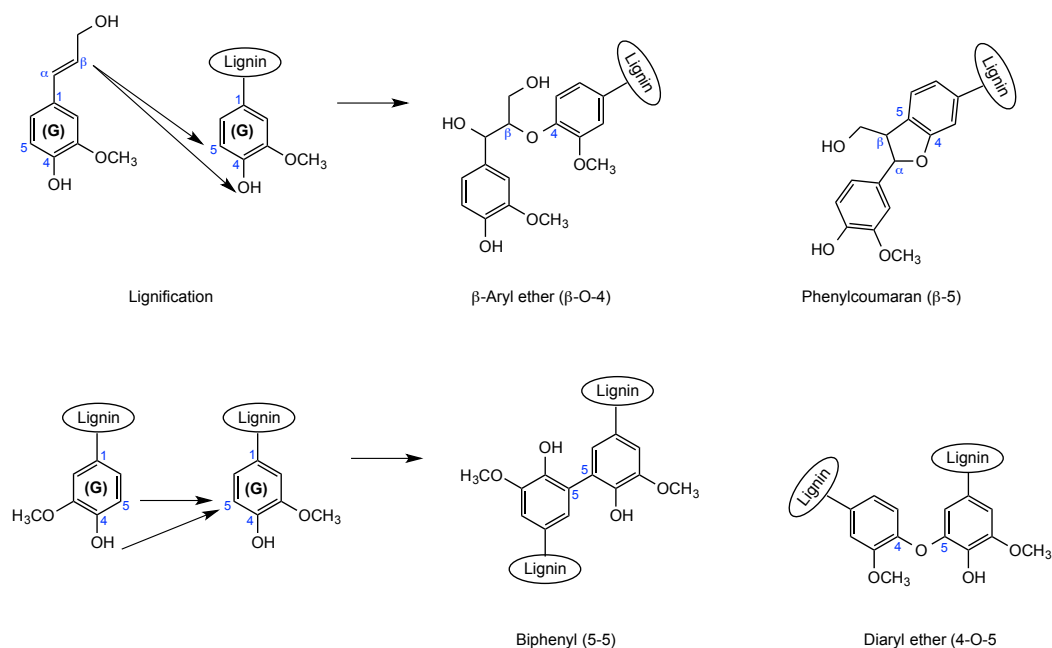


Figure 11: Continuing lignification of the G type lignin results in mainly β -aryl ether, phenylcoumarin, biphenyl and diaryl ether linkages.

Outcomes from reactions involving tri-substituted sinapyl alcohols are far more restricted than coniferyl alcohol. It is suggested in these instances that *p*-coumaryl alcohol acts as the intermediate oxidized by a plant peroxidase or laccase and then transfers its radical to sinapyl alcohol.^[30] A dimerisation produces only β -aryl ether (β -O-4) and pinoresinol (β - β) units and lignification of either coniferyl or sinapyl alcohol to an S unit results solely in β -aryl ether (β -O-4) linkages.

Reactions connecting the *p*-coumaryl alcohols are similar to those of coniferyl alcohols but are said not to occur until stores of sinapyl alcohol have been exhausted.

It can be seen from this brief outline why the β -aryl ether (β -O-4) unit is the most common found within lignin from across all species of plants, accounting for 45–50% of linkages in softwoods and 60% in hardwoods.^{[26], [31]}

Whilst cellulose and hemicellulose can be converted to C₆ and C₅ sugars for fermentation, lignin is currently intractable but provides a potential source of aromatic chemicals

1.3 Commercial sources of lignin

Although lignocellulosic biomass delivers an abundant source of raw material, industrial processes for isolating the cellulosic and hemicellulosic components from the lignin are often expensive and energy intensive.

As a by-product of the pulp and paper industry for example, unwanted lignin has historically been solubilised in either a sulphite or sulphate process and results in various types of the polymer with different characteristics than the natural-state lignin. Understanding the nature and structure of these waste products is key to identifying the potential aromatic chemicals that may be extracted.

1.3.1 Kraft lignin

Most widely used of these chemical techniques is the sulphate (kraft) process in which sodium hydroxide and sodium sulphide (Na₂S) are cooked with the wood at elevated temperatures, generally in the range of 160 to 190°C.^[32]

The predominant lignin degradation reactions that occur during the kraft pulping are cleavage of α -aryl ether and β -aryl ether bonds. However, the reactivity of such linkages is dependent on the free phenolic group present. If the free phenolic group is at the *para* position relative to an α -aryl ether unit, then the linkage is readily cleaved via a highly reactive quinone methide intermediate (4). Quinone methide (4) can also undergo further degradation with the loss of formaldehyde (CH₂O) to form enol ether (5). It has also been observed in the kraft process that generated hydrosulphide ions

are nucleophilic enough to restore the aromaticity to the ring to form thiirane intermediate (6) cleaving the β -aryl ether unit in the process (Figure 12). Any etherified non-phenolic α -aryl ether linkages are stable and do not react.^[33]

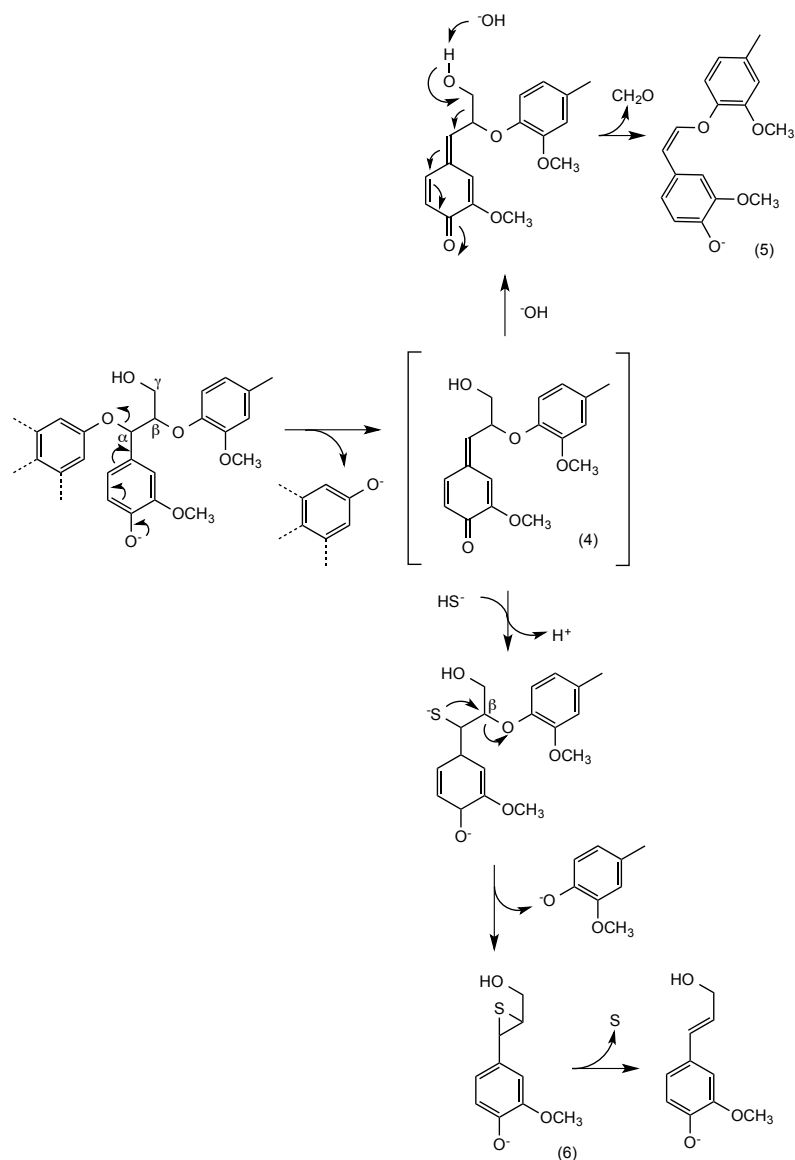


Figure 12: The α -aryl ether of a para phenolic unit is cleaved during the kraft process via quinone methide intermediate (4) that can then undergo further degradation with the loss of formaldehyde (CH_2O) to form enol ether (5). The hydrosulphide ions generated during the kraft process can also form thiirane intermediate (6) to cleave the β -aryl ether.

The cleavage of non-phenolic aryl ether structures happens less frequently and is resultant from the formation of an alkoxide anion on the α - or γ -carbon. The

nucleophilic attack from this neighbouring alkoxide can result in the elimination of the β -aryl ether via an oxirane intermediate (Figure 13).

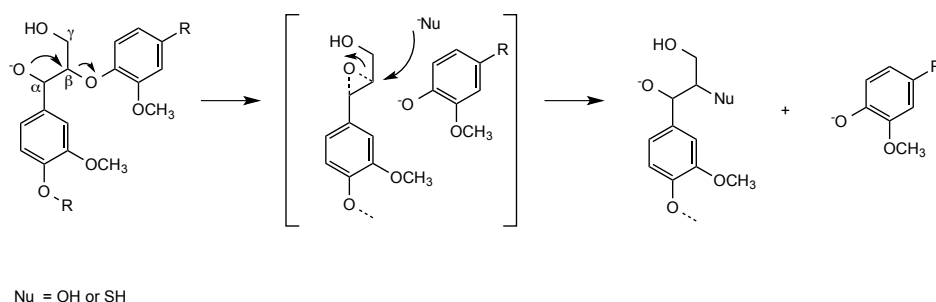


Figure 13: The cleavage of a β -aryl ether in non-phenolic units can occur from a nucleophilic attack of an alkoxide ion formed on the neighbouring α -C via the formation of an oxirane intermediate.

These reactions also form a number of electrophilic and nucleophilic intermediates and leaving groups that not only result in the discussed cleavage of aryl ethers, but also participate in competing condensation reactions with each other. The resultant condensed form of lignin that is produced from the kraft process is suggested to be even more resistant to microbial degradation. [34]–[36]

1.3.2 Sulphite pulping

The sulphite process is the second most common technique used by the paper and pulping industry, although is less favoured due to the acidic nature of the process hydrolysing some of the cellulose resulting in a weaker end use fibre. The methods can vary due to end use but primarily revolve around a complex use of sulphur dioxide (SO_2) in aqueous solution (H_2SO_3) in the presence of alkali at temperatures ranging from 130 to 160°C. The combination of released H_2SO_3 , bisulphites (HSO_3^-), monosulphites (SO_3^{2-}) and counter ion from the base used (calcium, magnesium, ammonium or potassium) all have an effect on the pH level (between pH 1.5 and 5). [37]

Lignin is made water soluble in the sulphite pulping process by the introduction of sulphonate groups to cations formed by acid cleaved α -aryl ethers (Figure 14).

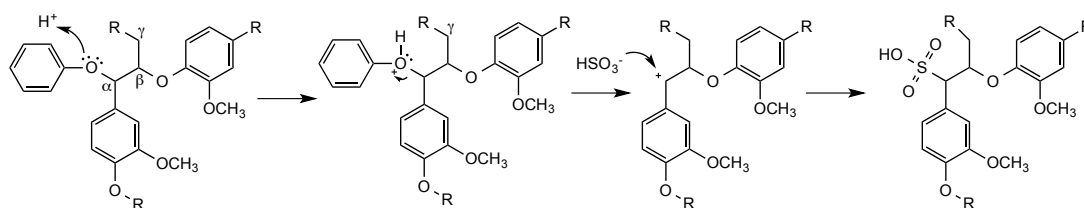


Figure 14: Cations formed from acid cleaved α -aryl ether units are readily sulphonated during the sulphite pulping process.

This selective cleavage also ensures most of the recovered solubilised lignin fragments remain largely intact and these so-called lignosulphonates retain unique properties that make them useful for dispersants, plasticisers and binders.^{[38]–[40]} The process is less favoured by the pulping industry however, as some of the acid-sensitive glycosidic bonds in cellulose are cleaved resulting in weaker fibres for making paper.^[41]

1.3.3 Organosolv lignin

Preferred for environmental factors such as solvent recycling and absence of sulphur, a refined form of lignin can also be produced from lignocellulose by the Organosolv process. Unlike the lignin recovered from sulphite and sulphate processes, organosolv lignin retains a high proportion of the acid-sensitive -O-4 (aryl ether) linkages found in native lignin.^[42] Organosolv pulping involves heating the lignocellulosic feedstock in an aqueous organic solvent, such as ethanol, at temperatures ranging from 180-220°C. Although temperatures under 190°C still require an acid catalyst, effective hydrolysis of esters can be achieved at higher temperatures due to the acidic nature of superheated water.^[43] The resulting hydrolytic cleavage of the ester linkages between hemicellulose and lignin and between hemicellulose and cellulose lignin

achieves almost complete separation of the different components into the solvent system.^[44]

At present most of the lignin recovered by these techniques is burned for heat generation, but if it could be converted into commodity and high-value chemicals, this would be a more profitable and more sustainable use of this abundant bio-material.

With advances in protein engineering in the 80's, the potential for an efficient and more controlled enzymatic lignin removal process for the paper and pulp industry was heavily investigated.^[45] These methods could not only be used to separate the lignin from the hemicellulose and cellulose components but may also influence any potential range of substances, materials and products obtainable from the recovered lignin.

1.4 Enzymatic breakdown of lignin

The microbial breakdown of lignocellulose to carbon dioxide, organic acids, methane and water is clearly an important and vital part of recycling the carbon on Earth. What is apparent is that organisms involved in this activity must be equipped with a suite of cellulases, hemicellulases and ligninases capable of cleaving the C-C and C-O bonds of the various linkages within the secondary cell wall.

Kirk and Yang reported for the first time delignification of unbleached Kraft pulp by the white-rot basidiomycete *Phanerochaete chrysosporium* in 1979. Shortly after in 1982, the discovery of the first ligninase from *P. chrysosporium* was confirmed by Tien and Kirk^[46] and throughout the 80's and early 90's a number of lignolytic enzymes from white and brown-rot fungi were identified.^{[31], [47]–[50]}

The basidiomycetes have since then been highlighted as the main decomposers of lignin containing biomass and are classified into white- and brown-rot fungi, due to

the decolourisation of the woody material by their primary enzymatic activities. The term white-rot fungus is coined due to the lignin and hemicellulose being removed in the early stages leaving the white fibrous cellulose. Brown-rot fungi on the other hand target cellulose and hemicellulosic carbohydrates leaving the brown lignin.^[25]

The main fungal ligninases have since been mainly classified as heme-peroxidases, such as lignin peroxidase (LiP), manganese peroxidase (MnP) and versatile peroxidase (VP) or copper-containing phenol oxidases (laccase).^{[51]–[57]}

Lignin-modifying heme-peroxidases are oxidative systems capable of performing one-electron reaction steps creating cation radicals that attack the C-C and C-O bonds. These lignolytic enzymes are believed too large to diffuse through secondary wood cell walls and degradation is effectuated by low-molecular mass radical mediators such as hydrogen peroxide, veratryl alcohol (7) and oxalate chelates (8).^{[58]–[63]}

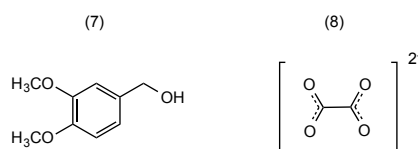


Figure 15: Heme-peroxidases initiate lignin degradation reactions via the use of radical mediators such as hydrogen peroxide, veratryl alcohol (7) and metal chelates of the oxalate anion (8).

The general mechanism of these peroxidase enzymes follows a reaction where one equivalent of H_2O_2 (or organic peroxide) reacts to give a porphyrin cation radical containing Fe(IV). This compound then oxidises a substrate to give a radical mediator that enables oxidation of the aromatic rings found within the lignin structure. A subsequent one-electron step oxidises a further reducing substrate returning the enzyme to its resting state (Figure 16).

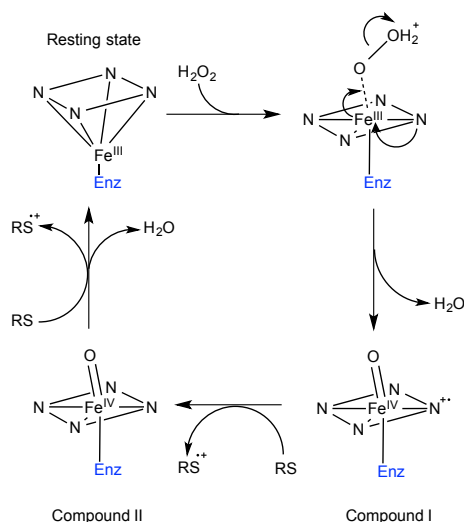


Figure 16: After initial oxidation of the native enzyme with hydrogen peroxide to form compound I, a generic mechanism of a heme-peroxidase shows compound I existing as an iron porphyrin radical cation intermediate. This intermediate can then oxidise reducing substrates (RS) such as veratryl alcohol by a one electron steps to give Compound II which again oxidises reducing substrates by a subsequent one electron step returning the enzyme to its resting state. In the manganese peroxidase (MnP) reaction, Mn^{2+} is oxidized by compounds I and II to generate Mn^{3+} , which by various means diffuses to the surface to oxidize the lignin structure.

1.4.1 Lignin Peroxidase (LiP)

LiPs are hydrogen peroxide (H_2O_2) dependent glycoproteins that catalyse the oxidative depolymerisation lignin and have a wide range of phenolic and non-phenolic substrates.^[64]

After the first LiP had been crystallised, it became apparent that the buried heme group was not capable of directly accessing the lignin polymer.^[65]

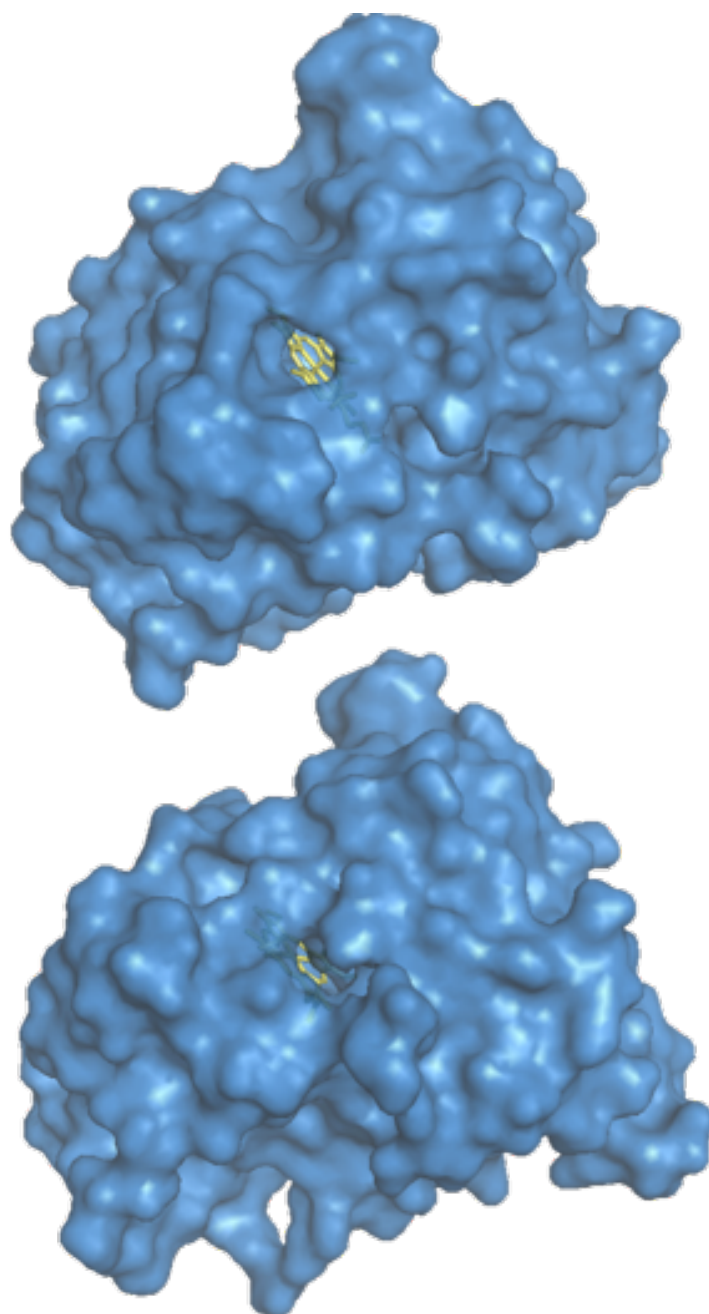


Figure 17: The buried heme group of lignin peroxidase (LiP) is accessible through two small channels and cannot directly access the lignin polymer. The slightly larger opening (top) is assumed accessible only by small substrates such as veratryl alcohol. An even smaller channel on the distal side of the protein (bottom) appears to only be suitable for the transport and occupancy of one hydrogen peroxide molecule. PDB ID: 1LLP^[63]

Accessible through two small channels from the outer surface, it was surmised that one very small channel led to a peroxide-binding pocket and the other slightly larger channel from the exterior of the protein led to a proximal heme-binding pocket (visible in Figure 17). This heme binding pocket in which an Asp-His-Fe triad stabilises the Fe(IV)-O intermediate of compound I is also conserved in other peroxidases (Figure 18).^[66]

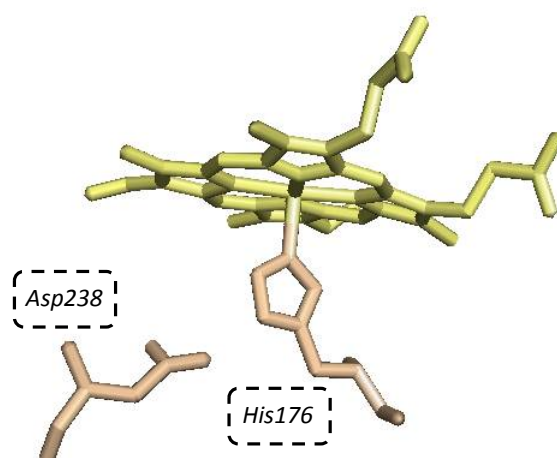


Figure 18: The Asp-His-Fe triad is a common stabilizer of the heme Fe in peroxidases. PDB ID: 1LLP^[63]

Early work assumed LiP mediated the oxidation of intermediate radicals such as veratryl alcohol that diffused to the enzyme surface and initiated a non-enzymatic deconstruction of the lignin polymer. The predominant suggested mechanism for this is via the formation of an aryl cation radical that results in a cleavage between the α - β carbons (Figure 19).^{[67], [68]} Mechanisms for cleavage of aryl ether side chains or ring opening have also been proposed.^{[69]-[71]}

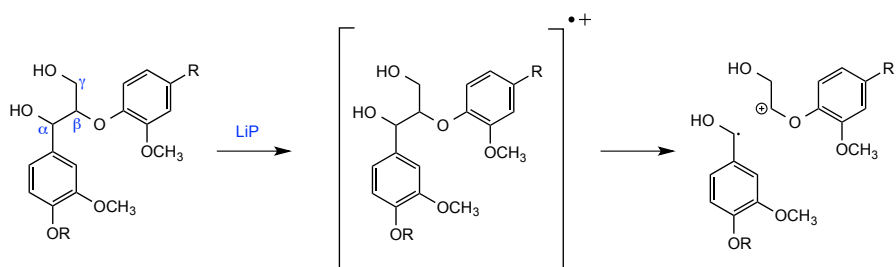


Figure 19: Cleavage between the α -C and β -C in non-phenolic lignin substructures can proceed after the formation of an aryl cation radical

Further analysis of the crystal structures suggested however, that the opening of the active site channel was far too small for reducing substrates and current evidence has since pointed to the substrate being oxidized via a long-range electron transfer mechanism, likely mediated by a conserved Trp171 residue on the enzyme surface.^[63]
^[72] Site-directed mutagenesis of the Trp171 residue has led to complete loss of activity when replaced with phenylalanine, reinforcing the evidence for Trp171 being involved in the binding and oxidation of intermediate radicals.^[73]

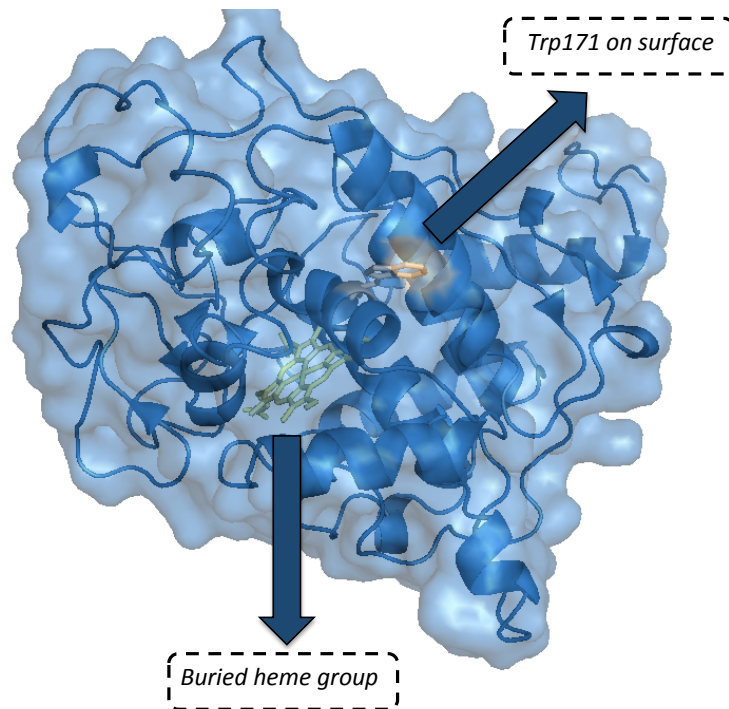


Figure 20: The oxidation of the substrate is thought initiated via long-range electron transfer to the Trp171 residue on the protein surface. This residue is conserved in all lignin peroxidases and mutation leads to complete loss of activity. PDB ID: 1LLP^[63]

Although a LiP has been reportedly identified in brown-rot fungi *Polyporus ostreiformi*,^[74] there are far many more in white-rot fungi, with at least ten isozymes found in the most studied basidiomycete *P. chrysosporium*.^[63]

1.4.2 Manganese Peroxidase (MnP)

Another major lignolytic enzyme is the manganese peroxidase (MnP), so called for its preferred substrate of Mn^{2+} ubiquitous in ecological environments. Discovered in 1985 in *P. chrysosporium*, manganese peroxidase was thought only to oxidise phenolic substrates and its lignolytic activity second to that of the LiP.^{[75], [76]} However, since the availability of genome-scale data more MnPs have been found in different basidiomycetes, in particular *Ceriporiopsis subvervispora* a white-rot fungus, notable for having a higher activity for lignin degradation than *P. chrysosporium* and producing up to thirteen isozymes of MnP and only 1 putative LiP.^[77] The discovery

of MnP in *C. subvervispora* suggests that MnP may catalyse the breakdown of lignin not only from the phenolic ends but also from the non-phenolic main body via hydrogen and one-electron abstraction (Figure 21).^[78]

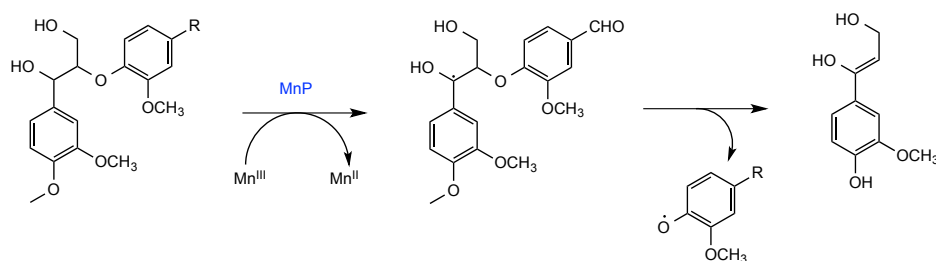


Figure 21: The α -C and β -C bond in non-phenolic lignin structures are cleaved via hydrogen and one electron abstraction

The crystal structure of MnP revealed a similar tertiary structure with other heme peroxidases, but with a notable Mn^{2+} binding site at the surface of the protein coordinating to the carboxylate oxygens of Glu35, Glu39, and Asp179, the heme propionate, and two water molecules (Figure 22).^[79]

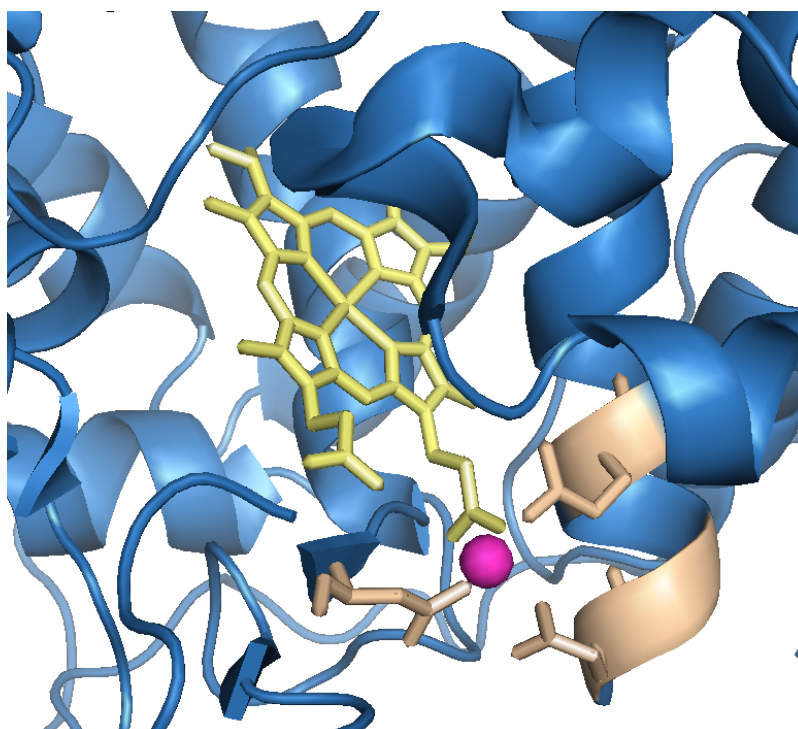


Figure 22: The manganese is coordinated by a Glu-Glu-Asp triad and the propionate of a heme moiety. PDB ID: 1MNP^[80]

The mechanism proceeds in a similar fashion to LiP only the $2e^-$ required to reduce compounds I and II are provided by 2 Mn^{2+} ions oxidised to Mn^{3+} . The Mn^{3+} formed is chelated and stabilised by organic acids such as oxalic acid and then diffuses to the surface where it can attack the lignin polymer.

1.4.3 Versatile Peroxidase (VP)

Characterised from *Pleurotus ostreatus* in 1999, the versatile peroxidase (VP) showed striking similarities in topology and function with both MnP and LiP.^[81] Glu-Glu-Asp residues in the heme-binding site coordinate a Mn^{2+} cation in keeping with MnP, however a surface based tryptophan residue, such as that seen in LiP was also observed.^[82]

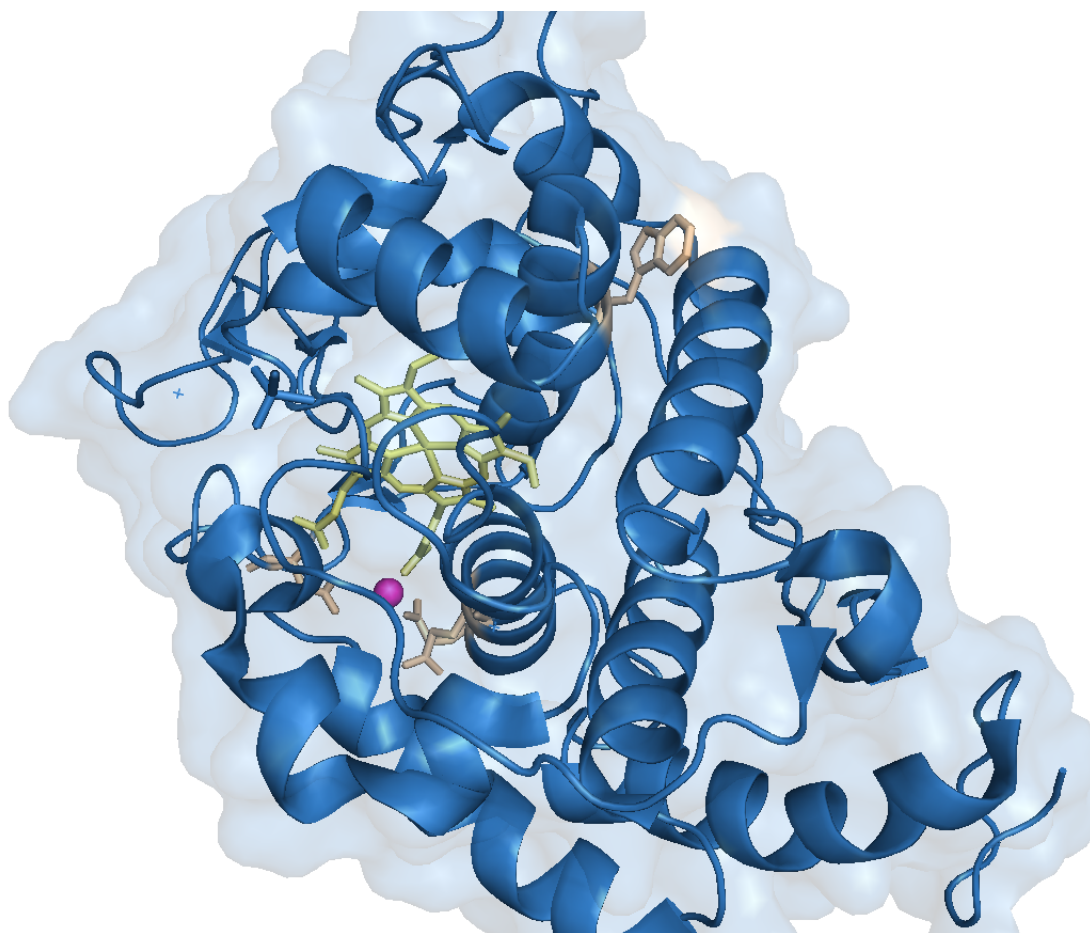


Figure 23: The versatile peroxidase (VP) shares a heme binding site coordinating a Mn^{2+} cation in keeping with MnP and a surface based tryptophan residue as seen in LiP. PDB ID: 2BOQ^[83]

The Trp170 residue was shown by site-directed mutagenesis to be essential in the oxidation of aromatic substrates in the absence of manganese, suggesting a similar long-range electron transfer system used by the LiPs.^{[84], [85]} The reintroduction of manganese to the medium restored lignolytic activity to the Trp170 knockout mutants reinforcing the evidence of a true hybrid lignolytic enzyme.^[86]

1.4.4 Laccase

Some involvement of copper containing fungal laccases in lignin degradation is clear, but the role they play is contentious due to the contrasting involvement of the enzymes in lignin biosynthesis and polymerisation.^{[87], [88]} Laccases are part of the

multicopper oxidoreductase family and oxidise a broad spectrum of phenolic compounds including the substructures typically found within the lignin polymer (Figure 24).^{[45], [47], [48], [89], [90]}

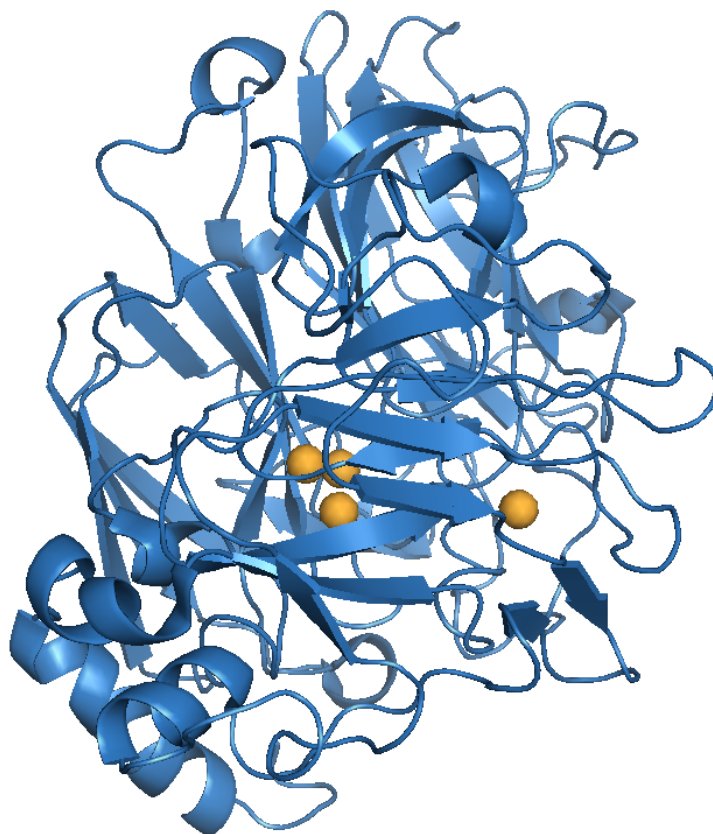


Figure 24: Fungal laccases contain 4 copper atoms, three of which are orientated in a trinuclear cluster, typical of laccases. PDB ID: 2H5U^[91]

The accepted mechanism for laccase-mediated oxidation involves four successive $1e^-$ oxidation (from four substrate molecules) that are transferred to 4 x central copper atoms in the Cu^{2+} oxidation state. The electrons are rapidly transferred to molecular oxygen via a peroxide intermediate to release 2 molecules of water (Figure 25).

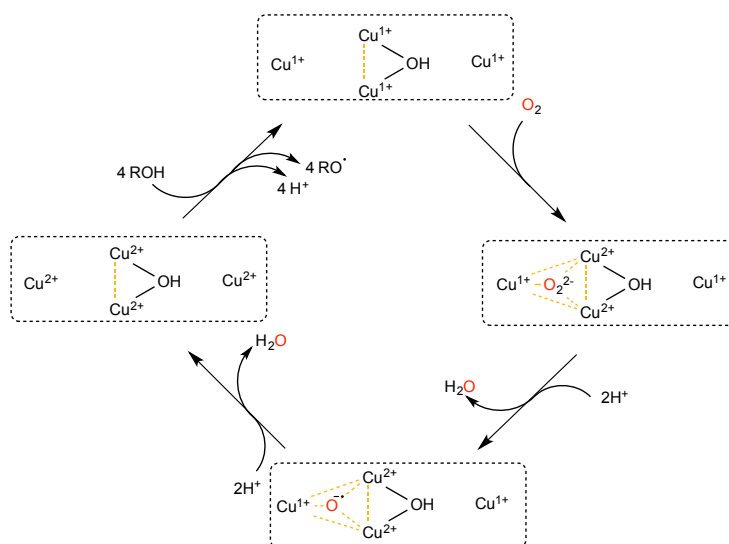


Figure 25: General laccase mediated oxidation of phenolic compounds results in the concomitant release of two molecules of water

Phenolic molecules are oxidised by the abstraction of $1e^-$ from the phenolic hydroxyl group to form a highly reactive phenoxy radicals. The polymerisation by radical-radical coupling accounts for the plant laccase mediated role in lignin biosynthesis, but in fungal lignin degradation an alternative process must also be occurring. Certain white-rot fungi, such as *Pycnoporus cinnabarinus* are assumed lignolytic without possessing the previously mentioned suite of peroxidases.^[92] The natural action of laccase on a phenolic substrate does however restrict the direct action of the enzymes on only a small percentage of the polymer. Degradation of any non-phenolic moieties within the lignin structure is assumed initiated by the production of reactive phenolic radicals – possibly liberated from the lignin matrix - acting as mediators, however evidence based on interactions with lignin model compounds has so-far proved inconclusive.^[93]

Degradation of lignin is a slow process that occurs in a select few organisms and only after nutrient depletion elicits secondary metabolism, ensuring the longevity of the kingdom Plantae.^[94] However, it is noted conversely that certain lignin-containing

species of plants decompose relatively quickly in moist soils suggesting the involving of a number of different organisms not just limited to the basidiomycetes. Cereal crop residues for instance, are regularly returned to the soil for microbial decomposition to sustain soil fertility.^[95]

1.4.5 Evidence of bacterial lignin degradation

Studies of non-fungal lignin degradation implicate bacterial involvement and highlight a number species capable of interacting with industrial lignin and synthetic lignin model compounds.^{[56], [57], [96]}

The first reported lignin-degrading bacterium was *Streptomyces viridosporus* T7A. When grown on corn stover lignocellulose, *S. viridosporus* T7A produces an extracellular peroxidase capable of generating aromatic intermediates, which indicates lignin metabolism.^{[97], [98]} Other studies have investigated the involvement of soil bacteria in lignin degradation using ¹⁴C-labelled maize-lignin or ¹⁴C-labelled synthetic lignins.^{[99], [100]} These experiments allowed researchers to measure ¹⁴CO₂ formed as a percentage of the original substrate and identified *Nocardia*, *Pseudomonas* and *Bacillus* strains as lignin degraders with varying degrees of metabolic efficacy from 0.3% (*Bacillus megaterium*) to 7% (*Nocardia*). Research using synthetic model dimers also identified a number of species capable of metabolising a non-phenolic substructure of lignin, vital if significant bacterial lignin degradation was to occur.^{[101]-[103]}

Conclusions so far have been made with synthetic lignin model dimers or laborious and often unreliable ¹⁴C-labelled experiments that until recently hampered major progress in the field. However, in 2011 Ahmad *et al* published work detailing a novel colorimetric assay that used a milled wheat straw lignin preparation (MWL) as a

substrate for rapid screening of lignin degrading microbes. A UV/vis assay using a chemically nitrated MWL was developed enabling the spectrophotometric monitoring of nitrated polysubstituted aromatic degradation products at 430 nm (Figure 26).

The assay confirmed lignin degradation of *P. chrysosporium* the white-rot fungi and also identified lignin-degrading activity in the actinomycetes *Rhodococcus erthyropolis* and *Rhodococcus jostii* RHA1. These bacteria showed higher increases in absorbance at 430 nm using the UV/vis assay when compared with non-degrading microbial controls.^[104]

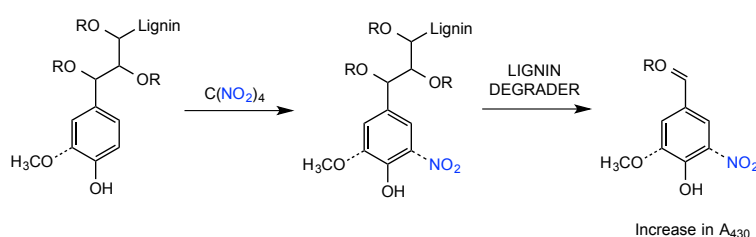


Figure 26: In the nitrated lignin assay tetranitromethane (C(NO₂)₄) is used to nitrate the milled wheat straw lignin. Positive microbial degradation of this substrate releases nitrated aromatic products that cause an increase in absorbance at A₄₃₀.

Although this work added weight to bacteria possessing extracellular lignin degrading enzymes, little had been published with respect to the specific enzymes involved.

However, advances in bioinformatics and genome sequencing have made it easier to identify potential enzymes involved in degrading lignin. After the genome sequence for *R. jostii* RHA1 was published,^[103] a possible involvement of two dye-decolourising peroxidases DypA and DypB were identified based on bioinformatics analysis.^[105] A $\Delta dypB$ gene deletion was later shown to have greatly reduced activity in the colorimetric assays than controls and recombinant DypB

protein displayed Michaelis-Menten kinetic behaviour when assayed with kraft lignin as a substrate.^[106]

Both DypA and DypB were also found to display peroxidase-type activity in the presence of the peroxidase reductant 2,2'-azino-bis-(3-ethylbenzothiazoline-6-sulfonic acid (ABTS). Further evidence was also obtained using the nitrated lignin assay in the presence of 2 mM hydrogen peroxide, where it was shown that DypB retained activity in the presence of hydrogen peroxide, but not without. DypA did not show any sign of activity in the presence or absence of hydrogen peroxide reaffirming conclusions made using the gene deletion strains that DypB was a bacterial lignin degrading peroxidase. DypB was also found to oxidise Mn^{2+} to Mn^{3+} and furthermore capable of oxidising a β -aryl ether model compound via resulting in C_{α} - C_{β} bond cleavage.^[106]

1.4.6 Dye-decolorizing peroxidases

Since the identification of DypB in *R. jostii* RHA1, a further three genes encoding dye-decolourising peroxidases (DyPs) have been reported in another actinomycetes strain *Amycolatopsis* sp. 75iv2 by Brown *et al* (2012).^[107] In all cases the bacterial DyP enzymes had a manganese dependent mode of action, signifying similarities with the fungal manganese peroxidase in which the oxidation of Mn^{2+} to Mn^{3+} initiates the oxidative degradation of lignin (Figure 27).^[106]

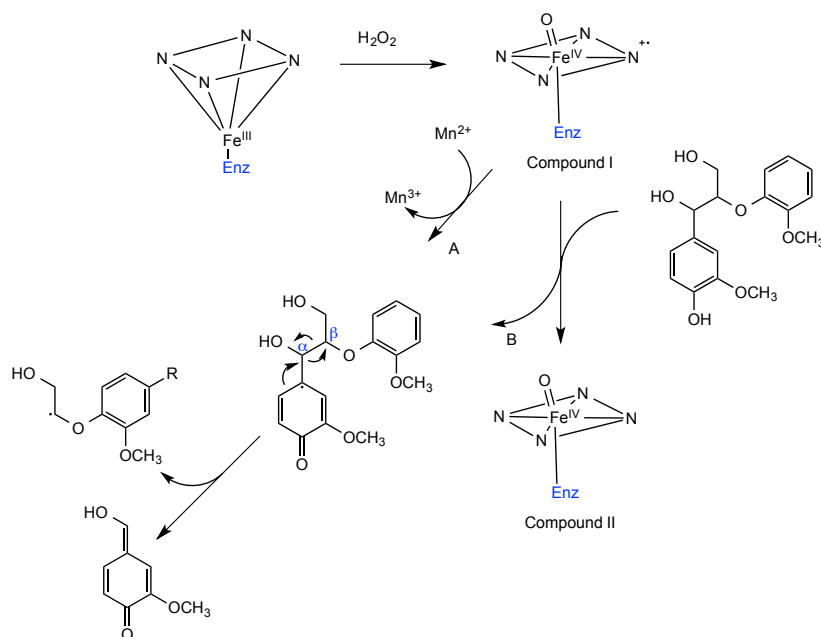


Figure 27: An enzymatic reaction with hydrogen peroxide forms compound I with a porphyrin located radical. Reduction of compound II proceeds either via the oxidation of Mn^{II} to Mn^{III} (Pathway A) or direct interaction with a reducing substrate such as the β-aryl ether dimer (Pathway B). Either pathway can create an aryl radical that can undergo non-enzymatic cleavage of the C_α-C_β bond.^[106]

The catalytic mechanism of DyPs has been suggested to proceed similar to the fungal peroxidases.^{[106], [108], [109]} The resting enzyme reacts with hydrogen peroxide to form the semi-stable reactive intermediate Compound I. Compound I may then react directly with the substrate (Pathway B, Figure 27) or via a single-electron oxidation of Mn^{II} (Pathway A, Figure 27). Subsequent non-enzymatic degradation would then proceed after the formation of an aryl cation, as discussed earlier in this chapter.

For complete biodegradation of plant biomass it most likely requires a suite of different enzymes and microbial degradation is by no means limited to the discussed enzyme groups. These enzymes have a wide spectrum of substrates and can often work optimally at different pH levels suggesting their expression and excretion may

be a response to the degradation products released during the different stages of lignin decomposition.

1.4.7 Existence of aromatic degradation pathways in bacteria

Aromatic degradation pathways conserved in bacterial soil species are indicative of an ability to metabolise lignin breakdown products.^{[106], [110]–[113]} A better understanding of these pathways may provide a route to making lignin sources an economically viable feedstock alternative to petroleum by identifying key metabolites that may be of commercial value.

Despite the random occurrence of the linkages within the lignin structure, aerobic biodegradation of lignin by soil-dwelling bacteria must proceed via the formation of central aromatic intermediates substrates for ring-cleaving dioxygenase enzymes. Bacterial aromatic degradation pathways typically involve catechol intermediates, which are substrates for oxidative ring cleavage by the catechol dioxygenases. Ring cleavage of these substrates is termed *ortho*-cleavage when it occurs between the two hydroxyl groups and *meta*-cleavage when it occurs adjacent to one of the hydroxyl groups (Figure 28). *Ortho* cleavage is catalysed by iron (III) dependent intradiol catechol dioxygenases, while *meta*-cleavage is catalysed by iron (II) dependent extradiol catechol dioxygenases (Figure 29).

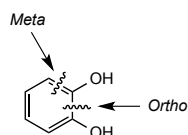


Figure 28: *meta* and *ortho* cleavage of catechol

The *ortho*-cleavage pathway (or β -ketoacid pathway) has been comprehensively studied in soil bacteria and assumed the main route for aromatic compounds in bacterial lignin degradation (Figure 29).^[114]

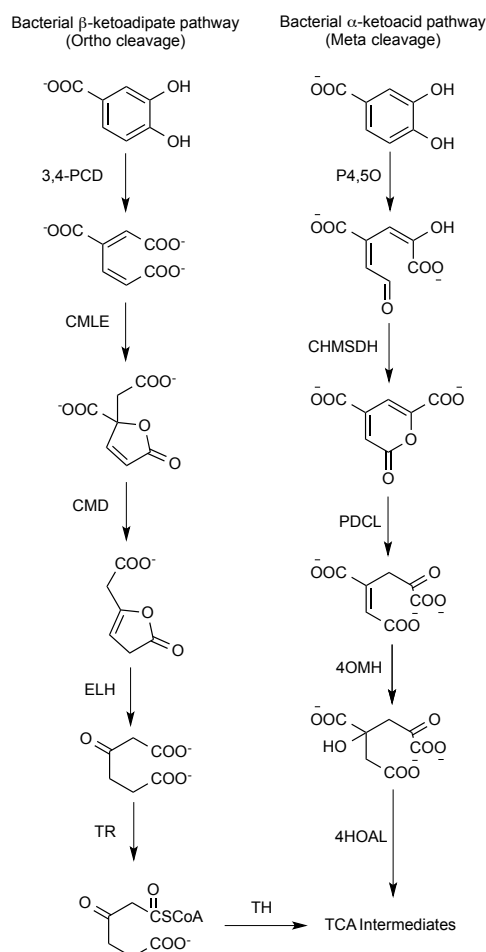


Figure 29: Bacterial β -ketoacid and α -ketoacid pathways for the substituted catechol protocatechuate. Enzymatic steps are indicated by initials. β -ketoacid pathway steps: 3,4-PCD protocatechuate 3,4-dioxygenase; CMLE β -carboxymuconate lactonizing enzyme; CMD γ -carboxymuconolactone decarboxylase; ELH enolactone hydrolase; TR β -ketoacid:succinyl-CoA transferase; TH β -ketoacid-pyruvate thiolase. α -ketoacid pathway steps: P4,5O protocatechuate 4,5-dioxygenase; CHMSDH 4-carboxy-2-hydroxymuconate-6-semialdehyde dehydrogenase; PDCL 2-pyrone-4,6-dicarboxylate lactonase; 4OMH 4-oxalomesaconate hydratase; 4HOAL 4-hydroxy-4-methyl-2-oxoglutarate aldolase.^[114]

The *meta*-cleavage pathways appear to be generally plasmid-borne in microorganisms that have evolved to degrade environmental pollutants^[115]. Sequence data of the enzymes involved in aromatic degradation has shown however that the β -ketoadipate pathway (*ortho*) is the most highly conserved in soil-dwelling bacteria and can be observed in species such as *Pseudomonas*, *Azotobacter*, *Arthrobacter*, *Acinetobacter* and *Rhodococcus*.^{[114]-[116]}

However, it should not be overlooked that once a cluster of genes has evolved as a plasmid in a bacterium, it can spread rapidly by bacterial conjugation to other species if advantageous for them to utilise the genetic trait. *Sphingomonas paucimobilis* sp. SYK-6 is reported as a Gram-negative soil bacillus that has been studied in detail by Masai et al (2007), and is an example of such a bacterium that utilises the *meta*-cleavage pathway in degradation of lignin type structures.^{[60], [117]-[119]}

The degradation of lignin and the catabolic pathways that feed into the convergent ring fission pathways are dependant on the composition of the initial substructure.

The β -aryl ether, phenylcoumaran and diarylpropane have been identified as the most common type of linkage found in lignin representing as much as 70% of all linkages between the G, S and H subunits. However, the breakdown pathways for these structural units are still poorly understood.^{[120], [121]}

In previous work by Dr Mark Ahmad, University of Warwick, incubations of *R. jostii* RHA1 grown on manganese supplemented liquid media containing 1% (w/v) milled wheat straw lignocellulose led to the identification of several metabolites derived from lignin, although in low yield.

Two observed products β -hydroxypropiovanillone (9) and vanillic acid (10) could each be derived from degradation of the β -aryl ether component of lignin. It was also observed *in vitro* that peroxidase DypB could generate vanillin (11) by oxidative C_{α} - C_{β} bond cleavage of β -aryl-ether. Vanillin could then be oxidised via a dehydrogenase, which would account for the observed vanillic acid (Figure 30).^[106] In theory (9) could also be generated by an α,β -elimination reaction, followed by tautomerisation of the enol product.

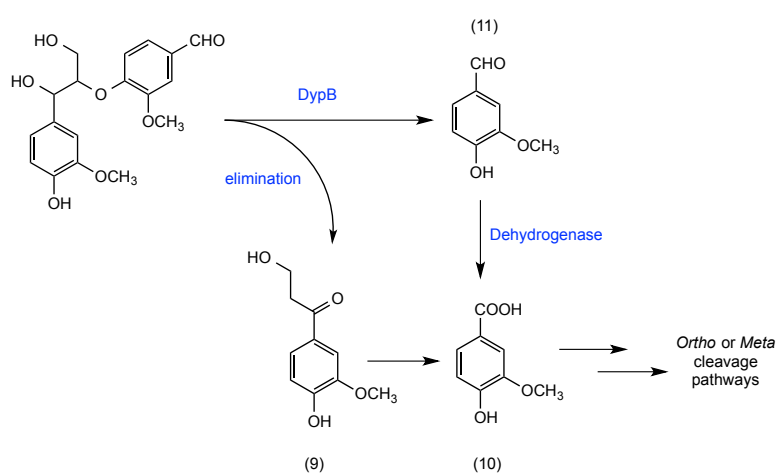


Figure 30: It is hypothesised that the DypB catalysed degradation of the β -aryl ether component of lignin could release vanillin (11). Vanillin may be further oxidised via a dehydrogenase to vanillic acid (10).

Another metabolite, 5-carboxyvanillic acid (12), was also observed in the same experiment and could potentially arise from the degradation of a biphenyl lignin component (Figure 31). The biphenyl pathway is well reported in soil bacteria^{[103], [122]} and the enzymes that catalyse the degradation of 5,5'-dehydrodivanillate (13), a lignin-related biphenyl compound, were characterised by Peng *et al* in 2002 as LigXYZ.^[123]

Peng *et al* determined the substructure could be demethylated in the first instance by 5,5'-dehydrodivanillate O-demethylase (LigX), then cleaved in the 1,2 position by an

extradiol ring cleavage dioxygenase (LigZ). Compound (12) could then be released by a concomitant hydrolysis by the C-C hydrolase (LigY). Vanillic acid (10) may also arise as the decarboxylated product of 5-carboxyvanillic acid from the same pathway (Figure 31).

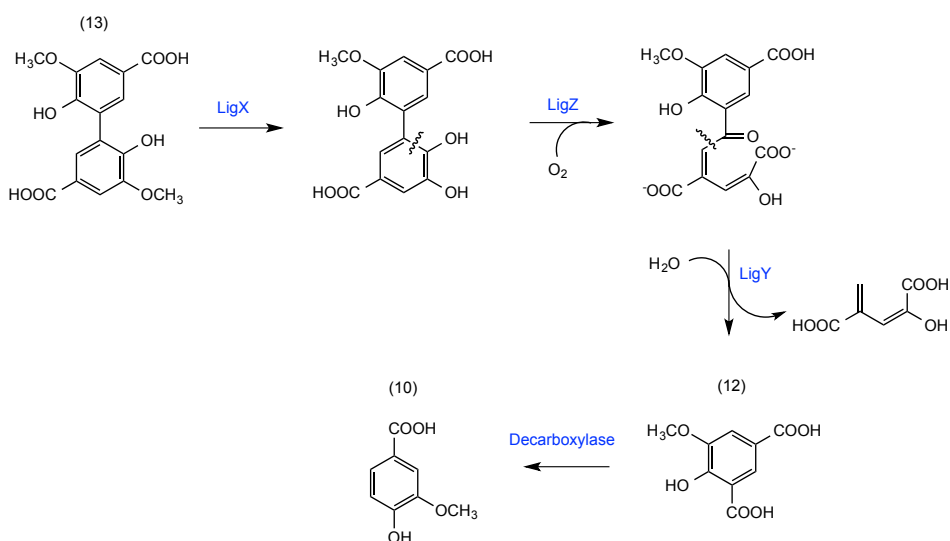


Figure 31: 5-carboxyvanillic acid (12) could potentially arise from lignin related structure 5,5'-dehydrodivanillate (13) by a demethylation catalysed by LigX, a concomitant ring cleavage by LigZ followed by a C-C hydrolase step (LigY) step of the biphenyl component of lignin. Vanillic acid (10) may also be formed by a decarboxylation of 5-carboxyvanillic acid.

Umezawa *et al* (1982) showed that a synthetic phenylcoumaran dimer could be first oxidized in the coumaran ring to give a propiosyringone derivative by the action of a peroxidase.^[71] This oxidative reaction could then be followed by a reduction to form a diarylpropane structure. An alternative pathway from the propiosyringone derivative however, could involve cleavage between the C_α-C_β bond to vanillic or syringic acid dependant on the initial substructure unit. The diarylpropane degradation pathway itself may also proceed via a cleavage between the C_α-C_β bond by a peroxidase or alternatively via a cleavage of the inter-phenyl double bonds of lignostilbene (14) by lignostilbene dioxygenases (Figure 32).^[124]

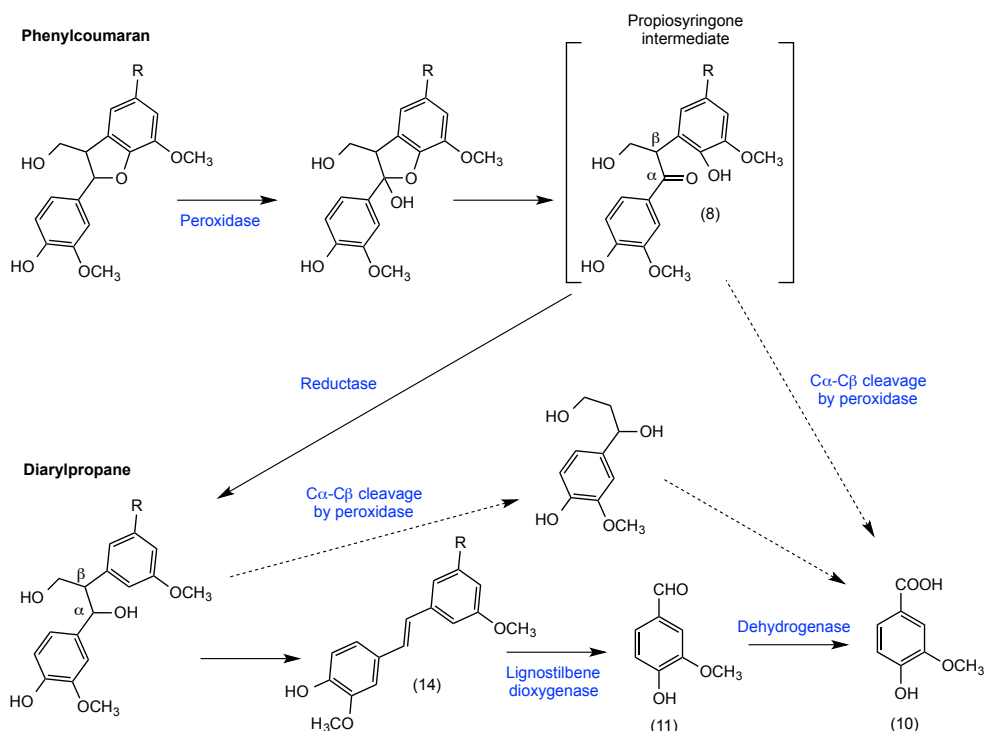


Figure 32: A phenylcoumaran model compound is first oxidized in the coumaran ring to give the propiosyringone derivative by the action of a peroxidase.^[71] This may then be followed by a reduction to form the diarylpropane structure. An alternative pathway from the propiosyringone derivative could involve cleavage between C α and C β to vanillic acid (10). The diarylpropane degradation pathway itself may also proceed via a cleavage between C α and C β by a peroxidase or alternatively via a cleavage of the inter phenyl double bonds of lignostilbene (14) by lignostilbene dioxygenases

Whilst there seems to be a number of oxidative breakdown pathways of the initial dimeric and polymeric structures, many of the pathways converge on the production of key intermediates such as vanillin (11) and vanillic acid (10), which are then converted via enzymatic transformations to protocatechuic acid (15) for entry into the β -ketoacid pathway.

These compounds have been consistently and repeatedly found in experiments with microbial lignin degraders, highlighting potential enzymes that may be important in lignin degradation.^{[59], [60], [125]–[130]}

1.5 Extracting value from lignin

Table 1 shows a number of products that may be gained from the degradation of lignin and their respective value.^{[127], [129], [131]–[133]} It can also be seen from the table that if a method to obtain vanillin from lignocellulose can be termed as a natural biosynthetic process then the economic potential of acquiring this metabolite is of great interest.

Table 1: Current value of identified potential lignin breakdown products. (Prices obtained from Borregaard Ingredients, ICIS Pricing and Rhodia Group. Correct as of 12/09/13)

PRODUCT	\$		PRODUCT	\$	
Process Heat & Power	10.00	per 106 BTU*	Biosynthetic Vanillin	700.00	per kg
Methanol/Dimethyl ether (DME)	0.22	per litre	Petrochemical Vanillin	15.00	per kg
Ethanol/mixed alcohols	0.88	per litre	Aromatic Acids	1.32	per kg
Fischer Tropsch Liquids	0.66	per litre	Aliphatic Acids	1.54	per kg
Mixed Liquid Fuels	0.66	per litre	Cyclohexanol/al	1.76	per kg
BTX (benzene-toluene-xylene) and Higher Alkylates	0.66	per litre	Quinones	2.20	per kg
Cyclohexane	0.48	per litre	Styrenes	1.76	per kg
Phenol	1.65	per kg	Polyelectrolytes	7.05	per kg
Substituted Phenols	4.85	per kg	Polymer Alloys	4.63	per kg
Catechols, cresols, resorcinols	3.96	per kg	Fillers, Polymer Extender	3.08	per kg

*BTU (British Thermal Unit)

Whilst the identification of metabolites found on the pathways of microbial lignin deconstruction may give an indication as to potential aromatic chemicals of commercial value, the main barrier to unlocking its potential would have to involve an efficient targeted depolymerisation process.

1.5.1 Chemocatalytic approaches to obtaining high value chemicals

A number of pyrolytic and chemocatalytic redox methods have been shown to depolymerise lignin and lignin model compounds and is comprehensively reviewed by Zakzeski *et al.*^[10]

Obtaining chemicals from lignin pyrolysis is particularly challenging. The kinetics of pyrolytic techniques can markedly influence the mixture of products reflecting the complex nature of the initial lignin source as highlighted earlier.^[134] Monomeric phenolic products such as guaiacol (16), syringol (17), vanillic acid (10) and catechol (18) have been found in the bio-oil, but as a complex mixture.

The most promising recovery from the pyrolysis of wheat straw in the last five years has been reported in a study by de Wild *et al* (2012).^[135] Wild achieved a monomeric phenolic fraction of approximately 2.8-4.4% (w/v), with the major phenolic monomers formed being derivatives of guaiacol (16).

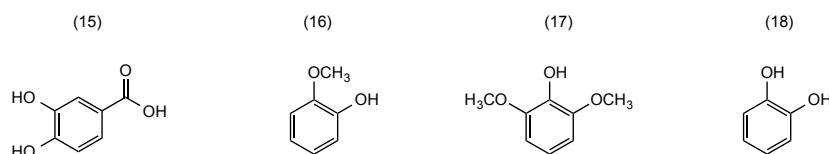


Figure 33: Protocatechuic acid (15), guaiacol (16), syringol (17) and catechol (18)

Catalytic reduction or hydro-deoxygenation of the components in bio-oil obtained from lignin pyrolysis provides a possible route from lignin to the BTX (benzene-toluene-xylene) fraction needed as a jet fuel additive, if a significant amount of the oxygen content could be removed whilst minimising hydrogen consumption.^[10] This is a challenging catalysis problem, but Jongerius *et al* (2012) have found using a pre-sulfided CoMo/Al₂O₃ catalyst that hydrodeoxygenation of the monomeric products of

pyrolysis, such as guaiacol (16) (Figure 34), syringol (17) and catechol (18) gave demethylated and ring methylated products in high selectivities.^[136]

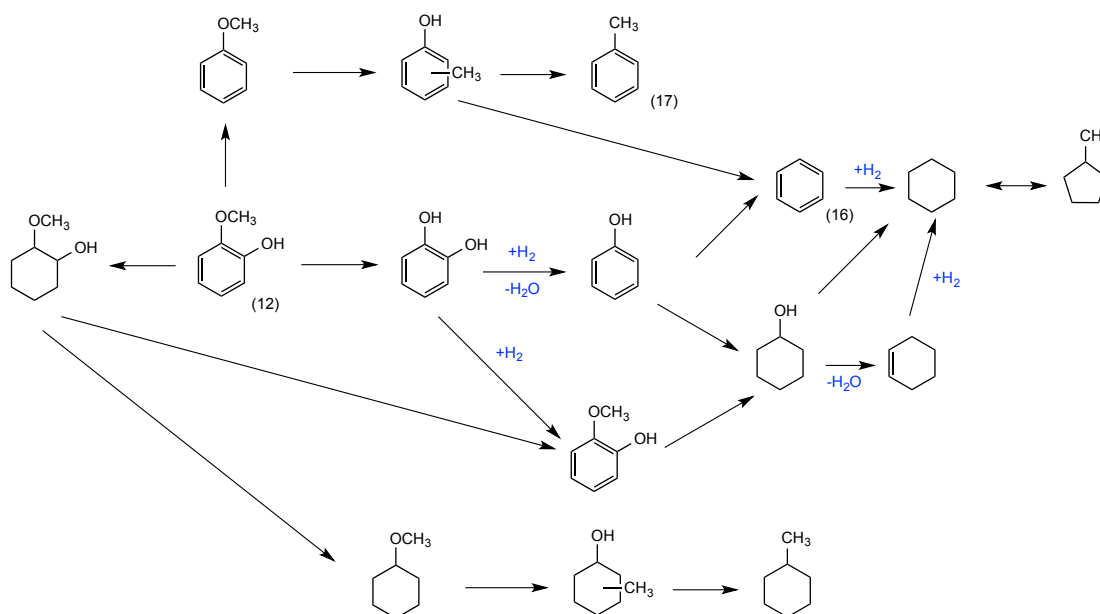


Figure 34: Catalytic hydrodeoxygenation of guaiacol (16) found in high percentage in the bio-oil from lignin pyrolysis can proceed via a number demethylated and ring methylated products to form benzene and toluene. This provides a possible route from lignin to the BTX (benzene-toluene-xylene) fraction require for jet fuel.^[137]

Overcoming the problems associated with unselective hydro-deoxygenation of a complex mixture of products found in biomass and bio-oil based products has encouraged some researchers to adopt techniques based on selectivity. A milder hydrogenolysis method for the selective catalytic cleavage of diaryl ether and alkyl-aryl ether linkages has recently been published, in which an exclusive range of arene and alcohol products could be formed using a soluble nickel carbene catalyst. It was found that ether substrates were selectively cleaved in the order of Ar-OAr >> Ar-OMe > ArCH₂-OMe without further hydrogenation and loss of aromaticity (Figure 35). The procedure was also found to work with lignin model compounds providing a potentially new hydrogenolytic deconstruction route for lignocellulosic biomass.^[138]

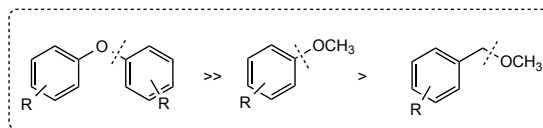


Figure 35: Ether substrates were selectively cleaved in the order of Ar-OAr >> Ar-OMe > ArCH₂-OMe without further hydrogenation and loss of aromaticity when treated with H₂ and a soluble nickel carbene catalyst.^[138]

Gasification approaches have also been successful. Gasification of lignin produces biogas (mainly CO/H₂) and activated carbon when carried out by treatment with O₂ and steam at elevated temperature (350°C) and pressure (3000 psi) in the presence of Ru/C catalysts.^{[139], [140]} The biogas can then be converted to methanol or dimethyl ether via chemocatalysis, followed by methanol to gasoline (MTG) or methanol to olefins (MTO) processes on acidic zeolites.^[141]

1.5.2 Vanillic acid pathway as a target for pathway engineering

In recent years the ability to genetically manipulate bacterial metabolic and catabolic pathways has become commonplace due to advances in genome technology and systems biology. This offers scientists a potential route to upgrading lignin sources to a valuable source of aromatic chemicals by using relatively inexpensive and environmentally sound enzymatic alternatives to chemocatalytic approaches.

A simplified diagram of possible bacterial breakdown of lignin substructures, based on the metabolites observed by research within the group highlights the prominent involvement of the vanillic acid pathway (Figure 36).

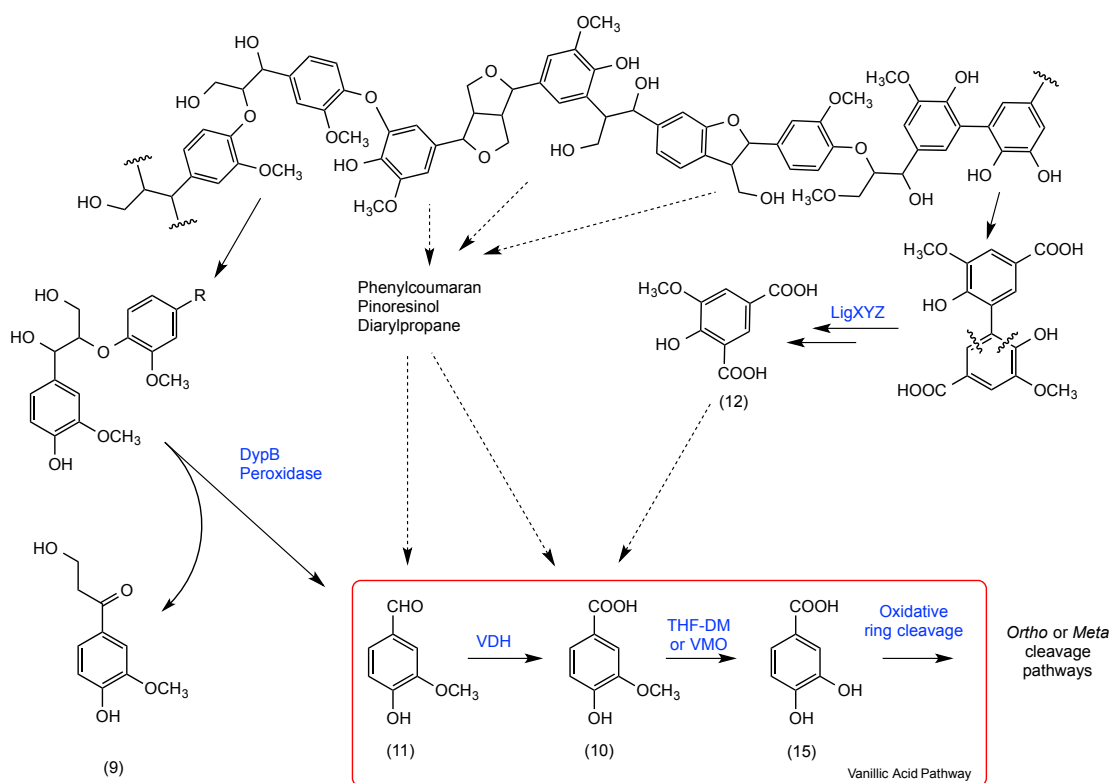


Figure 36: Postulated bacterial breakdown pathways of lignin substructures based on metabolites (9, 10, 11 and 12) observed by research within the group highlights the prominent involvement of the vanillic acid pathway. In the pathway, it is suggested vanillin (11) is oxidised by a vanillin dehydrogenase (VDH) to vanillic acid (10), which is further demethylated by either a tetrahydrofolate dependent demethylase (THF-DM) or vanillate mono-oxygenase (VMO) to protocatechuic acid (15) for entry into ring cleavage pathways.

The inhibition, introduction or deletion of selected enzymes responsible for the transformations on the vanillic acid pathway could lead to accumulation of target metabolites.

1.5.2.1 Vanillin aldehyde dehydrogenase

Vanillin is a particular metabolite of interest as it is an important aromatic flavour compounds used in foods, beverages and perfumes and produced on a massive scale. Its value varies widely, with natural biosynthetic vanillin worth almost 50 times that of petrochemical vanillin (Table 1). Genes encoding for vanillin aldehyde

dehydrogenase have been isolated in a number of soil bacteria including *Bacillus subtilus*^[142], *Rhodococcus jostii* RHA1^[143], *Pseudomonas putida*^[144] and *Sphingomonas paucimobis* SYK-6^[119].

The biotransformation by bacteria of cheaper substrates to vanillin has already been established. Vanillin production from ferulic acid by *P putida* >2 g/L (Ryu *et al* 2005)^[145], *Pseudomonas fluorescens* >0.1 g/L (Calisti *et al* 2008)^[146], *Streptomyces setonii* >10 g/L (Achterholt *et al* 2004)^[147] and *E. coli* >2.5 g/L (Barghini *et al* 2007)^[148] have all been reported in the last decade. Most recently Fleige *et al* (2013) have reported that a *vdh* gene deletion strain of *Amycolatopsis sp.* was capable of synthesising vanillin to a final concentration of approximately 1 g/L from ferulic acid, approximately 4 times that of the wild type strain.^[149]

Isoeugenol and eugenol obtained from the essential oils of plants have also been used as a cheaper substrate for biotransformation to vanillin. Overhage and Priefert (1999) were one of the first to use a combination of gene deletion and heterologous gene expression techniques to show *P. putida* was capable of converting eugenol to vanillin and in 2006, Zhang *et al* obtained yields >1.3 g/L using a strain of *Bacillus subtilus* to transform isoeugenol.^[150]

However, trying to increase the concentrations of any targeted metabolite, such as vanillin may present a problem of bacterial toxicity. It is therefore worth considering not only selecting strains able to tolerate high concentrations of these chemicals, but also finding novel ways to remove the metabolite from the reaction system.

The orchid *Vanilla planifolia* solves the problem of the toxic release of vanillin into the cells by glycosylation.^[151] This strategy has been successfully implemented in *Schizosaccharomyces pombe*, also called “fission yeast”, by Hansen *et al.* (2009).

Hansen et al report an extracellular concentration of up to 25 g/L of the vanillin β -D-glucoside was shown not to affect growth. This suggests a potentially more suitable metabolite for *in vivo* accumulation than the toxic vanillin (Figure 37).^{[152], [153]}

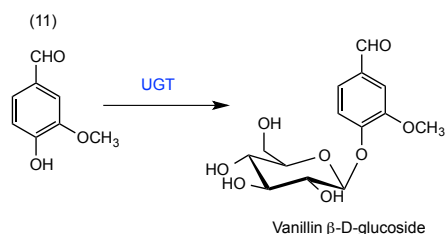


Figure 37: Glycosylation of vanillin by nucleotide-sugar dependent glycosyltransferases (UGTs) produces the far less toxic metabolite vanillin β -D-glucoside.

1.5.2.2 Demethylation of vanillate

Enzymes systems capable of the demethylation of vanillate to protocatechuate (3,4-dihydroxybenzoate) have been identified in a wide range of Gram positive and Gram negative bacterial species with two distinct aromatic demethylation enzyme systems identified. One of these systems is vanillate monooxygenase composed of ferredoxin oxygenase and reductase components. The other demethylase is a tetrahydrofolate (THF) dependant enzyme.^{[154], [155]}

Less studied than the bio-technological production of vanillin, enzymatic conversions of substrates with the intention to accrue vanillic acid have still been published. Most notably ferulic acid was converted to vanillic acid by a transposon mutant of *Pseudomonas fluorescens* strain (BF13) pre-grown on M9 medium containing 0.1% *p*-coumaric acid (w/v) as a sole source of carbon. The mutant was able to convert almost as high as 25% (w/w) of ferulic acid to vanillic acid per hour under optimum conditions.^[156]

As bacterial metabolic engineering involves the introduction or removal of genes in a naturally occurring microbial metabolic pathway unpredictable physiological responses in the organism resulting from genetic engineering can cause metabolic imbalances leading to unsatisfactory metabolite yields. Stephanopoulos *et al* (1991) remind us that a coordinated amplification or deletion of other enzymes in the same or closely related pathways may be required to maintain an environment to support the initial genetic modification.^[157] Their most current work on the lysine production pathway in *Corynebacterium glutamicum*^[158] continues to support the hypothesis and their work is often cited and considered, especially when using overexpression techniques.^{[159]-[161]}

Elucidating pathways and targeting enzymes for deletion or overexpression is often not a sure-fire predictable way to increase the yield of a target compound and many experimental approaches also rely on a degree of serendipity. Bacteria have developed sophisticated mechanisms for the regulation of both catabolic and anabolic pathways and readily shut down metabolic pathways when the end product of the pathway is not needed or readily obtained by uptake from the environment.

Using this information on the microbial degradation of lignin and current advances in microbiology, it seems possible that the metabolic pathways of previously identified lignin degrading bacteria can be altered. This could be done with chemical methods, the deletion of genes from the organism by genetic engineering or a combination of the two.

Not only could this yield metabolites with significant commercial interest but may also further the knowledge of the lignin bio-catabolic pathway in bacteria and find economic value in what has essentially been seen as a waste product for many years.

1.6 Aims and Objectives

The lignin content of plant biomass represents a major source of renewable carbon that could be used to produce chemical feedstocks for commercial use. Two colorimetric assays for lignin degradation had identified a number of bacterial strains capable of lignin degradation.^[104]

The objective of this PhD project is to examine the effects of disrupting the lignin degradation pathways via a) gene knockouts or b) enzyme inhibition for the production of aromatic chemicals.

In preliminary work, metabolites had been identified from the breakdown of lignocellulose by bacterial degraders, which have been used to postulate key pathways for manipulation.

A collaboration with Prof. Lindsay Eltis (Univ. British Columbia, Canada), whose group has determined the genome sequence of *Rhodococcus jostii* RHA1, can provide us with genetic mutants of *R. jostii* RHA1 in which (putative) genes involved in lignin degradation can be deleted targeting the assumed lignin degradation pathways. The effects of these gene knockouts on the production of useful chemicals from lignocellulose by the *R. jostii* RHA1 mutants will be examined with the use of analytical methods (HPLC, LC-MS, GC-MS).

The final objective of the thesis is to examine the effects of chemical inhibitors on putative enzymes on lignin degradation pathways. Enzymes on the vanillic acid pathway will be targeted, using novel and existing chemical inhibitors with the primary aim of increasing levels of lignin breakdown metabolites as a novel method for the production of useful chemicals from lignocellulosic feedstocks.

Results and Discussion I

Some of the results from this chapter have been published in ACS Chemical Biology.

Sainsbury, P. D. et al. Breaking down lignin to high-value chemicals: the conversion of lignocellulose to vanillin in a gene deletion mutant of *Rhodococcus jostii* RHA1. ACS Chem. Biol. 8, 2151–6 (2013)

<http://pubs.acs.org/doi/abs/10.1021/cb400505a>

2: Results and Discussion I: The use of *Rhodococcus jostii* RHA1 gene deletion strains for targeted metabolite production from the breakdown of lignocellulose

It is proposed that by using synthetic biology techniques, an approach can be taken in which genes hypothesised to be involved in lignin degradation are selectively chosen for deletion to increase target metabolite production.

As metabolites indicating bacterial lignin degradation had previously been observed in incubations from the group, the experiments were repeated using *R. jostii* RHA1 grown in Luria-Bertani broth (LB) supplemented with 2.5% (w/v) milled wheat straw lignocellulose.

2.1 Investigation into lignin degradation by *R. jostii* RHA1

During a seven day incubation period at 30°C, with shaking, samples were taken from the fermentations after 0, 6 and 24 h and then every 24 h for 7 days and the optical density at 600 nm (OD₆₀₀) was measured. The samples were then centrifuged at maximum speed (10 min, 13000 rpm) and supernatant removed with the cell pellet being kept for intracellular metabolite analysis (Section 5.2.5.2). The supernatant was adjusted to pH 2 with 6N HCl and left on ice for 3 minutes. The samples were again centrifuged (10 min, 13000 rpm) and the supernatant extracted into an equal volume ethyl acetate. The organic layer was dried and dissolved in methanol/H₂O (1:1 v/v) for HPLC analysis or into DCM for GC-MS analysis.

Using high performance liquid chromatography (HPLC) with diode array ultraviolet (UV) detection on samples from each time point provided inconclusive data and variable results. The spectra presented a complex mixture of peaks with no clear

difference between time points or between control incubations with and without bacteria (data not shown).

Gas chromatography-mass spectrometry (GC-MS) on organic extracts offered a slightly more sensitive approach. Bis(trimethylsilyl)trifluoroacetamide (BSTFA) was added to the extractions that had been dissolved in DCM one hour prior to injection to derivatise alcohols, acids, and amines to their respective trimethylsilyl (TMS) ethers. This technique is a common and a convenient way increase the volatility of potential metabolites prior to GC analysis. With the spectra being much less convoluted, individual new peaks not present in the controls were easier to single out and attempt to identify.

In the experiments with the nutrient-rich LB media, evidence of lignin degradation by *R. jostii* RHA1 was not entirely conclusive. However, a peak with a retention time of 4.4 seconds did occur in some GC-MS chromatograms taken from the incubations with wheat straw lignocellulose. This peak was not present in controls and was later identified to be oxalic acid (ethanedioic acid), confirmed by comparing its fragmentation pattern and retention time with that of the authentic standard (Figure 38).

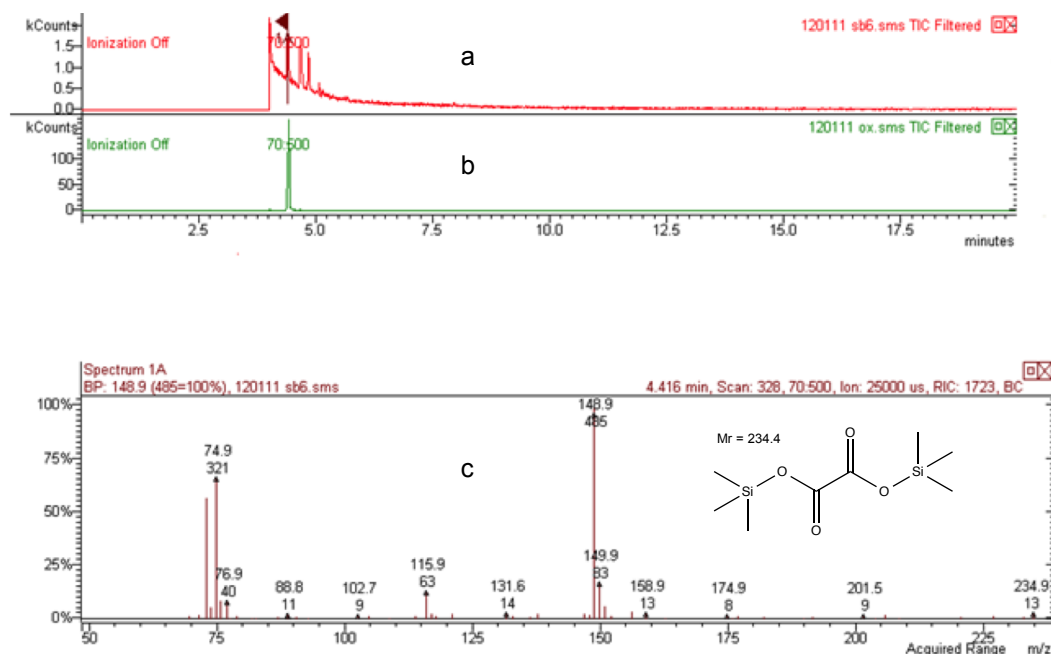


Figure 38: Total ion chromatogram by GC/MS with EI ionisation from a sample taken after 6 days from an incubation with *R. jostii* RHA1 and 2.5% w/v wheat straw lignocellulose in LB media (a), the total ion chromatogram of an oxalic acid standard (b) and the mass spectrum fragmentation pattern of the peak that was also consistent with that of the standard (c).

Oxalic acid biosynthesis in bacteria has been already been documented and linked to functions such as metal tolerance and for use as a pathogenic agent in a competitive environment.^[162]

Interestingly, it has also been suggested that oxalic acid acts as a possible regulation mechanism in white-rot fungi by the inhibition of both lignin peroxidase (LiP) and manganese-peroxidase (MnP). In the brown-rot fungal decay of lignocellulose it can serve as an electron donor in a Fenton-type catalytic breakdown process.^[163]

It could be hypothesised that the oxalic acid be formed from the cleavage of a β -aryl ether link releasing a two-carbon fragment glyceraldehyde that proceeds to undergo two subsequent oxidations to oxalic acid (Figure 39). The formation of oxalic acid via this mechanism is also noteworthy because metabolism of the glyoxal fragment via

aldehyde oxidases (ALOD) would replenish two equivalents of H₂O₂ for use by a peroxidase enzyme such as DypB.

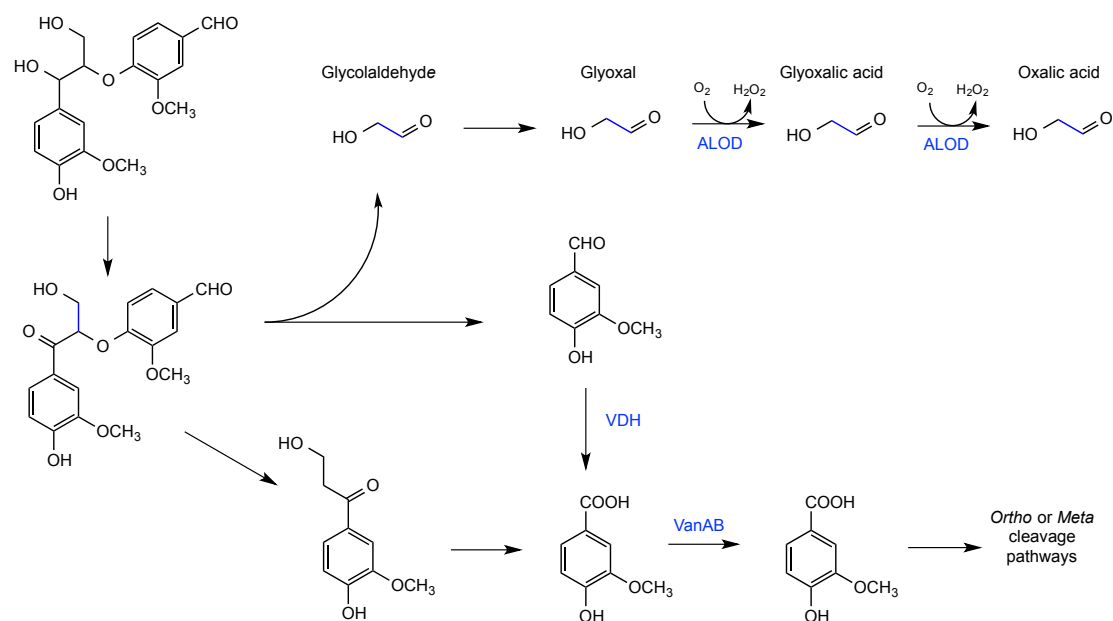


Figure 39: A hypothetical pathway for the production of oxalic acid by *R. jostii* RHA1. The breakdown of a β-aryl ether type linkage could release a glycoaldehyde fragment that with subsequent oxidations by aldehyde oxidase (ALOD) could form a route to oxalic acid biosynthesis.

These initial observations and the metabolites observed previously in the group suggested that a vanillic acid catabolic pathway in *R. jostii* RHA1 maybe important in the breakdown of lignocellulose.

2.2 Identification of vanillin catabolic genes in *Rhodococcus jostii* RHA1

It is hypothesised that three enzymes are involved in the *R. jostii* RHA1 vanillic acid catabolic pathway. A vanillin dehydrogenase (VDH) that converts vanillin to vanillate with the concomitant reduction of NAD⁺, a vanillin mono-oxygenase system composed of ferredoxin oxygenase (VanA) and reductase (VanB) components that convert vanillate to protocatechuate and finally a intradiol ring opening catechol dioxygenase (3,4-PCD) that provides entry to the β-ketoadipate pathway.

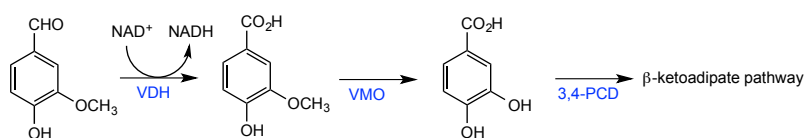


Figure 40: Enzymes hypothesised to responsible for the bacterial degradation of vanillin via the vanillic acid catabolic pathway include vanillin aldehyde dehydrogenase (VDH), vanillate monooxygenase (VMO) and 3,4-protocatechuate dioxygenase (3,4-PCD)

The oxidation of vanillin by bacteria to vanillate is via a vanillin aldehyde dehydrogenase (VDH) part of the oxidoreductase family of benzaldehyde dehydrogenases.^[60-63] In common with all benzaldehyde dehydrogenases vanillin is converted to the carboxylic acid derivative in a reversible reaction with concomitant reduction of NAD^+ .

The overall chemical mechanism involves an initial nucleophilic attack of a catalytic cysteine residue on the carbonyl carbon of the aldehyde to form a tetrahedral hemithioacetal intermediate bound to the enzyme. A hydride transfer then follows this from the tetrahedral hemithioacetal to the pyridine ring of NAD^+ and forms a thioester. The final steps of the reaction involve the nucleophilic attack of an activated water molecule on the thioester to produce the unstable tetrahedral intermediate which rapidly breaks down to expel the acid product (Figure 41).

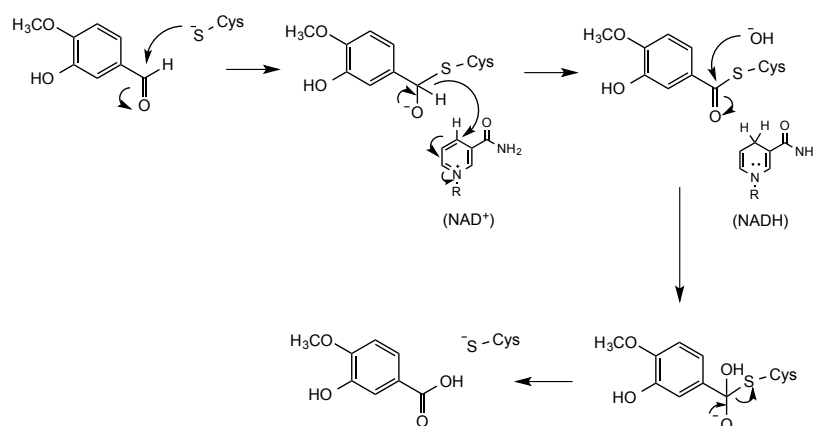


Figure 41: Oxidation of vanillin to form vanillic acid catalysed by the cysteine residue of a vanillin dehydrogenase with a concomitant reduction of NAD⁺

The catalytic cysteine residue conserved across all aldehyde dehydrogenases also makes them susceptible to varying extents of chemical inhibition by reagents commonly used to modify active site thiol residues such as *N*-ethylmaleimide (NEM)^[166] (19) and the pharmaceutical disulfiram^[167] (20) used in the treatment of alcohol abuse (Figure 42).

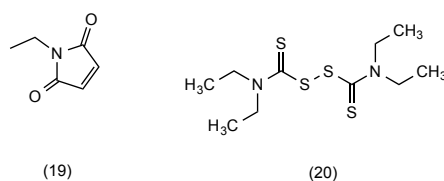


Figure 42: Chemical inhibitors of the catalytic cysteine residues of benzaldehyde dehydrogenases include disulfiram (20) and *N*-ethylmaleimide (19)

The conversion of vanillate to protocatechuic acid is catalysed by enzyme systems capable of demethylation. One of these systems is vanillate monooxygenase composed of ferredoxin oxygenase and reductase components (Figure 43). The other demethylase is the tetrahydrofolate (THF) dependant vanillate monooxygenase which is an example of a non-heme enzyme system containing the type of iron-sulphur clusters found in many proteins involved in electron transport. Vanillate monooxygenase is used by most aerobic vanillate-degrading bacteria to catalyse the

demethylation of vanillate to protocatechuate (Figure 36).^[155] The complex has wide substrate specificity and is able to transform a number of aromatic vanillate analogs with a methyl or methoxy group in the *meta* position.^{[143], [155]}

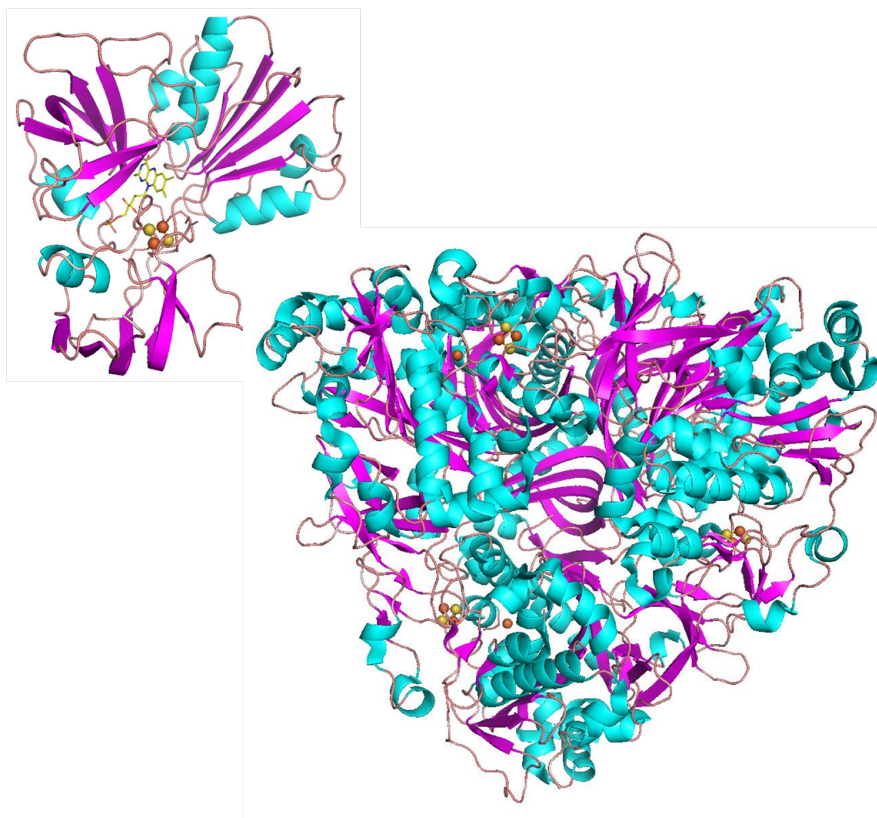


Figure 43: The monooxygenase system of vanillate mono-oxygenase contains ferredoxin reductase (VanB) (left) and oxygenase (VanA) (right) components. PDB ID: 3GLO^[168] & PDB ID: 1Q1R^[169]

The oxygenase component (VanA) contains a so-called “Rieske type” [2Fe-2S] iron-sulphur cluster that shuttles electrons to the mononuclear ferrous iron to ultimately activate molecular oxygen enabling the oxygenation of the substrate (Figure 44).

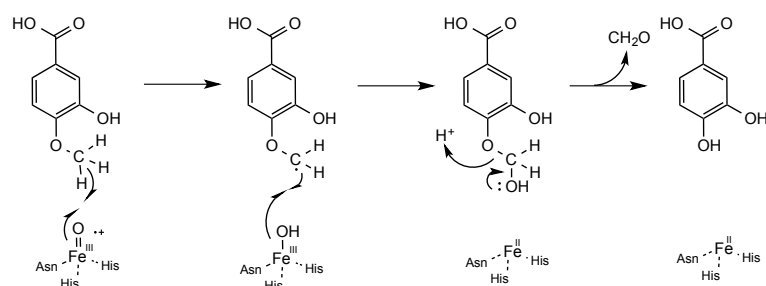


Figure 44: VMO catalysed conversion of vanillic acid to protocatechuic acid is initiated by oxygenation from the mononuclear ferrous iron within the oxygenase component.

The Rieske type [2Fe-2S] cluster accepts electrons from the “plant type” [2Fe-2S] iron-sulphur cluster within the reductase (VanB) component. The reductase uses NADH as a source of reducing equivalents exchanging electrons via the transfer of hydrides to flavin mononucleotide (FMN) and then on to the plant type [2Fe-2S] cluster.

Another enzymatic aromatic demethylation system that has been reported, used mainly by anaerobic bacteria, is tetrahydrofolate-dependent. This method of aromatic O-demethylation is achieved using up to four proteins and utilises enzymes and coenzymes involved in primary metabolism. In particular the tetrahydrofolate from the reaction acts as the contributor of one-carbon atoms in primary metabolite synthesis.^{[170], [171]}

In the first step a methyltransferase (methyltransferase I) mediates the transfer of a methyl group from the aromatic methyl ether to the cobalt of a vitamin B12 containing corrinoid protein. The methyl group is then transferred to tetrahydrofolate by a second methyl transferase (methyltransferase II) with the concomitant formation of 5-methyl-THF (Figure 45). A fourth protein is thought to act as a repairing ATP-dependent enzyme that reduces the oxidized corrinoid.^[158]

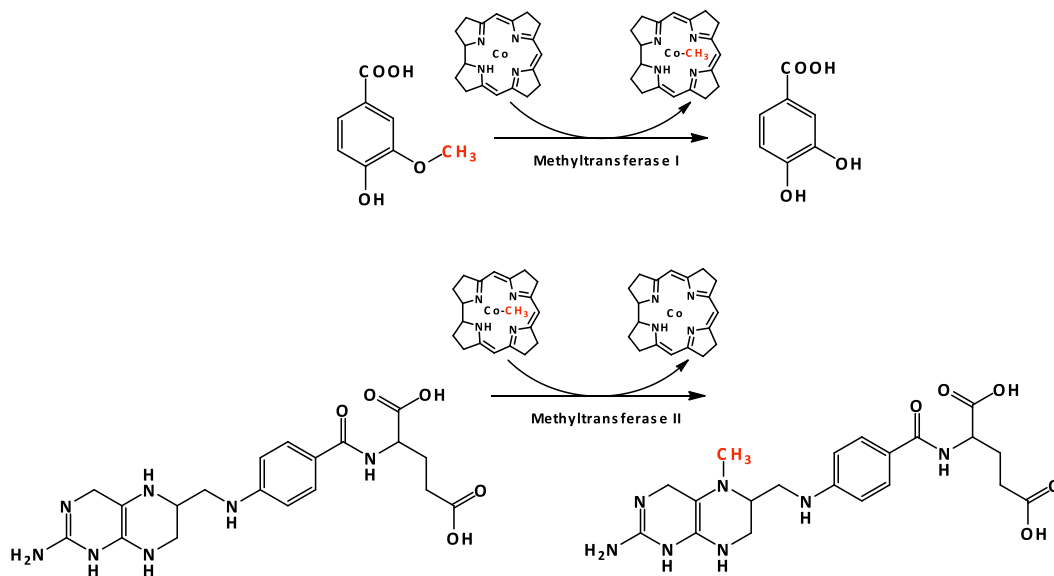


Figure 45: One-carbon movement by the THF-dependent methyltransferases from vanillate to tetrahydrofolate

Using a BLAST search of the *R. jostii* RHA1 genome, Professor Lindsay Eltis (UBC) was able to identify a homolog gene for *vdh*, ro02986 and a homolog gene for *vanA* ro04165 that shared high sequence identity with the same components from *Pseudomonas* sp. strain HR199. Using reverse transcription quantitative-PCR to monitor expression of putative genes during growth on vanillin and vanillic acid and traditional PCR to amplify genes for cloning in *Escherichia coli* he was able to confirm these genes as targets for deletion.^[143]

The genes ro02986 and ro04165 were disrupted in *R. jostii* RHA1 by targeted mutagenesis using a *sacB* counterselection by Prof. Eltis to create the gene deletion mutants. RHA045, the Δvdh deletion strain, was incapable of growing on vanillin but capable of growing on vanillate and RHA046, the $\Delta vanA$ deletion strain, was unable to grow on medium containing vanillin or vanillate, but able to grow on pyruvate. These gene deletion strains were then provided to us for use in the incubations with lignocellulose.

2.3 Testing of Δvdh and $\Delta vanA$ gene deletion strains in incubations with wheat straw lignocellulose.

It is presumed *R. jostii* RHA1 carrying a deletion of one of these genes may form a bottleneck in the metabolic flux of lignin degradation and potentiate a build-up of observable intracellular or extracellular metabolites.

Incubations with the gene deletion strains of *R. jostii* RHA1 were conducted using the method previously utilised with the wild type experiments. Initial data gained from HPLC-UV and GC-MS did not indicate the presence of any new peaks not present in the controls.

However, a nutrient-rich environment such as that provided by the LB broth is tailored to suit the requirements of *Escherichia coli* and may not afford a situation that promotes lignocellulose degradation in soil bacteria. Thus, a new method was required to stimulate and encourage growth on lignocellulose as a carbon source. Both mutants and wild type strain of *R. jostii* RHA1 were grown, with shaking, for a total of three days at 30 °C in a sterile filtered minimal media, named growth media P1 (pH 7.0) containing 42.3 mM Na₂HPO₄ (anhydrous), 22.0 mM KH₂PO₄, 8.5 mM NaCl, 18.6 mM NH₄Cl, 1 mM MgSO₄, 100 µM CaCl₂, 100 µM MnCl₂ and 10 µM FeSO₄. This was then supplemented with 1% glucose (w/v) and 2.5% milled wheat straw lignocellulose (w/v) as the carbon source.

Subsequent subculturing on growth media P1 agar plates supplemented with 2.5% milled wheat straw (w/v) and a decreasing gradient of glucose concentrations, yielded a final bacterial strain capable of growing on 2.5% milled wheat straw (w/v) and just 0.05% glucose (w/v). The bacteria were kept on plates at 4°C for a maximum of 2 months.

2.3.1 Growth observations with the Δvdh and $\Delta vanA$ gene deletion strains in incubations with wheat straw lignocellulose in liquid growth media P1.

A single colony from the subcultured plates was grown for 2 days in liquid M9 minimal media and 0.1% glucose and then used in incubations with 2.5% wheat straw lignocellulose (w/v) and 0.1% w/v glucose in growth media P1 over a period of 7 to 10 days. A lag phase of between 2-4 days was observed in all growth experiments.

Interestingly, a pattern in growth was observed using the mutant strains of *R. jostii* RHA1 and was consistently seen in repeated incubations (Figure 46). Whilst the timing of the pattern in OD₆₀₀ was erratic over many experiments, the general shape was consistent.

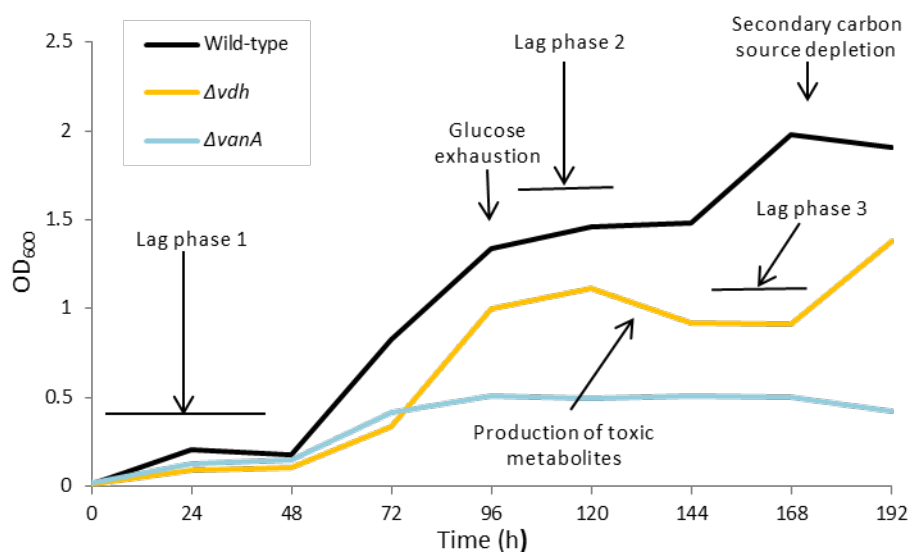


Figure 46: An example of the cell growth of *R. jostii* RHA1 wild type and the Δvdh and $\Delta vanA$ gene deletion strains grown in growth media P1 with 2.5% lignocellulose (w/v) and 0.1% glucose (w/v) appears to show a pattern of cellular growth in two to three phases, and illustrates a diauxic-type growth curve.

The initially long lag phase before the start of exponential growth exhibited by *R. jostii* RHA1 has been observed previously in experiments by researchers using this

organism.^{[172]–[174]} A secondary lag phase however, also seems to be occurring in incubations with the subcultured wild type and *Δvdh* mutant, RHA045. This could indicate a period of diauxic growth, which sees a degree of glucose exhaustion and a period in which *R. jostii* synthesises the necessary enzymes involved in lignocellulose degradation. The wild type strain exhibits a spurt of exponential growth after the second lag phase consistent with this premise, however, the incubations with the *Δvdh* mutant show a period in which the OD₆₀₀ decreases. A decrease in OD₆₀₀ could signify cell lysis due to the accumulation of toxic metabolites within the cell. Interestingly, in the growth curve of the *Δvdh* mutant a possible further, almost triaaxic-like period of growth is observed.

2.3.2 Metabolite analysis on samples taken from the *Δvdh* and *ΔvanA* incubations with wheat straw lignocellulose in liquid growth media P1.

Samples were taken and processed as previously mentioned and this time the results did provide evidence of new metabolites in the growth media. In the case of the *ΔvanA* mutant, RHA046 there was no detectable metabolite concentrations that differed from controls. However, samples taken from incubations with the *Δvdh* mutant showed a remarkable increase in quantity and concentration of metabolites.^[175]

This can be most clearly observed in a GC-MS total ion chromatogram (TIC) taken from the incubations with *Δvdh* mutant, RHA045 after 120 hours (Figure 47). In comparison with a sample taken from the wild type incubation at the same time point, it can be evidently seen that fermentations with the gene deletion strain of *R. jostii* RHA1 results in a substantial increase in both quantity and intensity of peaks in the chromatogram.

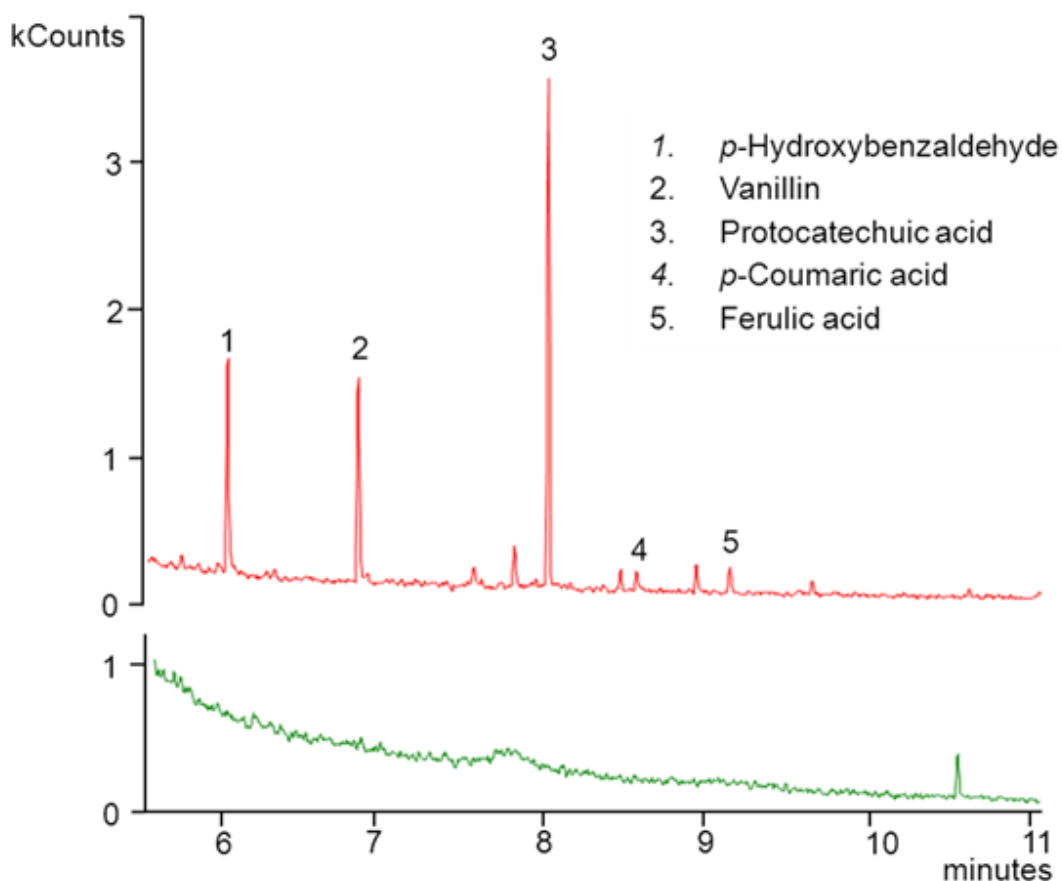


Figure 47: Detection by GC–MS of aromatic metabolites from cultures of Δvdh mutant RHA045 (top), compared with wild-type strain (bottom), grown on minimal media containing 2.5% wheat straw lignocellulose (w/v) and 0.1% glucose (w/v) in M9 minimal media, after 120 h.

Identification of the peaks was made by comparison of fragmentation patterns and retention times of compounds in a customised reference library created by the author (Appendix I). This approach in metabolomics using standard reagents can be prohibitively labour-intensive and the resulting library often inadequate because many compounds of interest are unknown or just not commercially available. A number of the peaks, however, were identified and the presence of aldehydes: 4-hydroxy-3-methoxybenzaldehyde (vanillin), 4-hydroxybenzaldehyde (*p*-hydroxybenzaldehyde) and organic acids: 3,4-dihydroxybenzoic acid (protocatechuic acid), (3-(4-hydroxyphenyl)-2-propenoic acid (*p*-coumaric acid) and 3-(4-hydroxy-3-methoxyphenyl)-2-propenoic acid (ferulic acid) was confirmed.

The presence of the aldehydes is especially significant and is consistent with the hypothesis that the *vdh*-knockout-mediated blockage of the vanillic acid pathway greatly increases levels of target metabolites in incubations with lignocellulose. Both vanillin and *p*-hydroxybenzaldehyde are potential aromatic intermediates in the oxidation of the *p*-hydroxyphenyl (H) and guaiacyl (G) phenylpropanoid components of lignin, both present in wheat straw.

The detection of protocatechuic acid in the incubations is unexpected, since it occurs after the *vdh* gene on the vanillic acid catabolic pathway. Its metabolism via the β -ketoacid pathway in *R. jostii* RHA1 should be unchallenged. One hypothesis could be that protocatechuic acid is formed by slow demethylation of vanillin by vanillic acid demethylase, generating a reactive 3,4-dihydroxybenzaldehyde shunt metabolite that is further oxidized to PCA (Figure 48).

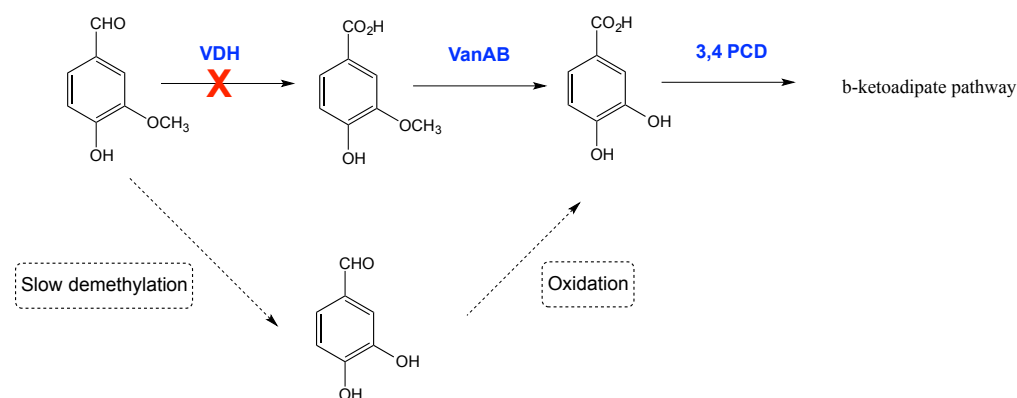


Figure 48: The protocatechuic acid observed in GC-MS spectra could be formed by the oxidation of 3,4-dihydroxybenzaldehyde formed from a slow enzymatic demethylation of vanillin.

After identification by GC-MS the detected metabolites were followed using LC-MS analysis on samples taken from the incubations. Metabolites were extracted using ethyl acetate, solvent removed *in vacuo* and analysed by LC-MS in positive and negative modes. Protocatechuic acid, *p*-coumaric acid and vanillin were all monitored

at 280 nm; 254 nm was used to detect vanillic acid and 325 nm for ferulic acid. Calibration curves were made for all compounds. Stock solutions were prepared in methanol/water (1:1 v/v) using the following range of concentrations: 300 to 0.10 mg/L.

It can be seen within the EIC for m/z 153.8 (corresponding to the positively charged ion of vanillin) a peak is observed with a retention time (RT) of 15.0 mins (Figure 49). Peaks corresponding to the positively charged ions of other compounds were also observed within EICs for m/z 124.0 (Figure 50), 165.7 (Figure 51), 195.5 (Figure 52) and 169.7 (Figure 53). These corresponded to *p*-hydroxybenzaldehyde (RT 13.2 mins), *p*-coumaric acid (RT 15.6 mins), ferulic acid (RT 17.1 mins) and vanillic acid (RT 11.1 mins) respectively.

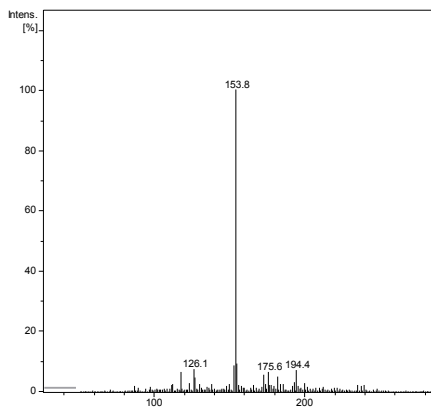
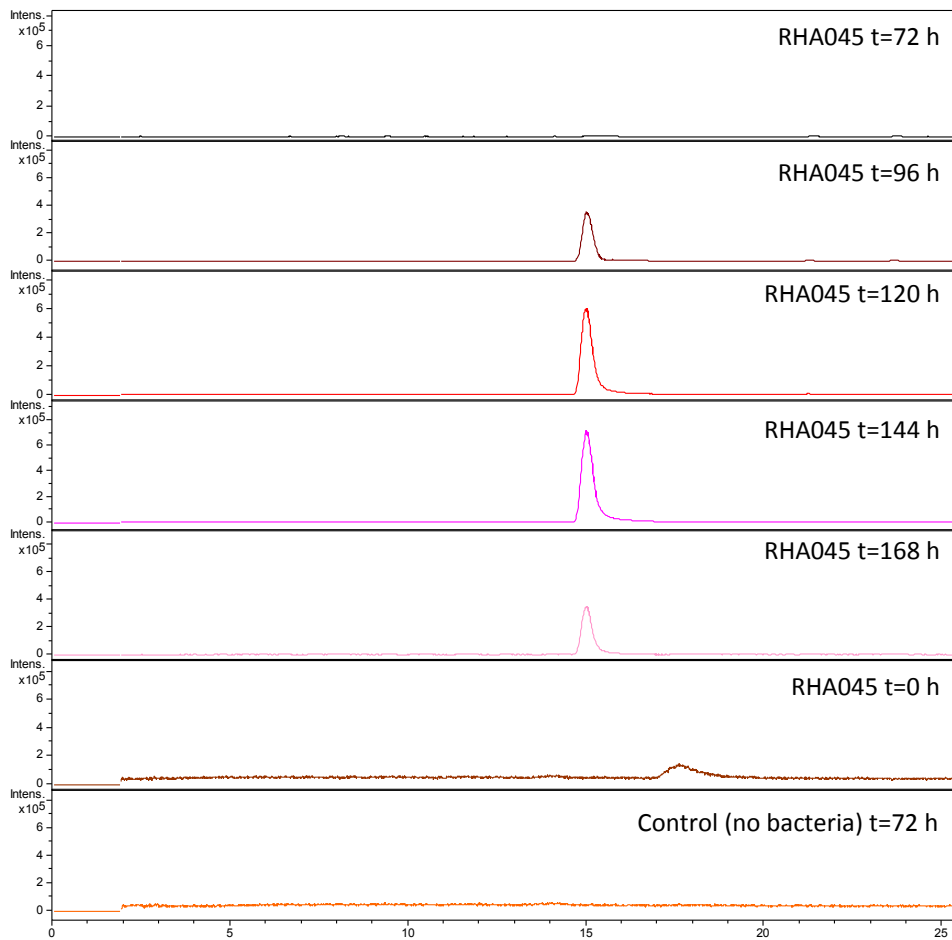


Figure 49: EIC for m/z 153.8 corresponding to the positively charged ions of vanillin (RT 15.0 min) from cultures of Δvdh mutant RHA045 (top), compared with control @ t=72h (no bacteria), grown on minimal media containing 2.5% wheat straw lignocellulose (w/v) and 0.1% glucose (w/v) in M9 minimal media. (LC-MS was unable to detect the appearance of any metabolites not in control samples before t=72 h)

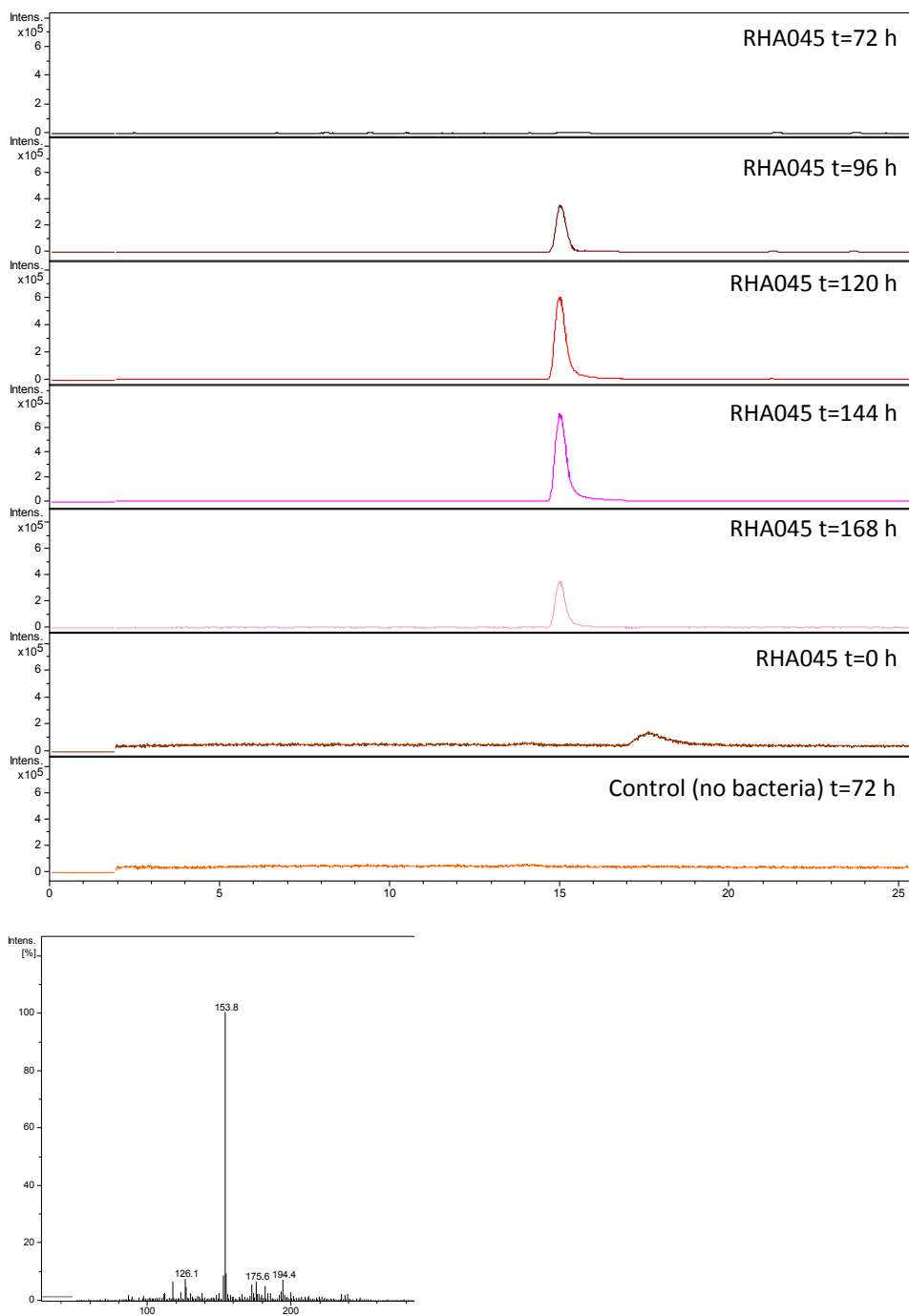


Figure 50: EIC for m/z 124.0 corresponding to the positively charged ions of p-hydroxybenzaldehyde (RT 13.2 mins) from cultures of Δvdh mutant RHA045 (top), compared with control @ t=72h (no bacteria), grown on minimal media containing 2.5% wheat straw lignocellulose (w/v) and 0.1% glucose (w/v) in M9 minimal media. (LC-MS was unable to detect the appearance of any metabolites not in control samples before t=72 h)

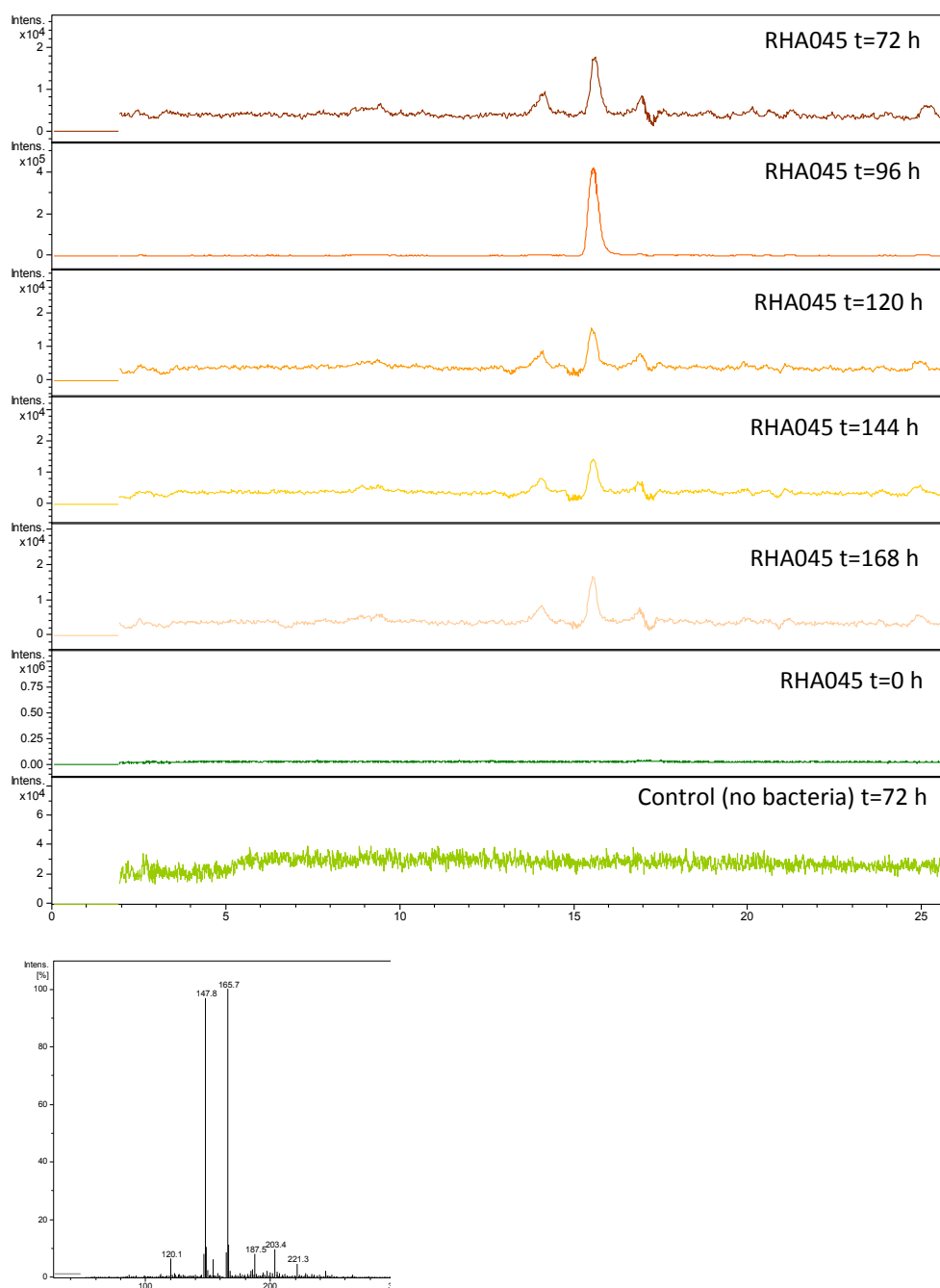


Figure 51: EIC for m/z 165.7 corresponding to the positively charged ions of p-coumaric acid (RT 15.6 mins) from cultures of Δvdh mutant RHA045 (top), compared with control @ t=72h (no bacteria), grown on minimal media containing 2.5% wheat straw lignocellulose (w/v) and 0.1% glucose (w/v) in M9 minimal media. (LC-MS was unable to detect the appearance of any metabolites not in control samples before t=72 h)

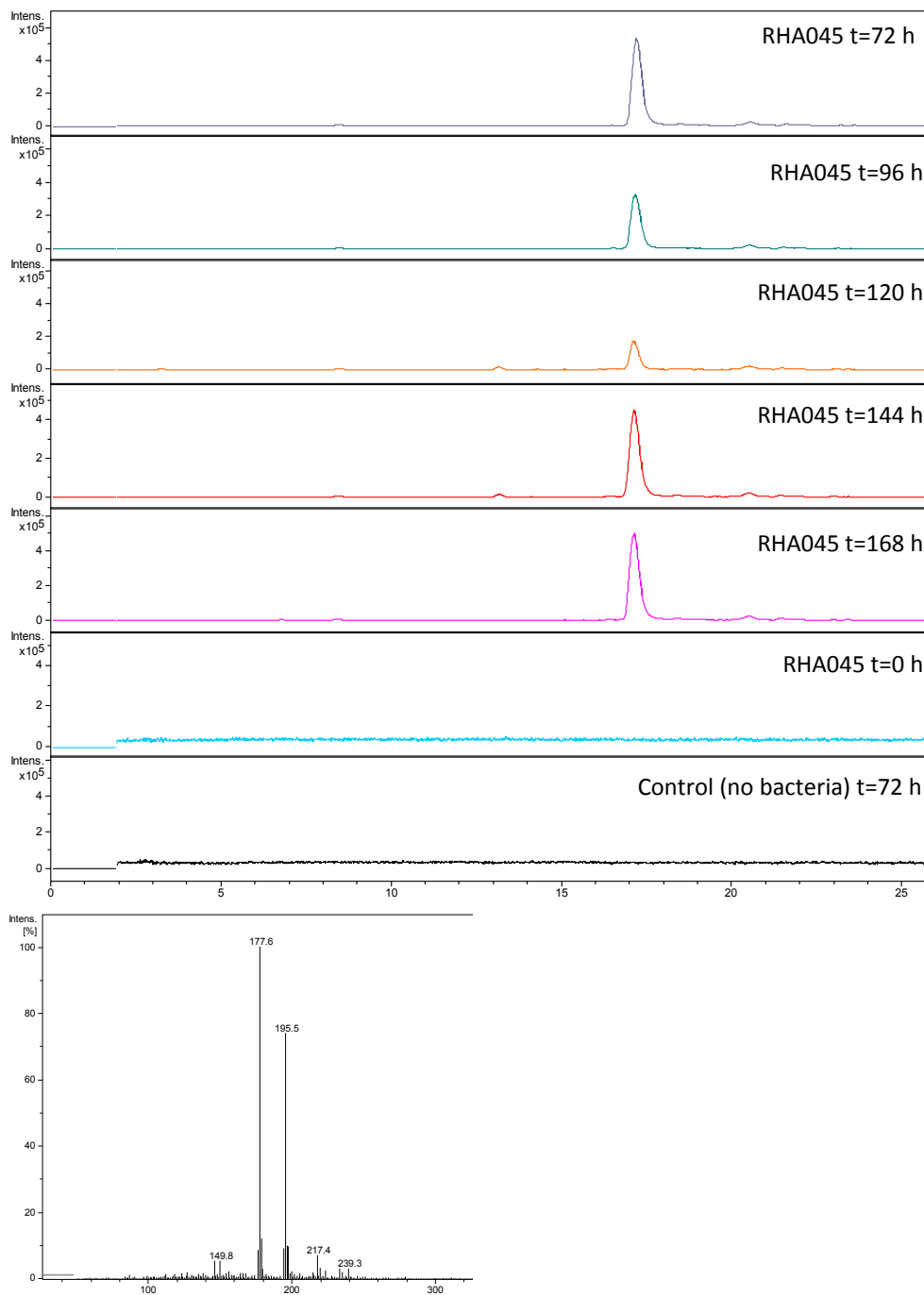


Figure 52: EIC for m/z 195.5 corresponding to the positively charged ions of ferulic acid (RT 17.1 mins) from cultures of Δvdh mutant RHA045 (top), compared with control @ $t=72h$ (no bacteria), grown on minimal media containing 2.5% wheat straw lignocellulose (w/v) and 0.1% glucose (w/v) in M9 minimal media. (LC-MS was unable to detect the appearance of any metabolites not in control samples before $t=72 h$)

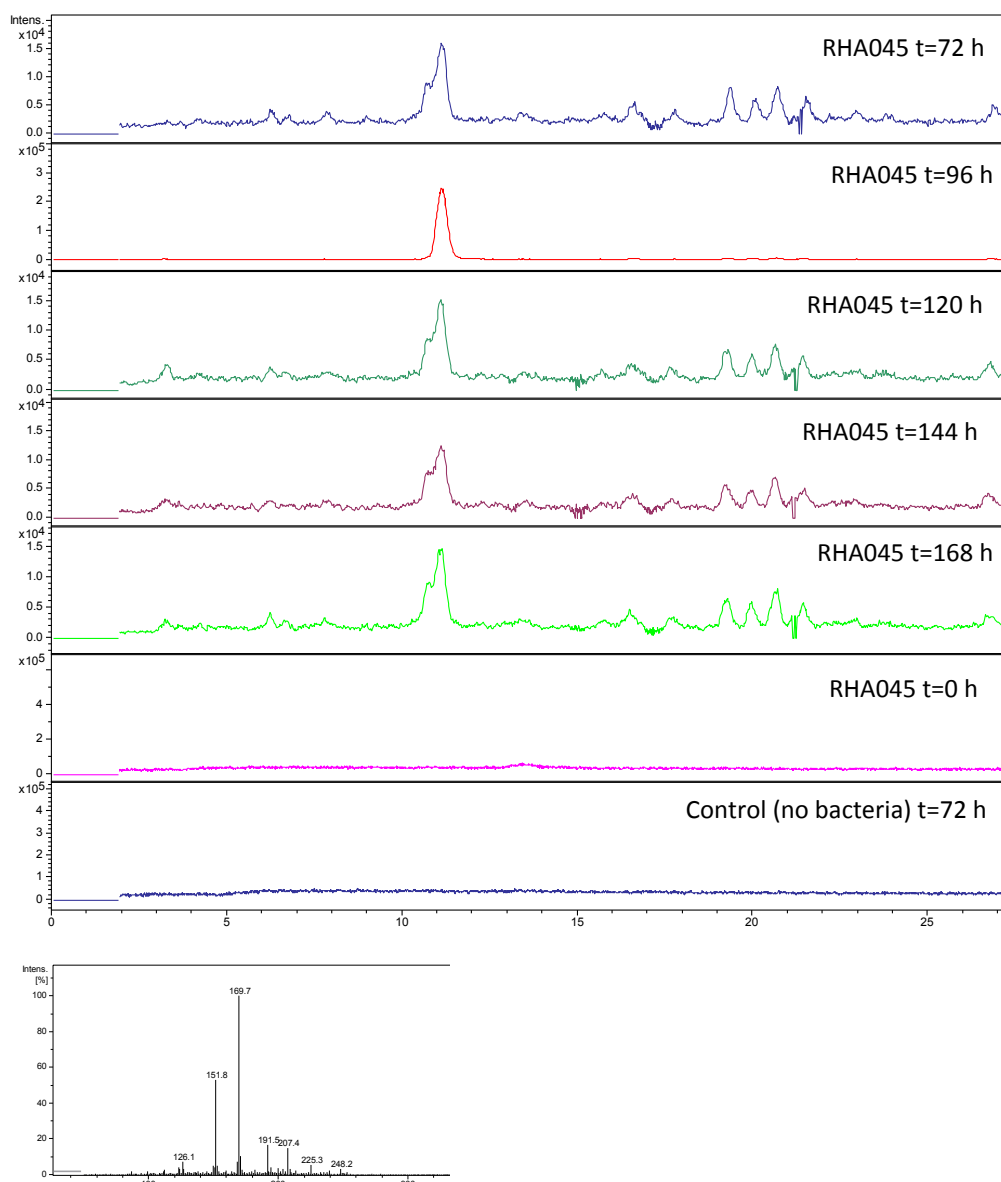


Figure 53: EIC for m/z 169.7 corresponding to the positively charged ions of vanillic acid (RT 11.1 mins) from cultures of Δvdh mutant RHA045 (top), compared with control @ $t=72h$ (no bacteria), grown on minimal media containing 2.5% wheat straw lignocellulose (w/v) and 0.1% glucose (w/v) in M9 minimal media. (LC-MS was unable to detect the appearance of any metabolites not in control samples before $t=72 h$)

Protocatechuic acid was not detected in any of the samples prepared for LC-MS, the appearance of vanillic acid in samples after 96 hours was however noted in these experiments. Compounds were confirmed by the retention time of analytical standards.

The highest concentrations of vanillin extracted from each experiment with the milled wheat straw lignocellulose ranged from approximately 1 to 96 mg/L. Concentrations (mg/L) were approximated by 6-point calibration curves of authentic standards. An example of concentrations extracted from the incubation producing the highest yield of target metabolites is presented in Table 2 and the growth curve from the same experiment is displayed in Figure 54.

Metabolite concentrations in experiments could vary 100 fold under the same conditions for the same time period, but a similar pattern between the growth curve and detection was still observed.

Table 2: The highest concentrations of detected metabolites found during an experiment are displayed. The metabolites were identified using LC-MS and their concentrations determined by plotting calibration curves (mg/L)

Time (h)	<i>p</i> -Hydroxybenzaldehyde (mg/L)	Vanillic Acid (mg/L)	Ferulic acid (mg/L)	Vanillin (mg/L)	<i>R. jostii</i> RHA1O45 OD ₆₀₀
0	0.00	0.00	0.00	0.00	0.035
3	0.00	0.00	0.00	0.00	0.011
6	0.00	0.00	0.00	0.00	0.121
24	0.00	0.00	0.00	0.00	0.098
48	0.00	0.00	0.00	0.00	1.321
72	0.00	2.52	114.33	0.00	1.311
96	0.74	121.34	54.35	37.07	1.295
120	53.11	4.52	23.23	85.59	1.118

144	49.79	2.88	86.38	96.20	1.007
168	0.78	4.05	101.94	39.34	0.998
172	<0.01	<0.01	97.73	<0.01	1.295

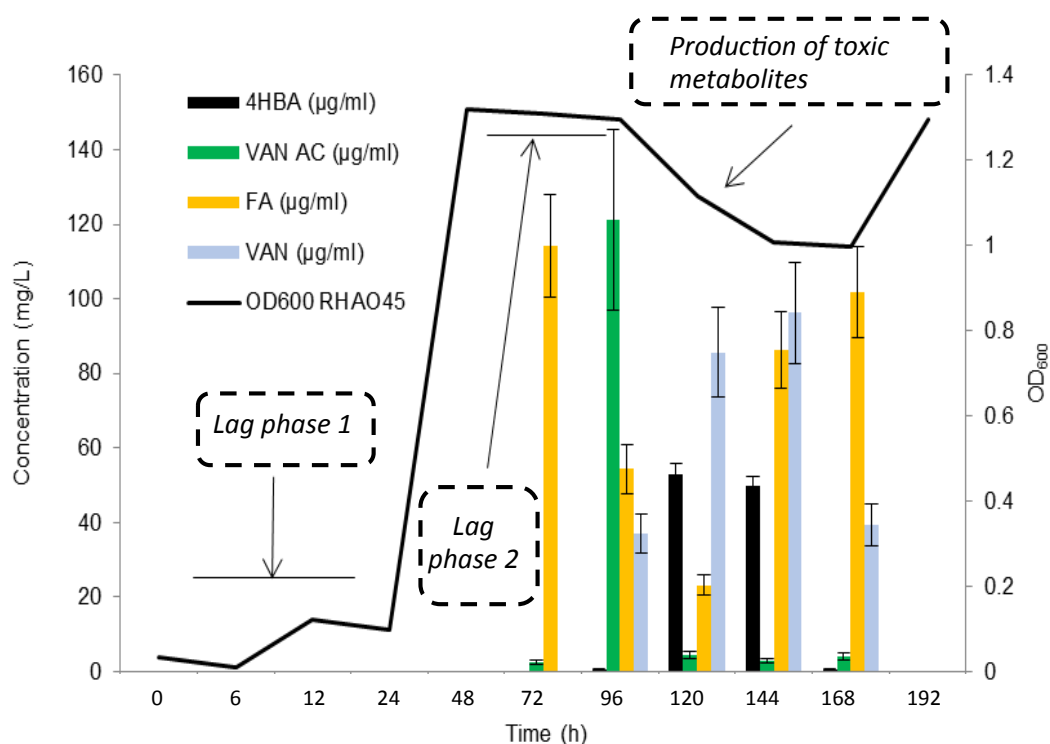


Figure 54: Concentrations of detected metabolites plotted against growth curve from same experiment.

It can be seen from the graph that the appearance of vanillin does indeed seem to coincide with a decrease in the OD₆₀₀ reading in this experiment (Figure 54). Vanillin is a highly toxic metabolite to many bacteria, including *R. jostii* RHA1, and has previously been shown to inhibit growth at concentrations >1 mM. The maximum concentration of vanillin ever detected in all incubations performed was 630 µM and approaches the maximum level tolerated by *R. jostii* RHA1 (1-1.5 mM).^[143]

This seems to support the earlier notion that a blockage in the metabolic flux of the gene deletion strain may cause cell lysis and a fall in observable cell density. A reduction in vanillin concentration coupled with a triauxic-like period of growth is also seen from 192 hours in this experiment could indicate a potential compensation for the blockage of individual reactions by the rerouting of metabolic flux through other pathways. A period of high concentrations of ferulic acid at 72 hours and again at 144 hours can also be visualised in the graph.

Ferulic acid was also identified by GC-MS in the incubations with lignocellulose in with concentrations high enough to monitor by LC-MS. The GC-MS analysis on samples from many of the incubations, including the controls without bacteria, ambiguously indicated the possible presence of other ferulate-type molecules such as dimeric ferulates and dehydroferulates.

The mass spectrum fragmentation patterns of these molecules displayed some similarities, but not enough detail for reliable identification. A common base peak in the mass spectra of these compounds appeared at m/z 194 and could correspond to the ferulate ion. An ion at m/z 177 was also seen that could have arisen from the cleavage of the ferulate ester bond. Whilst these observations were not enough for positive characterisations, it indicated the possible presence of trace amounts of ferulates in the autoclaved milled wheat.[176]

2.3.3 Testing of Δvdh and $\Delta vanA$ gene deletion strains in incubations with hemicellulose.

Ferulic acid is joined to the arabinoglucuronoxylans in the hemicellulose layer of lignocellulose via ester bonds and acts as a linkage to the lignin matrix via ester and ether linkages (Figure 55).[177] The bacterial conversion of free ferulic acid to

vanillin has been studied in pseudomonads, bacillales and actinomyces.[144], [149], [178]–[180]

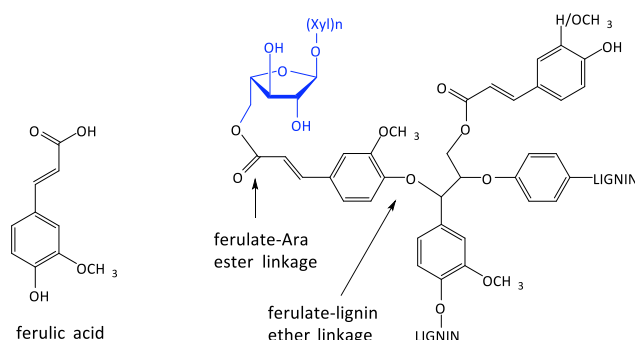


Figure 55: A simplified example of how ferulic acid may crosslink the arabinoglucuronoxylan hemicellulose to lignin

To identify whether the metabolites were coming from this more accessible hemicellulose layer or from linkages within the more fortified lignin structure, experiments were undertaken to ascertain if *R. jostii* RHA1 could metabolise the hemicellulosic xylan polysaccharide and ferulic acid to produce a similar spectrum of products.

Wild type and both gene deletion strains were grown on M9 minimal media containing 0.1% glucose (w/v) and in the presence of 0.1% beechwood xylan (w/v) (Sigma Aldrich, UK). The experiments were performed under the same conditions as in the lignocellulose experiments. It was not possible to obtain growth curves due to the turbidity of the solution, but samples taken from the experiments were re-streaked on LB agar plates to indicate growth. Samples taken from the media after 60 hours failed to grow on LB plates perhaps suggesting that the beechwood xylan was in fact toxic to the organism at the levels used for this experiment.

LC-MS and GC-MS were used as with previous experiments, but did not reveal any indication of identifiable metabolites. Whilst these growth experiments on beechwood

xylan cannot offer definitive answers on bacterial interactions with the complex hemicellulose layer of plant cell walls, further analysis is beyond the scope of this project.

2.3.4 Testing of Δvdh and $\Delta vanA$ gene deletion strains in incubations with ferulic acid.

The bioconversion of ferulic acid to vanillin from a cleaved ferulate linker could be responsible for the identified metabolites, and experiments detailing the production of vanillin from ferulic acid have been reported.[179]–[184]

The two gene deletion strains and the wild type *R. jostii* RHA1 were grown on 0.1% ferulic acid and 0.1% glucose in M9 minimal media (pH adjusted to 7).

Only trace amounts of vanillin <0.5 mg/L were observed in the experiments with the Δvdh mutant, but conversely relatively high concentrations of vanillic acid were observed (>100 mg/L).

Samples taken from experiments using the $\Delta vanA$ mutant also presented with similarly high concentrations of vanillic acid (Figure 56).

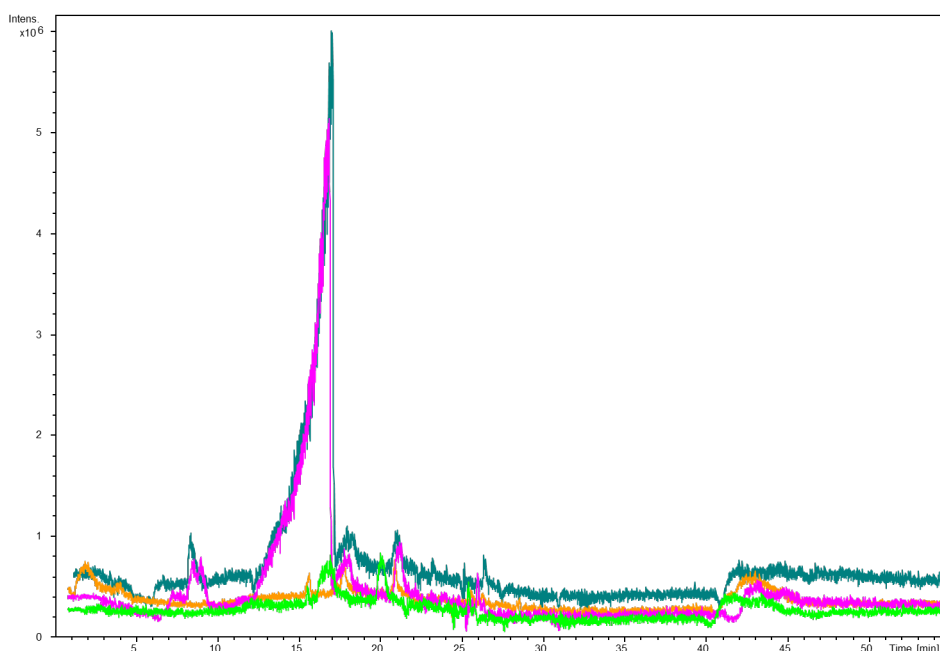


Figure 56: Strains of *R. jostii* RHA1 grown on 0.1% ferulic acid and 0.1% glucose in M9 minimal media. Samples taken at 96 h. EIC 169.2 m/z for Δ vanA mutant (blue), Δ vdh mutant (pink) wild type (green) control with no bacteria (orange). The peaks were confirmed as vanillic acid from the EIC of an authentic standard with a retention time of 15.9 min.

This new data was also the first time evidence of metabolic flux disruption in the Δ vanA mutant had been seen, in contrast with experiments using the previous alternative carbon sources.

2.4 Attempts to confirm partial bacterial lignin degradation pathways

In combination, the data starts to provide a clearer picture of the enzymatic breakdown of the wheat straw lignocellulose by *R. jostii* RHA1. The results indicate an initial hydrolysis of ester linkages in the lignocellulose and can explain the appearance of ferulic acid quantified by LC-MS and the GC-MS detection of *p*-coumaric acid seen after 72 hours.

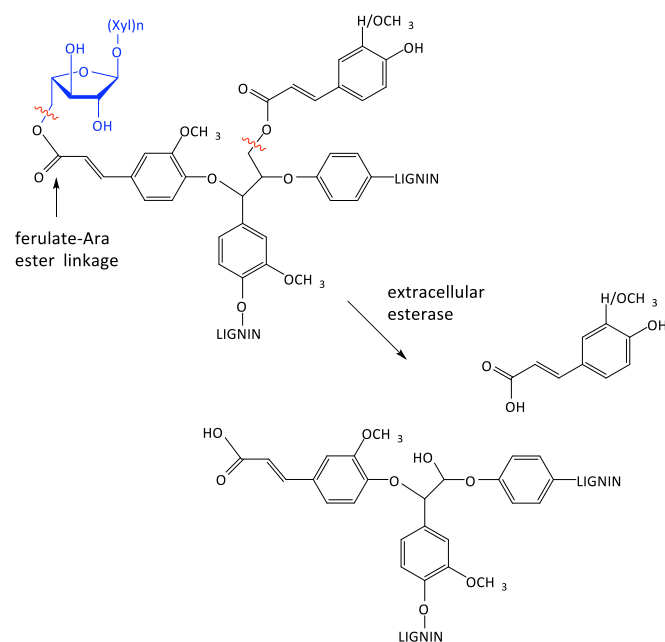


Figure 57: A hydrolysis of the ester linkages in lignocellulose could account for the initial release of the phenylpropanoid units seen after 72 hours. Theoretically this would also be accompanied by the simultaneous release of a lignin fragment

The detection of vanillic acid after 96 hours in incubations with the Δvdh gene deletion strain is unpredicted as the metabolic pathway to vanillic acid was considered blocked in this mutant. It could therefore be hypothesised that ferulic acid may be converted directly to vanillic acid via β -oxidation rather than via vanillin, as has been documented in a number of other bacterial strains (Figure 58).[164], [185]

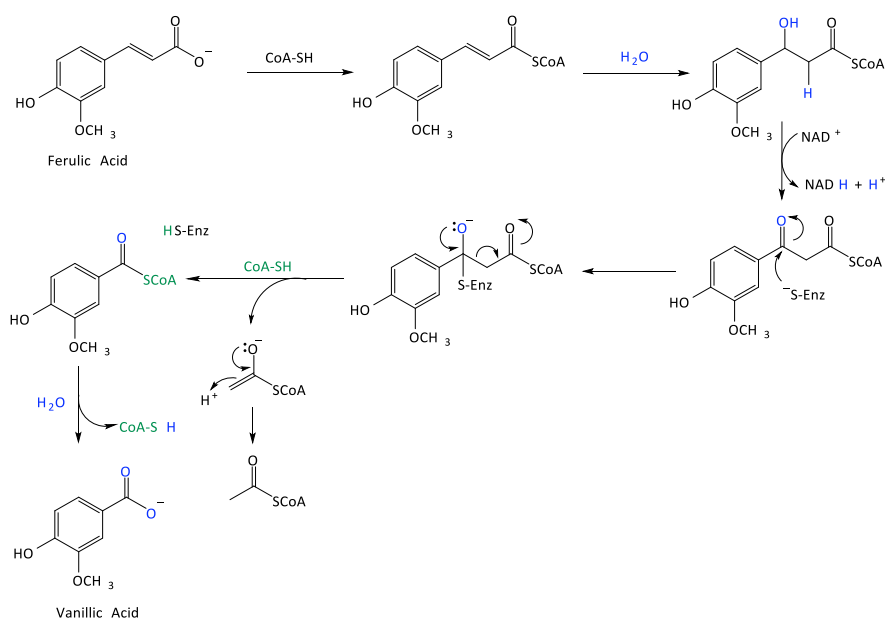


Figure 58: The β -oxidation pathway for the metabolism of ferulic acid to vanillic acid.

Should the ester hydrolysis of lignocellulose be responsible for the release of hemicellulosic phenylpropanoid linker units, it could be inferred that a lignin fragment would also be cleaved and responsible for the metabolites extracted in the later samples.

This lignin fraction could undergo an oxidative cleavage of the C_α - C_β bond and the benzylic C-O bond to generate vanillin and the second appearance of ferulic acid seen from 120 hours.

The oxidative cleavage of C_α - C_β bonds by a DypB peroxidase from *R. jostii* RHA1 has already been observed on a similar model compound by Ahmad *et al* (2011) and lends weight to the explanation.^[106]

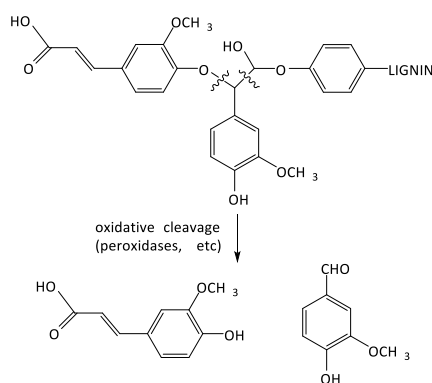


Figure 59: In this example of a lignin fragment it can be seen how an oxidative cleavage of the α - β carbon bond and the benzylic C-O bond could generate vanillin and ferulic acid linkages in lignocellulose

2.4.1 Testing of Δvdh and $\Delta vanA$ gene deletion strains in incubations with alkali treated wheat straw lignocellulose

To establish that vanillin is formed from the lignin fragment, the milled wheat straw was subjected to an alkaline treatment to replicate the enzymatic hydrolysis of ester linkages before incubations.

Adapted from the procedure of Sun *et al* (1996)^[120] milled wheat straw (15 g) was added to 1.5% wt/v NaOH (300 ml) and left to stir in a glass beaker for two hours. The slurry was filtered through Whatman # 1 filter paper using a Buchner funnel. The solid residue was removed and washed several times with H₂O and then freeze dried. The filtrate was acidified to pH 6.5 with acetic acid and then concentrated *in vacuo*. The extract was then mixed with five volumes of ethanol and left overnight. Any precipitated hemicelluloses and hemicellulosic-lignin was removed by Buchner filtration and the filtrate then acidified to pH 1.5 with 6N HCl and left for 24 hours. The alkali-soluble lignin precipitate was collected by centrifugation at 4702 x g for 10 minutes and the pellets freeze-dried overnight to give a 1.2% yield (180 mg).

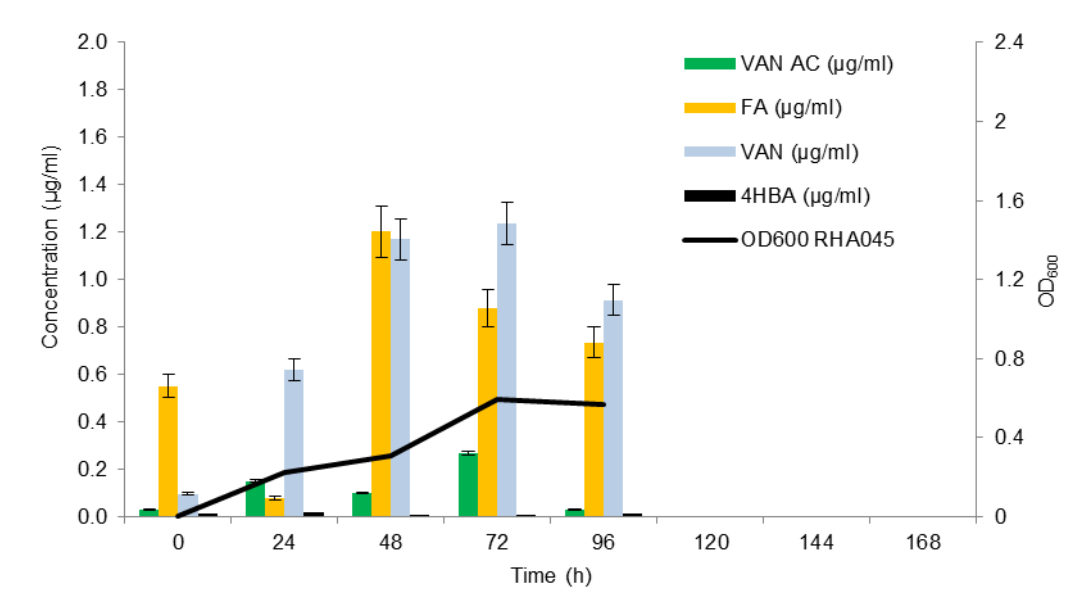


Figure 60: Concentrations of detected metabolites from incubations with wheat straw alkali lignin plotted against growth curve from same experiment.

Fermentations were performed as previous with RHA045 and 0.5% w/v of the solid NaOH treated wheat straw residue, but these did not see the production of any detectable metabolites, with the bacteria showing a death phase in the growth curve after 4 days. In comparison, the conversion of the alkali lignin fraction (0.5% w/v) by RHA045 to generate detectable metabolites occurred much more rapidly than any previous incubation (Figure 60). Vanillin was detected after 24 hours, with the highest concentration of approx. 1.3 mg/L being observed in a sample taken after 48 hours. A similar concentration of 1.3 mg/L for ferulic acid was also detected in the samples taken at 48 hours.

The data obtained with the alkali treated lignocellulose is consistent with the theory that metabolite production is initiated by an extracellular esterase and the production of vanillin is by degradation of the lignin fraction.

Although there are no annotated ferulic acid esterases in the *R. jostii* RHA1 genome that might initiate the first step, there are some putative extracellular hydrolases

(ro08551, ro02616, ro03139) sharing sequence similarity with an extracellular *Streptomyces* esterase EstA.

2.5 Kraft lignin

As a by-product of the paper/pulp industry, Kraft lignin is of particular interest as a potential source of aromatic chemicals. The Kraft lignin already has an intrinsic value for paper mills by being burnt for fuel, but potentially its value could be upgraded should it become a source of chemical feedstocks. There are many factors involving analysis on Kraft lignin that have to be considered, such as whether the source is hardwoods or softwoods and also the sulphate, carbonate and protolignin content. Traditionally, it is believed industrial kraft lignin has a lower sulphate and carbonate content and a higher condensed protolignin content than laboratory lignin reproduced by a 'kraft-like' process. In an attempt to recognise these differences, within the resources available, experiments were performed on a laboratory lignin (Sigma-Aldrich, UK) and an industrial lignin from spruce, a softwood (BillerudKorsnäs, Sweden).

Both of the highly condensed lignin preparations were first examined as a carbon source for growth. Slow growth of all strains of *R. jostii* RHA1 was observed on P1 media containing 0.5% (w/v) industrial and laboratory Kraft lignin and 0.05% (w/v) glucose over 14 days. A modified method was employed to study metabolites via LC-MS analysis in which an isocratic gradient was used from 3 to 5 minutes to separate polar compounds that may have previously been eluting too quickly from the column using the earlier method. Trace amounts of vanillin and vanillic acid were again observed using EICs on extractions from both types of Kraft lignin controls without bacteria (Figure 62).

When observing the growth curve of the strains on the Sigma Kraft lignin (Figure 61), the initial growth could be explained by glucose consumption that ceases rapidly in the experiments with the mutant strains. Growth by the Δvdh mutant RHA045 appeared to be hindered whilst further growth by $\Delta vanA$ mutant RHA046 was not possible at all suggesting a catabolic pathway that proceeds via vanillic acid is important for growth on this carbon source.

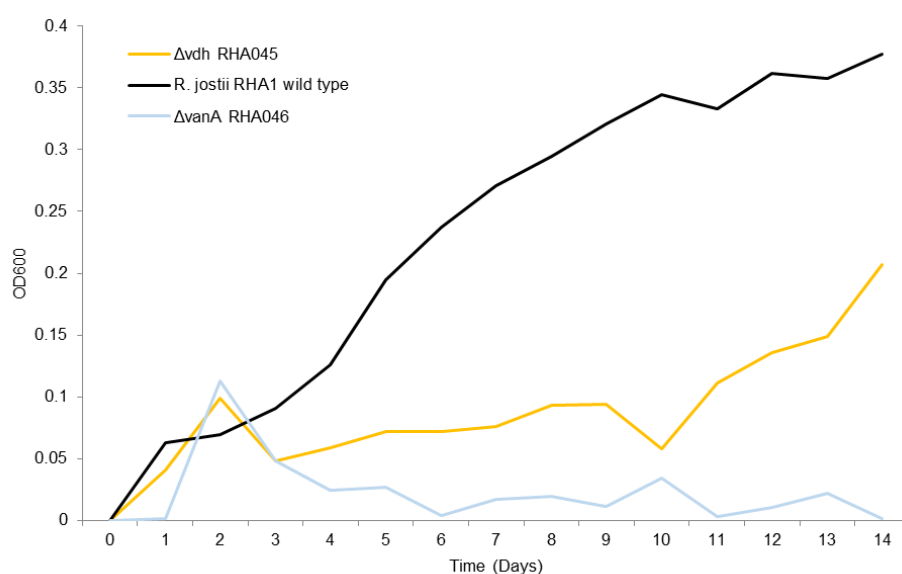


Figure 61: Cell growth of *R. jostii* wild type and the Δvdh and $\Delta vanA$ strains grown in growth media P1 with 0.5% kraft lignin and 0.1% glucose.

Kraft lignin is produced in a highly alkaline process and is not the same as the native lignin found in wood matrix. The alkali depolymerizes lignin by ether bond cleavage and the resulting products could already include some low molecular weight compounds, explaining the trace metabolites observed in controls. Metabolite production when grown on kraft lignin was rather variable. however, the EIC using samples from cultures of the RHA045 mutant did appear to show an accumulation of vanillin up to a maximum of 13 mg/L vanillin after 5 days in one incubation (Figure 62).

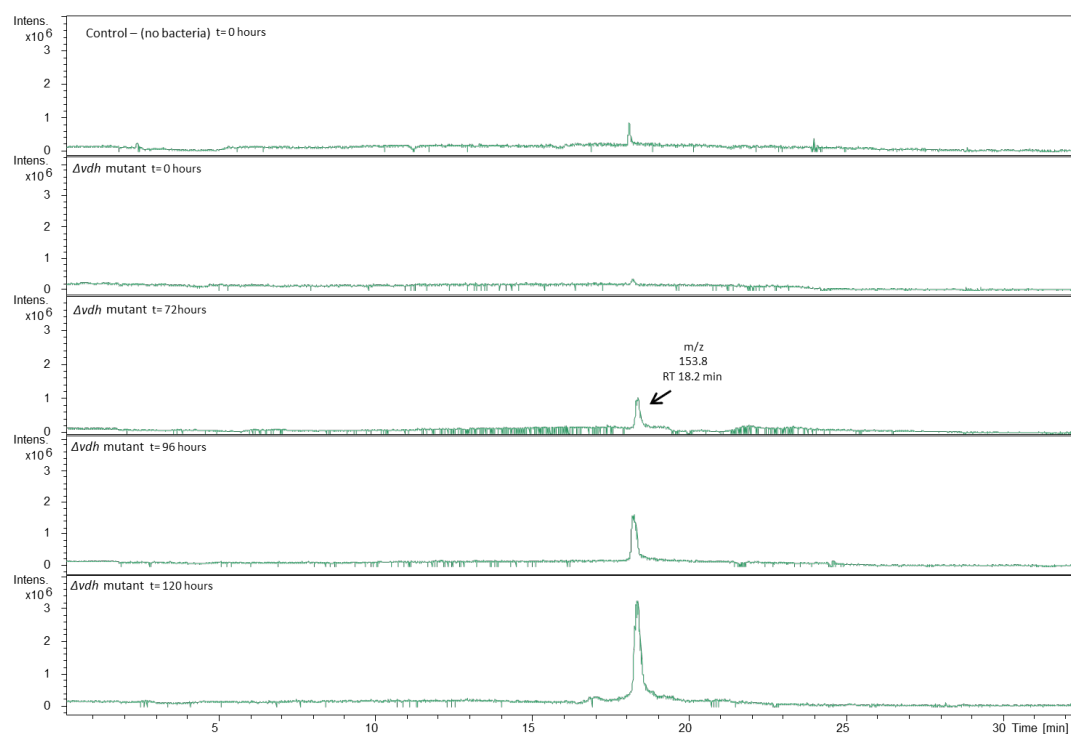


Figure 62: EIC for m/z 153.8 corresponding to the positively charged ions of vanillin (RT 18.2 min) on extractions from samples taken from incubations with *R. jostii* RHA1 Δvdh with 0.5% industrial Kraft lignin (BillerudKorsnäs, Sweden). Samples taken at $t= 0, 72, 96$ and 120 h

Similarly, cultures of the RHA046 were shown to accumulate up to 0.1 mg/L vanillic acid after 4 days of incubation (data not shown).

Most experiments performed using Kraft lignin rarely produced yields above 1 mg/L of target products, even when a pattern of accumulation was observed. In addition, the amounts of each of the compounds that accumulated did vary significantly from one run to the next, and no meaningful accumulation at all was observed when laboratory Kraft lignin (Sigma-Aldrich) was used as a substrate.

Occasionally, during some of the incubations, a gelatinous layer could be visibly seen accumulating over time indicating a potential radical repolymerisation of lower molecular weight products or the production of lipids. HPLC-UV and FT-IR spectral data was inconclusive, but it is possible that the DYP peroxidases identified in

R. jostii RHA1 could cause radical formed hydroxyl groups of low molecular weight products, which re-polymerise and become more insoluble.

The investigations into bacterial metabolism of Kraft lignin by *R. jostii* RHA1 is thus complicated as the results could indicate that bacteria cannot metabolise either the condensed or repolymerised fraction of the Kraft lignin but only the low molecular weight products that were produced during the Kraft process itself. This explanation would account for the pattern in growth curve, the low level of target products produced after incubations and the identification of metabolites in the starting material.

In any case, metabolic degradation of the Kraft lignin structure by *R. jostii* RHA1 by this process is rather slow and only proceeds to a limited extent, if at all. Incubations were generally unreliable in producing any useful products and proved a much less efficient process than successful experiments with lignocellulose.

Results and Discussion II

3: Results and Discussion II: Chemical inhibition of selected enzymes proposed to be involved in lignin breakdown

Having successfully developed a gene knockout technique to yield target metabolites from the bacterial breakdown of lignin, attention was then focused on an alternative chemical approach. As a technique that may be used with bacteria not amenable to genetic modification chemical inhibition presents a great advantage. The inhibitor must however, be selective and readily transported through a cellular membrane in concentrations significant enough to have an inhibitory effect.

If an enzyme on a chosen pathway was chemically inhibited, the substrate for that enzyme would again theoretically build up and this blockage in metabolic flux may be detectable. In attempts to increase target metabolite production from the bacterial breakdown of lignin, enzyme inhibitors could be tested on bacteria capable of degrading aromatic compounds.

Chemical compounds designed to inhibit the enzymes on the vanillic acid pathway (Figure 63), investigated via gene deletion in chapter 2, could be used to support this hypothesis.

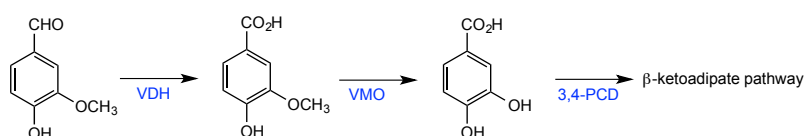


Figure 63: The enzymes selected for chemical inhibition on the vanillic acid pathway include vanillin aldehyde dehydrogenase (VDH), vanillate monooxygenase (VMO) and 3,4-protocatechuate dioxygenase (3,4-PCD)

3.1 Vanillin aldehyde dehydrogenase (VDH) as a target for chemical inhibition

The oxidation of vanillin to vanillic acid is the initial step of the vanillic acid catabolic pathway and is catalysed by a vanillin aldehyde dehydrogenase (VDH). An increase in concentration of vanillin was observed in chapter 2 in the incubations with lignocellulosic biomass using the genetically manipulated strain of *R. jostii* RHA1. This enzyme could be again be targeted for the chemical inhibition approach with the aim of reproducing the Δvdh gene deletion strain effect on lignocellulose breakdown.

Genes encoding for a vanillin aldehyde dehydrogenase (*vdh*) have been identified in a number of Gram positive and Gram negative bacteria such as *Pseudomonas fluorescens*^[180], *Pseudomonas putida*^{[144], [186]}, *Rhodococcus opacus*^[179] and *Bacillus subtilis*.^[181] Together with the *Rhodococcus jostii* RHA1 used extensively throughout this project and the *Sphingobacterium*^[110] and *Microbacterium*^[110] isolates thought to have lignin degrading capability, this represented a small collection of soil bacteria for use in the chemical inhibition experiments.^{[110], [142]–[144], [179]–[181], [187], [188]}

3.1.1 Inhibition of aldehyde dehydrogenase by disulfiram

The catalytic cysteine residue conserved across all aldehyde dehydrogenases also makes them susceptible to varying extents of chemical inhibition by reagents commonly used to modify active site thiol residues such as *N*-ethylmaleimide (NEM)^[166] (19) and the pharmaceutical disulfiram^[167] (20) used in the treatment of alcohol abuse (Figure 42).

The drug disulfiram (tetraethylthioperoxydicarbonic diamide) is a known inhibitor of human aldehyde dehydrogenase (ALDH) and a common treatment for alcohol dependence.^[167] Patients treated with therapeutic doses of the drug develop rapid and

severe negative effects upon ingestion of ethanol due to the accumulation of acetaldehyde in the blood (Figure 64).^[189]

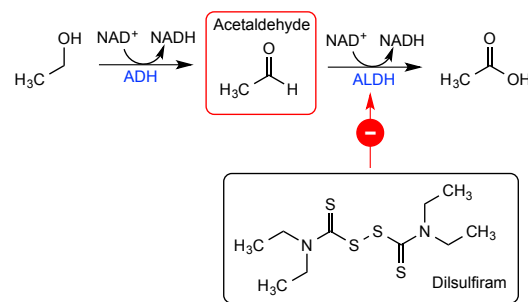


Figure 64: The oxidation of alcohol to acetaldehyde and then to acetic acid is disrupted by inhibition of aldehyde dehydrogenase (ALDH) and leads to a toxic build-up of the intermediate.

Aldehyde dehydrogenase enzymes contain a catalytic cysteine residue that is conserved in sequence alignments across all ALDHs. A covalent modification of this residue by disulfiram is thought to proceed via an initial intracellular reduction of the disulfide bond by a glutathione reductase (GSR) to liberate diethyldithiocarbamate (DDTC). Current evidence then suggests subsequent oxidation steps return a sulfoxide or sulfone metabolite capable of irreversible dithiocarbamylation of the active site cysteine (Figure 100).^{[167], [189], [190]}

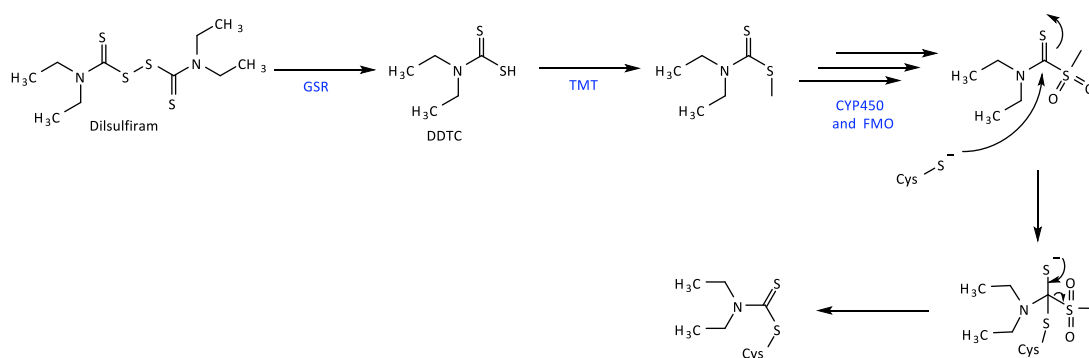


Figure 65: Intracellular glutathione reductase (GSR) is thought responsible for the liberation of DDTC which is further metabolised via a thiol methyl transferase (TMT) and then several oxidative transformations to produce a toxic metabolite capable of irreversible carbamylation to the catalytic cysteine residue.^[187]

Hypothetically, this presents the opportunity to increase vanillin concentration if the disulfiram-like reaction occurred within a lignin degrading bacterial cell targeting the bacterial vanillin ALDH and potentiate an increase in the substrate concentration.^[191]

3.1.2 Growth studies in the presence of disulfiram

The toxicity of disulfiram to the chosen strains of bacteria was evaluated by comparing the optical density at 600 nm (OD₆₀₀) over a range of time points and disulfiram concentrations. As disulfiram is practically insoluble in water the drug was first dissolved in DMSO before adding to M9 minimal media and 0.1% glucose (w/v). Concentrations above 150 µM instantly precipitated when introduced to the medium and therefore experimental conditions were limited to concentrations below this amount. Investigations were then undertaken to see which concentration of disulfiram was tolerable by the strains chosen and their ability to grow in its presence.

Before testing a chemical for its growth-inhibiting abilities it was important to understand if there are any chemical changes to the structure caused by reactions with media constituents. With this in mind, all *in vivo* chemical experiments performed during this project included controls where an identical medium was made up and inoculated after 2 days incubation.

The exposure of the bacterial strains to disulfiram had markedly varied effects on growth across the different phyla. The *Sphingobacterium* strain showed complete growth inhibition after 96 h in the presence of disulfiram even at the lowest concentration of 5 µM. *B. subtilis*, *R. opacus* and *R. jostii* RHA1 displayed complete growth inhibition at concentrations of 50 µM and over. *P. fluorescens* and *P. putida* and *M. phyllosphaerae* displayed almost normal growth patterns at all concentrations of disulfiram, compared with the experiments without any inhibitor (Figure 66).

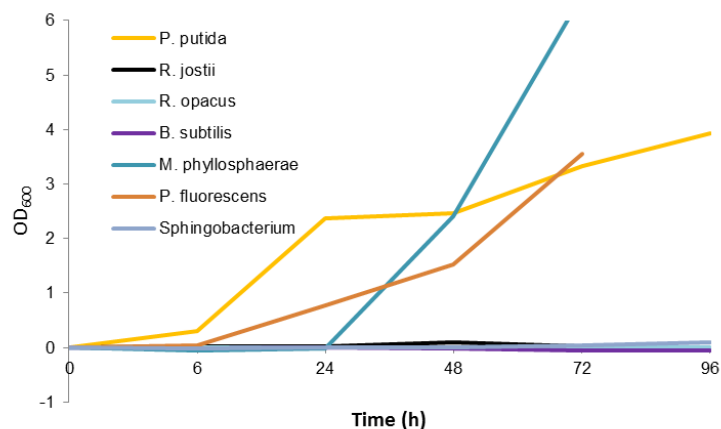


Figure 66: Growth of selected bacteria observed at OD600 in incubations with M9 minimal media, 0.1% glucose (w/v) and 100 μ M disulfiram

Samples taken from incubations in which growth was severely retarded were streaked on LB agar plates and failed to show signs of growth, this indicated disulfiram was acutely toxic to the primary metabolism of those species at these concentrations. As the purpose of these experiments was not to fatally harm the bacteria, it was decided that only the strains *M. phyllosphaerae*, *P. fluorescens* and *P. putida* would be selected for vdh inhibition experiments.

Incubations with *M. phyllosphaerae*, *P. fluorescens* and *P. putida* exhibited initial strong growth when incubated in growth media P1 supplemented with 0.1% (w/v) glucose and either 2.5% wheat straw lignocellulose or 0.5% industrial Kraft lignin in the presence of disulfiram at a final concentration of 100 μ M. A drop in growth was observed after 24 h in the incubations with *P. fluorescens* and the wheat straw lignocellulose (in contrast to controls with just growth media P1 and disulfiram and the experiments with *M. phyllosphaerae* and *P. putida*). This was a promising observation as Narbad *et al* had shown in previous work that *P. fluorescens* growth could not be supported at concentrations of 10 mM and higher.^[180]

The extracellular fractions after centrifugation were analysed by LC-MS and GC-MS. EICs for m/z 153.8 did not indicate any trace amounts of vanillin, in fact no detectable difference was seen between any of the incubations after close analysis of the UV spectra and base peak chromatograms.

Intracellular metabolites were then extracted from cell pellets using the boiling ethanol method (Section 5.2.3.2) and analysed by LC-MS. This time a distinctive broad peak in the base peak chromatogram (BPC) at 2.6 minutes was seen in the sample taken at 24 h from the *P. fluorescens* incubation. The mass spectrum showed dominant ions at m/z 120.0 (Figure 67).

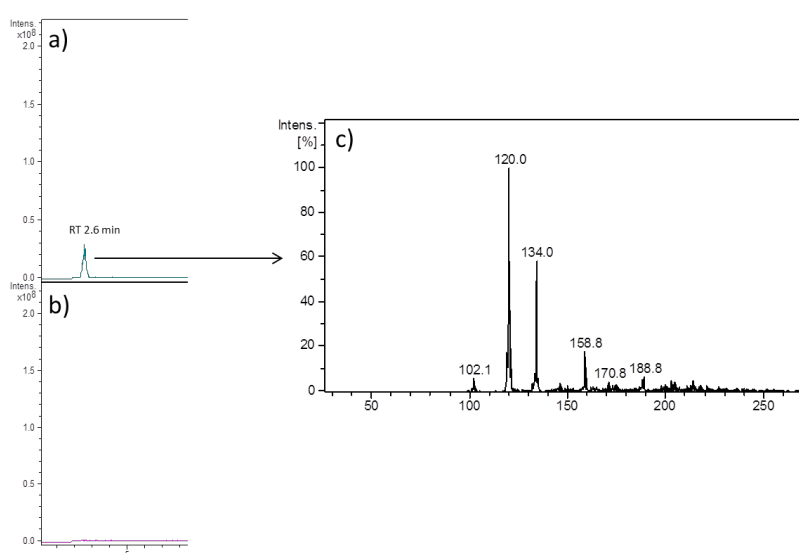


Figure 67: The base peak chromatogram shows a peak with a retention time of 2.6 min obtained the sample taken at 24 h from the *P. fluorescens* incubation (a) in comparison with that of a control incubation without disulfiram (b) for the same time period. The dominant ions at m/z 120.0 and 134.0 are displayed in the spectrum (c). Incubations were performed in M9 minimal media, 2.5% wheat straw lignocellulose (w/v), 0.1% glucose (w/v) and with or without 100 μ M disulfiram.

The peak was isolated by collecting the fraction at the retention time and HR-ESI-MS analysis by the University of Warwick Mass Spectrometry Service indicated the

presence of a compound with the molecular formula $C_5H_{12}NO$ (calculated for $[C_5H_{12}NO]^+$: 102.0913 found 102.0912) (Figure 68).

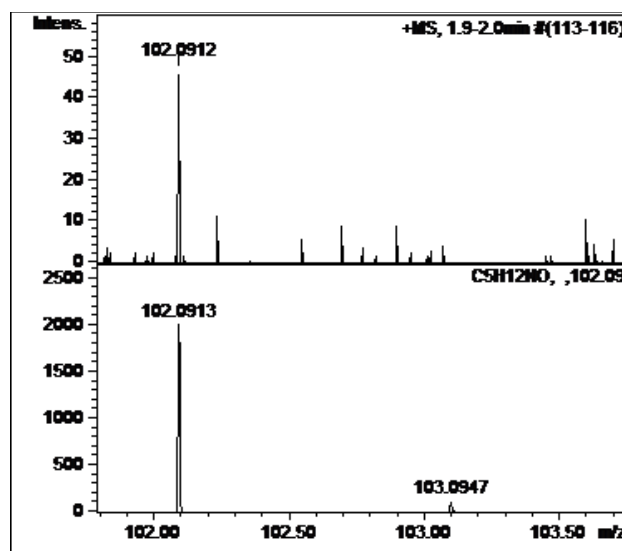


Figure 68: HR-MS analysis identified a molecular formula of $C_5H_{12}NO$

A database search returned the possibility of glycine betaine aldehyde (GBA) (*N,N,N*-trimethyl-2-oxoethanaminium) for the $C_5H_{12}NO$ and the hydrated form of glycine betaine aldehyde, known as betaine aldehyde hydrate (BAH) (2,2-Dihydroxy-*N,N,N*-trimethylethanaminium) could account for the ions at m/z 120 for $C_5H_{12}NO_2$ (Figure 69).

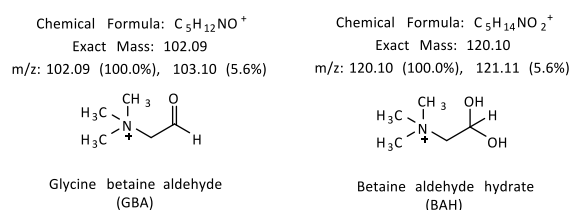


Figure 69: Glycine betaine aldehyde (*N,N,N*-trimethyl-2-oxoethanaminium) and betaine aldehyde hydrate (2,2 Dihydroxy-*N,N,N*-trimethylethanaminium) were identified as potential compounds isolated from the intracellular metabolite extraction, of *P. fluorescens* from a 24 hour incubation with 2.5% wheat straw lignocellulose (w/v) and 100 μ M disulfiram in P1 growth media.

The use of a reference standard and spiking experiments to compare retention times confirmed the analyte to be GBA for m/z 102.1 with a retention time of 2.6 minutes (Figure 70).

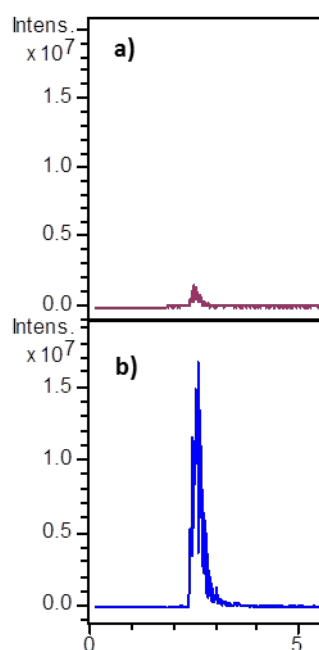


Figure 70: An EIC chromatogram for m/z 102.1 ($m+H$)⁺ shows a peak with a retention time of 2.6 min obtained from the sample taken at 24 h from the *P. fluorescens* incubation (a) in comparison with that of an analytical standard (b) confirming the compound to be glycine betaine aldehyde.

3.1.3 Inhibition of betaine aldehyde dehydrogenase (BADH)

The appearance of GBA indicated a possible inhibition of a betaine aldehyde dehydrogenase (BADH) a key enzyme used in the metabolic pathway of glycine from choline. BADH catalyses the second step in the pathway, namely the transformation of betaine aldehyde (*N,N,N*-trimethyl-2-oxoethanaminium) to glycine betaine (*N,N,N*-trimethylglycine) (Figure 71). It has also been observed that in aqueous solution GBA exists predominantly in a hydrate diol form which accounts for the predominant ions at m/z 120.0 in the chromatogram.

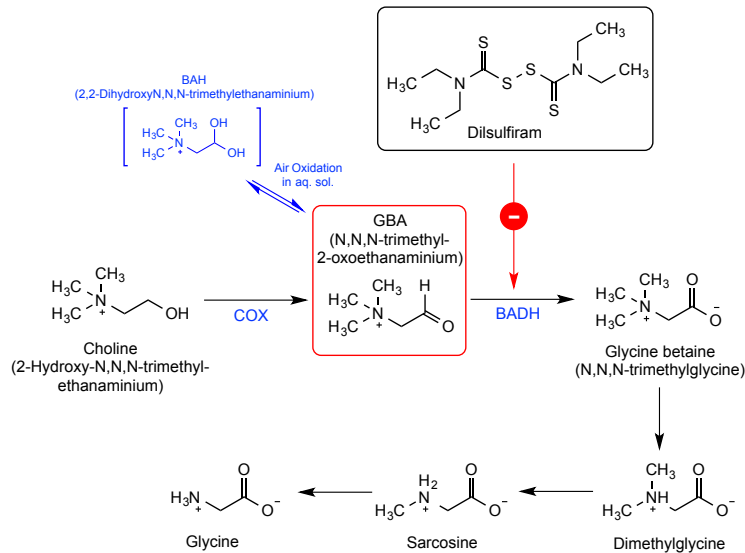


Figure 71: The metabolic pathway of glycine from choline is disrupted after the oxidation of choline by a choline oxidase oxidase (COX).^[192]

The use of glycine betaine as an osmoprotectant has been observed in a number of Gram negative and Gram positive bacteria.

Kappes *et al* (1996) identified multiple glycine betaine uptake systems in *Bacillus subtilis* that were employed as a defence in laboratory imposed hostile environmental conditions.^[193] Landfield and Strom (1986) observed glycine betaine accumulated to high levels in the osmotically stressed cells of *E. coli* and Graham and Wilkinson (1992) made the same observation in the cells of *Staphylococcus aureus* when choline was present in the media.^{[194], [195]}

In Gram negative bacteria such as these, it is reported either a choline dehydrogenase (CDH) or alcohol dehydrogenase (ADH) is responsible for the intracellular conversion of betaine aldehyde to glycine betaine.

In the Gram positive bacteria *Arthrobacter pascens*, Rozwadowski *et al* (1991) proved the choline to glycine betaine pathway proceeded via a choline oxidase (COX) and a betaine aldehyde dehydrogenase (BALDH).^[196] This pathway has also been

observed earlier by Ikuta *et al* (1977) from another Gram positive soil bacterium, *Arthrobacter globiformis*.^[197]

Whilst particularly not extensive, research into glycine betaine metabolism in bacteria has shown this pathway present in some form in a wide range of bacterial species. It is also evident that bacteria, whilst not able to produce glycine betaine directly, take up the compound from their environment or synthesise it from choline in times of oxidative or osmotic stress.

The media used in these incubations could provide a number of ions which may give rise to an environment that interferes with the movement of water into the bacterial cell. It is also reported that choline is found in relatively large quantities in wheat germ (152 mg/100 g), a possible component of the wheat straw lignocellulose used in the incubations.^[198] Together these could provide the necessary conditions for the induction of enzymes involved in glycine betaine biosynthesis.

A search in the genomic data for *P. fluorescens* strain Pf-5 on the Uniprot protein knowledgebase identified a gene (betA PFL_5768) that had already been characterised as a NAD/NADP-dependent betaine aldehyde dehydrogenase.

The chemical inhibition of BADH to trigger a build-up of the toxic betaine aldehyde has already been reported and searches of the literature found two papers including one that had already investigated the antibiotic properties of disulfiram due to inhibition of BALDH in *P. aeruginosa*.^{[190], [199]}

The identification of GBA in the wheat straw incubations of *P. aeruginosa* grown in the presence of disulfiram may also explain the effects on growth seen with the other

bacteria used. Whilst this metabolite was not observed in other incubations, this does not rule out the blockage of this pathway as the fundamental cause of cell death.

3.2 Known inhibitors of mono-oxygenase enzymes

The second step on the vanillic acid catabolic pathway is the conversion of vanillate acid to protocatechuate (Figure 63). The ability of certain soil bacteria to metabolise methoxylated lignin metabolites such as vanillate and anisate (Figure 72) has been widely studied with two distinct bacterial aromatic demethylation enzyme systems identified.^{[143], [170], [200]–[202]}

One of these systems is a vanillate monooxygenase (VMO) a non-heme enzyme system composed of ferredoxin oxygenase and reductase components and the other a tetrahydrofolate (THF) dependant system.

Studies have shown that the demethylation of vanillate by *P. putida* and *R. jostii* RHA1 is via the VMO oxygenase and reductase system.^{[143], [201]} However, it has also been reported that certain bacteria possess both demethylation systems. In *Sphingomonas paucimobilis* SYK-6 the H-type lignin metabolite anisate is selectively degraded via a THF-dependent methyltransferase system whilst vanillate is reportedly metabolised through a separate VMO system (Figure 72).^[202]

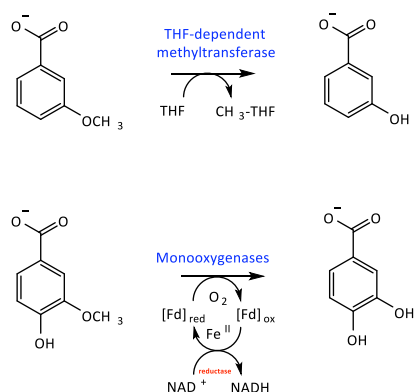


Figure 72: *m*-Anisic acid (3-methoxy benzoic acid) shown to be degraded via the THF-dependent methyltransferase system in certain bacteria and vanillic acid (4-hydroxy-3-methoxybenzoic acid) thought to be degraded by an oxygenase and reductase system.

It is proposed by de Montellano and Komives that a cytochrome P450 (CYP) isoform, also responsible for O-demethylation, metabolised aryl acetylenes to their corresponding carboxylic acids with a concomitant loss of protein activity.[203] It was thought the reactive ketene intermediate produced in the process formed covalent bonds with nucleophilic active site residues and caused complete enzyme inactivation.

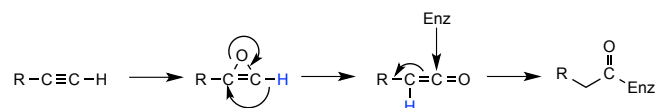


Figure 73: De Montelano and Komives proposed activation of acetylene to ketene via a hydride shift and concomitant reaction with a nucleophilic active site residue

Analogues containing a terminal alkyne could be designed as potent small molecule inhibitors of the demethylase systems. Provided that these inhibitors are taken up into the cell and brought into close proximity of the active site of the protein target, they may initiate a deactivation of the enzyme similar to that reported by de Montellano and Komives.

3.2.1 Design of potential mechanism-based inhibitors of vanillate monooxygenase (VMO)

Based on the results of de Montellano and Komives, substrate analogues were designed containing a terminal alkyne, which could potentially act as mechanism-based inhibitors of the vanillate monooxygenase system.^[203] Therefore two potential inhibitors (21) and (22) with an alkoxy alkyne moiety introduced were synthesised.

3.2.1.1 Synthesis of 3-(prop-2-ynyloxy)-4-hydroxybenzoic acid (21)

Figure 74 illustrates the approach taken for the synthesis of the inhibitors.

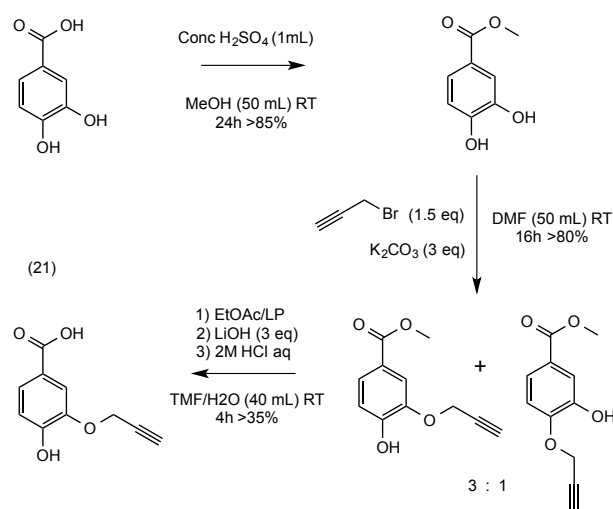


Figure 74: Synthesis of 3-(prop-2-ynyloxy)-4-hydroxybenzoic acid (21) from 3,4-dihydroxybenzoic acid

Firstly, in a classic example of Fischer esterification to protect the carboxyl group, commercially available 3,4-dihydroxybenzoic acid was stirred overnight in methanol at RT with concentrated H₂SO₄ to afford the methyl benzoate at >85% yield. Alkylation of the phenolic group was then achieved using an adapted procedure based on the work by Ishii *et al* (1991) using propargyl bromide in the presence of K₂CO₃ as

a base.^[204] The best yields were achieved at RT over 48 h, as low-res mass spectrometry and TLC indicated that when the mixture was refluxed, only the di-substituted alkylated product was formed. At room temperature however the mono-substituted alkylated product was the major product, however NMR experiments still indicated that two isomeric compounds at a ratio of 3:1 had been formed. Cross-peaks on a correlated spectroscopy (COSY) NMR experiment showed formation of both the *para* and *meta* substituted compounds. Column chromatography (20% EtOAc/LP) enabled separation of the two isomers and further treatment with aqueous LiOH saponified the recovered ester to produce 3-(prop-2-ynyloxy)-4-hydroxybenzoic acid.

3.2.1.2 Synthesis of 3-(prop-2-ynyloxy) benzoic acid (22)

The same approach was followed using commercially available 3-hydroxybenzoic acid as the starting reagent to generate 3-(prop-2-ynyloxy) benzoic acid (22) (Figure 75).

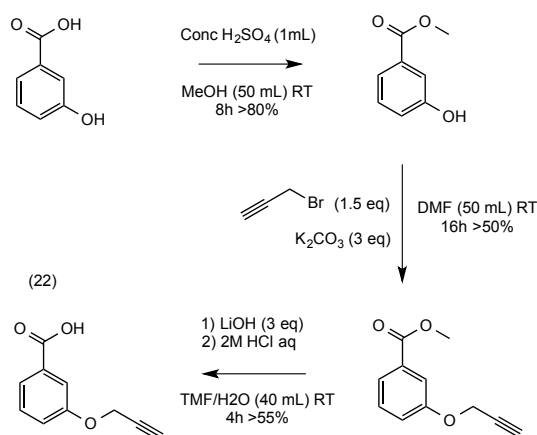


Figure 75: Synthesis of 3-(prop-2-ynyloxy) benzoic acid (22) from 3,4-dihydroxybenzoic acid

3.2.2 Testing *in vivo* of potential mechanism-based inhibitors of VMO

To investigate the efficacy of these compounds *in vivo*, the strains *P. fluorescens*, *P. putida*, *R. opacus*, *B. subtilis* R. *jostii* RHA1, *M. phyllosphaerae* and the *Sphingobacterium* isolate were again selected for the experiments. As the demethylation enzyme systems can vary across the species, it was decided to test the inhibitors *in vivo* for any sign of pathway inhibition or build-up of metabolic flux.

To examine the effect of (21) and (22) on bacterial growth, the strains were grown under the conditions stated for the disulfiram experiment. The inhibitors need to be specific enough to target the specific vanillate monooxygenase without killing the host cell outright.

The putative inhibitors remained soluble up to 500 μM and incubations were performed using concentrations ranging from 100 to 500 μM . The strains were grown over 72 h and bacterial growth was determined using optical density data (OD) recorded for triplicates at 600 nm using samples taken at 0, 3, 6, 24, 48 and 72 h. Initial observations indicated the inhibitors enhanced growth in experiments with the pseudomonads and rhodococci strains (Figure 76).

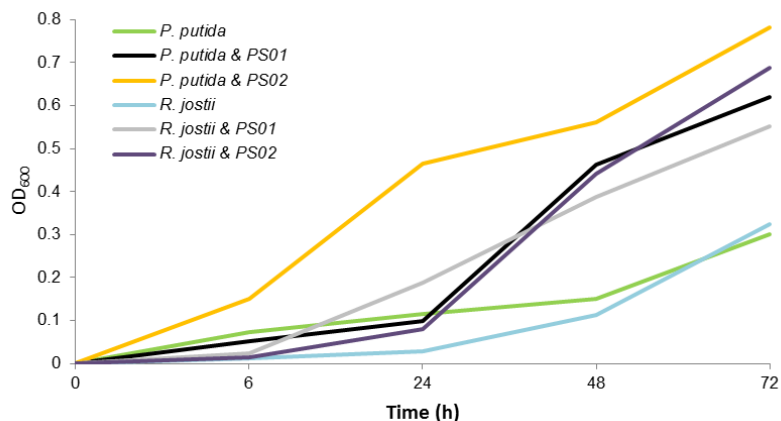


Figure 76: Growth curve for *P. putida* and *R. jostii* RHA1 in liquid M9 minimal media with 0.1% glucose and 500 μ M of putative inhibitor.

Although the most likely explanation for the above observations was that as aromatic degraders the strains were able to utilise the inhibitors as an extra source of carbon. The measurement of turbidity as an indicator of bacterial growth was confirmed by the use of the spread count method and serial dilutions. Viable colony forming units (CFU) for samples taken from the *R. jostii* RHA1 and *P. putida* experiments were counted and also indicated higher and faster bacterial growth in the incubations with inhibitors (21) and (22).

Nonetheless, incubations were performed where bacteria had been grown with 2.5% wheat straw (w/v) or industrial 0.5% Kraft lignin (w/v) in growth media P1 inoculated with (21) or (22). LC-MS and GC-MS analysis was performed on samples taken from the experiments. A search through the chromatograms did not identify expected product vanillic acid (M_r 168.14) or any distinguishable metabolites indicative of a block in metabolic flux.

With the lack of positive experimental data in regards to inhibition of the vanillate monooxygenase system and growth data signifying bacterial consumption of the inhibitors, it was decided to proceed with another target for chemical inhibition.

3.3 Hydroxamic acid based inhibitors for non-heme iron oxygenases

Further dissimilation of vanillic acid is via the diphenolic compound protocatechuate. Bacterial metabolism of this diphenol proceeds by either *meta* or *ortho* cleavage of the hydroxyl groups on the aromatic ring and yields a ring fission product that is further metabolized to TCA cycle intermediates.

Within the degradation pathways conserved in many aromatic degrading soil bacteria are the catechol dioxygenases. These non-heme iron oxygenase enzymes catalyse the incorporation of molecular oxygen into catechol or substituted catechol substrates, such as protocatechuate resulting in the critical ring opening step and also offer an opportunity as targets for chemical inhibition.

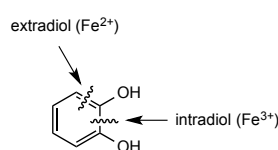


Figure 77: Two subfamilies of catechol dioxygenase enzymes exist; the extradiol and intradiol dioxygenases that incorporate molecular oxygen to break open the aromatic ring structure.

Two subfamilies of these catechol dioxygenase enzymes exist, the extradiol catechol dioxygenases and the intradiol catechol dioxygenases.[205] Extradiol catechol dioxygenases cleave the carbon-carbon bond adjacent to the phenolic hydroxyl group and require Fe²⁺ as a cofactor, whereas intradiol catechol dioxygenases cleave the carbon-carbon bond between the phenolic hydroxyl and require Fe³⁺ as a cofactor (Figure 77).

The differing use of iron oxidation states by these enzymes presents an opportunity for inhibition. Corey *et al* in 1984 identified hydroxamic acids as selective chelators of the ferric iron (Fe³⁺) (Figure 78).^[206]

Hydroxamic acid core structure

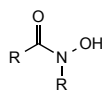


Figure 78: Core structure of hydroxamic acid reported as a selective chelator of the ferric Fe^{3+} ion

A number of hydroxamic analogues had previously been synthesised in our research group as selective inhibitors of the carotenoid cleavage dioxygenases (CCDs).[207] The oxidative cleavage of carotenoids results in the release of signalling molecules with a wide range of functions such as the cleavage of β -carotene by the CCD enzyme β -carotene-15,15'-dioxygenase to retinal, a form of vitamin A - important for sight.[208]

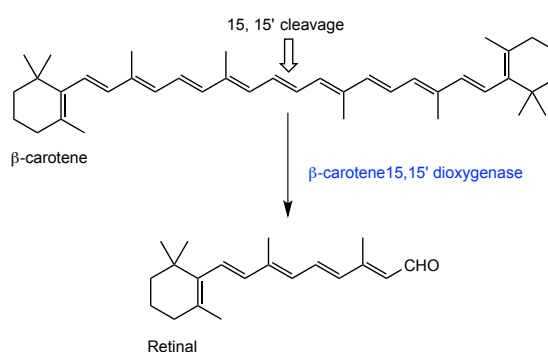


Figure 79: Cleavage of β -carotene by β -carotene-15,15'-dioxygenase to retinal

To test the selective effectiveness of these so-called 'D-Series' of hydroxamic acid chemicals on oxidative ring cleavage enzymes, an example of both extradiol and intradiol dioxygenases were selected for inhibition assays. A screening method was initially developed, followed by more detailed kinetic analysis and finally any potential inhibitors were used for experiments *in vivo*.

3.3.1 Chemical inhibition of *E. coli* 2,3-dihydroxyphenyl propionate 1,2-dioxygenase (MhpB)

The enzyme MhpB is an example of an extradiol catechol dioxygenase that requires Fe^{2+} as a cofactor, catalysing the cleavage of 2,3-dihydroxyphenyl propionate (DHPP) to give 2-hydroxy-6-oxo-nona-2,4-diene-1,9-dicarboxylate (Figure 80). Previous work by Professor Tim Bugg had enabled the overexpression and characterisation of this tetrameric enzyme.^{[209], [210]} As the ring cleavage product of DHPP has a distinctive yellow appearance, its formation is easily monitored visually. Hence MhpB was used to investigate whether a selective extradiol catechol dioxygenase inhibitor could be found.

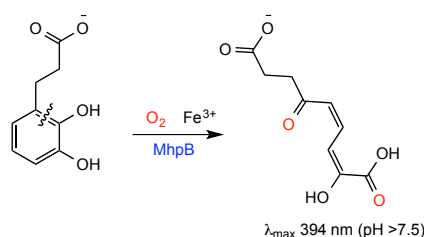


Figure 80: The enzyme 2,3-dihydroxyphenyl propionate 1,2-dioxygenase (MhpB) from *E. coli* catalyses the extradiol cleavage of 2,3-dihydroxyphenyl propionate (DHPP) to give 2-hydroxy-6-oxo-nona-2,4-diene-1,9-dicarboxylate

MhpB was over-produced in *E. coli* strain TB1 DH5 α /pIPB and the apoenzyme purified.^[210] The cells were first grown in LB and induced by IPTG at OD₆₀₀ 0.6-0.8. The cells were then harvested by centrifugation and resuspended in approximately 10 mL of buffer B per g of pellet. Cell lysis was carried out on a cell disrupter and the cell debris removed by centrifugation. Powdered ammonium sulphate (NH_4SO_4) was added to the cell free extract to 25% saturation and the suspension stirred for 1 h. After centrifugation the supernatant was collected and $(\text{NH}_4)_2\text{SO}_4$ added to 50% saturation and the suspension stirred for a further 1 h. After centrifugation the pellet

was resuspended in buffer A and loaded onto a pre-equilibrated phenyl agarose column. The proteins were then eluted by fast protein liquid chromatography with a linear gradient of 0 to 100% buffer B at a flow rate of 0.25 mL/min. Each fraction was monitored at 280 nm, and collected in glass tubes at a volume of 1.5 mL to a final yield of about 26 mg/L of culture. SDS-PAGE was used to determine the relative abundance of proteins in each fraction, which showed a main band at $\sim 33 \text{ kDa} \pm 3$ in keeping with the published value for the subunit of 33.8 kDa (Figure 81).

The fractions with the highest concentrations were pooled, concentrated and used in assays without further purification at the pH-optimum for MhpB (pH 8.0).[209]

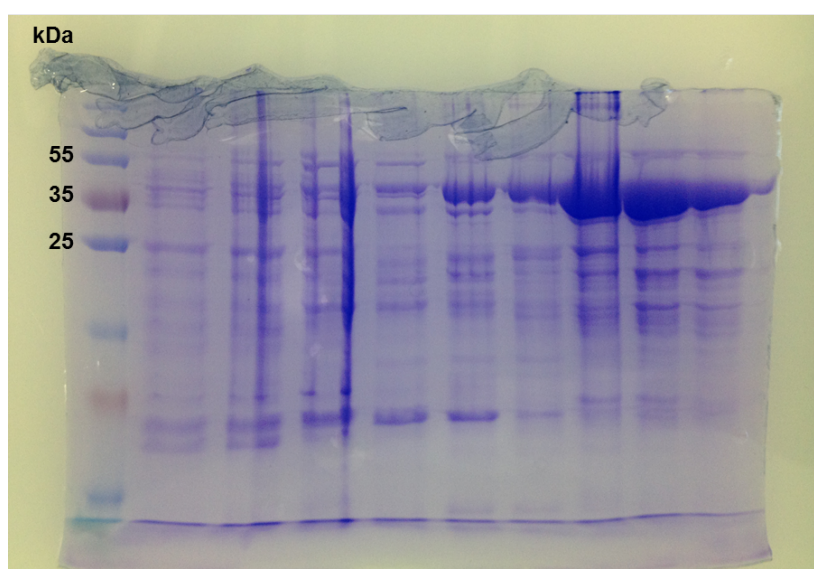


Figure 81: SDS-PAGE gel showing the relative abundance of MhpB in each fraction, which showed a main band at $\sim 33 \text{ kDa} \pm 3$

Once activated with sodium ascorbate (5 mM) and ammonium Fe (II) sulphate (5 mM), MhpB displayed Michaelis-Menten type kinetics for activity in assays with DHPP (data not shown). The holoenzyme showed affinity for the substrate with a K_m value of $27 \mu\text{M} \pm 0.5$, similar to the reported literature value of $26 \mu\text{M}$.^[209] DHPP was used at a final concentration of $30 \mu\text{M}$ in the inhibitor-screening assay.

3.3.1.1 Initial *in vitro* 96 well plate screening of hydroxamic acid inhibitors on MhpB

To select potential inhibitors of MhpB activity, 30 of the ‘D-Series’ of hydroxamic acids were initially screened using a microtitre plate. Each inhibitor at final concentrations of 50, 100, 200 and 300 μM was incubated with 30 μM DHPP for 5 minutes before initiation of reaction by the addition of enzyme. Two additional controls were added to each plate, which included replicates containing inhibitor and no enzyme, which would highlight any visual reaction between the inhibitor and substrate, and a replicate without any inhibitor as described in the assay conditions (Section 5.2.10.1.1).

Inhibitors D3, D7 and D8 at 50-200 μM concentrations slowed or stopped the formation of the yellow coloured product over 60 minutes (Figure 82).

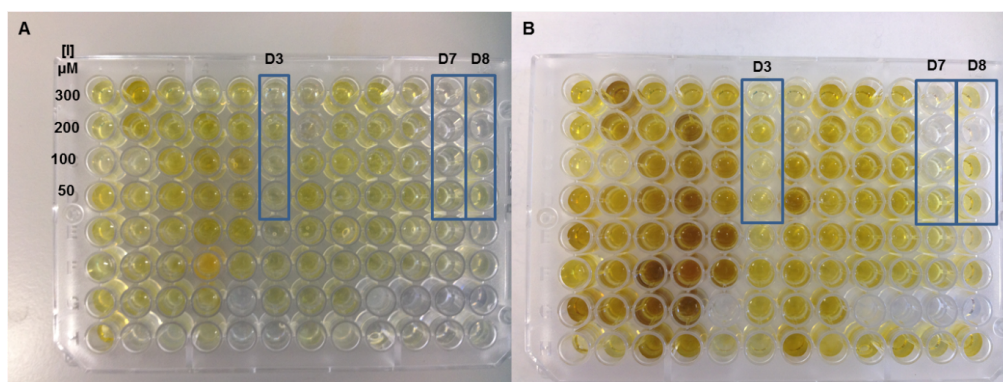


Figure 82: Microtitre plate experiments in which inhibitors at various concentrations slowed or stopped the formation of the yellow coloured MhpB catalysed reaction product over 1 min (A) and 60 min (B). D3, D7 and D8 were highlighted as potentiating a negative effect on enzyme activity.

Compounds D3, D7 and D8 were then selected for retesting and more detailed kinetic analysis. The structures are shown below (Figure 83).

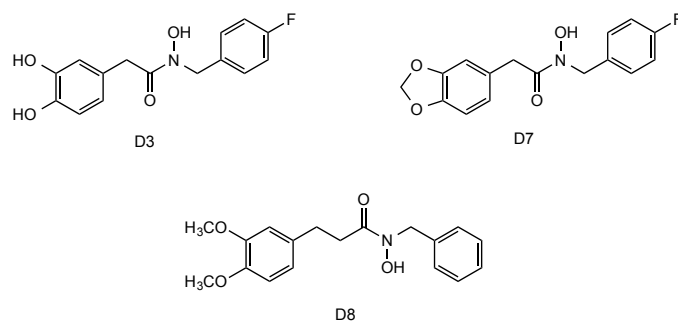


Figure 83: Potential inhibitors D3, D7 and D8

3.3.1.2 Determining IC_{50} values for the potential inhibitors of MhpB

UV/vis kinetic assays were used to study the inhibitory effect of D3, D7 and D8. The three compounds were tested at concentrations ranging from 62 to 250 μ M with 30 μ M DHPP to determine IC_{50} values (concentration required for 50% inhibition). The increase of absorbance at 394 nm was measured and a graph of concentration of drug against activity was produced. The results demonstrate that at the concentrations of inhibitor used, the compound D8 had only 20% inhibitory effect on the reaction (Figure 84).

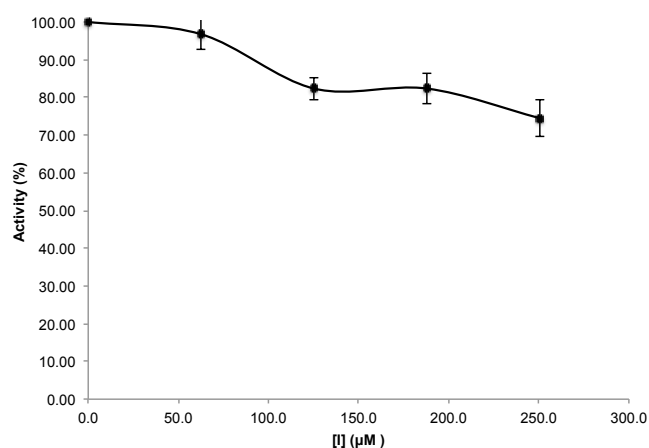


Figure 84: Inhibition of the MhpB by D8

D3 was the most potent inhibitor of MhpB with an IC_{50} value of $110 \mu\text{M} \pm 5$, and showed $>95\%$ inhibition of MhpB *in vitro* at $250 \mu\text{M}$ concentration (Figure 85). D7 failed to show any inhibition effect at all (data not shown).

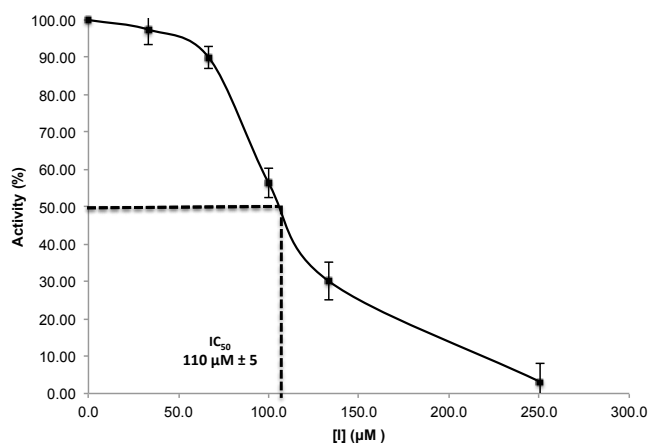


Figure 85: Hydroxamic acid D3 proved to be the most effective on enzyme activity with an IC_{50} value of approximately $110 \mu\text{M} \pm 5$.

Notably the structure of D3 contains a catechol group found in the structure of the MhpB substrate. On the basis of this initial screening, the effects of D3 on MhpB activity *in vivo* were investigated.

3.3.1.3 Colour Enhancing Media (CEM) assay for determining *in vivo* inhibition of D3 on MhpB activity

Research by R Burlingame (1986) to isolate mutants of *E. coli* defective in catabolism of 3-phenylpropionate described a method to characterise mutant strains of MhpB using a visible assay. *E. coli* mutants lacking either MhpB or MhpC (the C-C bond hydrolase required to cleave the 2-hydroxy-6-oxo-nona-2,4-diene-1,9-dicarboxylate ring cleavage product) were grown in indicator media (CEM) in which accumulation of substrate led to the formation of dark red or bright yellow colours in the medium (Figure 86).^[211]

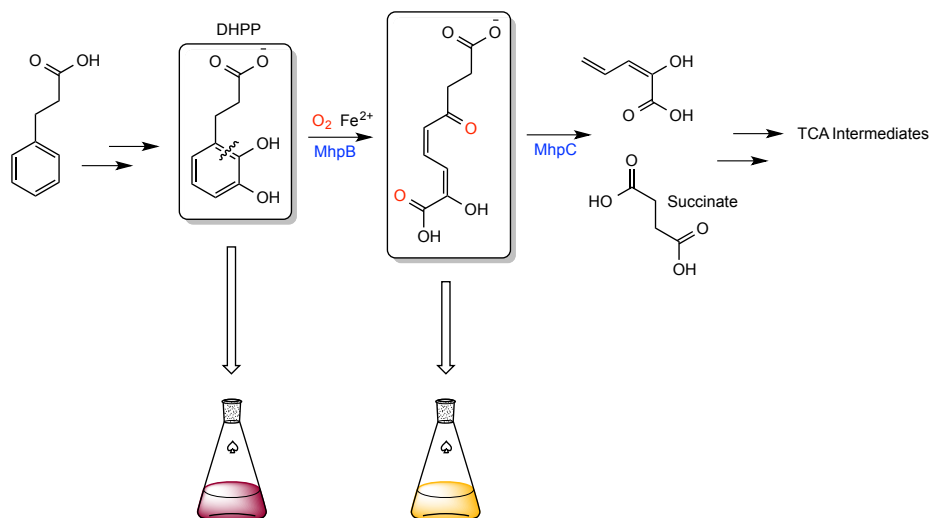


Figure 86: Mutants of *E. coli* lacking MhpB or MhpC and defective in catabolism of 3-phenylpropionate accumulated colourful substrates when grown in colour enhancing indicator media (CEM)

The dark red colour is due to the oxidation of the catechol DHPP to a reactive quinone that forms a coloured charge-transfer complex with the proline in the CEM media. The ring fission product has a yellow colour as discussed previously.

It was assumed that if chemical inhibition of these enzymes was achieved in whole bacterial cells then a similar effect could be observed, providing a useful assay for detecting inhibition *in vivo*.

The procedure was repeated in which *E. coli* strains K-12 LW366 $\Delta mhpB$ and K-12 LW353 $\Delta mhpC$ were incubated at 30°C a medium for several days. As expected, after 36 h the media inoculated with the $\Delta mhpB$ mutant turned a vibrant dark purple and the $\Delta mhpC$ inoculated media appeared bright orange (Figure 87).

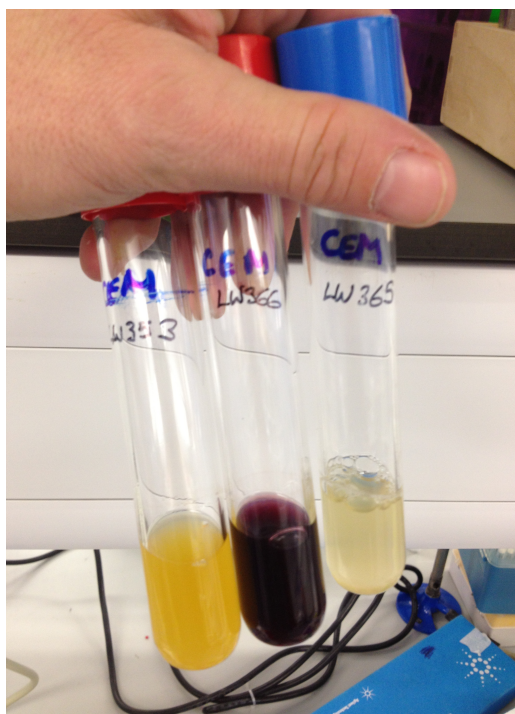


Figure 87: Accumulation of 2,3-dihydroxyphenyl propionate (in LW 366) or 2-hydroxy-6-oxonona-2,4-diene-1,9-dicarboxylic acid (in LW353) in indicator media (CEM) led to the formation of dark red or bright yellow colours respectively.

The CEM inoculations were repeated with *E. coli* K-12 W3747 (parent strain) in the presence of D3 at final concentrations of 110 μM , 220 μM and 330 μM . Once again the tubes were left with shaking at 180 rpm in a 30°C incubator for several days. A slight change in colour was observed after 24 h in the 220 μM D3 experiment, but the expected dark purple was not observed (Figure 88).

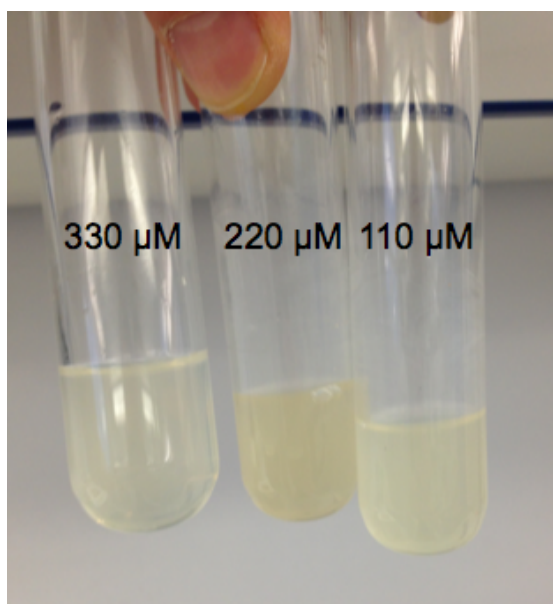


Figure 88: Inoculations in the presence of D3 at final concentrations of 110 μM , 220 μM and 330 μM failed to reproduce the vibrant purple colour expected with inhibition of MhpB and accumulation of DHPP. A darker slight colour change was observed with 220 μM D3 but subsequent analysis did not reveal expected products.

Samples were taken from the experiment and centrifuged at 13000 rpm for 10 min. Subsequent analysis of the samples by LC-MS failed to reveal the presence of DHPP. Hence it appears that D3 is not taken up into *E. coli* cells

3.3.2 Chemical inhibition of protocatechuate 3,4-dioxygenase (3,4-PCD)

Protocatechuate 3,4-dioxygenase (3,4-PCD) is the intradiol dioxygenase used on the β -keto adipate pathway and catalyses the cleavage of protocatechuic acid (PCA) to produce 3-carboxy-*cis,cis*-muconate (Figure 89). This enzyme is conserved across a number of soil degrading bacteria and is the first enzyme catalysed step in the β -keto adipate pathway.

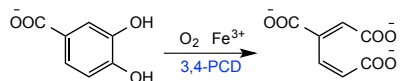


Figure 89: Protocatechuate 3,4-dioxygenase (3,4-PCD) catalyses the cleavage of protocatechuic acid (PCA) to produce 3-carboxy-*cis,cis*-muconate.

The enzyme isolated from *Pseudomonas sp.*, is commercially available from Sigma Aldrich (UK).

3.3.2.1 Plate reader assay for determining in vitro inhibition of ‘D-Series’ on 3,4-PCD activity

A plate reader assay was used to examine substrate consumption by monitoring a decrease in absorbance at 294 nm. Modified from the assay described by Fujisawa *et al* (1974), 150 μL of 0.5 mM PCA stock solution in tris acetate buffer (final concentration 0.38 mM pH7.5) and 45 μL of an inhibitor stock solution in tris acetate buffer were added to the wells of a Greiner UV star 96 well plate followed by 5 μL of enzyme solution to initiate the reaction. The microplate was then read at 280 nm every 5 s for 2 min.

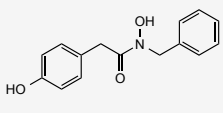
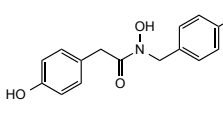
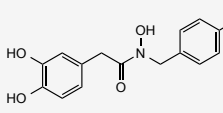
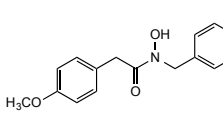
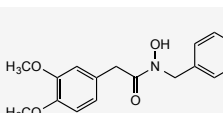
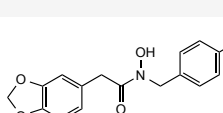
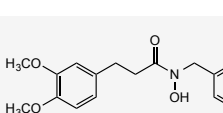
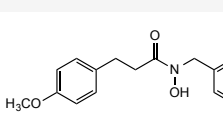
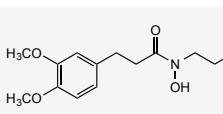
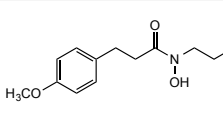
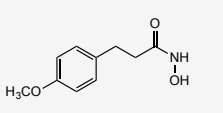
The library of 30 ‘D-Series’ at a nominal final concentration of 200 μM , were screened and the change in absorption of the reactions was measured and enzyme activity was calculated in $\mu\text{moles}/\text{min}$. Specific activity was calculated as the activity of 3,4-PCD per mg of protein and was compared to that of the assay using PCA without any inhibitor. Every experiment was done in triplicate.

3.3.2.2 UV/Vis assay for determining in vitro inhibition of ‘D-Series’ compounds D7, D10 and D13 on 3,4-PCD activity

The *in vitro* effect of each ‘D-Series’ compound investigated revealed 11 compounds displaying varying degrees of efficacy of 3,4-PCD inhibition (Table 1). Data from the

plate reader assay indicated hydroxamic acids D7, D10 and D13 as the most potent inhibition agents with an approximate loss of enzyme activity ranging from 59 to 79%, at 200 μ M inhibitor concentration.

Table 3: The percentage decrease in specific activity for the 11 hydroxamic acid based ‘D-Series’ at 200 μ M concentration that tested positive in the plate reader screening assay

Name	Structure	Activity (U / mL) \pm 0.2	Specific Activity (U / mg)	% Decrease in specific activity
D1		0.126	4.60	32
D2		0.145	5.29	22
D3		0.132	4.80	30
D4		0.141	5.15	24
D5		0.122	4.46	35
D7		0.075	2.74	60
D8		0.175	6.38	6
D9		0.152	5.54	19
D10		0.079	2.90	57
D11		0.185	6.68	2
D13		0.038	1.38	80

The assay was repeated in a quartz cuvette using a spectrophotometer to give a more accurate picture of inhibition. D7 and D10 were this time shown not to inhibit 3,4-PCD to the same extent (<20% decrease in specific activity). D13 displayed similar levels of inhibition (69% decrease in specific activity) toward 3,4-PCD.

It is worth noting that D13 is the only compound with no N substituent. It could be hypothesised that a smaller hydroxamic analogue is required to fit into the 3,4-PCD active site.

3.3.2.3 Design of analogues of hydroxamic acid D13

As described above, D13 was identified as the best candidate for 3,4-PCD inhibition, and its behaviour in the assays established it as the standard for further inhibitor design. Using the D13 (4-methoxycinnamohydroxamic acid) structure as a scaffold, a further three chemicals, 3,4-dimethoxy-cinnamohydroxamic acid (23), 3-(4-methoxyphenyl)- propiohydroxamic acid (24), and (3-(3,4-dimethoxyphenyl) propiohydroxamic acid (25) were synthesised (Figure 90).

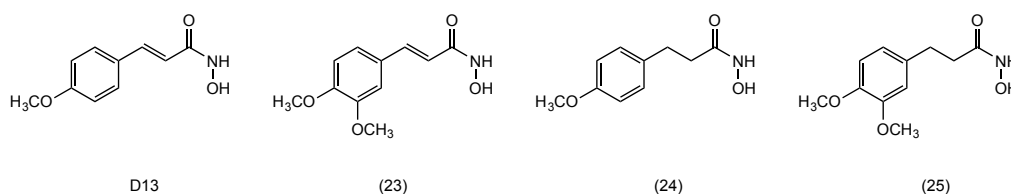


Figure 90: Using the D13 structure as a scaffold, (23), (24) and (25) were synthesised.

3.3.2.4 Synthesis of 3,4-dimethoxy-cinnamohydroxamic acids (D13) and (23)

The Tanaka procedure was followed for the preparation of the substituted cinnamohydroxamic acids.[212] Commercially available 3,4-dimethoxy-cinnamic acid was first converted to the carboxylic acid chloride after refluxing with thionyl chloride acid to 80% yield (Figure 91).

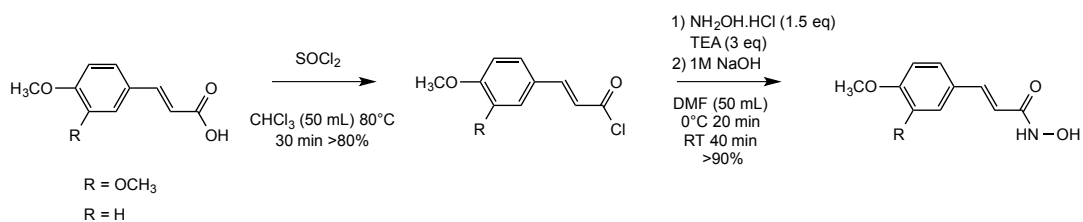


Figure 91: Synthesis of 3,4 dimethoxy-cinnamohydroxamic acid from 3,4 dimethoxycinnamic acid.

The solvent was evaporated and an ice-cold solution of hydroxylamine hydrochloride ($\text{NH}_3\text{OH}\cdot\text{HCl}$) and triethylamine (TEA) in chloroform (CH_3Cl) was added dropwise with stirring over 20 minutes at 0°C . The reaction was allowed to come to room temperature over 40 minutes. The hydroxamic acid was extracted and then recrystallised from EtOH in excellent yields. D13 was also resynthesised using the above procedure.

3.3.2.5 Synthesis of (3-(4-methoxyphenyl)-propiohydroxamic acid) and (3-(3,4-dimethoxyphenyl) propiohydroxamic acid (24) and (25)

The reduction of the substituted cinnamohydroxamic acids was carried out using 10% palladium on carbon (Pd/C) and hydrogen gas (H_2) in MeOH. The reaction was left stirring overnight and then the mixture filtered over diatomaceous earth. The propiohydroxamic acids were recovered in almost quantitative yields.

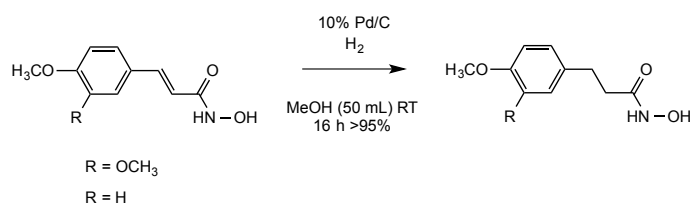


Figure 92: Reduction of substituted cinnamohydroxamic acids.

3.3.2.6 Testing *in vitro* the inhibition of 3,4-PCD using analogues of D13

The inhibitors were assayed *in vitro* against the commercially available 3,4-PCD utilising a fixed final concentration of 0.4 μM PCA. Data was obtained using the earlier UV/Vis method to estimate the IC_{50} of D13 and the new analogues. Final concentrations of inhibitor were 500, 250, 100, 50 and 5 μM and all experiments repeated in triplicate. Pre-incubation for <10 mins of 3,4-PCD with inhibitors D13, (23) and (25) at concentrations >5 μM saw complete deactivation of the enzyme.

The concentration-dependent inhibition effect of the new hydroxamic analogues on 3,4-PCD was determined over 2 min. D13 still proved the most potent inhibitor of activity, with an IC_{50} of 16 μM (Figure 96). Interestingly it was observed that inhibition with the reduced analogous 4-methoxy substituted (24) was not significant even at the highest concentration of 500 μM (Figure 93). The 3,4-methoxy substituted (23) and its reduced equivalent (25) with an IC_{50} of 19 and 158 μM , respectively, did however show concentration-dependent inhibition with time (Figure 94 and Figure 95).

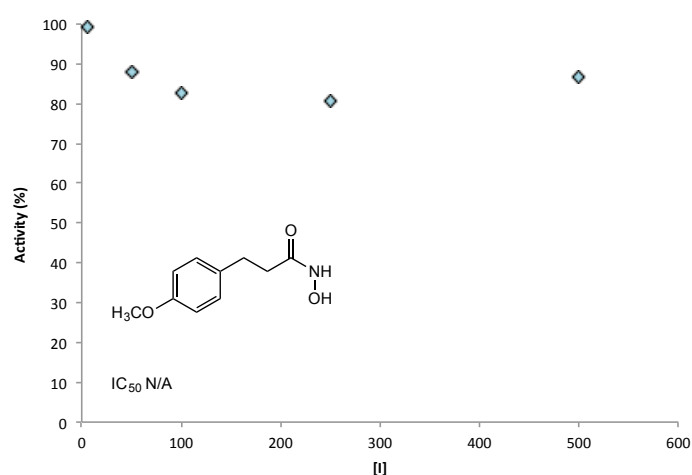


Figure 93: The IC_{50} of 3,4-methoxyphenyl propiohydroxamic acid (24) was obtained by plotting the data as % inhibition as a function of inhibitor concentration

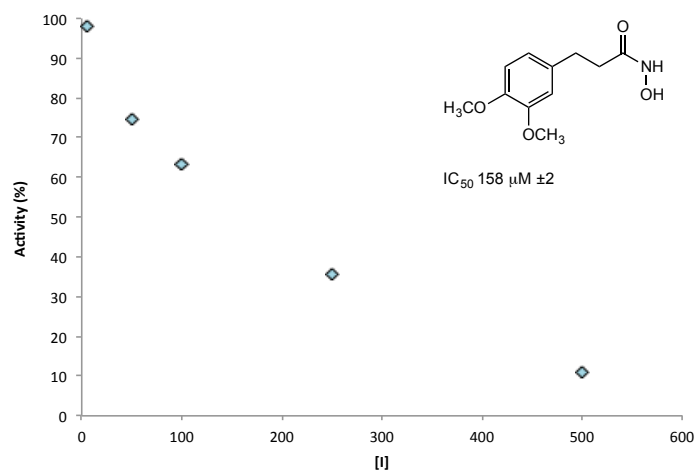


Figure 94: The IC_{50} of 3,4-dimethoxyphenyl propiohydroxamic acid (25) was obtained by plotting the data as % inhibition as a function of inhibitor concentration.

From these experiments, the inclusion of a double bond between the α and β carbons on the inhibitor was found to be important for enzyme inhibition.

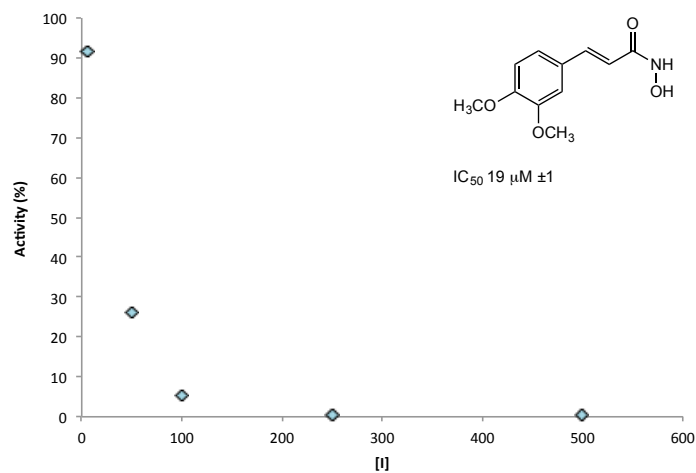


Figure 95: The IC_{50} of 3,4 dimethoxy cinnamohydroxamic acid (23) was obtained by plotting the data as % inhibition as a function of inhibitor concentration.

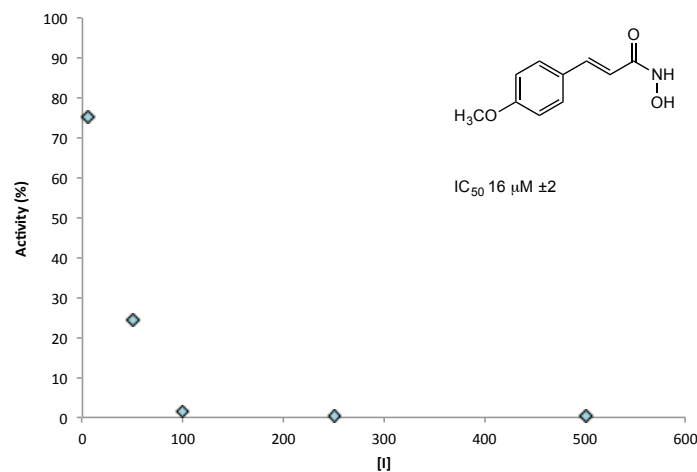


Figure 96: The IC_{50} of 4-methoxycinnamohydroxamic acid (D13) was obtained by plotting the data as % inhibition as a function of inhibitor concentration.

With the D13 and (23) inhibitors appearing to be active *in vitro* they were retested against expressed and purified extradiol dioxygenase MhpB. Neither compound had any discernable impact on enzyme activity. Therefore, the data suggests D13 and (23) are potent and selective *in vitro* inhibitors of the intradiol dioxygenase 3,4-PCD.

3.3.2.7 Evaluating *in vivo* chemical inhibition of 3,4-PCD in *R. jostii* RHA1 by D13 and (23)

The concentration for *in vivo* inhibition of 3,4 PCD in *R. jostii* RHA1 was chosen above the IC_{50} of the two compounds and set at 50 μ M. In incubations with *R. jostii* RHA1 in M9 minimal media with 5 mM protocatechuic acid (PCA) as a sole source of carbon in the presence of both inhibitors (final concentrations of 50 and 100 μ M) failed to show any signs of growth at all. Interestingly this could signify the compounds are taken up into the cell.

R. jostii RHA1 was then grown in M9 minimal medium supplemented with 0.4% glucose (w/v) and 5 mM PCA as an additional source of carbon (pH 7). The inhibitors were introduced to the medium after 16 hours.

R. jostii RHA1 displayed varied growth after timed exposure to the inhibitors. Inhibitor D13 at a concentration of 50 μM had a dramatic effect on *R. jostii* RHA1 and within 24 h of addition, less than 1% of colonies were viable. In contrast, bacteria exposed to 50 μM of (23) appeared to show a stable growth pattern up to approximately 48 h of incubation and was not significantly different from the control experiments without inhibitor. After this time, growth of bacteria grown with PCA as an additional source of carbon in the presence of (23) began to decrease slightly (Figure 97).

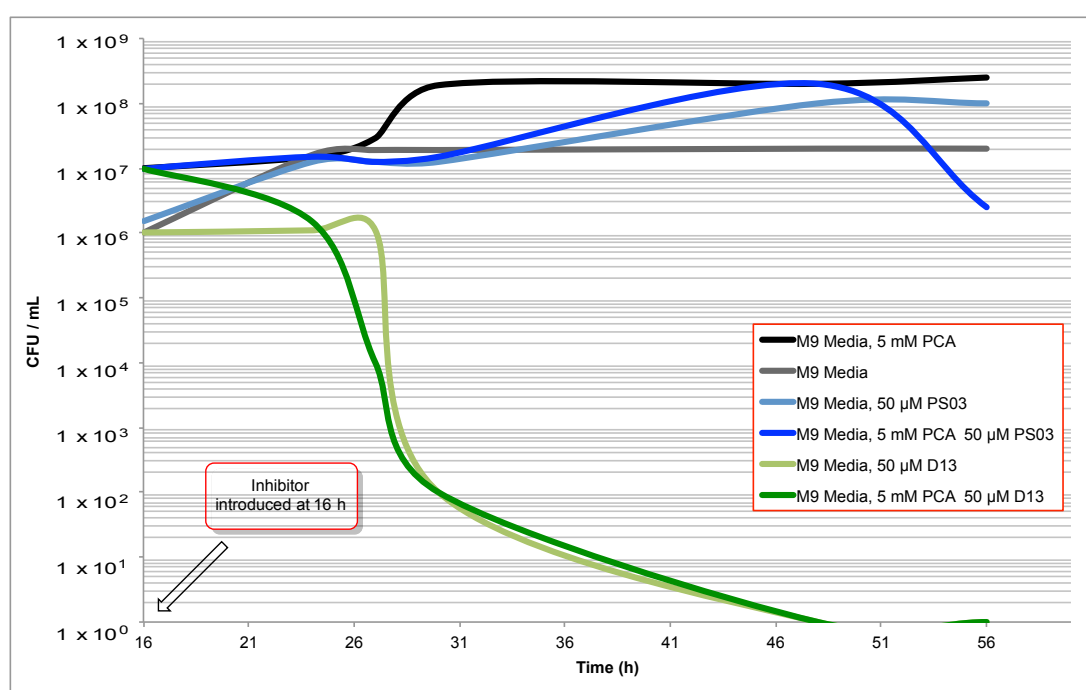


Figure 97: Logarithmic growth curve showing the effects of 3,4-dimethoxycinnamohydroxamic acid (23) and 4-methoxycinnamohydroxamic acid (D13) on *R. jostii* RHA1. Bacteria grown with 0.4% glucose (w/v) were exposed to inhibitors at a concentration of 50 μM for up to 46 h. Controls without inhibitor and without additional PCA carbon source were also monitored. Each data point is an average of three samples counted from the same time point.

The mechanism of toxicity by D13 is not entirely understood, the glucose should provide as an alternative source of carbon if the route to degrading protocatechuate is

blocked. The decrease in CFU however, was observed in the culture inoculated without PCA, indicating another method of toxicity affecting primary metabolism. Experiments were repeated and the addition of inhibitor staggered at different time points and the toxicity was still apparent.

One potential cause of toxicity may arise from enzymatic hydrolysis of the hydroxamic acid to release hydroxylamine (NH_2OH). Hydroxylamine has been known toxic to bacteria since 1964.^[213] An example of how the catalytic triad of a serine protease could catalyse this reaction is shown below. The serine proteases are just one of a number of enzymes capable of this reaction.^[214]

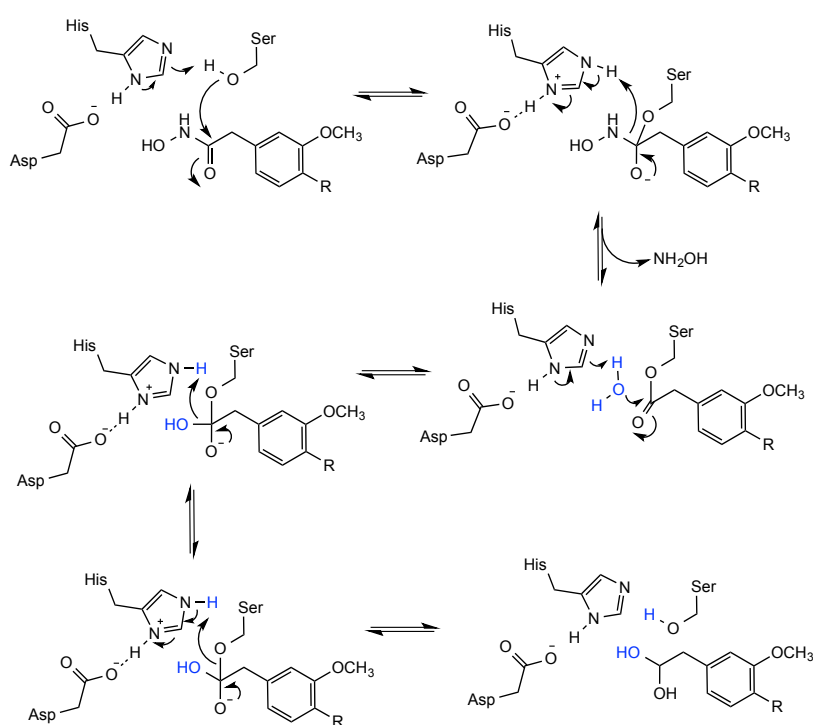


Figure 98: Proposed mechanism of the hydrolysis of a hydroxamic acid structure by a serine protease to release the bacteria toxin hydroxylamine (NH_2OH)

Incubations were then performed with *R. jostii* RHA1 in P1 media (500 mL) supplemented with 2.5% wheat straw lignocellulose (w/v). Inhibitor (23) was introduced to the medium (final concentration of 50 μM) after 16 hours and 50 mL

samples taken after 48, 72 and 96 hours. Analysis of extracellular and intracellular extractions of the samples were inconclusive by LC-MS analysis and did not indicate detectable levels of PCA or any other metabolites distinguishable from those in relevant control experiments.

Incubations were repeated under the same conditions using 10 mM ferulic acid and 0.1% glucose (w/v) in P1 media with samples extracted as per the lignocellulose experiment. Inhibitor (23) was introduced to the medium (final concentration of 50 μ M) after 36 hours. Within the EIC for m/z 153.3 (corresponding to the negatively charged ion of PCA) from the LC-MS analysis of an intracellular extraction from a sample taken at 96 h, a low intensity peak with a retention time of 15.6 minutes was observed and confirmed as PCA by comparing the retention time of an analytical standard (Figure 99).

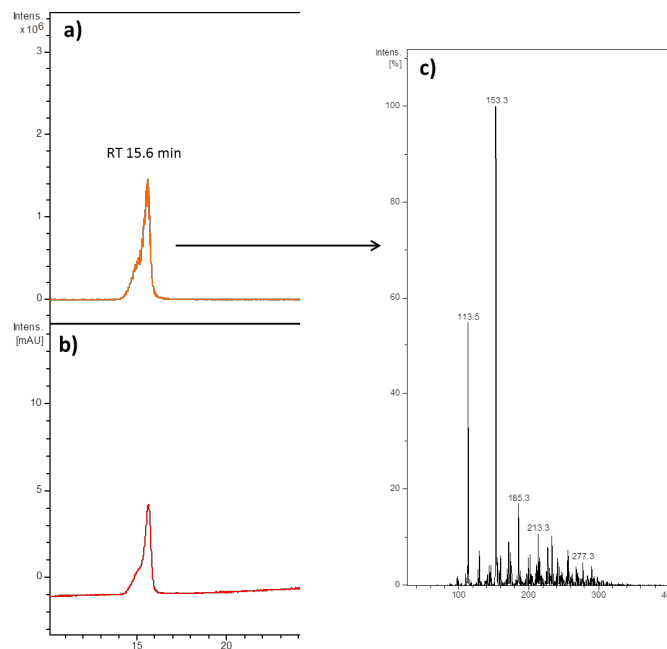


Figure 99: An EIC for m/z 153.12 shows a peak with a retention time of 15.6 min obtained in the sample taken at 96 h from the *R. jostii* RHA1 incubation (a). The small peak was first observed in the UV chromatogram @ 280 nm and not present in controls. The dominant ions at m/z 153.3

correspond to the expected $[M-H]^-$ ion (c). Incubations were performed in P1 media, 10 mM ferulic acid and 0.1% glucose (w/v) with inhibitor (23) introduced after 16 h (final concentration 50 μ M).

Using the result as a tentative inference that PCA accumulation in the cell may be occurring but below the levels of detection by LC-MS, it was hypothesised that the concentration could be determined by spectrophotometric analysis. Using a quartz cuvette, 1 mL of the intracellular extractions were run on the UV/Vis spectrophotometer @ 294 nm.

Table 4: Concentrations of PCA from the intracellular extractions obtained from incubations of *R. jostii* RHA1 with 10 mM ferulic acid in P1 media (inhibitor (23) concentration 50 μ M) by application of the Beer-Lambert law. The molar absorption coefficient value used for protocatechuate was 3800 $M^{-1} cm^{-1}$ @290 nm (pH7.5) in a 1 cm path length quartz cuvette. Absorbance values are the average of triplicate reads

Time	Absorbance (A) @ 294 nm	ΔA	Concentration μ M	Mg/L
Blank	0.2611	n/a	n/a	n/a
24	0.2659	0.0048	1.26	0.19
48	0.2698	0.0087	2.29	0.35
72	0.2789	0.0178	4.68	0.72
96	0.3048	0.0437	11.50	1.77

Application of the Beer-Lambert law on the data obtained did in fact show an increase in absorption at 294 nm. The molar absorption coefficient value used to calculate concentrations for protocatechuate was 3800 $M^{-1} cm^{-1}$ as established by the method of Stanier and Ingraham (1954).^[215]

Although the results from the spectrophotometric analysis remain uncorroborated by an alternative method, coupled with the data obtained from growth experiments they do suggest *in vivo* chemical inhibition of 3,4-protocatechuate dioxygenase by inhibitor (23), a novel hydroxamic acid.

4: Conclusions

Throughout the duration of this PhD it has been demonstrated that a targeted pathway engineering approach to enzyme inhibition can alter the metabolic flux of bacterial lignin degradation.

It was shown that a vanillin dehydrogenase gene knockout mutant of *R. jostii* RHA1 when grown on lignocellulose wheat straw displayed a remarkable increase in concentration of metabolites consistent with a blockage in the lignin degradation pathways. Furthermore, the levels of metabolites were at a concentration high enough to measure by LC-MS, potentially representing a novel method for discovering new lignin degradation pathways in other gene deletion bacterial strains.

A chemical approach also identified hydroxamic acids as potent and selective inhibitors *in vitro* of extradiol and intradiol iron dependent catechol dioxygenases. Tentative evidence also indicated *in vivo* inhibition of the intradiol catechol dioxygenase 3,4-PCD by a newly synthesised hydroxamic acid.

The discovery of further pathways and gene products for lignin breakdown in bacteria using the techniques developed in the PhD could in principle enable synthetic biology to be used to engineer new routes for production of chemicals from renewable feedstocks via catabolic pathways. Currently the methods developed in this PhD are being used within the group to identify other metabolites formed from the bacterial enzymatic degradation of lignin.

It was identified in the group that the peroxidase DypB could release vanillin when grown on a synthetic β -aryl ether dimer. Homologous gene overexpression of *dypB* could be coupled with deletion of vanillin aldehyde dehydrogenase in a directed

attempt to increase the metabolite of interest. The experiments could be monitored using the methods developed in chapter II.

The results from this PhD have also enabled a successful funding application in conjunction with a small biotech firm via a KTP fellowship. A large scale 5L fermentation with the gene deletion mutant of *R. jostii* RHA1 grown on lignocellulose is currently being attempted within that fellowship to garner whether the approach has any commercial value. The fermentations could indicate whether these techniques can be applied on a larger scale and also to alternative target enzymes of interest.

Vanillin is a toxic intermediate and not well tolerated by *R. jostii* RHA1. The production of vanillin in experiments with gene deletion mutants of *R. jostii* RHA1 when grown on lignocellulose was accompanied by a sharp decrease in CFU. Current studies in our group are investigating whether a mechanism to reduce vanillin toxicity could be implemented such as the introduction of a nucleotide-sugar dependent glycosyltransferase (UGTs) to *R. jostii* RHA1 with the aim of creating a vanillin β -D-glucoside that may accrue in the media from the cell.

A technique is also being explored within the group to combine the results gained during this PhD to use both chemical inhibition and genetic engineering for pathway manipulation. If the intradiol dioxygenase pathway in aromatic degrading bacteria could be blocked using chemical inhibitors, flux could be diverted into an alternative pathway, for example via introduction of an extradiol dioxygenase cloned and expressed in the same organism.

For example, the extradiol cleavage product could be treated with ammonium chloride (NH_4Cl) potentially generating a pyridine dicarboxylic acid product.

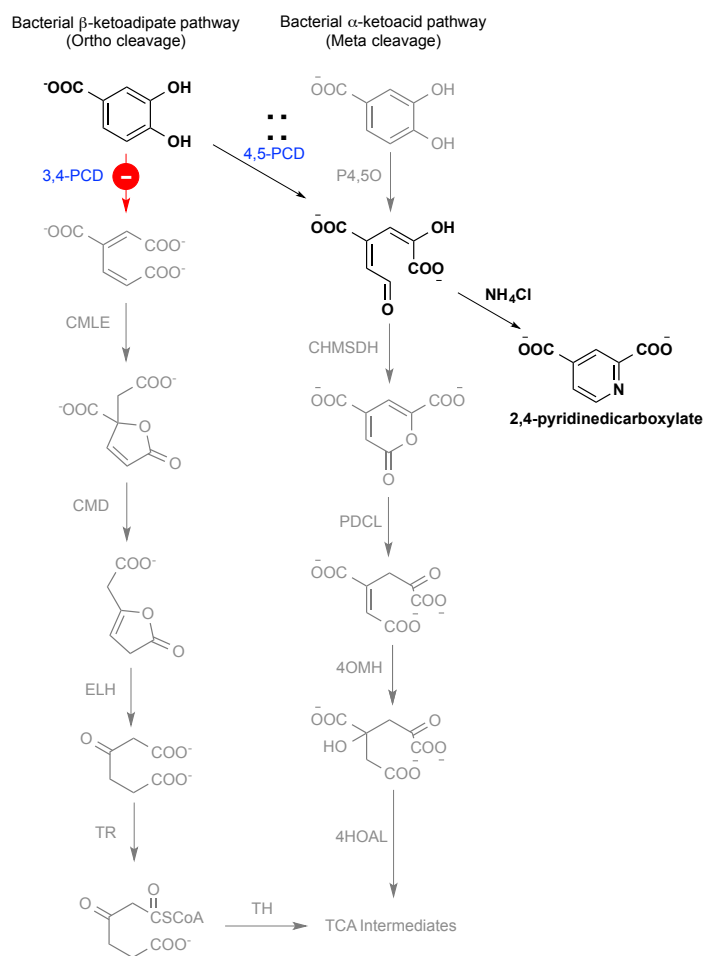


Figure 100: The bacterial *ortho* and *meta* catechol cleavage routes offer an opportunity to combine chemical and genetic pathway manipulation to afford useful agrochemical such as 1,3-pyridinedicarboxylate.

5: Experimental

5.1: General experimental

5.1.1 Chemicals and reagents

All common chemicals were purchased from VWR, UK Sigma-Aldrich, UK, Fischer Scientific, UK and Difco Laboratories, UK unless specified below or in the text. LC-MS and HPLC-UV was carried out using HPLC grade water and methanol from Fischer Scientific filtered through a 0.2 micron glass filter prior to use. All water used was deionised unless indicated otherwise

The source of lignocellulose in experiments was wheat straw milled in a Retsch grinding mill (model RM 200) sieved through a 0.5 mm mesh. Alkali lignin, purchased from Sigma-Aldrich, UK was used to represent an unknown source of Kraft lignin produced in a laboratory setting. Industrial Kraft lignin, manufactured from spruce, was kindly supplied by Billerud, Sweden.

5.1.2 Instruments and equipment

High-performance liquid chromatography (HPLC) was performed with an Agilent 1200 Series liquid chromatograph (Agilent Technologies, Cheshire, UK) equipped either with a G1311A quaternary pump and a variable-wavelength UV detector. Separations carried out over an Agilent reversed-phase Zorbax Eclipse XDB-C18 column (250 by 4.6 mm, 50 μ m particle size).

Gas chromatography mass spectrometry (GC-MS) was performed through a fused silica capillary column (30 m x 0.25 mm) conducted on a Varian 4000 GC-MS system consisting of a gas chromatograph (Varian 3800) and fitted with an ion trap mass spectrometer (Varian 4000) using an mass analyser and ion multiplier detector

Liquid chromatography mass spectrometry (LC-MS) analysis was accomplished using an Agilent 1200 Series system, equipped with a DAD photodiode detector (G1315B) connected to a Bruker HTC-Ultra ESI mass spectrometer (Coventry, UK) both coupled to an Agilent ChemStation (Version B.01.03) for data processing. Low-resolution ESI mass spectra were recorded with a Bruker Esquire 2000 spectrometer and high-resolution LC-MS spectra obtained by submission to the University of Warwick Mass Spectrometry service on a Bruker MaXis ESI spectrometer.

The NMR spectra were recorded on a Bruker AM-300 (^1H 300MHz and ^{13}C 75MHz) instrument. Chemical shifts are given in ppm with TMS as an internal standard.

Melting points were determined using a Stuart SMP10 melting point apparatus, and are uncorrected. Flash chromatography was carried out on silica gel (Fluorochem LC60A40-63 micron. Thin layer chromatography (TLC) was performed on 0.25 mm thick TLC F254 aluminium plates precoated with silica gel (art. no. 1.05554.001) (Merck, Germany) and visualised under a low-frequency UV lamp.

The optical density of bacterial cultures was measured using a Thermo BioMate3 spectrophotometer. SDS page was carried out using a BioRad Mini-protein electrophoresis system. The centrifuges used were Eppendorf models 5424 and 5810 and a Fisher Scientific AccuSpin Microcentrifuges. A Varian Cary 50 Bio UV/ Visible Spectrophotometer was used to monitor the absorbance and measurements taken using a 1 mL quartz cuvette.

A pneumatic cell disrupter (ConstantSystems, UK) was used to lyse cells (20 KPSI)

Fast Protein Liquid Chromatography (FPLC) was carried out on an ÄKTAFPLC system consisting of a P-920 system pump connected to a UPC-900 monitor (GE Healthcare, UK).

For the plate reader assays, each sample was transferred into 370 μ L Greiner UV star 96 well plates and read using a GENios Microplate Reader (Tecan, Switzerland).

5.1.3 Enzymes and commercially prepared kits

Bradford reagent, bovine serum albumin (BSA) and protocatechuate 3,4-Dioxygenase (3,4-PCD) from *Pseudomonas* sp. were purchased from Sigma-Aldrich UK

5.1.4 Solutions and buffers

Unless otherwise stated, all buffers and solutions were prepared according to standard procedures.^[216]

5.1.4.1 Potassium phosphate 0.1M buffer stock solution (pH 8)

94 mL of 1M K_2HPO_4 , 6 mL of 1M KH_2PO_4 and bring to 1 L with deionised water.

5.1.4.2 MhpB Suspension buffer A^[209] (pH 8)

250 mL 0.1M phosphate buffer, 66.07 g $(NH_4)SO_4$, 50 mL glycerol, 50 mL ethanol, 350 μ L β -mercaptoethanol and bring to 500 mL with deionised water.

5.1.4.3 MhpB Purification buffer B^[209] (pH 8)

250 mL 0.1M phosphate buffer, 50 mL glycerol, 50 mL ethanol, 350 μ L β -mercaptoethanol and bring to 500 mL with deionised water.

5.1.4.4 Tris acetate buffer (50x) (pH 8)

242 g Tris base, 57.1 mL glacial acetic acid and bring to 1 L with deionised water.

5.1.4.5 SDS loading sample (5x)

3 mL of 1M Tris-HCl, pH 6.8, 5 mL of Glycerol, 1 g of SDS powder, 0.05 g of Bromophenol blue and 500 μ L β -mercaptoethanol, Bring to 10 mL with deionised water. Final concentrations (in a 1x solution): 60 mM Tris, 10% glycerol, 2% SDS, 0.1% bromophenol blue, 1% β -mercaptoethanol.

5.1.4.6 SDS running buffer

57.6 g Glycine, 12 g Tris base, 4 g SDS, deionised water to 4 L

5.1.4.7 Coomassie staining solution

1 g Coomassie R250, 100 mL glacial acetic acid, 400 mL methanol, 500 mL deionised water

5.1.4.8 De-stain for Coomassie

200 mL methanol, 100 mL glacial acetic acid 700 mL deionised water

5.1.5 Media

All media were prepared in deionised water and either autoclaved or filter-sterilised prior to use. Where appropriate filter-sterilised Ampicillin (dissolved in water, and stored at -20°C) was added to media at a final concentration of 100 μ g/ml.

5.1.5.1 LB

Tryptone 10g/L, yeast Extract 5 g/L, NaCl 10 g/L. (For LB plates, 15 g/L agar was added prior to autoclaving)

5.1.5.2 Growth media P1 (pH 7)

Na₂HPO₄·12H₂O 0.85 g/L, NH₄Cl 1 g/L, KH₂PO₄ 3 g/L, 0.5 g/L NaCl, 0.24 g/L MgSO₄ were dissolved in water and autoclaved. Following autoclaving 1 mL of 1 M MgSO₄ (final concentration 1 mM), 1 mL of 100 mM CaCl₂ (final concentration 100 μM), 1 mL of 100 mM MnCl₂ (final concentration 100 μM) and 1 mL of 50 mM FeCl₃ solution (final concentration 50 μM) The solution are filter sterilised and added as separate solutions to prevent precipitation problems. When not in use the solutions were stored in the stored at 4 °C. FeCl₃ stock solution (50 mM in 100 mM citric acid) contains 1.35 g FeCl₃·6H₂O and 2.10 g citric acid·H₂O in 100 mL deionised water. The FeCl₃ is particularly unstable and the stock solution was wrapped in foil before storage at 4°C.

5.1.5.3 Minimal medium M9 (M9) (pH 7)

Na₂HPO₄·12H₂O 0.85 g/L, NH₄Cl 1 g/L, KH₂PO₄ 3 g/L and NaCl 0.5 g/L were added to water and autoclaved. Following autoclaving 1 mL of 1 M MgSO₄ (final concentration 1 mM) 20 mL of 20% (w/v) glucose (final concentration 0.4% (w/v) glucose). (For M9 plates, 15 g/L agar was added prior to autoclaving and the additional supplements were introduced just before pouring)

5.1.5.4 Colour enhancing media (CEM)^[211] (pH 7)

Bactopeptone 5g/L, Na₂HPO₄·12H₂O 1.5 g/L, NaCl 5 g/L, yeast extract 3 g/L and L-proline 2 g/L were added to water and autoclaved. Following autoclaving, the indicator carbon source 3-phenylpropionic acid (0.2g in 50 mL of deionised water), was filter sterilised and added for a final concentration of 1.3 mM.

5.1.5.5 Trace element solution (P2)

Citric acid 5 g/L, ZnSO₄ • 7H₂O 5 g/L, Fe(NH₄)₂(SO₄)₂•6H₂O 1 g/L, CuSO₄•5H₂O 0.25 g/L, H₃BO₃ 0.05 g/L mg, Na₂MoO₄•2H₂O 0.05 g/L were added to water and autoclaved.

5.1.6 Bacterial Strains

All bacterial strains were the property of the chemical biology department, University of Warwick unless stated otherwise.

The following Rhodococcus strains were used:

- *R. jostii* RHA1 wild type
- *R. jostii* RHA1 Δ *vdh* (ro02986) and Δ *vanA* (ro04165) provided by Prof. Lindsay Eltis (University of British Columbia)
- *R. opacus* DSMZ 069

The following Pseudomonas strains were used:

- *P. putida* MT2
- *P. fluorescens* PF5 DSMZ 289

The following Escherichia coli were used:

- *E. coli* TB1 DH5 α /pIPB
- *E. coli* K-12 W3747 (parent strain)
- *E. coli* K-12 LW366 Δ MhpB
- *E. coli* K-12 LW353 Δ MhpC
- *E. coli* K-12 LW293 Δ MhpC (2)

The following other strains were used:

- *Microbacterium phyllosphaerae*
- *Sphingobacterium sp. T2*
- *Bacillus subtilis* DSMZ 10

5.2: Methods

5.2.1 Culture growth conditions and storage of cells

Bacteria were grown in either an incubator or a New Brunswick Scientific Innova shaker at 180 rpm. All *E. coli* strains were grown at 37°C, The Sphingobacterium isolate was grown at 45°C and all other strains were grown at 30°C. Cell growth was measured spectrophotometrically by measuring the optical density (OD) of each sample at 600 nm in a Thermo Biomate 3 spectrophotometer. When the spread count method was employed, a volume of culture (~0.1 mL) was spread over the surface of an agar plate by using a sterile glass spreader and the plate left to incubate and develop colonies. The number of colonies was then counted.

For frozen storage, 1 mL of bacterial culture was added into 2 mL sterile polypropylene microfuge screw top tubes containing 1 mL of sterile 50% glycerol (v/v) and mixed using a vortex mixer. Vials were frozen in liquid nitrogen and stored at -80°C. Cells were recovered by thawing at RT.

5.2.1.1 Overnight cultures

Bacterial isolates were streaked from glycerol stocks onto M9 agar plates and incubated for 18 to 42 h to obtain individual (clonal) colonies of bacteria unless stated otherwise. A single colony from a freshly streaked plate was then used to inoculate a sterile glass tube with cap (13 x 100 mm) containing 3 mL M9 liquid media unless

stated. The tubes were incubated in a shaker and grown to mid-log phase OD (OD 0.3-0.5).

5.2.2 Incubations with sources of lignin

Overnight cultures of bacterial strains used in incubations were prepared as detailed in section 5.2.1.1. All bacterial strains used were plated from existing glycerol stocks apart from those pertaining to *R. jostii* RHA1, which were cultured by the manner detailed in section 5.2.2.1.

5.2.2.1 Isolation and subculturing of activated R. jostii RHA1 strains

Strains of *R. jostii* RHA1 were enriched and isolated from lignin sources using the medium described below containing either 2.5% (w/v) wheat straw lignocellulose or 0.5% (w/v) Kraft lignin plus a decreasing gradient of glucose as a complimentary energy sources. The bacteria were initially grown under sterile aerobic conditions with the lignin source in growth media P1 (Section 5.1.5.2), 0.2% (v/v) trace element solution P2 (Section 5.1.5.5) and 1% (w/v) glucose. The glucose solution was sterilised by filtration and added after later following autoclaving. To obtain single colonies, the bacteria were repeatedly subcultured on agar plates with a 50% decrease in glucose concentrations until growth was not observed. Cultures of *R. jostii* RHA1 able to grown on a minimum of 0.05% glucose and lignin source were stored on plates at 4°C for a maximum of 4 weeks.

5.2.2.2 Fermentations with the selected lignocellulosic carbon source

A 2 mL aliquot of an overnight culture of the bacterial strain grown in P1 growth media and 0.1% (w/v) glucose was used to inoculate fermentations supplemented with the appropriate sterile carbon source. The fermentations were performed in

100 mL of growth media P1 in conical flasks stoppered with a foam bung and incubated at 30°C with shaking at 180 rpm. Solutions were left to shake for 7 to 14 days. For the growth analysis and investigations of metabolites in the cultures, 1 mL samples were taken from the liquid phase at time point 0, after 3 and 6 h and then every 24 hours days until growth was not observed in any strain. The OD at 600 nm was recorded for each sample before metabolite extraction (see 5.2.3.1).

5.2.2.3 Wheat straw Alkali Lignin preparation^[120]

Adapted from the procedure of R Sun (1996) milled wheat straw (15 g) was added to 1.5% wt/v NaOH (300 mL) and left to stir in a glass beaker for two h. The slurry was filtered through Whatman # 1 filter paper using a Buchner funnel. The solid residue was removed and washed several times with H₂O and then freeze dried. The filtrate was acidified to pH 6.5 with acetic acid and then concentrated in vacuo. The extract was then mixed with 5 volumes of ethanol and left overnight. Any precipitated hemicelluloses and hemicellulosic-lignin was removed by Buchner filtration and the filtrate then acidified to pH 1.5 with 6M HCl and left for 24 h. The alkali-soluble lignin precipitate was collected by centrifugation in 50 mL falcon tubes (Fischer Scientific, UK) at 4702 x g for 10 minutes and the pellets freeze-dried overnight to give a 1.2% yield (180 mg).

5.2.2.4 Incubations in Colour enhancing Media (CEM) for isolation of E. coli strains defective in MhpB and MhpC activity.^[211]

Without modification from the procedure of R Burlingame (1986), a single colony of the appropriate E. coli mutant grown on an LB agar plate was used to inoculate 10 mL of CEM (Section 5.1.5.4) in a glass tube. Solutions were left to shake at 180 rpm for

2 days in an incubator set to 30°C. The appearance and change in colour was documented or photographed.

5.2.3 Metabolite extractions

5.2.3.1 Ethyl Acetate Extraction

Samples taken from the fermentations (Section 5.2.2.2) were centrifuged at maximum speed (10min, 13000 rpm) and the supernatant was removed with the cell pellet being kept for intracellular metabolite analysis (Section 5.2.5.2). The supernatant was then adjusted to pH 2 with 6N HCl and left on ice for 3 minutes. The samples were again centrifuged (10min, 13000 rpm) and the supernatant extracted into an equal volume ethyl acetate. The organic layer was dried under nitrogen. (Samples over 10 mL taken from larger scale experiments were mechanically shaken solvent removed *in vacuo*). All samples were prepared in triplicate.

5.2.3.2 Hot ethanol extraction

Hot ethanol extractions were performed on 100 mL extractions from larger scale fermentations (500 mL). The cell pellet was resuspended in 500 µL of boiling ethanol and placed into a hot water bath (90°C) for 10 min. The suspension was vortexed twice during the 10 minutes and finally the sample was frozen in liquid nitrogen. The boiling and freezing process was repeated twice and samples then stored at -80°C overnight. After rapid thawing in a hot water bath (50°C) for 1 minutes the samples were centrifuged at maximum speed (10min, 13000 rpm) and the supernatants filtered through 0.20 µm Minisart filters (Sartorius, Germany) into clean glass vials before analysis.

5.2.4 Thin layer chromatography

Analytical grade solvents were used for TLC chromatography. Phenolic compounds were occasionally visualized with ferric (III) chloride (FeCl_3) (2% in methanol). Aldehydes and ketones were also detected with a 2,4,-dinitrophenylhydrazine (2,4-DNP) 0.4% (w/v) in 2 N HCl. Choosing the right elutant or elutant mixture for the TLC varied, requiring some trial and error and is noted where appropriate.

5.2.5 HPLC-UV analysis

Samples were injected onto a C18 Zorbax Eclipse plus (Agilent Technologies, UK). The solvents used were water and MeOH. The flow rate was 1 mL/min. The linear gradient for solvent B was as follows: 0 min, 5%; 15 min, 35%; 30 min, 43%; 32 min, 100%; 40 min, 5%. Eluted peaks were detected at 280 nm or at 325 nm and identified by comparison with authentic standards at a flow rate of 0.1 mL/min.

5.2.6 LC-MS analysis

The organic residue from extractions was re-dissolved in 1 mL 50% v/v methanol and samples were injected onto a C18 Zorbax Eclipse plus (Agilent Technologies, UK). The solvents for positive ionisation mode were water / 0.1% (v/v) trifluoroacetic acid (TFA) as solvent A and MeOH / 0.1% (v/v) TFA as solvent B. For negative ionisation the solvents used were water / 0.1% (v/v) ammonium hydroxide (NH_4OH) as solvent A and MeOH / 0.1% (v/v) TFA as solvent B. The flow rate was 1 mL/min. The linear gradient for solvent B was as follows: 0 min, 5%; 15 min, 25%; 23 min, 25%; 35 min, 70%; 42 min, 0%, 45 min, 0%, 49 min, 95%, 50 min, 95%. Eluted peaks were detected at 254, 280 nm or at 325 nm and identified by comparison with authentic standards at a flow rate of 0.1 mL/min. Standard curves for these compounds were established over the range of 0.3 to 3 $\mu\text{g/ml}$.

5.2.7 GC-MS analysis

Samples were prepared for GC-MS from dried organic extracts reconstituted in dichloromethane 1 mL DCM and dried through glass pipettes filled with 50 mg of magnesium sulphate. The samples were then derivatised with 200 μ L of N,O-bis(trimethylsilyl)acetamide (BSA) and 10 μ L of chlorotrimethylsilane (TMCS), left for at least 2 hours and diluted by a factor of 100. For metabolite reference and quantification, stock solutions were made from analytical standards. Helium was used as carrier gas (0.7 bar) at a flow rate of 1.3 mL/min. The splitter/injector was kept at 300°C and the column temperature was programmed as follows: 100°C held for 4 minutes then increased by 4°C/min until 270°C where it was held for 4 minutes. The ion source temperature was 150°C. The chromatograms were recorded by ion monitoring in the m/z range 50- 500.

5.2.8 Protein purification

5.2.8.1 *Overexpression of E. coli 2,3-dihydroxyphenyl propionate 1,2-dioxygenase (MhpB).*^[209]

Unless otherwise stated, all the overexpression and purification steps were carried out at 4°C. The procedure has been slightly modified from that described by TDH Bugg (1993). Buffer ingredients listed in section 5.1.4. A single colony of TB1/pIPB was used to inoculate a 50 mL culture of LB containing 100 μ g/mL AMP and grown overnight at 30°C. A 2 L culture of LB containing 100 μ g/mL AMP was diluted with 2 mL of the overnight culture (1:1000) dilution and grown at 37°C for at least 4 h. Once the OD at 600nm had reached 0.6-0.8, the cells were induced by the addition of IPTG to a final concentration of 0.5 mM and grown with shaking at 15°C for 16 h.

5.2.8.2 MhpB purification

The cells were harvested by centrifugation for 10 minutes at 5000 x g and resuspended in approximately 10 mL of buffer B per g of pellet. Cell lysis was carried out by a cell disrupter and cell debris removed by centrifugation at 25000 x g for 30 min. Powdered ammonium sulphate (NH₄SO₄) was added to the cell free extract to 25% saturation (139 g/L) and the suspension stirred for 1 h. After centrifugation at 25000 x g for 20 min, the supernatant was collected and NH₄SO₄ added to 50% saturation (301 g/L) and the suspension stirred for a further 1 h. After centrifugation at 25000 x g for 30 min, the pellet was resuspended in buffer A and loaded onto a pre-equilibrated phenyl agarose column. The cell free extract was injected via a 50 mL superloop (GE Healthcare, UK) equilibrated with buffer A at a flow rate of 0.25 mL/min. The proteins were then eluted with a linear gradient of 0 to 100% buffer B at a flow rate of 0.25 mL/min. Each fraction was monitored at 280 nm, and collected in glass tubes at a volume of 1.5 mL.

5.2.8.3 Electrophoresis of proteins using sodium dodecyl sulfate–12% polyacrylamide gel electrophoresis (SDS-PAGE)

When SDS-PAGE was used to monitor collected FPLC fractions, proteins were resolved using a 12% separating gel, with a 5% stacking gel prepared to standard protocols.[216] The protein ladder used was PageRuler Plus Prestained Protein Ladder (ThermoScientific, UK). In 100 µl polypropylene microtubes (Eppendorf, Germany), 20 µl of each fraction and 5 µl of SDS-PAGE loading buffer (Section 5.1.4) were heated at 95°C in a heating block for 5-10 minutes alongside 10 µl of cell free extract and 10 µl of SDS-PAGE loading buffer in a separate tube. The tubes were all centrifuged at maximum speed for 2 minutes and 20 µl of the supernatant loaded

directly into a well of an SDS-PAGE gel. Gels were run at 150 V for approximately 80 min. Fractions identified to be containing purified MhpB were pooled, concentrated and stored at 4°C.

5.2.8.4 Bradford assay^[217]

Protein concentrations were determined by the method of Bradford with bovine serum albumin (BSA) as a standard. Purified protein solutions were made at 0 x, 2 x, 5 x and 10 x dilutions. A 5 mg/mL of BSA stock solution (5 mg BSA in 1 mL water) was further diluted with water to obtain the following standards for the assay; 1.40 mg/mL, 1.00 mg/mL, 0.50 mg/mL and 0.25 mg/mL. The Bradford reagent was brought to room temperature and 50 µl of each standard dilution was pipetted into a disposable 2 mL polypropylene microtube (Eppendorf, Germany) and 1.5 mL of Bradford reagent added. Each sample was incubated at room temperature for approximately 5 minutes and lightly centrifuged (30 sec, 5000 x g) prior to measuring. A cuvette of 1.5 mL Bradford reagent was used to blank the spectrophotometer. The absorbance of each sample was measured at 595 nm to obtain the data needed to plot a standard curve. Then 50 µl of the protein dilution was combined with 1.5 mL of Bradford reagent and the OD at 595 nm measured. This was repeated twice for each dilution and the protein concentration of each sample was calculated considering the dilution factor.

5.2.9 Enzyme assays

5.2.9.1 MhpB Assay^[209]

Purified samples of the inactive apoenzyme (100 µL) were re-activated by treatment with 5 µL of 100 mM stock solution of sodium ascorbate (5 mM) and 5 µL of a saturated stock solution of ammonium Fe (II) sulphate (5 mM) and kept on ice for 1-2 minutes prior to assay. MhpB was assayed spectrophotometrically at RT by

monitoring the increase in absorbance at 394 nm in 50 mM. The reaction was initiated by the addition of 5 μ L enzyme solution to a solution of 2,3-dihydroxyphenylpropionic acid (DHPP) in a 1 mL quartz cuvette and mixed by inversion. The reaction was scanned every 0.1 sec for 2 min. A stock solution of DHPP (13.73 mM) was made in potassium phosphate buffer (pH 8.0) (Section 5.1.4.1).

The enzyme kinetics for MhpB was determined at a range of substrate concentrations (0.21 to 0.08 mM) V_{\max} and K_m values were determined from triplicate rate determinations by plotting Michaelis-Menten and Lineweaver-Burk graphs. A solution containing 1.4 mg/ml of MhpB in ice-cold potassium phosphate buffer (pH 8) buffer was activated just before use. One unit of enzyme is defined as the amount that oxidizes 2,3-dihydroxyphenylpropionic acid to 2-hydroxy-6-oxo-nona-2,4-diene 1,9-di-carboxylate at an initial rate of 1 μ M/min. Specific activity was calculated as units per milligram of protein. The millimolar extinction coefficient of 2-hydroxy-6-oxo-nona-2,4-diene 1,9-di-carboxylate at 394 nm is 15.6 mM⁻¹ cm⁻¹ as described by TDH Bugg (1993).^[209]

5.2.9.2 Protocatechuate-3,4-Dioxygenase Assay^[218]

Protocatechuate 3,4-dioxygenase (3,4-PCD) activity was measured at RT by measuring the decrease in absorbance at 290nm spectrophotometrically using commercially obtained enzyme (Sigma-Aldrich, UK). Immediately before use a solution containing 0.15 mg/ml of Protocatechuate 3,4-Dioxygenase in ice-cold 50 mM Tris-acetate buffer was prepared. The reaction was initiated by the addition of 25 μ L enzyme solution to 975 μ L of a stock solution of protocatechuic acid (580 μ g in 100 mL 50 mM Tris-acetate buffer (Section 5.1.4.4) pH 7.5) in a 1mL quartz

cuvette and mixed by inversion. The reaction was scanned every 0.1 sec for 2 min. The concentrations in the final reaction mixture were 0.39 mM protocatechuic acid, 50 mM Tris-Acetate buffer (pH 7.5) and 0.015 mg 3,4-PCD in a total volume of 1 mL. One unit of enzyme is defined as the amount that oxidizes protocatechuate to 3-carboxy-*cis,cis*-muconate at an initial rate of 1 $\mu\text{M}/\text{min}$. Specific activity was calculated as units per milligram of protein. The millimolar extinction coefficient of protocatechuic acid at 290 nm is 3.8 $\text{mM}^{-1} \text{cm}^{-1}$ as described by DL MacDonald (1954).^[218]

5.2.10 In-vitro Chemical Inhibition Assays

All experiments were performed at RT and in triplicate.

5.2.10.1 Chemical inhibition of MhpB

5.2.10.1.1 Plate reader assay

Screening for potential MhpB inhibitors was initially performed colourimetrically in a 96 well plate by visually observing the degree of colour change in each well. Each sample was performed in triplicate and final concentrations of inhibitors were 50, 100, 200 and 500 μM . The final concentration of the substrate DHPP in the reactions was 0.03 mM and the reaction, initiated by addition of 1 μL enzyme and mixed by pipetting up and down.

5.2.10.1.2 UV/Vis Inhibition assay

Inhibition of MhpB activity was measured spectrophotometrically under the same conditions as previously stated (Section 5.2.9.1). The final concentration of substrate DHPP in the reactions was 0.03 mM. Concentrations of inhibitors were staggered from 0 to 250 μM . The final reaction volume was 1 mL and the reaction, initiated by

addition of 5 μ L enzyme and mixed by inversion. An estimate of IC₅₀ was measured by plotting a graph of concentration of drug via activity (Abs (with inhibitor) / Abs (control without inhibitor addition) x 100%. The IC₅₀ was read at the 50% activity position.

5.2.10.2 Chemical inhibition of 3,4-PCD

5.2.11.1.1 Plate reader assay

Screening for potential 3,4-PCD inhibitors was performed using a Greiner UV star 96 well plate and the decrease in absorbance measured at 280 nm. 150 μ L of a 0.5 mM PCA stock solution in tris acetate buffer (final concentration 0.38 mM) and 45 μ L of an inhibitor stock solution in tris acetate buffer were added to the wells followed by 5 μ L of enzyme solution to initiate the reaction. The microplate was then read at 280 nm every 5 s for 2 min. Final concentration of inhibitors was 200 μ L

5.2.11.1.2 UV/Vis Inhibition assay

Inhibition of 3,4-PCD activity was measured spectrophotometrically under the same conditions as previously stated (Section 5.2.9.2). The final concentration of PCA in the reactions was 0.4 μ M. Final concentrations of inhibitor were 500, 250, 100, 50 and 5 μ M. The final reaction volume was 1 mL and the reaction, initiated by addition of 5 μ L enzyme and mixed by inversion. An estimate of IC₅₀ was obtained by plotting the data as % inhibition as a function of log inhibitor concentration. The IC₅₀ was read at the 50% activity position.

5.2.11 In-vivo Chemical Inhibition Assays

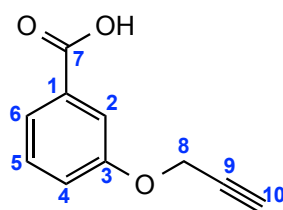
All experiments were performed at RT in triplicate and performed with appropriate controls. The IC₅₀ levels were used to determine the concentrations of inhibitor unless

stated otherwise. Incubations were performed as described in section 5.2.2 with filter-sterilised inhibitors introduced after 16 hours.

5.3: Synthesis

The abbreviations used for the ^1H and ^{13}C NMR spectral data are as follows: s, singlet; d, doublet; t, triplet. All compounds were synthesised following experimental data using the references provided.

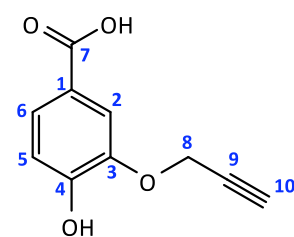
5.3.1 Synthesis of 3-(prop-2-ynoxy)benzoic acid (21)^[219]



To a stirred solution of 3-hydroxybenzoic acid (1.12 g, 8.11 mmol) in MeOH (50 mL) at room temperature was added 1 mL of concentrated H_2SO_4 . After stirring for 8 h, water (10 mL) was added and MeOH removed in vacuo. The reaction mixture extracted with EtOAc (3 x 10 mL). The combined organic layers were washed with NaHCO_3 (2 x 10 mL), brine (2 x 10 mL, dried over MgSO_4 , filtered and concentrated in vacuo. The methyl-3-hydroxybenzoate as a clear oil (0.95 g, 6.25 mmol) that crystallised at room temperature was dissolved in DMF (50 mL). To this stirred solution was added K_2CO_3 (2.85 g, 20.62 mmol) and propargyl bromide (~80% in toluene) solution (1.332 g, 1 mL, 9.4 mmol). After stirring for 16 h at ambient room temperature, the solution was diluted with EtOAc (30 mL) and washed with H_2O (15 mL), 0.2M HCl (15 mL), H_2O (15 mL), saturated NaHCO_3 (aq) (15 mL), H_2O (15

mL), and brine (15 mL). The organic layer was dried over MgSO₄, filtered and concentrated *in vacuo*. The pale yellow waxy solid was shown to be pure by NMR. The product (0.90 g, 4.73 mmol) was dissolved in TMF (40 mL) and stirred with Lithium Hydroxide and water LiOH.H₂O (0.38g, 9.27 mmol) for four hours. The mixture was acidified to pH 4 with 2M HCl and extracted into DCM, dried with MgSO₄ and concentrated *in vacuo*. The product, 3-(prop-2-ynyloxy benzoic acid), recrystallised in H₂O and was collected as off white crystals (0.81 g, 4.60 mmol, 57%) mp 92-93°C ¹H-NMR (400MHz, DMSO-*d*₆) δ_H: 7.59 (1H, d, J=7, **H6**) 7.54 (1H, s, **H2**) 7.44 (1H, t, J=8, **H5**) 7.20 (1H, d, J=8, **H4**) 4.86 (2H, d, J=2, **H8**) 3.55 (1H, t, J=2 **H10**) ¹³C-NMR (100MHz, DMSO-*d*₆) δ_C: 165.92 (**C7**) 157.15 (**C3**) 130.93 (**C1**) 129.80 (**C5**) 122.48 (**C6**) 120.06 (**C2**) 114.82 (**C4**) 78.34 (**C9**) 75.56 (**C10**) 52.12 (**C8**) HR-MS (ES+) *m/z* calculated for [C₁₀H₉O₃]⁺ 177.0703 found 177.0707

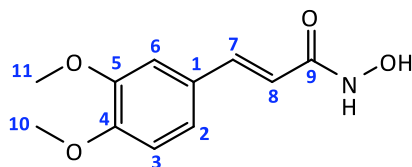
5.3.1 Synthesis of 3-(prop-2-ynyloxy)-4-hydroxy benzoic acid (**22**)^[219]



To a stirred solution of 3,4-dihydroxybenzoic acid (1.08 g, 7.01 mmol) in MeOH (50 mL) at room temperature was added 7 drops of H₂SO₄. After stirring for 24 h, water (10 mL) was added and MeOH removed *in vacuo*. The reaction mixture extracted with EtOAc (3 x 10 mL). The combined organic layers were dried over MgSO₄, filtered and concentrated *in vacuo* as a white solid. To a stirred solution of methyl

3,4-dihydroxybenzoate (0.90 g, 5.35 mmol) and propargyl bromide (~80% in toluene) solution (1.5 g, 1.1 mL, 8.15 mmol) in DMF (50 mL) at room temperature was added K₂CO₃ (2.60 g, 18.82 mmol). After stirring for 48 h, the solution was diluted with EtOAc (30 mL) and washed with H₂O (15 mL), 0.2M HCl (15 mL), H₂O (15 mL), saturated NaHCO₃ (aq) (15 mL), H₂O (15 mL), and brine (15 mL). The organic layer was dried over MgSO₄, filtered and concentrated *in vacuo*. The crude product was shown by NMR to contain a 3:1 ratio of methyl (3-propargyloxy-4-hydroxy) benzoate and methyl (3-hydroxy-4-propargyloxy) benzoate. TLC analysis (20% EtOAc/LP) revealed the presence of two UV-absorbing spots (R_f = 0.60 and 0.62) with the slightly higher spot corresponding to the product. The two isomers were dissolved in EtOAc and applied to a silica gel column (3.8 cm x 16.5 cm) and eluted with 20% EtOAc in LP. Fractions of approximately 5 mL each were collected and analyzed by TLC. Fractions containing a single R_f = 0.62) were pooled and solvent removed under reduced pressure to yield the required isomer as a white solid. The product (0.61 g, 3.19 mmol) was dissolved in TMF (40 mL) and stirred with Lithium Hydroxide and water LiOH.H₂O (0.38g, 9.27 mmol) for four hours. The mixture was then acidified to pH 4 with 2M HCl and extracted with DCM. The organic phase was dried with MgSO₄ and concentrated *in vacuo*. The product was recrystallised in H₂O and collected as a fluffy white solid 3-(prop-2-ynoxy)-4-hydroxy benzoic acid (0.63 g, 3.05 mmol, 57%) (Mp 78°C) ¹H-NMR (400MHz, DMSO-*d*₆) δ_H: 7.60 (1H, s, **H6**) 7.54 (1H, d, J=6, **H2**) 7.44 (1H, d, J=8, **H5**) 4.86 (2H, d, J=2, **H8**) 3.61 (1H, t, J=1 **H10**) ¹³C-NMR (100MHz, DMSO-*d*₆) δ_C: 164.12 (**C7**) 153.45 (**C3**) 132.43 (**C4**) 127.77 (**C1**) 121.11 (**C6**) 116.42 (**C5**) 113.32 (**C2**) 77.14 (**C9**) 74.51 (**C10**) 51.11 (**C8**) HR-MS (ES-) *m/z* calculated for [C₁₀H₇O₄]⁻ 191.0354 found 191.0350

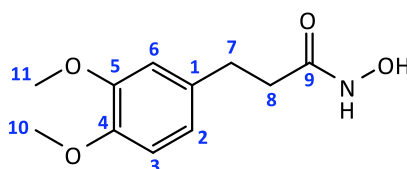
5.3.7 Synthesis of 3,4-Dimethoxycinnamohydroxamic acid (**23**)^[212]



Adapted from the procedure of Tanaka[212], thionyl chloride was added dropwise to a solution of 3,4-dimethoxycinnamic acid (5.01g, 24.06 mmol) and CHCl_3 (50 mL) in a RBF equipped with a magnetic stirrer bar. The reaction mixture was heated on a water bath under reflux at 40°C for approximately 30 minutes. The solvent was evaporated *in vacuo* and the acid chloride confirmed by ESI was used in the next step without purification. The acid chloride was then dissolved in CHCl_3 (50 mL) and added dropwise to another RBF equipped with a magnetic stirrer bar containing a cooled solution of hydroxylamine hydrochloride (2.64 g, 37.99 mmol), triethylamine (7.58 g, 10.45 mL, 74.91 mmol) and CHCl_3 (50 mL). Stirring was continued at ice temperature for twenty minutes and then for a further 40 minutes at RT. The solvent was removed *in vacuo* and residue dissolved in 1 M NaOH aqueous solution (50 mL) and the mixture was filtered through a Buchner filter under reduced pressure. The filtrate was cooled using an ice bath and acidified to pH 4 to precipitate the crude hydroxamic acid. The product was recrystallized from EtOH to give pale yellow crystals (4.71 g, 21.11 mmol, 84.4%). mp $188\text{-}189^\circ\text{C}$ (lit^[212] $188\text{-}190^\circ\text{C}$) $^1\text{H-NMR}$ (300MHz, $\text{DMSO-}d_6$) δ_{H} : 7.39 (1H, d, $J=15$, **H7**) 7.18 (1H, s, **H6**) 7.11 (1H, d, $J=8$, **H3**) 7.05 (1H, d, $J=8$, **H2**) 6.32 (1H, d, $J=15$, **H8**) 3.80 (3H, s, **H10**) 3.78 (3H, s, **H11**) $^{13}\text{C-NMR}$ (75MHz, $\text{DMSO-}d_6$) δ_{C} : 163.7 (**C9**) 150.0 (**C4**) 148.8 (**C5**) 138.41 (**C7**)

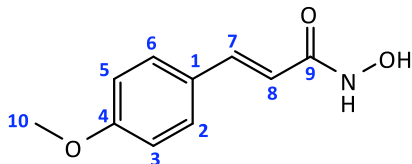
127.56 (C1) 121.22 (C2) 116.65 (C8) 111.65 (C3) 109.99 (C6) 55.32 (C10) 55.17 (C11) HR-MS (ES+) m/z calculated for $[C_{11}H_{13}NNaO_4]^+$: 246.0737 found 246.0737

5.3.8 Synthesis of 3-(3,4-Dimethoxyphenyl)propiohydroxamic acid (24)



To a suspension of (23) (2.51g, 11.25 mmol) in MeOH was added 10% Pd/C (0.25g)[220] to a RBF equipped with a magnetic stirrer bar and closed with a rubber bung. The solution was degassed, the saturated with hydrogen gas supplied from a balloon and stirred for 16 h. The reaction mixture was then filtered through a sintered glass Büchner funnel containing diatomaceous earth and solvent removed under reduced pressure to give the pure product as a dark yellow oil. (2.11 g, 9.37 mmol, 93.8%). $^1\text{H-NMR}$ (300MHz, DMSO- d_6) δ_{H} : 6.92 (1H, s, H6) 6.79 (1H, d, J=8, H3) 6.68 (1H, d, J=8, H2) 3.72 (3H, s, H10) 3.69 (3H, s, H11) 2.73 (2H, t, J=7, H7) 2.22 (2H, t, J=7, H8) $^{13}\text{C-NMR}$ (75MHz, DMSO- d_6) δ_{C} : 168.42 (C9) 148.51 (C3) 147.02 (C4) 133.44 (C2) 119.89 (C5) 112.08 (C1) 111.74 (C6) 55.43 (C10) 55.29 (C11) 34.12 (C8) 30.45 (C7) HR-MS (ES+) m/z calculated for $[C_{11}H_{15}NNaO_4]^+$: 248.0893 found 248.0895

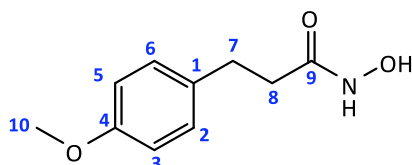
5.3.9 Synthesis of 4-methoxycinnamohydroxamic acid (D13)^[212]



Adapted from the work of Tanaka^[212], 4-methoxycinnamic acid (4.97 g, 27.90 mmol) was refluxed with MeOH (15 mL) and H₂SO₄ (0.7 mL) in a RBF equipped with a magnetic stirrer bar for 3 h. Excess solvent was removed under reduced pressure and the residue was poured into water and extracted into ether. The solvent removed *in vacuo* and the methyl ester recrystallized from methanol and used in the next step. hydroxylamine hydrochloride (5.63 g, 81.02 mmol) in MeOH (40 mL) was added to a solution of 1 M methanolic KOH (50 mL) and the mixture was left to cool in an ice bath for twenty minutes. The precipitated KCl solution was removed by filtration and the filtrate collected in a RBF. To the solution of hydroxylamine in MeOH was added methyl-4-methoxycinnamic acid (5.11 g, 26.59 mmol) and the mixture left to stir at room temperature for 24 h. The solvent was removed *in vacuo* and the residue dissolved in H₂O (50 mL) and filtered to remove insoluble impurities. The filtrate was cooled on ice and acidified to pH 4 by adding concentrated HCl dropwise. The solid was collected and recrystallized in MeOH as orange crystals (4.37 g, 22.63 mmol, 80.8%). mp 141-142°C (lit^[212] 143.5-144°C) ¹H-NMR (300MHz, DMSO-*d*₆) δ_H: 7.54 (1H, d, J=8, **H6** and **H2**) 7.44 (1H, d, J=15, **H7**) 7.01 (1H, d, J=8, **H5** and **H3**) 6.47 (1H, d, J=15, **H8**) 3.82 (3H, s, **H10**) ¹³C-NMR (75MHz, DMSO-*d*₆) δ_C: 163.16 (**C9**) 160.27 (**C4**) 138.04 (**C7**) 129.01 (**C6** and **C2**) 127.33

(**C1**) 116.42 (**C8**) 114.30 (**C5** and **C3**) 55.01 (**C10**) HR-MS (ES+) m/z calculated for $[\text{C}_{10}\text{H}_{11}\text{NNaO}_3]^+$: 216.0631 found 216.0627

5.3.10 Synthesis of 3-(4-methoxyphenyl)propiohydroxamic acid (**25**)



A suspension of D13 (2.01 g, 10.42 mmol) in EtOH was added 10% Pd/C (0.2g)[220] and procedure followed as 5.3.8. to give the pure product as pale pink crystals. (1.73 g, 8.87 mmol, 88.7%). mp 109-110°C (lit^[221] 113-114°C) ¹H-NMR (300MHz, DMSO-*d*₆) δ_H: 7.10 (1H, d, J=8, **H6** and **H2**) 6.82 (1H, d, J=8, **H5** and **H3**) 3.71 (3H, s, **H10**) 2.74 (2H, t, J=7, **H7**) 2.20 (2H, t, J=7, **H8**) ¹³C-NMR (75MHz, DMSO-*d*₆) δ_C: 168.25 (**C9**) 161.94 (**C4**) 161.94 (**C1**) 129.13 (**C6** and **C2**) 113.65 (**C5** and **C3**) 51.15 (**C10**) 36.81 (**C8**) 34.12 (**C7**) HR-MS (ES+) m/z calculated for $[\text{C}_{10}\text{H}_{13}\text{NNaO}_3]^+$: 218.0788 found 218.0787

6: References

- [1] IEA Publications (2013) *Oil Information 2013 with 2012 data*. IEA Publications Bookshop, Paris
- [2] “Oil reserves | About BP | BP Global.” [Online]. Available: http://www.bp.com/en/global/corporate/about-bp/energy-economics/statistical-review-of-world-energy-2013/review-by-energy-type/oil/oil-reserves.html?gclid=CNSBptDB1r0CFScHwwodbbsA_Q. [Accessed: 10-Apr-2014].
- [3] J. K. Weng, X. Li, N. D. Bonawitz, and C. Chapple, “Emerging strategies of lignin engineering and degradation for cellulosic biofuel production.,” *Curr. Opin. Biotechnol.*, vol. 19, no. 2, pp. 166–72, Apr. 2008.
- [4] L. C. Basso, H. V de Amorim, A. J. de Oliveira, and M. L. Lopes, “Yeast selection for fuel ethanol production in Brazil.,” *FEMS Yeast Res.*, vol. 8, no. 7, pp. 1155–63, Nov. 2008.
- [5] A. Gasparatos, P. Stromberg, and K. Takeuchi, “Sustainability impacts of first-generation biofuels,” *Anim. Front.*, vol. 3, no. 2, pp. 12–26, Mar. 2013.
- [6] S. N. Naik, V. V. Goud, P. K. Rout, and A. K. Dalai, “Production of first and second generation biofuels: A comprehensive review,” *Renew. Sustain. Energy Rev.*, vol. 14, no. 2, pp. 578–597, Feb. 2010.
- [7] S. P. Singh and D. Singh, “Biodiesel production through the use of different sources and characterization of oils and their esters as the substitute of diesel: A review,” *Renew. Sustain. Energy Rev.*, vol. 14, no. 1, pp. 200–216, Jan. 2010.
- [8] R. E. H. Sims, W. Mabee, J. N. Saddler, and M. Taylor, “An overview of second generation biofuel technologies.,” *Bioresour. Technol.*, vol. 101, no. 6, pp. 1570–80, Mar. 2010.
- [9] P. M. Schenk, S. R. Thomas-Hall, E. Stephens, U. C. Marx, J. H. Mussgnug, C. Posten, O. Kruse, and B. Hankamer, “Second Generation Biofuels: High-Efficiency Microalgae for Biodiesel Production,” *BioEnergy Res.*, vol. 1, no. 1, pp. 20–43, Mar. 2008.
- [10] J. Zakzeski, P. C. a Bruijninx, A. L. Jongerius, and B. M. Weckhuysen, “The catalytic valorization of lignin for the production of renewable chemicals.,” *Chem. Rev.*, vol. 110, no. 6, pp. 3552–99, Jun. 2010.
- [11] D. K. Shen, S. Gu, K. H. Luo, S. R. Wang, and M. X. Fang, “The pyrolytic degradation of wood-derived lignin from pulping process.,” *Bioresour. Technol.*, vol. 101, no. 15, pp. 6136–46, Aug. 2010.

- [12] D. Mohan, C. U. Pittman, and P. H. Steele, "Pyrolysis of Wood/Biomass for Bio-oil: A Critical Review," *Energy & Fuels*, vol. 20, no. 3, pp. 848–889, May 2006.
- [13] C. U. Pittman, D. Mohan, A. Eseyin, Q. Li, L. Ingram, E.-B. M. Hassan, B. Mitchell, H. Guo, and P. H. Steele, "Characterization of Bio-oils Produced from Fast Pyrolysis of Corn Stalks in an Auger Reactor," *Energy & Fuels*, vol. 26, no. 6, pp. 3816–3825, Jun. 2012.
- [14] L. Zhang, R. Liu, R. Yin, and Y. Mei, "Upgrading of bio-oil from biomass fast pyrolysis in China: A review," *Renew. Sustain. Energy Rev.*, vol. 24, pp. 66–72, Aug. 2013.
- [15] J. G. Rogers and J. G. Brammer, "Estimation of the production cost of fast pyrolysis bio-oil," *Biomass and Bioenergy*, vol. 36, no. 0, pp. 208–217, Jan. 2012.
- [16] L. Guzzi and A. Erd helyi, (2012) *Catalysis for Alternative Energy Generation*. Springer, New York
- [17] J. Perez-Carbajo, P. G mez- lvarez, R. Bueno-Perez, P. J. Merklings, and S. Calero, "Optimisation of the Fischer-Tropsch process using zeolites for tail gas separation.," *Phys. Chem. Chem. Phys.*, vol. 16, no. 12, pp. 5678–88, Mar. 2014.
- [18] K. Keegstra, "Plant cell walls.," *Plant Physiol.*, vol. 154, no. 2, pp. 483–6, Oct. 2010.
- [19] A. C. O’Sullivan, "Cellulose: the structure slowly unravels," *Cellulose*, vol. 4, no. 3, pp. 173–207, Jun. 1997.
- [20] H. Yang, R. Yan, H. Chen, C. Zheng, D. H. Lee, and D. T. Liang, "In-Depth Investigation of Biomass Pyrolysis Based on Three Major Components: Hemicellulose, Cellulose and Lignin," *Energy & Fuels*, vol. 20, no. 1, pp. 388–393, Jan. 2006.
- [21] P. Sannigrahi, A. J. Ragauskas, and G. A. Tuskan, "Poplar as a feedstock for biofuels: A review of compositional characteristics," *Biofuels, Bioprod. Biorefining*, vol. 4, no. 2, pp. 209–226, Mar. 2010.
- [22] J. M. Humphreys and C. Chapple, "Rewriting the lignin roadmap.," *Curr. Opin. Plant Biol.*, vol. 5, no. 3, pp. 224–9, Jun. 2002.
- [23] L. B. Davin and N. G. Lewis, "Lignin primary structures and dirigent sites.," *Curr. Opin. Biotechnol.*, vol. 16, no. 4, pp. 407–15, Aug. 2005.
- [24] G. Brunow, O. Karlsson, and K. Lundquist, "On the distribution of the diastereomers of the structural elements in lignins: the steric course of reactions mimicking lignin biosynthesis," *Wood Sci. Technol.*, vol. 27, no. 4, pp. 281–286, May 1993.

- [25] D. W. S. Wong, "Structure and action mechanism of ligninolytic enzymes.," *Appl. Biochem. Biotechnol.*, vol. 157, no. 2, pp. 174–209, May 2009.
- [26] R. Vanholme, B. Demedts, K. Morreel, J. Ralph, and W. Boerjan, "Lignin biosynthesis and structure.," *Plant Physiol.*, vol. 153, no. 3, pp. 895–905, Jul. 2010.
- [27] F. R. D. van Parijs, K. Morreel, J. Ralph, W. Boerjan, and R. M. H. Merks, "Modeling lignin polymerization. I. Simulation model of dehydrogenation polymers.," *Plant Physiol.*, vol. 153, no. 3, pp. 1332–44, Jul. 2010.
- [28] J. Ralph, K. Lundquist, G. Brunow, F. Lu, H. Kim, P. F. Schatz, J. M. Marita, R. D. Hatfield, S. a. Ralph, J. H. Christensen, and W. Boerjan, "Lignins: Natural polymers from oxidative coupling of 4-hydroxyphenylpropanoids," *Phytochem. Rev.*, vol. 3, no. 1/2, pp. 29–60, 2004.
- [29] W. Boerjan, J. Ralph, and M. Baucher, "Lignin biosynthesis.," *Annu. Rev. Plant Biol.*, vol. 54, pp. 519–46, Jan. 2003.
- [30] J. L. Ferrer, M. B. Austin, C. Stewart, and J. P. Noel, "Structure and function of enzymes involved in the biosynthesis of phenylpropanoids.," *Plant Physiol. Biochem.*, vol. 46, no. 3, pp. 356–70, Mar. 2008.
- [31] T. D. H. Bugg, M. Ahmad, E. M. Hardiman, and R. Rahmanpour, "Pathways for degradation of lignin in bacteria and fungi.," *Nat. Prod. Rep.*, vol. 28, no. 12, pp. 1883–96, Nov. 2011.
- [32] F. S. Chakar and A. J. Ragauskas, "Review of current and future softwood kraft lignin process chemistry," *Ind. Crops Prod.*, vol. 20, no. 2, pp. 131–141, Sep. 2004.
- [33] R. S. and C. J. A.-D. Oscar Sánchez (2011) Delignification Process of Agro-Industrial Wastes an Alternative to Obtain Fermentable Carbohydrates for Producing Fuel *Alternative Fuel*. InTech, Toronto.
- [34] T. K. Kirk, "Effects of Microorganisms on Lignin," *Annu. Rev. Phytopathol.*, vol. 9, no. 1, pp. 185–210, Sep. 1971.
- [35] D. L. Crawford and R. L. Crawford, "Microbial degradation of lignin," *Enzyme Microb. Technol.*, vol. 2, no. 1, pp. 11–22, Jan. 1980.
- [36] I. D. Reid, "Fate of Residual Lignin during Delignification of Kraft Pulp by *Trametes versicolor*," *Appl. Envir. Microbiol.*, vol. 64, no. 6, pp. 2117–2125, Jun. 1998.
- [37] D. Fengel and G. Wegener (1983), *Wood: chemistry, ultrastructure, reactions*. Walter de Gruyter & Co, New York

- [38] G. Rødsrud, M. Lersch, and A. Sjöde, “History and future of world’s most advanced biorefinery in operation,” *Biomass and Bioenergy*, vol. 46, no. null, pp. 46–59, Nov. 2012.
- [39] H. R. Bjørsvik and F. Minisci, “Fine Chemicals from Lignosulfonates. 1. Synthesis of Vanillin by Oxidation of Lignosulfonates,” *Org. Process Res. Dev.*, vol. 3, no. 5, pp. 330–340, Sep. 1999.
- [40] W. O. S. Doherty, P. Mousavioun, and C. M. Fellows, “Value-adding to cellulosic ethanol: Lignin polymers,” *Ind. Crops Prod.*, vol. 33, no. 2, pp. 259–276, Mar. 2011.
- [41] A. T. W. M. Hendriks and G. Zeeman, “Pretreatments to enhance the digestibility of lignocellulosic biomass.,” *Bioresour. Technol.*, vol. 100, no. 1, pp. 10–8, Jan. 2009.
- [42] X. Zhao, K. Cheng, and D. Liu, “Organosolv pretreatment of lignocellulosic biomass for enzymatic hydrolysis.,” *Appl. Microbiol. Biotechnol.*, vol. 82, no. 5, pp. 815–27, Apr. 2009.
- [43] Y. Kim, R. Hendrickson, N. S. Mosier, and M. R. Ladisch, “Liquid hot water pretreatment of cellulosic biomass.,” *Methods Mol. Biol.*, vol. 581, pp. 93–102, Jan. 2009.
- [44] M. J. de la Torre, A. Moral, M. D. Hernández, E. Cabeza, and A. Tijero, “Organosolv lignin for biofuel,” *Ind. Crops Prod.*, vol. 45, pp. 58–63, Feb. 2013.
- [45] H. P. Call and I. Mücke, “History, overview and applications of mediated lignolytic systems, especially laccase-mediator-systems (Lignozym®-process),” *J. Biotechnol.*, vol. 53, no. 2–3, pp. 163–202, Mar. 1997.
- [46] M. Tien and T. K. Kirk, “Lignin-Degrading Enzyme from the Hymenomycete *Phanerochaete chrysosporium*,” *Science*, vol. 221, no. 4611, pp. 661–3, Aug. 1983.
- [47] C. Srinivasan, T. M. Dsouza, K. Boominathan, and C. a Reddy, “Demonstration of Laccase in the White Rot Basidiomycete *Phanerochaete chrysosporium* BKM-F1767.,” *Appl. Environ. Microbiol.*, vol. 61, no. 12, pp. 4274–7, Dec. 1995.
- [48] H. D. Youn, Y. C. Hah, and S.-O. Kang, “Role of laccase in lignin degradation by white-rot fungi,” *FEMS Microbiol. Lett.*, vol. 132, no. 3, pp. 183–188, Oct. 1995.
- [49] A. Leonowicz, A. Matuszewska, J. Luterek, D. Ziegenhagen, M. Wojtaś-Wasilewska, N. S. Cho, M. Hofrichter, and J. Rogalski, “Biodegradation of lignin by white rot fungi.,” *Fungal Genet. Biol.*, vol. 27, no. 2–3, pp. 175–85, Jan. 1999.

- [50] I. D. Reid and M. G. Paice, "Biological bleaching of kraft pulps by white-rot fungi and their enzymes," *FEMS Microbiol. Rev.*, vol. 13, no. 2–3, pp. 369–375, Mar. 1994.
- [51] J. A. Souza-Corrêa, M. A. Ridenti, C. Oliveira, S. R. Araújo, and J. Amorim, "Decomposition of Lignin from Sugar Cane Bagasse during Ozonation Process Monitored by Optical and Mass Spectrometries.," *J. Phys. Chem. B*, vol. 117, no. 11, pp. 3110–9, Mar. 2013.
- [52] I. Brodin, E. Sjöholm, and G. Gellerstedt, "The behavior of kraft lignin during thermal treatment," *J. Anal. Appl. Pyrolysis*, vol. 87, no. 1, pp. 70–77, Jan. 2010.
- [53] B. Montie, J. Lallemand, and E. Guillet, "Ether linkage between phenolic acids and lignin fractions from wheat straw," *Phytochemistry* vol. 24, no. 6, pp. 1359–1362, 1985.
- [54] J. D. P. Araújo, C. a. Grande, and A. E. Rodrigues, "Vanillin production from lignin oxidation in a batch reactor," *Chem. Eng. Res. Des.*, vol. 88, no. 8, pp. 1024–1032, Aug. 2010.
- [55] R. Sun, J. M. Lawther, W. B. Banks, "A tentative chemical structure of wheat straw lignin," *Ind. Crops and Prod.* vol. 6, no. 1, pp 1-8, 1997.
- [56] J. R. Davis and J. K. Sello, "Regulation of genes in *Streptomyces* bacteria required for catabolism of lignin-derived aromatic compounds.," *Appl. Microbiol. Biotechnol.*, vol. 86, no. 3, pp. 921–9, Apr. 2010.
- [57] W. Zimmermann, "Degradation of lignin by bacteria," *J. Biotechnol.*, vol. 13, no. 2–3, pp. 119–130, Feb. 1990.
- [58] T. Watanabe, H. Teranishi, Y. Honda, and M. Kuwahara, "A selective lignin-degrading fungus, *Ceriporiopsis subvermispora*, produces alkylitaconates that inhibit the production of a cellulolytic active oxygen species, hydroxyl radical in the presence of iron and H₂O₂," *Biochem. Biophys. Res. Commun.*, vol. 297, no. 4, pp. 918–23, Oct. 2002.
- [59] T. K. Kirk and R. L. Farrell, "Enzymatic 'combustion': the microbial degradation of lignin.," *Annu. Rev. Microbiol.*, vol. 41, pp. 465–505, Jan. 1987.
- [60] E. Masai, Y. Katayama, and M. Fukuda, "Genetic and Biochemical Investigations on Bacterial Catabolic Pathways for Lignin-Derived Aromatic Compounds," *Biosci. Biotechnol. Biochem.*, vol. 71, no. 1, pp. 1–15, 2007.
- [61] K. Li, F. Xu, and K. E. Eriksson, "Comparison of fungal laccases and redox mediators in oxidation of a nonphenolic lignin model compound.," *Appl. Environ. Microbiol.*, vol. 65, no. 6, pp. 2654–60, Jun. 1999.

- [62] A K. Haritash and C. P. Kaushik, "Biodegradation aspects of polycyclic aromatic hydrocarbons (PAHs): a review.," *J. Hazard. Mater.*, vol. 169, no. 1–3, pp. 1–15, Sep. 2009.
- [63] T. Choinowski, W. Blodig, K. H. Winterhalter, and K. Piontek, "The crystal structure of lignin peroxidase at 1.70 Å resolution reveals a hydroxy group on the cβ of tryptophan 171: a novel radical site formed during the redox cycle.," *J. Mol. Biol.*, vol. 286, no. 3, pp. 809–27, Feb. 1999.
- [64] M. Tien, "Oxidation of Guaiacol by Lignin Peroxidase," *J. Biol. Chem.*, vol. 270, no. 38, pp. 22254–22258, Sep. 1995.
- [65] K. Piontek, T. Glumoff, and K. Winterhalter, "Low pH crystal structure of glycosylated lignin peroxidase from *Phanerochaete chrysosporium* at 2.5 Å resolution," *FEBS Lett.*, vol. 315, no. 2, pp. 119–124, Jan. 1993.
- [66] D. B. Goodin and D. E. McRee, "The Asp-His-Fe triad of cytochrome c peroxidase controls the reduction potential, electronic structure, and coupling of the tryptophan free radical to the heme.," *Biochemistry*, vol. 32, no. 13, pp. 3313–24, Apr. 1993.
- [67] M. Ohta, T. Higuchi, and S. Iwahara, "Microbial degradation of dehydrodiconiferyl alcohol, a lignin substructure model," *Arch. Microbiol.*, vol. 121, no. 1, pp. 23–28, 1979.
- [68] T. K. Kirk and F. Nakatsubo, "Chemical mechanism of an important cleavage reaction in the fungal degradation of lignin," *Biochim. Biophys. Acta - Gen. Subj.*, vol. 756, no. 3, pp. 376–384, Apr. 1983.
- [69] H. Takayoshi, "Plant Cell Wall Polymers", *A. Chem. Soc.*, vol. 399. pp. 482–502, 1989
- [70] T. Higuchi, "Lignin biochemistry: Biosynthesis and biodegradation," *Wood Sci. Technol.*, vol. 24, no. 1, 1990.
- [71] T. Umezawa, T. Nakatsubo, F. Higuchi, "Lignin degradation by *Phanerochaete chrysosporium*: Metabolism of phenolic phenylcoumaran substructure model compound," *Arch. Microbiol.*, vol. 131, pp. 124–128, Jan. 1982.
- [72] W. Blodig, a T. Smith, W. a Doyle, and K. Piontek, "Crystal structures of pristine and oxidatively processed lignin peroxidase expressed in *Escherichia coli* and of the W171F variant that eliminates the redox active tryptophan 171. Implications for the reaction mechanism.," *J. Mol. Biol.*, vol. 305, no. 4, pp. 851–61, Jan. 2001.
- [73] M. D. Sollewijn Gelpke, J. Lee, and M. H. Gold, "Lignin peroxidase oxidation of veratryl alcohol: effects of the mutants H82A, Q222A, W171A, and F267L.," *Biochemistry*, vol. 41, no. 10, pp. 3498–506, Mar. 2002.

- [74] S. Dey, T. K. Maiti, and B. C. Bhattacharyya, "Lignin peroxidase production by a brown-rot fungus *Polyporus ostreiformis*," *J. Ferment. Bioeng.*, vol. 72, no. 5, pp. 402–404, Jan. 1991.
- [75] J. K. Glenn and M. H. Gold, "Purification and characterization of an extracellular Mn(II)-dependent peroxidase from the lignin-degrading basidiomycete, *Phanerochaete chrysosporium*," *Arch. Biochem. Biophys.*, vol. 242, no. 2, pp. 329–341, Nov. 1985.
- [76] A. Paszczyński, V.-B. Huynh, and R. Crawford, "Enzymatic activities of an extracellular, manganese-dependent peroxidase from *Phanerochaete chrysosporium*," *FEMS Microbiol. Lett.*, vol. 29, no. 1, pp. 37–41, 1985.
- [77] E. Fernández-Fueyo, F. J. Ruiz-Dueñas, Y. Miki, M. J. Martínez, K. E. Hammel, and A. T. Martínez, "Lignin-degrading peroxidases from genome of selective ligninolytic fungus *Ceriporiopsis subvermispora*," *J. Biol. Chem.*, vol. 287, no. 20, pp. 16903–16, May 2012.
- [78] M. Hofrichter, "Review: lignin conversion by manganese peroxidase (MnP)," *Enzyme Microb. Technol.*, vol. 30, no. 4, pp. 454–466, Apr. 2002.
- [79] M. Sundaramoorthy, K. Kishi, M. H. Gold, and T. L. Poulos, "Crystal Structures of Substrate Binding Site Mutants of Manganese Peroxidase," *J. Biol. Chem.*, vol. 272, no. 28, pp. 17574–17580, Jul. 1997.
- [80] M. Sundaramoorthy, K. Kishi, M. H. Gold, and T. L. Poulos, "Preliminary crystallographic analysis of manganese peroxidase from *Phanerochaete chrysosporium*," *J. Mol. Biol.*, vol. 238, no. 5, pp. 845–8, May 1994.
- [81] F. J. Ruiz-Dueñas, M. J. Martínez, and A. T. Martínez, "Molecular characterization of a novel peroxidase isolated from the ligninolytic fungus *Pleurotus eryngii*," *Mol. Microbiol.*, vol. 31, no. 1, pp. 223–35, Jan. 1999.
- [82] E. Fernández-Fueyo, F. J. Ruiz-Dueñas, M. J. Martínez, A. Romero, K. E. Hammel, F. J. Medrano, and A. T. Martínez, "Ligninolytic peroxidase genes in the oyster mushroom genome: heterologous expression, molecular structure, catalytic and stability properties, and lignin-degrading ability," *Biotechnol. Biofuels*, vol. 7, no. 1, p. 2, Jan. 2014.
- [83] M. Pérez-Boada, F. J. Ruiz-Dueñas, R. Pogni, R. Basosi, T. Choinowski, M. J. Martínez, K. Piontek, and A. T. Martínez, "Versatile peroxidase oxidation of high redox potential aromatic compounds: site-directed mutagenesis, spectroscopic and crystallographic investigation of three long-range electron transfer pathways," *J. Mol. Biol.*, vol. 354, no. 2, pp. 385–402, Nov. 2005.
- [84] F. J. Ruiz-Dueñas, R. Pogni, M. Morales, S. Giansanti, M. J. Mate, A. Romero, M. J. Martínez, R. Basosi, and A. T. Martínez, "Protein radicals in fungal versatile peroxidase: catalytic tryptophan radical in both compound

- I and compound II and studies on W164Y, W164H, and W164S variants.,” *J. Biol. Chem.*, vol. 284, no. 12, pp. 7986–94, Mar. 2009.
- [85] F. J. Ruiz-Dueñas, M. Morales, M. J. Mate, A. Romero, M. J. Martínez, A. T. Smith, and A. T. Martínez, “Site-directed mutagenesis of the catalytic tryptophan environment in *Pleurotus eryngii* versatile peroxidase.,” *Biochemistry*, vol. 47, no. 6, pp. 1685–95, Feb. 2008.
- [86] R. Pogni, M. C. Baratto, S. Giansanti, C. Teutloff, J. Verdin, B. Valderrama, F. Lenzian, W. Lubitz, R. Vazquez-Duhalt, and R. Basosi, “Tryptophan-based radical in the catalytic mechanism of versatile peroxidase from *Bjerkandera adusta*.,” *Biochemistry*, vol. 44, no. 11, pp. 4267–74, Mar. 2005.
- [87] K. Rittstieg, A. Suurnakki, T. Suortti, K. Kruus, G. Guebitz, and J. Buchert, “Investigations on the laccase-catalyzed polymerization of lignin model compounds using size-exclusion HPLC,” *Enzyme Microb. Technol.*, vol. 31, no. 4, pp. 403–410, Sep. 2002.
- [88] Q. Zhao, J. Nakashima, F. Chen, Y. Yin, C. Fu, J. Yun, H. Shao, X. Wang, Z.-Y. Wang, and R. A. Dixon, “Laccase is necessary and nonredundant with peroxidase for lignin polymerization during vascular development in *Arabidopsis*.,” *Plant Cell*, vol. 25, no. 10, pp. 3976–87, Oct. 2013.
- [89] N. Xie, F. Chapeland-Leclerc, P. Silar, and G. Ruprich-Robert, “Systematic gene deletions evidences that laccases are involved in several stages of wood degradation in the filamentous fungus *Podospora anserina*.,” *Environ. Microbiol.*, vol. 16, no. 1, pp. 141–61, Jan. 2014.
- [90] H. Jung, “Purification and characterization of laccase from wood-degrading fungus *Trichophyton rubrum* LKY-7,” *Enzyme Microb. Technol.*, vol. 30, no. 2, pp. 161–168, Feb. 2002.
- [91] A. V Lyashenko, N. E. Zhukhlistova, A. G. Gabdoulkhakov, Y. N. Zhukova, W. Voelter, V. N. Zaitsev, I. Bento, E. V Stepanova, G. S. Kachalova, O. V Koroleva, E. A. Cherkashyn, V. I. Tishkov, V. S. Lamzin, K. Schirwitz, E. Y. Morgunova, C. Betzel, P. F. Lindley, and A. M. Mikhailov, “Purification, crystallization and preliminary X-ray study of the fungal laccase from *Cerrena maxima*.,” *Acta Crystallogr. Sect. F. Struct. Biol. Cryst. Commun.*, vol. 62, no. Pt 10, pp. 954–7, Oct. 2006.
- [92] C. Eggert, U. Temp, and K. Eriksson, “The ligninolytic system of the white rot fungus *Pycnoporus cinnabarinus*: purification and characterization of the laccase,” *Appl. Envir. Microbiol.*, vol. 62, no. 4, pp. 1151–1158, Apr. 1996.
- [93] L. Heap, A. Green, D. Brown, B. van Dongen, and N. Turner, “Role of laccase as an enzymatic pretreatment method to improve lignocellulosic saccharification,” *Catal. Sci. Technol.*, vol. 4, pp. 2251–2259, Mar. 2014.

- [94] J. A. Bumpus and S. D. Aust, "Biodegradation of environmental pollutants by the white rot fungus *Phanerochaete chrysosporium*: Involvement of the lignin degrading system," *BioEssays*, vol. 6, no. 4, pp. 166–170, Apr. 1987.
- [95] P. E. Rasmussen, R. R. Allmaras, C. R. Rohde, and N. C. Roager, "Crop Residue Influences on Soil Carbon and Nitrogen in a Wheat-Fallow System1," *Soil Sci. Soc. Am. J.*, vol. 44, no. 3, p. 596, Jan. 1980.
- [96] K. C. Yam, S. Okamoto, J. N. Roberts, and L. D. Eltis, "Adventures in *Rhodococcus* - from steroids to explosives.," *Can. J. Microbiol.*, vol. 57, no. 3, pp. 155–68, Mar. 2011.
- [97] D. L. Crawford, a L. Pometto, and R. L. Crawford, "Lignin Degradation by *Streptomyces viridosporus*: Isolation and Characterization of a New Polymeric Lignin Degradation Intermediate.," *Appl. Environ. Microbiol.*, vol. 45, no. 3, pp. 898–904, Mar. 1983.
- [98] M. Ramachandra, D. L. Crawford, and G. Hertel, "Characterization of an extracellular lignin peroxidase of the lignocellulolytic actinomycete *Streptomyces viridosporus*.,," *Appl. Environ. Microbiol.*, vol. 54, no. 12, pp. 3057–63, Dec. 1988.
- [99] R. Vicuña, "Bacterial degradation of lignin," *Enzyme Microb. Technol.*, vol. 10, no. 11, pp. 646–655, Nov. 1988.
- [100] J. Trojanowski, K. Haider, and V. Sundman, "Decomposition of ¹⁴C-labelled lignin and phenols by a *Nocardia sp.*," *Arch. Microbiol.*, vol. 114, no. 2, pp. 149–153, 1977.
- [101] A. Enoki and M. H. Gold, "Degradation of the diarylpropane lignin model compound 1-(3,4-diethoxyphenyl)-1,3-dihydroxy-2-(4'-methoxyphenyl)-propane and derivatives by the basidiomycete *Phanerochaete chrysosporium*," *Arch. Microbiol.*, vol. 132, no. 2, pp. 123–130, Aug. 1982.
- [102] J. Pellinen, E. Visnen, M. Salkinoja-Salonen, and G. Brunow, "Utilization of dimeric lignin model compounds by mixed bacterial cultures," *Appl. Microbiol. Biotechnol.*, vol. 20, no. 1, Jul. 1984.
- [103] M. P. McLeod, R. L. Warren, W. W. L. Hsiao, N. Araki, M. Myhre, C. Fernandes, D. Miyazawa, W. Wong, A. L. Lillquist, D. Wang, M. Dosanjh, H. Hara, A. Petrescu, R. D. Morin, G. Yang, J. M. Stott, J. E. Schein, H. Shin, D. Smailus, A. S. Siddiqui, M. A. Marra, S. J. M. Jones, R. Holt, F. S. L. Brinkman, K. Miyauchi, M. Fukuda, J. E. Davies, W. W. Mohn, and L. D. Eltis, "The complete genome of *Rhodococcus sp.* RHA1 provides insights into a catabolic powerhouse.," *Proc. Natl. Acad. Sci. U. S. A.*, vol. 103, no. 42, pp. 15582–7, Oct. 2006.
- [104] M. Ahmad, C. R. Taylor, D. Pink, K. Burton, D. Eastwood, G. D. Bending, and T. D. H. Bugg, "Development of novel assays for lignin degradation:

- comparative analysis of bacterial and fungal lignin degraders.,” *Mol. Biosyst.*, vol. 6, no. 5, pp. 815–21, May 2010.
- [105] C. Zubieta, R. Joseph, S. S. Krishna, D. McMullan, M. Kapoor, H. L. Axelrod, M. D. Miller, P. Abdubek, C. Acosta, T. Astakhova, D. Carlton, H.-J. Chiu, T. Clayton, M. C. Deller, L. Duan, Y. Elias, M.-A. Elsliger, J. Feuerhelm, S. K. Grzechnik, J. Hale, G. W. Han, L. Jaroszewski, K. K. Jin, H. E. Klock, M. W. Knuth, P. Kozbial, A. Kumar, D. Marciano, A. T. Morse, K. D. Murphy, E. Nigoghossian, L. Okach, S. Oommachen, R. Reyes, C. L. Rife, P. Schimmel, C. V Trout, H. van den Bedem, D. Weekes, A. White, Q. Xu, K. O. Hodgson, J. Wooley, A. M. Deacon, A. Godzik, S. A. Lesley, and I. A. Wilson, “Identification and structural characterization of heme binding in a novel dye-decolorizing peroxidase, TyrA.,” *Proteins*, vol. 69, no. 2, pp. 234–43, Nov. 2007.
- [106] M. Ahmad, J. N. Roberts, E. M. Hardiman, R. Singh, L. D. Eltis, and T. D. H. Bugg, “Identification of DypB from *Rhodococcus jostii* RHA1 as a Lignin Peroxidase.,” *Biochemistry*, vol. 50, no. 23, pp. 5096–107, Jun. 2011.
- [107] M. E. Brown, T. Barros, and M. C. Y. Chang, “Identification and characterization of a multifunctional dye peroxidase from a lignin-reactive bacterium.,” *ACS Chem. Biol.*, vol. 7, no. 12, pp. 2074–81, Dec. 2012.
- [108] Y. Sugano, R. Muramatsu, A. Ichiyanagi, T. Sato, and M. Shoda, “DyP, a unique dye-decolorizing peroxidase, represents a novel heme peroxidase family: ASP171 replaces the distal histidine of classical peroxidases.,” *J. Biol. Chem.*, vol. 282, no. 50, pp. 36652–8, Dec. 2007.
- [109] Y. Sugano, “DyP-type peroxidases comprise a novel heme peroxidase family.,” *Cell. Mol. Life Sci.*, vol. 66, no. 8, pp. 1387–403, Apr. 2009.
- [110] C. R. Taylor, E. M. Hardiman, M. Ahmad, P. D. Sainsbury, P. R. Norris, and T. D. H. Bugg, “Isolation of bacterial strains able to metabolize lignin from screening of environmental samples.,” *J. Appl. Microbiol.*, vol. 113, no. 3, pp. 521–30, Sep. 2012.
- [111] A. Raj, M. Krishnareddy, and R. Chandra, “Identification of low molecular weight aromatic compounds by gas chromatography–mass spectrometry (GC–MS) from kraft lignin degradation by three *Bacillus sp.*,” *Int. Biodeterior. Biodegradation*, vol. 59, no. 4, pp. 292–296, Jun. 2007.
- [112] D. L. Crawford, S. Floyd, a L. Pometto, and R. L. Crawford, “Degradation of natural and Kraft lignins by the microflora of soil and water.,” *Can. J. Microbiol.*, vol. 23, no. 4, pp. 434–40, Apr. 1977.
- [113] A. M. Deschamps, G. Mahoudeau, J. M. Lebeault, D. P. Biotechnologiques, and U. De Technologie, “Microbiology and Biotechnology Fast Degradation of Kraft Lignin by Bacteria Assimilation of Lignin Related Compounds The assimilation of phenolic compounds

- considered as monomers or monomer related,” *Microbios*, vol. 1, pp. 45–51, 1980.
- [114] C. S. Harwood and R. E. Parales, “The beta-ketoadipate pathway and the biology of self-identity,” *Annu. Rev. Microbiol.*, vol. 50, pp. 553–90, Jan. 1996.
- [115] G. M. Stephens and H. Dalton, “The effect of lipophilic weak acids on the segregational stability of TOL plasmids in *Pseudomonas putida*,” *J. Gen. Microbiol.*, vol. 133, no. 7, pp. 1891–9, Jul. 1987.
- [116] K. C. Yam, R. Van Der Geize, and L. D. Eltis, (2010) *Biology of Rhodococcus*, Springer, Berlin.
- [117] X. Peng, T. Egashira, K. Hanashiro, E. Masai, S. Nishikawa, Y. Katayama, K. Kimbara, and M. Fukuda, “Cloning of a *Sphingomonas paucimobilis* SYK-6 gene encoding a novel oxygenase that cleaves lignin-related biphenyl and characterization of the enzyme,” *Appl. Environ. Microbiol.*, vol. 64, no. 7, pp. 2520–7, Jul. 1998.
- [118] E. Masai, A. Ichimura, Y. Sato, K. Miyauchi, Y. Katayama, and M. Fukuda, “Roles of the Enantioselective Glutathione S-Transferases in Cleavage of β -Aryl Ether,” *Am. Soc. Microbiol.*, vol. 185, no. 6, pp. 1768–1775, 2003.
- [119] E. Masai, Y. Yamamoto, T. Inoue, K. Takamura, H. Hara, D. Kasai, Y. Katayama, and M. Fukuda, “Characterization of ligV Essential for Catabolism of Vanillin by *Sphingomonas paucimobilis* SYK-6,” *Biosci. Biotechnol. Biochem.*, vol. 71, no. 10, pp. 2487–2492, 2007.
- [120] R. Sun, “Fractional and structural characterization of wheat straw hemicelluloses,” *Carbohydr. Polym.*, vol. 29, no. 4, pp. 325–331, Apr. 1996.
- [121] Q. Yang, S. Wu, R. Lou, and G. LV, “Structural characterization of lignin from wheat straw,” *Wood Sci. Technol.*, pp. 1–13–13, May 2010.
- [122] E. Masai, A. Yamada, J. Healy, T. Hatta, K. Kimbara, M. Fukuda, and K. Yano, “Characterization of biphenyl catabolic genes of gram-positive polychlorinated biphenyl degrader *Rhodococcus sp.* strain RHA1,” *Appl. Envir. Microbiol.*, vol. 61, no. 6, pp. 2079–2085, Jun. 1995.
- [123] X. Peng, E. Masai, H. Kitayama, K. Harada, Y. Katayama, and M. Fukuda, “Characterization of the 5-Carboxyvanillate Decarboxylase Gene and Its Role in Lignin-Related Biphenyl Catabolism in *Sphingomonas paucimobilis* SYK-6,” *Appl. Environ. Microbiol.*, vol. 68, no. 9, pp. 4407–4415, Sep. 2002.

- [124] S. Kamoda, T. Terada, and Y. Saburi, "Production of heterogeneous dimer lignostilbenedioxygenase II from lsdA and lsdB in *Escherichia coli* cells.," *Biosci. Biotechnol. Biochem.*, vol. 69, no. 3, pp. 635–7, Mar. 2005.
- [125] V. V. Lozovaya, a. V. Lygin, O. V. Zernova, S. Li, J. M. Widholm, and G. L. Hartman, "Lignin Degradation by *Fusarium solani* sp. glycines," *Plant Dis.*, vol. 90, no. 1, pp. 77–82, Jan. 2006.
- [126] P. Ander and K. Messner, "Oxidation of 1-hydroxybenzotriazole by laccase and lignin peroxidase," *Biotechnology*, vol. 12, no. 3, pp. 191–195, 1998.
- [127] R. Pecina, P. Burtscher, G. Bonn, and O. Bobleter, "GC-MS and HPLC analyses of lignin degradation products in biomass hydrolyzates," *Fresenius' Zeitschrift fur Anal. Chemie*, vol. 325, no. 5, pp. 461–465, 1986.
- [128] M. Kato, K. Kozaki, S. Sakuranaga, "Degradation of lignin compounds by bacteria from termite guts," *Biotechnol. Lett.*, vol. 20, no. 5, pp. 459–462, 1998.
- [129] D. Takada, K. Ehara, and S. Saka, "Gas chromatographic and mass spectrometric (GC-MS) analysis of lignin-derived products from *Cryptomeria japonica* treated in supercritical water," *J. Wood Sci.*, vol. 50, no. 3, pp. 253–259, Jun. 2004.
- [130] D. W. Ribbons, "Chemicals from Lignin," *Philos. Trans. R. Soc. London. Ser. A, Math. Phys. Sci.*, vol. 321, no. 1561, pp. 485–494, 2011.
- [131] L. S. de Jager, G. a Perfetti, and G. W. Diachenko, "Determination of coumarin, vanillin, and ethyl vanillin in vanilla extract products: liquid chromatography mass spectrometry method development and validation studies.," *J. Chromatogr. A*, vol. 1145, no. 1–2, pp. 83–8, Mar. 2007.
- [132] O. Suparno, A. D. Covington, and C. S. Evans, "Kraft lignin degradation products for tanning and dyeing of leather," *J. Chem. Technol. Biotechnol.*, vol. 80, no. 1, pp. 44–49, Jan. 2005.
- [133] N. K. Nishikawa, R. Sutcliffe, and J. N. Saddler, "The influence of lignin degradation products on xylose fermentation by *Klebsiella pneumoniae*," *Culture*, vol. 5, pp. 549–552, 1988.
- [134] J. Cho, S. Chu, P. J. Dauenhauer, and G. W. Huber, "Kinetics and reaction chemistry for slow pyrolysis of enzymatic hydrolysis lignin and organosolv extracted lignin derived from maplewood," *Green Chem.*, vol. 14, no. 2, p. 428, 2012.
- [135] P. J. de Wild, W. J. J. Huijgen, and H. J. Heeres, "Pyrolysis of wheat straw-derived organosolv lignin," *J. Anal. Appl. Pyrolysis*, vol. 93, pp. 95–103, Jan. 2012.

- [136] A. L. Jongerius, R. Jastrzebski, P. C. a. Bruijninx, and B. M. Weckhuysen, “CoMo sulfide-catalyzed hydrodeoxygenation of lignin model compounds: An extended reaction network for the conversion of monomeric and dimeric substrates,” *J. Catal.*, vol. 285, no. 1, pp. 315–323, Jan. 2012.
- [137] Z. He and X. Wang, “Hydrodeoxygenation of model compounds and catalytic systems for pyrolysis bio-oils upgrading,” *Catal. Sustain. Energy*, vol. 1, pp. 28–52.
- [138] A. G. Sergeev and J. F. Hartwig, “Selective, nickel-catalyzed hydrogenolysis of aryl ethers.,” *Science*, vol. 332, no. 6028, pp. 439–43, Apr. 2011.
- [139] M. P. Pandey and C. S. Kim, “Lignin Depolymerization and Conversion: A Review of Thermochemical Methods,” *Chem. Eng. Technol.*, vol. 34, no. 1, pp. 29–41, Jan. 2011.
- [140] P. Azadi, O. R. Inderwildi, R. Farnood, and D. A. King, “Liquid fuels, hydrogen and chemicals from lignin: A critical review,” *Renew. Sustain. Energy Rev.*, vol. 21, pp. 506–523, May 2013.
- [141] J. Q. Chen, A. Bozzano, B. Glover, T. Fuglerud, and S. Kvisle, “Recent advancements in ethylene and propylene production using the UOP/Hydro MTO process,” *Catal. Today*, vol. 106, no. 1–4, pp. 103–107, Oct. 2005.
- [142] D. Hua, C. Ma, S. Lin, L. Song, Z. Deng, Z. Maomy, Z. Zhang, B. Yu, and P. Xu, “Biotransformation of isoeugenol to vanillin by a newly isolated *Bacillus pumilus* strain: identification of major metabolites.,” *J. Biotechnol.*, vol. 130, no. 4, pp. 463–70, Jul. 2007.
- [143] H.-P. Chen, M. Chow, C.-C. Liu, A. Lau, J. Liu, and L. D. Eltis, “Vanillin catabolism in *Rhodococcus jostii* RHA1.,” *Appl. Environ. Microbiol.*, vol. 78, no. 2, pp. 586–8, Jan. 2012.
- [144] M. Yamada, Y. Okada, T. Yoshida, and T. Nagasawa, “Biotransformation of isoeugenol to vanillin by *Pseudomonas putida* IE27 cells.,” *Appl. Microbiol. Biotechnol.*, vol. 73, no. 5, pp. 1025–30, Jan. 2007.
- [145] J. Ryu, J. Seo, Y. Lee, Y. Lim, J.-H. Ahn, and H.-G. Hur, “Identification of syn- and anti-anethole-2,3-epoxides in the metabolism of trans-anethole by the newly isolated bacterium *Pseudomonas putida* JYR-1.,” *J. Agric. Food Chem.*, vol. 53, no. 15, pp. 5954–8, Jul. 2005.
- [146] C. Calisti, A. G. Ficca, P. Barghini, and M. Ruzzi, “Regulation of ferulic catabolic genes in *Pseudomonas fluorescens* BF13: involvement of a MarR family regulator.,” *Appl. Microbiol. Biotechnol.*, vol. 80, no. 3, pp. 475–83, Sep. 2008.
- [147] S. Achterholt, H. Priefert, and A. Steinbüchel, “Identification of *Amycolatopsis* sp. strain HR167 genes, involved in the bioconversion of

- ferulic acid to vanillin,” *Appl. Microbiol. Biotechnol.*, vol. 54, no. 6, pp. 799–807, Dec. 2000.
- [148] P. Barghini, D. Di Gioia, F. Fava, and M. Ruzzi, “Vanillin production using metabolically engineered *Escherichia coli* under non-growing conditions,” *Microb. Cell Fact.*, vol. 6, no. 1, p. 13, Jan. 2007.
- [149] C. Fleige, G. Hansen, J. Kroll, and A. Steinbüchel, “Investigation of the *Amycolatopsis* sp. Strain ATCC 39116 Vanillin Dehydrogenase and Its Impact on the Biotechnical Production of Vanillin,” *Appl. Environ. Microbiol.*, vol. 79, no. 1, pp. 81–90, Jan. 2013.
- [150] Y. Zhang, P. Xu, S. Han, H. Yan, and C. Ma, “Metabolism of isoeugenol via isoeugenol-diol by a newly isolated strain of *Bacillus subtilis* HS8.,” *Appl. Microbiol. Biotechnol.*, vol. 73, no. 4, pp. 771–9, Dec. 2006.
- [151] D. Havkin-Frenkel and F. C. Belanger. (2007) *Application of metabolic engineering to vanillin biosynthetic pathways in vanilla planifolia*. Springer, Berlin.
- [152] K. Hansen, “The in vitro substrate regiospecificity of recombinant UGT85B1, the cyanohydrin glucosyltransferase from *Sorghum bicolor*,” *Phytochemistry*, vol. 64, no. 1, pp. 143–151, Sep. 2003.
- [153] E. H. Hansen, B. L. Møller, G. R. Kock, C. M. Büchner, C. Kristensen, O. R. Jensen, F. T. Okkels, C. E. Olsen, M. S. Motawia, and J. Hansen, “De novo biosynthesis of vanillin in fission yeast (*Schizosaccharomyces pombe*) and baker’s yeast (*Saccharomyces cerevisiae*).,” *Appl. Environ. Microbiol.*, vol. 75, no. 9, pp. 2765–74, May 2009.
- [154] M. a Providenti, J. M. O’Brien, J. Ruff, A. M. Cook, and I. B. Lambert, “Metabolism of isovanillate, vanillate, and vertrate by *Comamonas testosteroni* strain BR6020.,” *J. Bacteriol.*, vol. 188, no. 11, pp. 3862–9, Jun. 2006.
- [155] B. Morawski, a Segura, and L. N. Ornston, “Substrate range and genetic analysis of *Acinetobacter* vanillate demethylase.,” *J. Bacteriol.*, vol. 182, no. 5, pp. 1383–9, Mar. 2000.
- [156] C. Civolani, P. Barghini, A. R. Roncetti, M. Ruzzi, and A. Schiesser, “Bioconversion of ferulic acid into vanillic acid by means of a vanillate-negative mutant of *Pseudomonas fluorescens* strain BF13.,” *Appl. Environ. Microbiol.*, vol. 66, no. 6, pp. 2311–7, Jun. 2000.
- [157] G. Stephanopoulos and J. J. Vallino, “Network rigidity and metabolic engineering in metabolite overproduction.,” *Science*, vol. 252, no. 5013, pp. 1675–81, Jun. 1991.
- [158] M. A. G. Koffas, G. Y. Jung, and G. Stephanopoulos, “Engineering metabolism and product formation in *Corynebacterium glutamicum* by

- coordinated gene overexpression.,” *Metab. Eng.*, vol. 5, no. 1, pp. 32–41, Jan. 2003.
- [159] B. H. A. Rehm, (2009) *Microbial Production of Biopolymers and Polymer Precursors: Applications and Perspectives*. Horizon Scientific Press, California.
- [160] J. Bailey, “Toward a science of metabolic engineering,” *Science.*, vol. 252, no. 5013, pp. 1668–1675, Jun. 1991.
- [161] Y. Chen, M. J. Smanski, and B. Shen, “Improvement of secondary metabolite production in *Streptomyces* by manipulating pathway regulation.,” *Appl. Microbiol. Biotechnol.*, vol. 86, no. 1, pp. 19–25, Mar. 2010.
- [162] P. A. Nakata and C. He, “Oxalic acid biosynthesis is encoded by an operon in *Burkholderia glumae.*,” *FEMS Microbiol. Lett.*, vol. 304, no. 2, pp. 177–82, Mar. 2010.
- [163] M. Shimada, D.-B. Ma, Y. Akamatsu, and T. Hattori, “A proposed role of oxalic acid in wood decay systems of wood-rotting basidiomycetes,” *FEMS Microbiol. Rev.*, vol. 13, no. 2–3, pp. 285–295, Mar. 1994.
- [164] X. Peng, N. Misawa, and S. Harayama, “Isolation and Characterization of Thermophilic Bacilli Degrading Cinnamic, 4-Coumaric, and Ferulic Acids,” *Appl. Environ. Microbiol.*, vol. 69, no. 3, pp. 1417–1427, Mar. 2003.
- [165] P. Xu, D. Hua, and C. Ma, “Microbial transformation of propenylbenzenes for natural flavour production.,” *Trends Biotechnol.*, vol. 25, no. 12, pp. 571–6, Dec. 2007.
- [166] J. Farres, T. T. Y. Wang, S. J. Cunningham, and H. Weiner, “Investigation of the Active Site Cysteine Residue of Rat Liver Mitochondrial Aldehyde Dehydrogenase by Site-Directed Mutagenesis,” *Biochemistry*, vol. 34, no. 8, pp. 2592–2598, Feb. 1995.
- [167] R. C. Vallari and R. Pietruszko, “Human aldehyde dehydrogenase: mechanism of inhibition of disulfiram.,” *Science*, vol. 216, no. 4546, pp. 637–9, May 1982.
- [168] R. Dumitru, W. Z. Jiang, D. P. Weeks, and M. A. Wilson, “Crystal structure of dicamba monooxygenase: a Rieske nonheme oxygenase that catalyzes oxidative demethylation.,” *J. Mol. Biol.*, vol. 392, no. 2, pp. 498–510, Sep. 2009.
- [169] I. F. Sevrioukova, H. Li, and T. L. Poulos, “Crystal structure of putidaredoxin reductase from *Pseudomonas putida*, the final structural component of the cytochrome P450cam monooxygenase.,” *J. Mol. Biol.*, vol. 336, no. 4, pp. 889–902, Mar. 2004.

- [170] E. Masai, M. Sasaki, Y. Minakawa, T. Abe, T. Sonoki, K. Miyauchi, Y. Katayama, and M. Fukuda, "A Novel Tetrahydrofolate-Dependent O-Demethylase Gene Is Essential for Growth of *Sphingomonas paucimobilis* SYK-6 with Syringate," *J. Bacteriol.*, vol. 186, no. 9, pp. 2757–2765, Apr. 2004.
- [171] T. Abe, E. Masai, K. Miyauchi, Y. Katayama, and M. Fukuda, "A tetrahydrofolate-dependent O-demethylase, LigM, is crucial for catabolism of vanillate and syringate in *Sphingomonas paucimobilis* SYK-6.," *J. Bacteriol.*, vol. 187, no. 6, pp. 2030–7, Mar. 2005.
- [172] M. A. Patrauchan, C. Florizone, M. Dosanjh, W. W. Mohn, J. Davies, and L. D. Eltis, "Catabolism of Benzoate and Phthalate in *Rhodococcus sp.* Strain RHA1 : Redundancies and Convergence," *Am. Soc. Microbiol.*, vol. 187, no. 12, pp. 4050–4063, 2005.
- [173] K. C. Y. C. Yam, S. Okamoto, J. N. R. N. Roberts, and L. D. E. D. Eltis, "Adventures in *Rhodococcus* — from steroids to explosives," Mar. 2011.
- [174] M. Dosanjh, G. L. Newton, and J. Davies, "Characterization of a mycothiol ligase mutant of *Rhodococcus jostii* RHA1.," *Res. Microbiol.*, vol. 159, no. 9–10, pp. 643–50.
- [175] P. D. Sainsbury, E. M. Hardiman, M. Ahmad, H. Otani, N. Seghezzi, L. D. Eltis, and T. D. H. Bugg, "Breaking down lignin to high-value chemicals: the conversion of lignocellulose to vanillin in a gene deletion mutant of *Rhodococcus jostii* RHA1.," *ACS Chem. Biol.*, vol. 8, no. 10, pp. 2151–6, Oct. 2013.
- [176] D. J. Yelle, P. Kaparaju, C. G. Hunt, K. Hirth, H. Kim, J. Ralph, and C. Felby, "Two-Dimensional NMR Evidence for Cleavage of Lignin and Xylan Substituents in Wheat Straw Through Hydrothermal Pretreatment and Enzymatic Hydrolysis," *BioEnergy Res.*, vol. 6, no. 1, pp. 211–221, Sep. 2012.
- [177] A. P. Zhang, C.-F. Liu, and R.-C. Sun, "Fractional isolation and characterization of lignin and hemicelluloses from triploid of *Populus tomentosa*," *Ind. Crops Prod.*, vol. 31, no. 2, pp. 357–362, Mar. 2010.
- [178] A. Muheim and K. Lerch, "Towards a high-yield bioconversion of ferulic acid to vanillin," *Appl. Microbiol. Biotechnol.*, vol. 51, no. 4, pp. 456–461, Apr. 1999.
- [179] R. Plaggenborg, J. Overhage, A. Loos, J. A. C. Archer, P. Lessard, A. J. Sinskey, A. Steinbüchel, and H. Priefert, "Potential of *Rhodococcus* strains for biotechnological vanillin production from ferulic acid and eugenol.," *Appl. Microbiol. Biotechnol.*, vol. 72, no. 4, pp. 745–55, Oct. 2006.

- [180] A Narbad and M. J. Gasson, "Metabolism of ferulic acid via vanillin using a novel CoA-dependent pathway in a newly-isolated strain of *Pseudomonas fluorescens*," *Microbiology*, vol. 144 (Pt 5, pp. 1397–405, May 1998.
- [181] G. Gurujeyalakshmi and A. Mahadevan, "Dissimilation of ferulic acid by *Bacillus subtilis*," *Curr. Microbiol.*, vol. 16, no. 2, pp. 69–73, Mar. 1987.
- [182] G. Degrassi, R. Rizzo, and C. V Bruschi, "Degradation of trans-ferulic and p-coumaric acid by *Acinetobacter calcoaceticus* DSM 586," *Biochim. Biophys. Acta.*, vol. 1244, pp. 363–367, Jun. 1995.
- [183] A. Toms and J. M. Wood, "Degradation of trans-ferulic acid by *Pseudomonas acidovorans*," *Biochemistry*, vol. 9, no. 2, pp. 337–343, Jan. 1970.
- [184] P. Barghini, D. Di Gioia, F. Fava, and M. Ruzzi, "Vanillin production using metabolically engineered *Escherichia coli* under non-growing conditions," *Microb. Cell Fact.*, vol. 6, p. 13, Jan. 2007.
- [185] Z. Huang, L. Dostal, and J. Rosazza, "Mechanisms of ferulic acid conversions to vanillic acid and guaiacol by *Rhodotorula rubra*," *J. Biol. Chem.*, vol. 268, no. 32, pp. 23954–23958, Nov. 1993.
- [186] H. Furukawa, H. Morita, T. Yoshida, and T. Nagasawa, "Conversion of Isoeugenol into Vanillic Acid by *Pseudomonas putida* I58 Cells Exhibiting High Isoeugenol-Degrading Activity," *J. Biosci. Bioeng.*, vol. 96, no. 4, pp. 401–403, 2003.
- [187] V. Koppaka, D. C. Thompson, Y. Chen, M. Ellermann, K. C. Nicolaou, R. O. Juvonen, D. Petersen, R. A. Deitrich, T. D. Hurley, and V. Vasiliou, "Aldehyde dehydrogenase inhibitors: a comprehensive review of the pharmacology, mechanism of action, substrate specificity, and clinical application," *Pharmacol. Rev.*, vol. 64, no. 3, pp. 520–39, Jul. 2012.
- [188] E. Masai, Y. Yamamoto, T. Inoue, K. Takamura, H. Hara, D. Kasai, Y. Katayama, and M. Fukuda, "Characterization of ligV essential for catabolism of vanillin by *Sphingomonas paucimobilis* SYK-6," *Biosci. Biotechnol. Biochem.*, vol. 71, no. 10, pp. 2487–92, Oct. 2007.
- [189] D. C. Mays, a N. Nelson, a H. Fauq, Z. H. Shriver, K. a Veverka, S. Naylor, and J. J. Lipsky, "S-methyl N,N-diethylthiocarbamate sulfone, a potential metabolite of disulfiram and potent inhibitor of low Km mitochondrial aldehyde dehydrogenase," *Biochem. Pharmacol.*, vol. 49, no. 5, pp. 693–700, Mar. 1995.
- [190] V. J. Zaldívar-Machorro, M. López-Ortiz, P. Demare, I. Regla, and R. A. Muñoz-Clares, "The disulfiram metabolites S-methyl-N,N-diethyldithiocarbamoyl sulfoxide and S-methyl-N,N-diethylthiocarbamoyl sulfone irreversibly inactivate betaine aldehyde dehydrogenase from

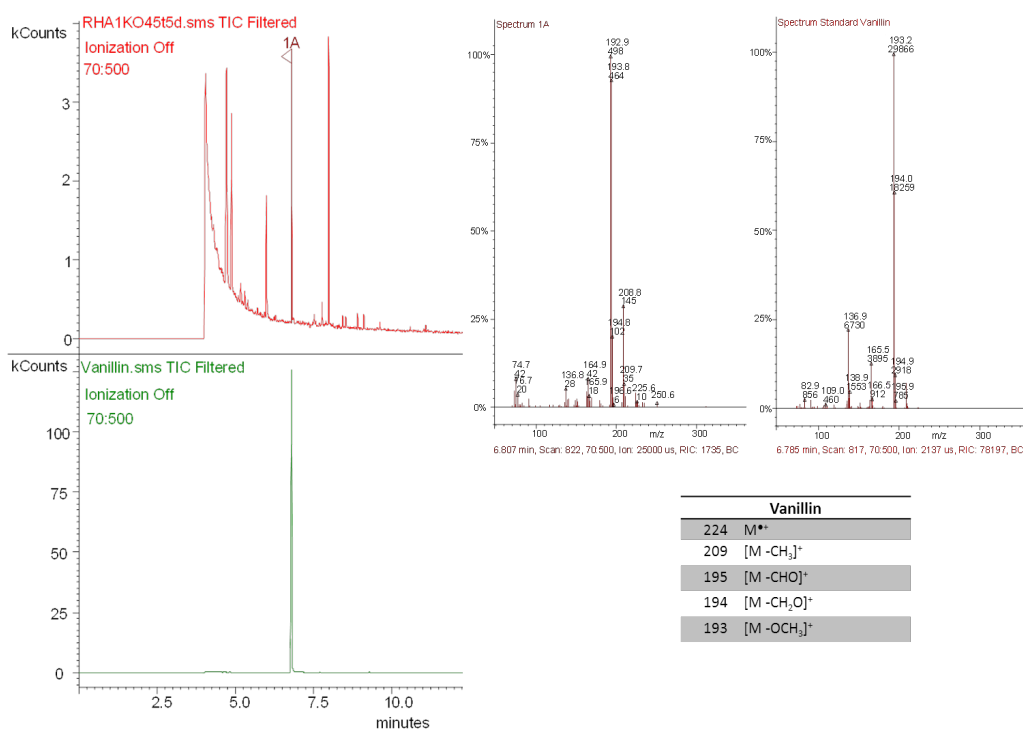
- Pseudomonas aeruginosa*, both in vitro and in situ, and arrest bacterial grow,” *Biochimie*, vol. 93, no. 2, pp. 286–95, Feb. 2011.
- [191] J. Perozich, H. Nicholas, B. C. Wang, R. Lindahl, and J. Hempel, “Relationships within the aldehyde dehydrogenase extended family.,” *Protein Sci.*, vol. 8, no. 1, pp. 137–46, Jan. 1999.
- [192] L. F. Fitzsimmons, S. Flemer, A. S. Wurthmann, P. B. Decker, I. N. Sarkar, and M. J. Wargo, “Small-molecule inhibition of choline catabolism in *Pseudomonas aeruginosa* and other aerobic choline-catabolizing bacteria.,” *Appl. Environ. Microbiol.*, vol. 77, no. 13, pp. 4383–9, Jul. 2011.
- [193] J. Boch, G. Nau-Wagner, S. Kneip, and E. Bremer, “Glycine betaine aldehyde dehydrogenase from *Bacillus subtilis*: characterization of an enzyme required for the synthesis of the osmoprotectant glycine betaine,” *Arch. Microbiol.*, vol. 168, no. 4, pp. 282–289, Sep. 1997.
- [194] B. Landfald and A. R. Strom, “Choline-glycine betaine pathway confers a high level of osmotic tolerance in *Escherichia coli*.,” *J. Bacteriol.*, vol. 165, no. 3, pp. 849–855, Mar. 1986.
- [195] J. E. Graham and B. J. Wilkinson, “*Staphylococcus aureus* osmoregulation: roles for choline, glycine betaine, proline, and taurine.,” *J. Bacteriol.*, vol. 174, no. 8, pp. 2711–2716, Apr. 1992.
- [196] K. L. Rozwadowski, G. G. Khachatourians, and G. Selvaraj, “Choline oxidase, a catabolic enzyme in *Arthrobacter pascens*, facilitates adaptation to osmotic stress in *Escherichia coli*.,” *J. Bacteriol.*, vol. 173, no. 2, pp. 472–8, Jan. 1991.
- [197] S. Ikuta, S. Imamura, H. Misaki, and Y. Horiuti, “Purification and Characterization of Choline Oxidase from *Arthrobacter globiformis*.,” *J. Biochem.*, vol. 82, no. 6, pp. 1741–1749, Dec. 1977.
- [198] S. H. Zeisel, M.-H. Mar, J. C. Howe, and J. M. Holden, “Concentrations of choline-containing compounds and betaine in common foods.,” *J. Nutr.*, vol. 133, no. 5, pp. 1302–7, May 2003.
- [199] M. Vojtěchová, R. Rodríguez-Sotres, E. M. Valenzuela-Soto, and R. A. Muñoz-Clares, “Substrate inhibition by betaine aldehyde of betaine aldehyde dehydrogenase from leaves of *Amaranthus hypochondriacus* L.,” *Biochim. Biophys. Acta - Protein Struct. Mol. Enzymol.*, vol. 1341, no. 1, pp. 49–57, 1997.
- [200] E. Stupperich and R. Konle, “Corrinoid-Dependent Methyl Transfer Reactions Are Involved in Methanol and 3,4-Dimethoxybenzoate Metabolism by *Sporomusa ovata*.,” *Appl. Environ. Microbiol.*, vol. 59, no. 9, pp. 3110–6, Sep. 1993.

- [201] F. Brunel and J. Davison, "Cloning and sequencing of *Pseudomonas* genes encoding vanillate demethylase.," *J. Bacteriol.*, vol. 170, no. 10, pp. 4924–4930, Oct. 1988.
- [202] T. Sonoki, T. Obi, S. Kubota, M. Higashi, E. Masai, and Y. Katayama, "Coexistence of two different O demethylation systems in lignin metabolism by *Sphingomonas paucimobilis* SYK-6: cloning and sequencing of the lignin biphenyl-specific O-demethylase (LigX) gene.," *Appl. Environ. Microbiol.*, vol. 66, no. 5, pp. 2125–32, May 2000.
- [203] P. Ortiz de Montellano and E. Komives, "Branchpoint for heme alkylation and metabolite formation in the oxidation of arylacetylenes by cytochrome P-450," *J. Biol. Chem.*, vol. 260, no. 6, pp. 3330–3336, Mar. 1985.
- [204] H. Ishii, T. Ishikawa, S. Takeda, S. Ueki, and M. Suzuki, "Cesium Fluoride-Mediated Claisen Rearrangement of Aryl Propargyl Ether. Exclusive Formation of 2-Methylarylfuran and Its Availability as a Masked Salicylaldehyde," *Chem. Pharm. Bull. (Tokyo)*, vol. 40, no. 5, pp. 1148–1153, May 1992.
- [205] T. D. H. Bugg, "Dioxygenase enzymes: catalytic mechanisms and chemical models," *Tetrahedron*, vol. 59, no. 36, pp. 7075–7101, Sep. 2003.
- [206] E. J. Corey, J. R. Cashman, S. S. Kantner, and S. W. Wright, "Rationally designed, potent competitive inhibitors of leukotriene biosynthesis," *J. Am. Chem. Soc.*, vol. 106, no. 5, pp. 1503–1504, Mar. 1984.
- [207] M. J. Sergeant, J.-J. Li, C. Fox, N. Brookbank, D. Rea, T. D. H. Bugg, and A. J. Thompson, "Selective inhibition of carotenoid cleavage dioxygenases: phenotypic effects on shoot branching.," *J. Biol. Chem.*, vol. 284, no. 8, pp. 5257–64, Feb. 2009.
- [208] P. J. Harrison and T. D. H. Bugg, "Enzymology of the carotenoid cleavage dioxygenases: Reaction mechanisms, inhibition and biochemical roles.," *Arch. Biochem. Biophys.*, vol. 544C, pp. 105–111, Feb. 2014.
- [209] T. D. Bugg, "Overproduction, purification and properties of 2,3-dihydroxyphenylpropionate 1,2-dioxygenase from *Escherichia coli*," *Biochim. Biophys. Acta*, vol. 1202, no. 2, pp. 258–64, Oct. 1993.
- [210] E. L. Spence, M. Kawamukai, J. Sanvoisin, H. Braven, and T. D. Bugg, "Catechol dioxygenases from *Escherichia coli* (MhpB) and *Alcaligenes eutrophus* (MpcI): sequence analysis and biochemical properties of a third family of extradiol dioxygenases.," *J. Bacteriol.*, vol. 178, no. 17, pp. 5249–56, Sep. 1996.
- [211] R. P. Burlingame, L. Wyman, and P. J. Chapman, "Isolation and characterization of *Escherichia coli* mutants defective for phenylpropionate degradation.," *J. Bacteriol.*, vol. 168, no. 1, pp. 55–64, Oct. 1986.

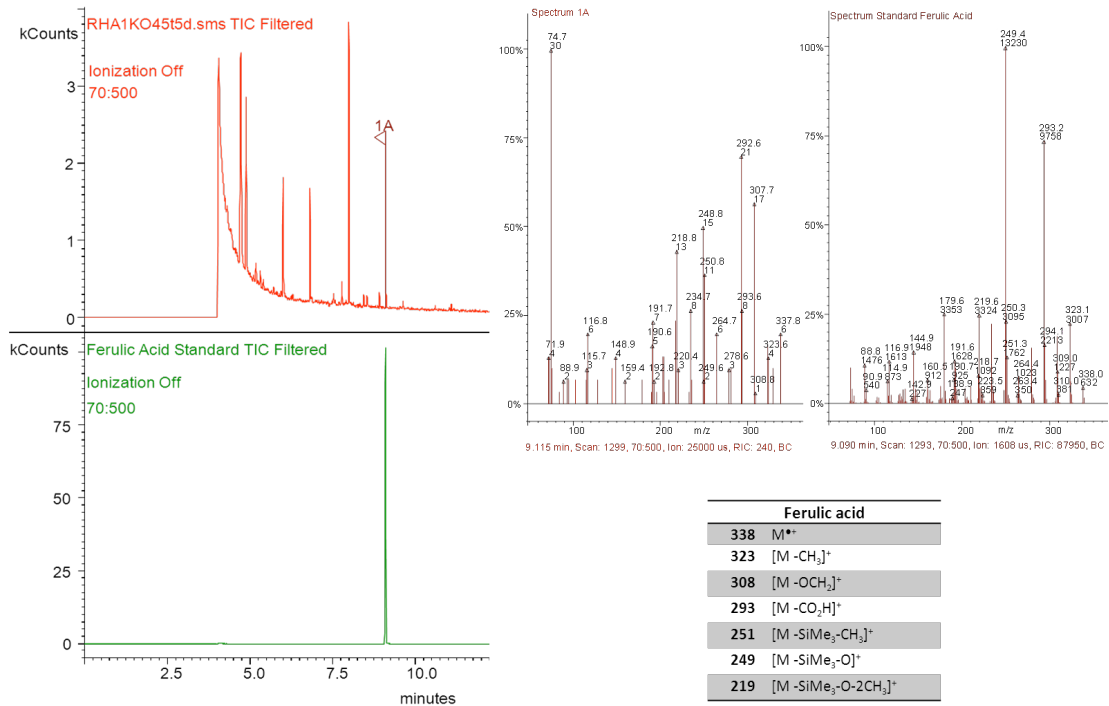
- [212] K. Tanaka, K. Matsuo, A. Nakanishi, T. Hatano, H. Izeki, Y. Ishida, and W. Mori, "Syntheses and anti-inflammatory and analgesic activities of hydroxamic acids and acid hydrazides.," *Chem. Pharm. Bull. (Tokyo)*., vol. 31, no. 8, pp. 2810–9, Aug. 1983.
- [213] T. Yoshida and M. Alexander, "Hydroxylamine formation by *Nitrosomonas europaea*," *Can. J. Microbiol.*, vol. 10, no. 6, pp. 923–926, Dec. 1964.
- [214] T. D. H. Bugg, (2012) *Introduction to Enzyme and Coenzyme Chemistry*, Wiley-Blackwell, New Jersey.
- [215] D. L. MacDonald, R. Y. Stanier, and J. L. Ingraham, "The enzymatic formation of beta-carboxymuconic acid.," *J. Biol. Chem.*, vol. 210, no. 2, pp. 809–20, Oct. 1954.
- [216] M. R. Green and J. Sambrook, (2012) *Molecular Cloning: A Laboratory Manual (Fourth Edition): Three-volume set*. Cold Spring Harbor Laboratory Press, New York
- [217] T. Zor and Z. Selinger, "Linearization of the Bradford protein assay increases its sensitivity: theoretical and experimental studies.," *Anal. Biochem.*, vol. 236, no. 2, pp. 302–8, May 1996.
- [218] H. Fujisawa and M. Uyeda, "Protocatechuate 3,4-Dioxygenase. Cobalt Substitution for Iron," *Eur. J. Biochem.*, vol. 45, no. 1, pp. 223–231, Jun. 1974.
- [219] I. Dijkgraaf, A. Y. Rijnders, A. Soede, A. C. Dechesne, G. W. van Esse, A. J. Brouwer, F. H. M. Corstens, O. C. Boerman, D. T. S. Rijkers, and R. M. J. Liskamp, "Synthesis of DOTA-conjugated multivalent cyclic-RGD peptide dendrimers via 1,3-dipolar cycloaddition and their biological evaluation: implications for tumor targeting and tumor imaging purposes.," *Org. Biomol. Chem.*, vol. 5, no. 6, pp. 935–44, Mar. 2007.
- [220] G. Brieger and T. J. Nestruck, "Catalytic transfer hydrogenation," *Chem. Rev.*, vol. 74, no. 5, pp. 567–580, Oct. 1974.
- [221] N. Usachova, G. Leitis, A. Jirgensons, and I. Kalvinsh, "Synthesis of Hydroxamic Acids by Activation of Carboxylic Acids with N , N '-Carbonyldiimidazole: Exploring the Efficiency of the Method," *Synth. Commun.*, vol. 40, no. 6, pp. 927–935, Feb. 2010.

7: Appendix

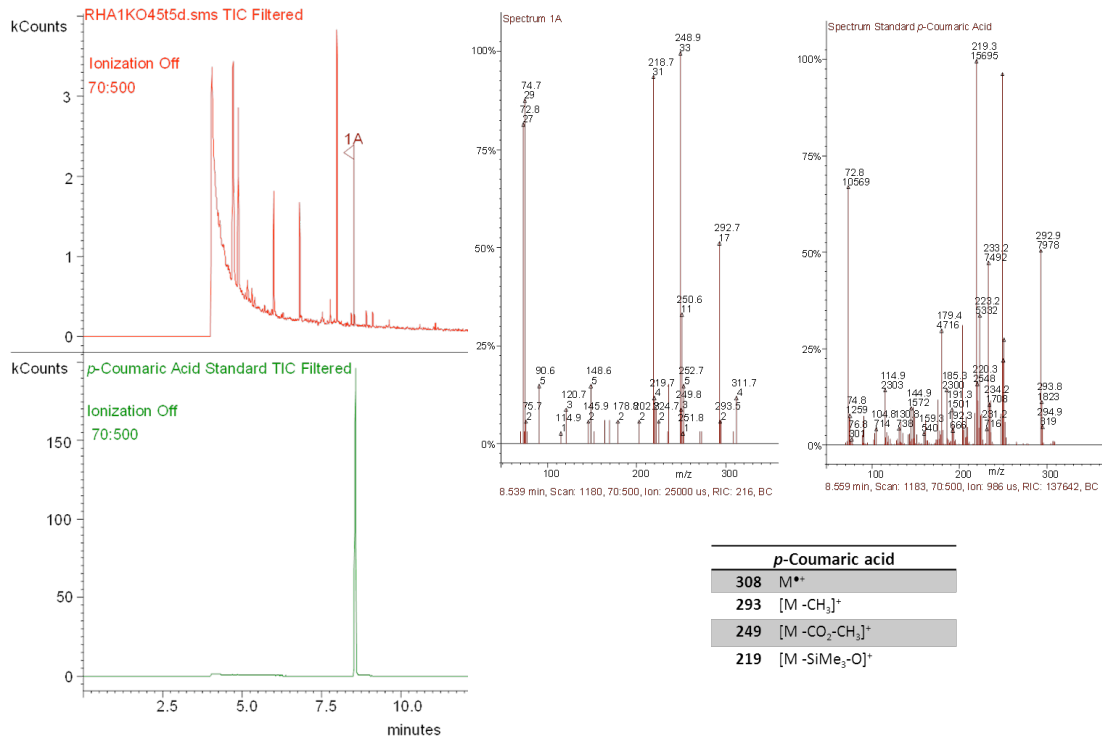
7.1 GC-MS Fragmentation patterns of identified metabolites and authentic standards



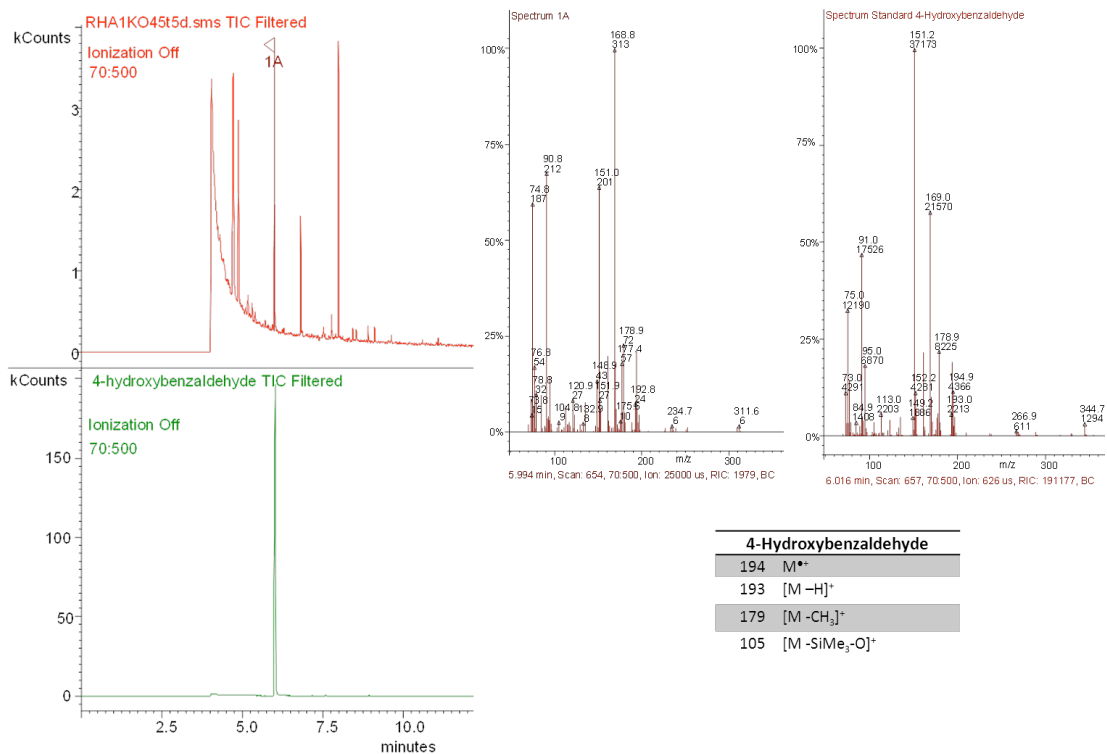
Appendix 1: GC-MS EI fragmentation pattern and retention time of detected metabolite after treatment with Bis(trimethylsilyl)trifluoroacetamide (BSTFA). The retention time and fragmentation pattern of a silylated vanillin standard.



Appendix 2: GC-MS EI fragmentation pattern and retention time of detected metabolite after treatment with Bis(trimethylsilyl)trifluoroacetamide (BSTFA). The retention time and fragmentation pattern of a silylated ferulic acid standard.



Appendix 3: GC-MS EI fragmentation pattern and retention time of detected metabolite after treatment with Bis(trimethylsilyl)trifluoroacetamide (BSTFA). The retention time and fragmentation pattern of a silylated *p*-coumaric acid standard.



Appendix 4: GC-MS EI fragmentation pattern and retention time of detected metabolite after treatment with Bis(trimethylsilyl)trifluoroacetamide (BSTFA). The retention time and fragmentation pattern of a silylated 4-hydroxybenzaldehyde standard.

Breaking Down Lignin to High-Value Chemicals: The Conversion of Lignocellulose to Vanillin in a Gene Deletion Mutant of *Rhodococcus jostii* RHA1

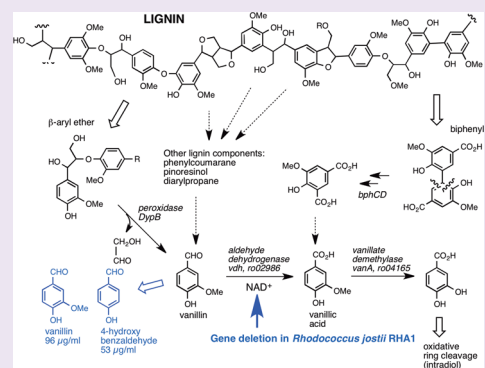
Paul D. Sainsbury,[†] Elizabeth M. Hardiman,[†] Mark Ahmad,[†] Hiroshi Otani,[‡] Nicolas Seghezzi,[‡] Lindsay D. Eltis,^{‡,*} and Timothy D. H. Bugg^{*,†}

[†]Department of Chemistry, University of Warwick, Coventry CV4 7AL, U.K.

[‡]Department of Microbiology and Immunology, University of British Columbia, 2350 Health Sciences Mall, Vancouver, British Columbia V6T 1Z3, Canada

Supporting Information

ABSTRACT: The aromatic polymer lignin represents a possible renewable source of aromatic chemicals, if biocatalytic routes for lignin breakdown can be developed. The availability of a genome sequence for *Rhodococcus jostii* RHA1, a bacterium that breaks down lignin, has allowed the application of a targeted pathway engineering strategy to lignin breakdown to produce vanillin, a valuable food/flavor chemical. A gene deletion strain of *R. jostii* RHA1 in which the vanillin dehydrogenase gene had been deleted, when grown on minimal medium containing 2.5% wheat straw lignocellulose and 0.05% glucose, was found to accumulate vanillin with yields of up to 96 mg/L after 144 h, together with smaller amounts of ferulic acid and 4-hydroxybenzaldehyde.



The industrial production of chemicals for fine chemicals manufacture, polymer synthesis, and food/flavor chemistry is currently a byproduct of the petrochemical industry: approximately 10% of oil refinery products are used to make feedstock chemicals. As supplies of crude oil begin to dwindle in the 21st century, scientists must find new routes to produce feedstock chemicals from renewable sources, for which metabolic engineering is an attractive approach.¹ Lignin, the aromatic polymer comprising 15–30% dry weight of lignocellulose, is a potential source of aromatic chemicals and is generated in large quantities as a byproduct of cellulosic biofuel and pulp/paper manufacture. However, lignin is refractory to hydrolysis, since it contains aryl C3 units linked via C–C and ether C–O bonds.² Chemical methods to depolymerize lignin currently generate low yields of complex mixtures of products and also result in the formation of insoluble high molecular weight “char”.² Microbial degradation of lignin has been investigated primarily in white-rot and brown-rot fungi: white-rot fungi such as *Phanerochaete chrysosporium* produce many extracellular lignin peroxidase and Mn peroxidase enzymes that can oxidize lignin; brown-rot fungi use iron and redox mediators to carry out Fenton chemistry to depolymerize lignin.³ Although fungal lignin breakdown has been studied for 30 years, there is no commercial biocatalytic process for lignin breakdown to date.

It is less well appreciated that several bacterial strains are also able to break down lignin, including actinobacteria such as *Streptomyces viridosporus*, which produces an extracellular

peroxidase,⁴ certain pseudomonads,⁵ and the anaerobic bacterium *Enterobacter lignolyticus* SCF1.⁶ In *Rhodococcus jostii* RHA1, whose genome sequence has been determined, we have reported the identification and characterization of peroxidase DypB, which can oxidize lignin model compounds, Kraft lignin, lignocellulose, and Mn²⁺.⁷ Two further bacterial peroxidase enzymes have been reported from *Amycolatopsis* sp. 75iv2: a heme-containing enzyme capable of oxidizing lignin model compounds⁸ and a Dyp2 peroxidase enzyme with higher catalytic activity for Mn²⁺ oxidation.⁹ The ability to genetically manipulate rhodococci, coupled with their use in fermentation and biotechnology, has prompted us to investigate whether *R. jostii* RHA1 could be used for synthetic biology applications in lignin depolymerisation. Synthetic biology has been used in *Escherichia coli* to engineer new biosynthetic routes to alkanol and biodiesel biofuels,^{10,11} but thus far there are limited applications toward biomass deconstruction and little use of other bacterial hosts for synthetic biology. Here we report the production of low molecular weight aromatic products using a *R. jostii* RHA1 gene deletion mutant, generating vanillin, a high value chemical product used in the food and flavor industry.¹²

Metabolite analysis of *R. jostii* RHA1 grown on liquid media containing 1% (w/v) milled wheat straw lignocellulose identified several metabolites (data shown in Supporting Information Table S1),

Received: April 5, 2013

Accepted: July 30, 2013

Published: July 30, 2013

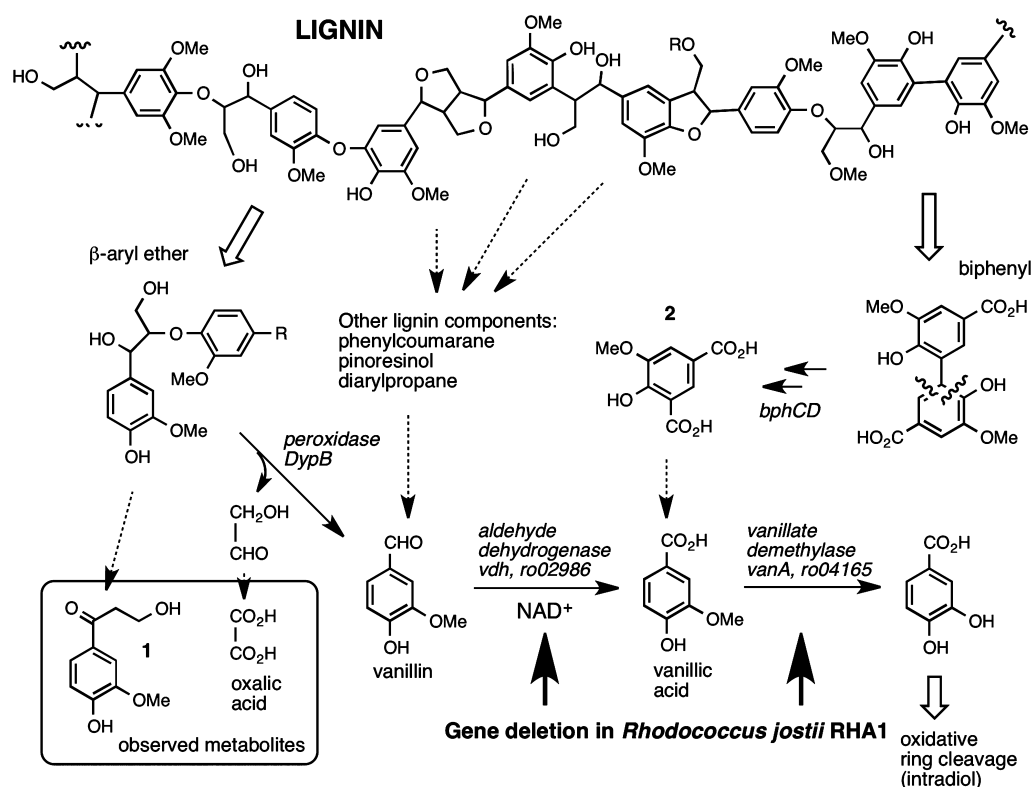


Figure 1. Hypothetical catabolic pathways in *R. jostii* RHA1 for breakdown of β -aryl ether and biphenyl components of lignin, based upon the structures of observed metabolites. Genes involved in vanillin catabolism in *R. jostii* RHA1 are indicated, which have been subjected to gene deletion.

whose structures are consistent with hypothetical catabolic pathways shown in Figure 1 for breakdown of β -aryl ether and biphenyl components of lignin.¹³ Major products 3-(3'-methoxy-4'-hydroxyphenyl)-3-keto-propan-1-ol (**1**) and oxalic acid and minor product vanillic acid could each be derived from the β -aryl ether component of lignin. We have previously shown that *R. jostii* RHA1 DypB (which is likely to be one of a group of lignin-oxidizing enzymes) is able to cleave a β -aryl ether lignin model compound to give vanillin⁷ and a two-carbon fragment glycoaldehyde, which we hypothesize could be oxidized to oxalic acid. The other aromatic metabolite, 5-carboxyvanillic acid (**2**), is a potential intermediate on the biphenyl catabolic pathway and can be decarboxylated to form vanillic acid.¹⁴ We have also found that environmental bacterial strains that are able to metabolize lignin can efficiently utilize vanillic acid for growth.¹⁵ Together, these observations suggested that the vanillic acid catabolic pathway might be important for lignin breakdown.

We have recently identified the *vdh* (ro02986) and *vanA* (ro4165) genes encoding vanillin dehydrogenase and vanillate demethylase, respectively, in *R. jostii* RHA1.¹⁶ RHA045, a Δ *vdh* gene deletion strain, was unable to grow on 1 mM vanillin but able to grow on 1 mM vanillic acid; RHA046, a Δ *vanA* gene deletion strain, was unable to grow on either vanillin or vanillic acid as sole organic substrate.¹⁶ These gene deletion strains allowed us to investigate the effect of disrupting the vanillic acid catabolic pathway on the metabolism of lignin by *R. jostii* RHA1.

Both mutants were able to grow on minimal media containing 1% (w/v) milled wheat straw lignocellulose. The production of low molecular weight metabolites was studied by GC-MS analysis of ethyl acetate extracts of the growth media. For the Δ *vanA* mutant, RHA046, no significant difference from wild-type levels of metabolites was observed. By contrast, in the

case of the Δ *vdh* mutant, a large increase in the quantity and intensity of metabolite peaks was observed, as illustrated in Figure 2a. Three large new peaks at retention time 6.0, 6.8, and 8.0 min were identified by comparison with authentic standards as *p*-hydroxybenzaldehyde, vanillin, and protocatechuic acid (4,5-dihydroxybenzoic acid), respectively. Small peaks corresponding to ferulic acid (9.1 min) and *p*-coumaric acid (8.6 min) were also observed. In each case the retention time and fragmentation pattern of the observed species matched authentic standards by GC-MS and LC-MS analysis (Supporting Information Figures S1–S8).

The accumulation of vanillin is consistent with a blockage in the flux of lignin metabolism caused by deletion of the *vdh* gene, and the accumulation of similar levels of *p*-hydroxybenzaldehyde is consistent with the processing of H- and G-type lignin (both present in wheat straw lignin) by the vanillin dehydrogenase on the vanillic acid catabolic pathway. Neither vanillin and *p*-hydroxybenzaldehyde were observed at all in fermentations using wild-type *R. jostii* (see Table 1), and the observed concentrations approach the maximum concentrations of these compounds tolerated by *R. jostii* RHA1 (toxic at >1 mM concentration).¹⁶

The levels of metabolite production were monitored by LC-MS analysis over 1–7 day fermentations, as shown in Figure 2b (yields shown in Table 1). Growth of RHA045 in minimal medium containing 2.5% wheat straw lignocellulose and 0.05% glucose resulted in production of ferulic acid after 72 h, then increasing production of vanillin from 96 to 144 h, with a maximum yield of 96 mg/L after 144 h. Production of 4-hydroxybenzaldehyde at 50–60 mg/L was also observed at 120–144 h. Cultures grew to A_{600} of 1.3 after 48 h, but growth was halted after metabolite production commenced, consistent with the production of a toxic metabolite. Assuming that wheat straw contains

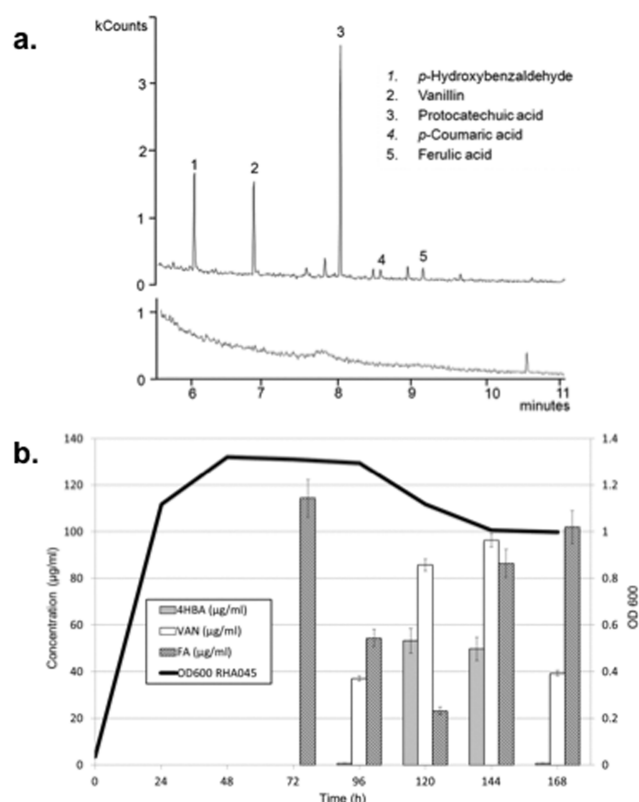


Figure 2. Production of aromatic metabolites from lignocellulose by RHA045. (a) Detection by GC–MS of aromatic metabolites from cultures of RHA045 (upper panel), compared with wild-type *R. jostii* RHA1 (lower panel), grown on minimal media containing 1 g/L wheat straw lignocellulose, after 120 h. Metabolites were extracted into dichloromethane and derivatized using bistrimethylsilylacetyl prior to GC–MS analysis. (b) Time-course of metabolite production from culture of RHA045 grown on minimal media containing 2.5% (w/v) wheat straw lignocellulose, over 1–7 days, by LC–MS analysis and bacterial growth, assessed by OD₆₀₀. VAN, vanillin; 4HBA, 4-hydroxybenzaldehyde; FA, ferulic acid. Yields and standard errors were calculated from averaging data from three separate 7-day experiments and three extractions/analyses at each time point in each experiment.

15–20% lignin, the conversion efficiency of lignin to vanillin in this experiment is approximately 2%, and that of total aromatic products 6–7%.

Table 1. Yields of Aromatic Products Obtained from *R. jostii* RHA1 and *R. jostii* RHA045 from Different Media and Carbon Sources

media	observed product (yield, time observed)				
	vanillin	<i>p</i> -hydroxybenzaldehyde	vanillic acid	ferulic acid	<i>p</i> -coumaric acid
<i>R. jostii</i> RHA1					
Luria–Bertani broth + 1% wheat straw lignocellulose	not observed	not observed	minor metabolite (GC–MS, 6 days)	major metabolite (GC–MS, 5 days)	not observed
M9 minimal medium + 1% wheat straw lignocellulose	not observed	not observed	0.2 mg/L (3 days)	20 mg/L (5 days)	not observed
M9 minimal medium + 0.1% beechwood xylan	not observed	not observed	<0.01 mg/L	0.01 mg/L	not observed
<i>R. jostii</i> RHA045 (Δ<i>vdh</i> mutant)					
M9 minimal medium + 1% wheat straw lignocellulose	major metabolite (GC–MS, 5 days)	major metabolite (GC–MS, 5 days)	minor metabolite (GC–MS, 5 days)	minor metabolite (GC–MS, 5 days)	minor metabolite (GC–MS, 5 days)
M9 minimal medium + 2.5% wheat straw lignocellulose	96 mg/L (6 days)	53 mg/L (5 days)	3–120 mg/L (4–6 days)	23–86 mg/L (4–6 days)	minor peak (not quantified)
M9 minimal medium + 0.1% beechwood xylan	not observed	not observed	<0.01 mg/L	0.01 mg/L	not observed

Wheat lignocellulose is known to contain ferulic acid, attached via ester linkages to hemicellulose and via ether linkages to lignin.^{17,18} In order to test whether the observed ferulic acid and vanillin are derived from the xylan polysaccharide in hemicellulose or from lignin, further experiments were carried out. First, RHA045 was grown on minimal medium containing 0.1% beechwood xylan: metabolite analysis after 72–96 h revealed no production of ferulic acid or vanillin. Second, to examine whether ferulic acid can be converted into vanillin in this host, RHA045 was grown on 0.1% ferulic acid as carbon source: low concentrations of vanillin (<0.5 mg/L) were observed, but high concentrations (>100 mg/L) of vanillic acid, implying that ferulic acid is not converted directly to vanillin but is converted to vanillic acid via β -oxidation. RHA046, lacking vanillate *O*-demethylase, grew to a much lower overall yield than the wild-type strain and accumulated an almost stoichiometric amount of vanillic acid (>85% of initial ferulic acid after 24 h, see Supporting Information Figure S10), but no vanillin was detected. Together, these results suggest that RHA1 degrades ferulic acid via β -oxidation, as has been documented in other bacterial strains.^{19,20} Finally, wheat straw was treated with 1.5% NaOH to cleave ester-linked material, and from the soluble lignin-carbohydrate fraction, alkali lignin was prepared by acidification to pH 6.5, precipitation with EtOH, and removal of hemicellulose at pH 1.5. From the solid residue remaining after NaOH treatment, fermentation with RHA045 for 7 days gave no aromatic metabolite production; however, treatment of the alkali lignin fraction with RHA045 resulted in production of vanillin and ferulic acid after 48–72 h, more rapidly than was observed from lignocellulose, albeit at reduced yields of 1.0–1.3 mg/L (see Supporting Information Figure S11). These data confirm that the observed aromatic metabolites are derived from the alkali lignin fraction of lignocellulose and suggest that metabolite production is probably initiated by hydrolysis of a ferulate ester linkage.

The detection of protocatechuic acid by GC–MS (Figure 2a) is surprising, since it occurs after the *vdh* gene on the vanillic acid catabolic pathway. Our hypothesis is that protocatechuic acid is formed by slow demethylation of vanillin by vanillic acid demethylase, generating a reactive 3,4-dihydroxybenzaldehyde shunt metabolite, which is oxidized upon cell export (see Figure 3).

Kraft lignin, a byproduct of the paper/pulp industry that has a more condensed structure,² was also examined as a substrate. *R. jostii* RHA1 and mutants RHA045 and RHA046 were grown on M9 minimal media and 0.05% glucose in the presence of each of two different types of Kraft lignin (at either 0.05% or

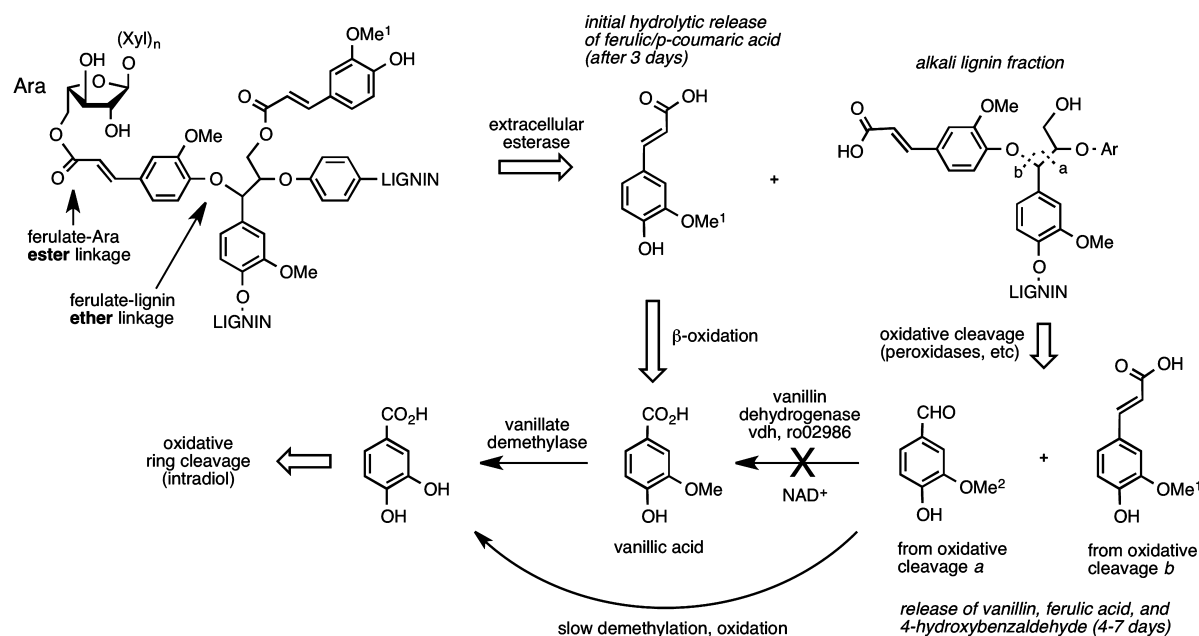


Figure 3. Catabolic steps that rationalize the observed aromatic products from gene deletion strain RHA045, starting from the documented structure of the wheat straw lignin–carbohydrate complex.^{17,18} Lignin structure is illustrated with G units, but wheat lignin contains a mixture of G and H units (label 1; 3-Ome replaced by H), whose breakdown gives rise to *p*-coumaric acid as well as ferulic acid (label 1; 3-Ome replaced by H) and 4-hydroxybenzaldehyde (label 2; 3-Ome replaced by H), as well as vanillin. Proposed conversion of vanillin to protocatechuic acid in RHA045 is illustrated. In the wild-type strain, 4-hydroxybenzaldehyde is oxidized to 4-hydroxybenzoic acid, which is then hydroxylated to protocatechuic acid. Ara, arabinofuranose, attached to xylan.

0.5% w/v) over 6–9 days. Cultures of the Δvdh mutant RHA045 accumulated up to 13 mg/L vanillin after 5 days of incubation on 0.5% w/v industrial Kraft lignin. Similarly, cultures of the Δvan mutant RHA046 accumulated up to 0.1 mg/L vanillic acid after 4–7 days of incubation on 0.05% industrial Kraft lignin. However, the amounts of each compound that accumulated varied significantly from one run to the next, and no significant accumulation was observed when alkali Kraft lignin (Sigma-Aldrich) was used as a substrate. Overall, *R. jostii* RHA1 transforms Kraft lignins much less efficiently than lignocellulose.

Vanillin is a high value chemical that is widely used in the food/flavor industry, for which biocatalytic routes are of considerable interest,¹¹ and for which there is a commercial process for production from lignosulfonates via a chemocatalytic route.²¹ During the completion of this work, it has been reported that deletion of the vanillin dehydrogenase gene in *Amycolatopsis* sp. strain ATCC 39116 can be used to produce vanillin from biotransformation of ferulic acid.²² This work establishes that vanillin can be produced from the lignin component of lignocellulose using a predictive gene deletion and therefore demonstrates that lignin breakdown pathways can in principle be engineered for production of aromatic chemicals. Although aromatic compounds can be produced from lignin through pyrolysis or chemocatalysis,² such approaches usually generate complex mixtures of products with total yields of 5–15%, whereas the pathway engineering approach reported here generates a small number of metabolites in a predictive way. *R. jostii* RHA1 has proved to be a robust organism for pathway engineering, the mutant strain growing to high cell density on minimal media containing lignocellulose and tolerating the production of toxic aldehyde metabolites. The discovery of further pathways and gene products for lignin breakdown in bacteria could in principle

enable synthetic biology to be used to engineer new routes for production of lignin-derived chemicals from renewable feedstocks via catabolic pathways.

METHODS

The source of lignocellulose in experiments was wheat straw (variety Hereward) milled in a Retsch grinding mill (model RM 200) sieved through a 0.5 mm mesh. Beechwood xylan (Sigma X4252, >90% xylose residues), chemicals, and solvents were purchased from Sigma-Aldrich. Industrial Kraft lignin, manufactured from spruce, was supplied by Billerud Ltd. *Rhodococcus jostii* RHA1 strains RHA045 (Δvdh) and RHA046 ($\Delta vanA$) were generated as previously described.¹⁶

Lignocellulose/Lignin Degradation Trials. Approximately 2.5 g (per liter) of milled wheat straw or Kraft Lignin was autoclaved with M9 salts (Na_2HPO_4 30.5 g, KH_2PO_4 15.0 g, NaCl 2.5 g, NH_4Cl 5.0 g per liter) supplemented with 2 mM MgSO_4 , 100 μM CaCl_2 , 100 μM FeCl_3 , and 100 μM MnCl_2 . Glucose (0.05% w/v) and additional supplements were filter sterilized and added preinoculation. A 2 mL overnight culture of the bacterial strain was used to inoculate the media (50 mL volume for initial trials, 1 L volume for LC–MS quantification). Solutions were left to shake (180 rpm) at 30 °C for 7 days, and samples taken after 0, 3, 6 h and after 1–7 days. Samples (5 mL) were removed and treated with 1 M HCl (50 μL) and left on ice for 3 min. The samples were centrifuged (10 min, 13000g), and the supernatant removed. To the supernatant was added ethyl acetate (1/3 volume), and the organic layer removed and dried under nitrogen. All extractions and analyses were carried out in triplicate, and each fermentation was carried out three times; estimated yields were averaged over all recorded samples at each time point. Control experiments with lignocellulose only (no bacteria) showed no detectable metabolite production, and incubations with wild-type *R. jostii* RHA1 showed low levels of production of ferulic acid and vanillic acid, but not vanillin (Supporting Information Table S2).

Preparation of Alkali Lignin Fraction. The procedure was adapted from the method of Sun et al.²³ Milled wheat straw (15 g) was stirred with 1.5% w/v NaOH (300 mL) for 2 h at RT. The slurry was

filtered through Whatman no. 1 filter paper, and the solid residue removed, washed several times with water, and then freeze-dried. The filtrate was acidified to pH 6.5 with acetic acid and then concentrated *in vacuo*. The extract was then mixed with 5 volumes of ethanol and left overnight. Precipitated hemicellulose was removed by filtration, and the filtrate then acidified to pH 1.5 with 6 M HCl and left for 24 h. The lignin precipitate was collected by centrifugation at 4700g (10 min), and the pellets freeze-dried overnight to give 180 mg of alkali lignin. Incubation of this material with *Rhodococcus jostii* RHA045 was carried out as described above, on a 50 mL scale.

GC–MS analysis was carried out on a Varian 4000 GC–MS system fitted with a mass spectrometer (Varian 4000) using an ion trap mass analyzer and ion multiplier detector with a capillary gas chromatograph (Varian 3800). Helium was used as carrier gas (0.7 bar) at a flow rate of 1.3 mL/min through a fused silica capillary column (30 m × 0.25 mm). The splitter/injector was kept at 300 °C, and the column temperature was programmed as follows: 100 °C held for 4 min then increased by 4 °C/min until 270 °C where it was held for 4 min. The ion source temperature was 150 °C. The chromatograms were recorded by ion monitoring in the *m/e* range of 50–500. Prior to GC–MS analysis, dry organic extracts were dissolved in dichloromethane (1 mL) and derivatized with *N,O*-bis(trimethylsilyl)acetamide (BSA, 200 μL) and chlorotrimethylsilane (TMCS, 10 μL), left overnight, and diluted by a factor of 100.

HPLC analysis was performed on an Agilent 1200 Series system (Agilent Technologies, Cheshire, UK), equipped with a DAD photodiode detector (G1315B) and an LC–MSD Trap VL (G2445C VL) electrospray ionization mass spectrometer (ESI/MS) system, both coupled to an Agilent ChemStation (Version B.01.03) for data processing. The organic residue was redissolved in 1 mL of 30% acetonitrile/70% H₂O, and samples were injected onto a reversed-phase column Zorbax Eclipse XDB-C18 (4.6 mm × 250 mm; 5 μm particle; Agilent). The solvents were water/trifluoroacetic acid (TFA) (99:1 v/v) as solvent A and MeOH with 0.1% TFA as solvent B. The flow rate was 1 mL/min. The linear gradient for solvent B was as follows: 0 min, 5%; 15 min, 35%; 30 min, 43%; 32 min, 100%; 40 min, 5%. The identity and quantification of each compound was established by comparing the retention times, uv–vis spectra, and mass spectra of the peaks in every sample with authentic standards. Standards of identified compounds were acquired from Sigma Aldrich (U.K.) and quantified.

■ ASSOCIATED CONTENT

📄 Supporting Information

Data for metabolites identified in the manuscript and metabolite time-course data. This material is available free of charge via the Internet at <http://pubs.acs.org>.

■ AUTHOR INFORMATION

Corresponding Author

*E-mail T.D.Bugg@warwick.ac.uk.

Notes

The authors declare no competing financial interest.

■ ACKNOWLEDGMENTS

Gene deletion strains RHA045 and RHA046 were previously constructed by Hao-Ping Chen (UBC). This work was supported by studentships from BBSRC (P.D.S.), the IMRC “Wealth out of waste” Project (M.A.), and research grants from the BBSRC IBTI Refinery Club (BB/H004270/1) and Genome Canada (LSARP 2108).

■ REFERENCES

(1) Lee, J. W., Na, D., Park, J. M., Lee, J., Choi, S., and Lee, S. Y. (2012) Systems metabolic engineering of micro-organisms for natural and non-natural chemicals. *Nat. Chem. Biol.* 8, 536–546.

(2) Zakzeski, J., Bruijninx, P. C. A., Jongerius, A. L., and Weckhuysen, B. M. (2010) The catalytic valorization of lignin for the production of renewable chemicals. *Chem. Rev.* 110, 3552–3599.

(3) Wong, D. W. S. (2009) Structure and action mechanism of lignolytic enzymes. *Appl. Biochem. Biotechnol.* 157, 174–209.

(4) Ramachandra, M., Crawford, D., and Hertel, G. (1988) Characterization of an extracellular lignin peroxidase of the lignocellulolytic actinomycete *Streptomyces viridosporus*. *Appl. Environ. Microbiol.* 54, 3057–3063.

(5) Ahmad, M., Taylor, C. R., Pink, D., Burton, K., Eastwood, D., Bending, G. D., and Bugg, T. D. H. (2010) Development of novel assays for lignin degradation: comparative analysis of bacterial and fungal lignin degraders. *Mol. Biosyst.* 6, 815–821.

(6) DeAngelis, K. M., D’Haeseleer, P., Chivian, D., Fortney, J. L., Khudyakov, J., Simmons, B., Woo, H., Arkin, A. P., Davenport, K. W., Goodwin, L., Chen, A., Ivanova, N., Kyrpides, N. C., Mavromatis, K., Woyke, T., and Hazen, T. C. (2011) Complete genome sequence of *Enterobacter lignolyticus* SCF1. *Stand. Genomic Sci.* 5, 69–85.

(7) Ahmad, M., Roberts, J. N., Hardiman, E. M., Singh, R., Eltis, L. D., and Bugg, T. D. H. (2011) Identification of DypB from *Rhodococcus jostii* RHA1 as a lignin peroxidase. *Biochemistry* 50, 5096–5107.

(8) Brown, M. E., Walker, M. C., Nakashige, T. G., Iavarone, A. T., and Chang, M. C. Y. (2011) Discovery and characterization of heme enzymes from unsequenced bacteria: application to microbial lignin degradation. *J. Am. Chem. Soc.* 133, 18006–18009.

(9) Brown, M. E., Barros, T., and Chang, M. C. Y. (2012) Identification and characterization of a multifunctional dye peroxidase from a lignin-reactive bacterium. *ACS Chem. Biol.* 7, 2074–2081.

(10) Atsumi, S., Hanai, T., and Liao, J. C. (2008) Non-fermentative pathways for synthesis of branched-chain higher alcohols as biofuels. *Nature* 451, 86–90.

(11) Steen, E. J., Kang, Y., Bokinsky, G., Hu, Z., Schirmer, A., McClure, A., del Cardayre, S. B., and Keasling, J. D. (2010) Microbial production of fatty-acid-derived fuels and chemicals from plant biomass. *Nature* 463, 559–563.

(12) Priefert, H., Rabenhorst, J., and Steinbüchel, A. (2001) Biotechnological production of vanillin. *Appl. Microbiol. Biotechnol.* 56, 296–314.

(13) Bugg, T. D. H., Ahmad, M., Hardiman, E. M., and Rahmanpour, R. (2011) Pathways for degradation of lignin in bacteria and fungi. *Nat. Prod. Rep.* 28, 1883–1896.

(14) Peng, X., Masai, E., Kitayama, H., Harada, K., Katayama, Y., and Fukuda, M. (2002) Characterization of the 5-carboxyvanillate decarboxylase gene and its role in lignin-related biphenyl catabolism in *Sphingomonas paucimobilis* SYK-6. *Appl. Environ. Microbiol.* 68, 4407–4415.

(15) Taylor, C. R., Hardiman, E. M., Ahmad, M., Sainsbury, P. D., Norris, P. R., and Bugg, T. D. H. (2012) Isolation of bacterial strains able to metabolise lignin from screening of environmental samples. *J. Appl. Microbiol.* 113, 521–530.

(16) Chen, H.-P., Chow, M., Liu, C. C., Lau, A., Liu, J., and Eltis, L. D. (2012) Vanillin catabolism in *Rhodococcus jostii* RHA1. *Appl. Environ. Microbiol.* 78, 586–588.

(17) Iiyama, K., Tuyet Lam, T. B., and Stone, B. A. (1990) Phenolic acid bridges between polysaccharides and lignin in wheat internodes. *Phytochemistry* 29, 733–737.

(18) Sun, X.-F., Sun, R., Fowler, P., and Baird, M. S. (2005) Extraction and characterization of original lignin and hemicelluloses from wheat straw. *J. Agric. Food Chem.* 53, 860–870.

(19) Huang, Z., Dostal, L., and Rosazza, J. P. (1993) Mechanisms of ferulic acid conversions to vanillic acid and guaiacol by *Rhodotorula rubra*. *J. Biol. Chem.* 268, 23954–23958.

(20) Peng, X., Misawa, N., and Harayama, S. (2003) Isolation and characterization of thermophilic Bacilli degrading cinnamic, 4-coumaric and ferulic acids. *Appl. Environ. Microbiol.* 69, 1417–1427.

(21) Bjørsvik, H. R., and Minisci, F. (1999) Fine chemicals from lignosulfonates. I. Synthesis of vanillin by oxidation of lignosulfonates. *Org. Process Res. Dev.* 3, 330–340.

(22) Fleige, C., Hansen, G., Kroll, J., and Steinbüchel, A. (2013) Investigation of the *Amycolatopsis* sp. strain ATCC 39116 vanillin dehydrogenase and its impact on the biotechnological production of vanillin. *Appl. Environ. Microbiol.* 79, 81–90.

(23) Sun, R., Lawther, J. M., and Banks, W. B. (1996) Fractional and structural characterization of wheat straw hemicelluloses. *Carbohydr. Polym.* 29, 325–331.